MODELING ETR1 WITH ISOLABE COINAGE METAL COMPLEXES SUPPORTED BY PARTIALLY FLUORINATED, AND METHYLATED SCORPIONATES

by

SHAWN GLEN RIDLEN

Presented to the Faculty of the Graduate School of

The University of Texas at Arlington in Partial Fulfillment

of the Requirements

for the Degree of

DOCTOR OF PHILOSOPHY

THE UNIVERSITY OF TEXAS AT ARLINGTON

May 2017

Acknowledgements

This work would not have been possible without the help and support of the many great people around me. I would first like to express my sincerest gratitude to my advisor, Professor H.V. Rasika Dias for his guidance, patience, and support during my graduate studies. I would next like to thank my graduate committee members: Professor Peter Kroll, Professor Fredrick MacDonnell, and Professor Junha Jeon. Thank you to the Dias group members, past and present. Especially to our post docs: Dr. Chandrakanta Dash, Dr. Animesh Das, Dr. Naveen Kulkarni, and Dr. Guocang Wang for their assistance and hands on training in the laboratory.

I greatly appreciate the assistance of all of the departmental faculty and staff. Thank you to Jill Howard, Debbie Cooke, Natalie Croy, Jim Garner, Jason Loyd, and Beth Klimeck for their behind-the-scenes support. My sincerest gratitude to Dr. Chuck Savage, Dr. Brian Edwards, and Dr. Roy McDougald for their training and assistance throughout my time at UTA.

My heartfelt gratitude to my friends and family for their endless support and encouragement. Thank you to my parents Ron and Glenda Ridlen, for their love and support throughout this difficult journey. Thank you to my good friend Josh Ward for being always there for me and helping me to remember to relax. Last and most importantly I would like to thank Brittany Baldwin, your endless love and support have made all of this possible and made each and every long night bearable.

April 12, 2017

Abstract

MODELING ETR1 WITH ISOLABE COINAGE METAL COMPLEXES SUPPORTED BY PARTIALLY FLUORINATED, AND METHYLATED SCORPIONATES

Shawn G. Ridlen, PhD

The University of Texas at Arlington, 2017

Supervising Professor: H. V. Rasika Dias

Ethylene is a small molecule that functions as a plant hormone that is closely associated with several vital plant functions ranging from germination, shoot and root growth, sex expression, fruit ripening, senescence and abscission. This gaseous hormone is produced by almost every part of the plant, and mediates these processes throughout out the life of the plant. The ethylene response in many plants is initiated by a group of 5 copper based membrane bound receptors, mainly ETR1 (ethylene receptor 1). These receptors are made up of homodimers linked at their N-termini by two disulfide bonds. Each of the monomer units is composed of three transmembrane α-helices followed by a GAF and kinase domain, and the copper ethylene binding site is located in the endoplasmic reticulum (ER).

While the native receptor is copper based, it has been shown that the group 11 metals (Cu, Ag, Au) can all support ethylene binding in the receptor.

Interestingly, silver is well known to block the ethylene response when applied as a pretreatment solution, whereas copper and gold are both known initiate the response. It is thought that the ethylene response is initiated by the binding of ethylene to the metal center in the receptor, followed by a conformational change, and the release of ethylene. It is not fully understood why silver blocks the signaling of the receptor, but it is probably due to the weak interactions of silver compared to copper and gold. In order to further explore the interactions of the coinage metals and ethylene we have isolated and fully characterized the group 11 metal adducts $[HB(3\text{-}(CF_3),5\text{-}(CH_3)Pz)_3]M(C_2H_4)$ (M = Au, Ag, and Cu; Pz = pyrazolyl) and $[HB(3\text{-}(CF_3),5\text{-}(Ph)Pz)_3]Ag(C_2H_4)$. The gold adduct adopts a trigonal planar geometry with a κ^2 bound scorpionate and has the strongest interaction between the metal center and ligands compared to the silver adducts which have distorted tetrahedral geometry and κ^3 bound scorpionates. The structure, ethylene-bonding, and the group trends in these two isoleptic coinage metal-ethylene adduct series are discussed in chapter 2.

The silver complexes $[HB(3\text{-}(CF_3),5\text{-}(Ph)Pz)_3]AgL$ (L = C_6H_6, CO, or PPh_3) have been synthesized and characterized by NMR spectroscopy, and by X-ray crystallography. In all cases the Scorpionate is bound to silver in typical κ^3-fashion. The benzene adduct is bound in η^2-fashion to silver and the room temperature solution NMR spectra show only one sharp proton and one carbon signal corresponding to benzene which points to fluxional behavior in solution. The

^{13}C NMR resonance corresponding to the CO moiety of [HB(3-(CF_3),5-(Ph)Pz)$_3$]Ag(CO) appears as a singlet at δ 177.4 ppm in CD_2Cl_2 and the characteristic carbonyl stretch appears at $\bar{\upsilon}$ 2148 cm^{-1}. These data indicate diminished Ag→CO π-backbonding. Interesting coupling is observed in the solution ^{19}F and ^{19}P NMR spectra of the Ag(I) adduct [HB(3-(CF_3),5-(Ph)Pz)$_3$]Ag(PPh_3). A detailed analysis of the spectral and structural features of these complexes has been described in chapter 3.

The new poly(pyrazolyl)methane based ligand [(Ph_3B)CH(3,5-(CH_3)$_2$Pz)$_2$]$^-$ has been prepared and the copper adducts [(Ph_3B)CH(3,5-(CH_3)$_2$Pz)$_2$]Cu(L) (where L = C_2H_4, and *cis*-$CH_3HC{=}CHCH_3$) have been isolated and characterized by NMR spectroscopy and X-ray crystallography. This monoanionic bidentate ligand analog of bis(pyrazolyl)borate has been prepared using closely related bis(pyrazolyl)methane and triarylboron, and has allowed for the isolation of the first copper-ethylene adduct of a bidentate poly(pyrazolyl) base ligand.

Table of Contents

List of Illustrations

List of Tables

Chapter 1

Introduction to Copper – Ethylene Chemistry

1.1 Biological Significance

1.1.1 Discovery of the Ethylene Response in Plants

Ethylene is a phytohormone that is associated with several plant functions ranging from germination, shoot and root growth, sex expression, fruit ripening, senescence and abscission.[1-5] Ethylene is produced in almost every part of the plant and mediates this wide range of plant responses and developmental steps.[6] While many of these processes are essential to nature, ethylene can also cause undesirable effects. Ethylene leads to significant economic losses in the agricultural and horticultural industries due to ethylene-accelerated post-harvest ripening and deterioration of perishable commodities.[3, 7] The biological activity of ethylene was first recognized due to the damage caused by the accidental exposure of cultivated plants to gas used in lamps, which was produced from the partial combustion of coal.[5] Leakage of illuminating gas was common at the time, with the Illuminating Gas Company in Massachusetts reporting that only 90% of gas it made reaching customers.[5] It was later discovered by many combined efforts that ethylene, even in trace amounts, could cause several growth abnormalities.[6]

1.1.2 The Ethylene Receptor (ETR1)

The ethylene response in many plants is initiated by a group of 5 membrane bound receptors, mainly ETR1 (ethylene receptor 1).[8] While the exact nature of

ETR1 is not known, as early as 1967 Burg and Burg[9] realized that the ethylene receptor most likely contained a transitional metal, and speculated that it may be zinc.[9] Later research pointed to the likelihood of a group 11 transition metal such as copper due the strong binding nature of ethylene and copper(I).[1] Several metals, including cobalt, copper, iron, nickel, and zinc, have been screened by using ETR1 in yeast that has been exogenously expressed with these cofactors.[10] It was found that only the group 11 metals Cu(I), Ag(I), and Au(I) support ethylene binding in ETR1.[11] Additional support comes from evidence that shows that the ETR1 mutant etr1-1(1-128)GST cannot coordinate copper and fails to bind ethylene.[10]

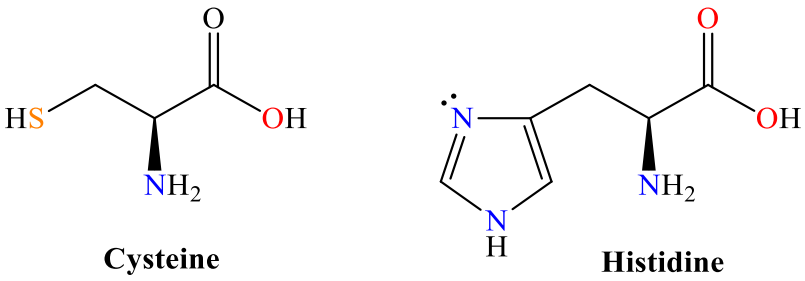

Figure 1.1. Structures of Cysteine and Histidine.

The ethylene receptors are homodimers linked at their N-termini by two disulfide bonds. Each of the monomer units is composed of three transmembrane α-helices followed by a GAF and kinase domain, and the copper ethylene binding site is located in the endoplasmic reticulum (ER).[12-13] Studies show that the copper

in ETR1 is housed in an electron rich hydrophobic pocket and structure-function studies have pointed to a putative ethylene-binding site in the transmembrane regions composed of from a copper ion ligated by essential cysteine and histidine residues (Figure 1.1).[10] Direct evidence has been shown histidine kinase activity in ETR1, and that cysteine is required as a cofactor for copper binding.[12, 14] These data give support that the active site may be a copper center chelated by nitrogen and/or sulfur based ligands.

1.1.3 Triggering the Ethylene Response in Plants

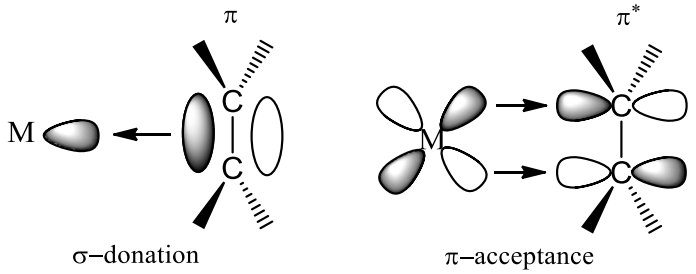

Figure 1.2. Dewar-Chatt-Duncanson model for metal-ethylene interaction.

It has been observed that a variety of π-acceptors induce the agonist, or decay, response similar to ethylene, however it is not well known exactly what is happening *in vivo*.[6] Ethylene, as well as other π-acceptors such as carbon monoxide, and isocyanides, can form a metal complex and back-accept electron density (Figure 1.2). All of these ligands induce the ethylene response, and it is thought that the backbonding from copper to the ligand initiates a change in the receptor due to

the *trans* effect. A three step process was proposed by Sisler, and Serek for the ethylene response (Figure 1.3, top).[15] The first step to initiating the agonist response must be the coordination of ethylene to the metal cite in the receptor. It is then speculated that the ligands associated with the metal center will go through a rearrangement due to the change in electron density and the π-acceptor is displaced. The displacement of ethylene is thought to be important to triggering the downfield signal. See a recent article by Mayerhofer et al. for a detailed discussion, including a crystal structure, of the cytosolic domain of ETR1.[8]

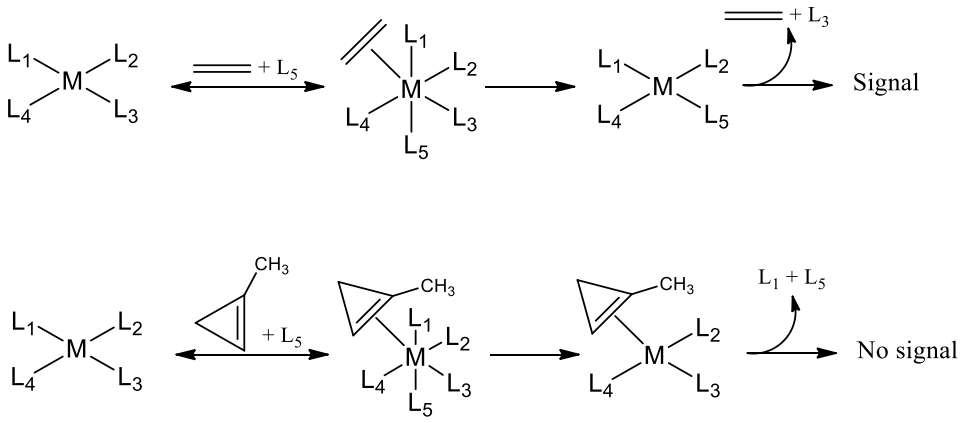

Figure 1.3. Possible sequence of events leading to the ethylene response (top) or signal blocking by 1-MCP (bottom). L_1, L_2, L_3, L_4, and L_5 are unknown chemical groups located on the protein.

1.1.4 Blocking the Ethylene Response in Plants

The ethylene response is commonly used in the agricultural industry to induce ripening, however preventing the response is equally important to prevent spoiling of crops due to ethylene-accelerated post-harvest ripening and deterioration as they travel from the farm to be sold. In 1996 Sisler and Blankenship received a patent for the use of cyclopropenes and its derivatives for the prevention of the ethylene response. Ultimately, 1-methylcyclopropene (1-MCP, Figure 1.4) was found the be the most effective.[16] Several other antagonists including silver thiosulfate (STS), 2,5-norbornadiene, strained alkenes, and several cyclopropenes have been examined for activity but so far no comparable antagonists have been reported.[7, 17] It is not known how antagonists react differently than agonist, however, it is speculated that antagonist form π-acceptor complexes, similar to those formed by ethylene, but are not easily displaced (Figure 1.3, bottom). There is other thought that suggests 1-MCP binds to the metal center and undergoes a ring opening reaction to form a reactive species that can damage the surrounding proteins of the receptor.[17]

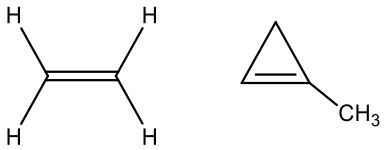

Figure 1.4. Ethylene and 1-Methylcyclopropene (1-MCP).

1-MCP (Figure 1.4) is currently the most widely used ethylene antagonist and is now commonly sold by the two American companies Floralife Inc. and ArgoFresh Inc. under the name EthylBloc® and SmartFresh™, respectively. The former is sold for applications in ornamental crops, and the ladder is sold for application on fresh produce. In both cases, these products are sold as powders with 1-MCP complexed with γ-cyclodextrin. When this powder is mixed with water or buffer solution, 1-MCP is released as a gas.[18]

It is not well known what happens when cyclopropene interacts with the copper site found in ETR1, although there is some speculation that the cyclopropene undergoes a ring opening reaction to form a carbene.[17] It is theorized that the long lasting protection against the ethylene response is due to permanent damage being caused by a reactive carbene species. The major driving force for this work is to further understand the interaction between cyclopropenes and the copper(I) active site, and ultimately to isolate a copper(I)-cyclopropene adduct.

Copper, silver, and gold have been shown to support the binding of ethylene in ETR1.[10] In fact, of the 11 metals tested for this function, only the coinage metals

exhibit the binding of ethylene. Interestingly, of these three, only silver is known to inhibit the ethylene action in ornamental crops.[19] Initially silver nitrate (AgNO3) was examined for anti-ethylene activity.[19] However, it was later found that AgNO3 had poor mobility in plant tissue and that silver thiosulfate (STS) was a more convenient ethylene inhibitor due to higher uptake and mobility in plant tissue.[20] STS is applied as a pretreatment to cut flowers by soaking the stems in a water solution containing STS. STS was the only commercially treatment used to protect ornamental crops against ethylene for many years, and is mandatory at flower auctions in the Netherlands.[21]

It has been suggested that Ag(I) ions can replace Cu(I) ions in the ETR1 binding pocket.[11] However, it is more likely that there are multiple metal binding sites on the receptors mediating the effects of ethylene bind and silver ions.[12] It appears that while silver ions support ethylene binding in the receptor, they prevent the secondary conformational change and prevent the signal transduction.[22] We have explored ethylene binding with the coinage metals in chapter 2 and have further explored silver adducts in chapter 3. Our results suggest show that copper and gold interact strongly with ethylene, whereas silver form only very weak interactions.

Over the past decades polymers have replaced conventional materials in food packaging applications and there are several examples of nanocomposite materials used for this application.[23] There has been recent interest in the

devolvement of storage devices that actively participate in the control of the properties of product and the surrounding environment. These materials include substances embedded in the matrix that interact either directly with the food or the surrounding environment by either releasing or absorbing substances.[23] For example, the antimicrobial activity of silver nanoparticles have dominated the idea of active packaging. The nanocomposite martials generally suffer from has permeability, but there is some thought that gold and silver nanoparticles could be used in food or flower storage containers to remove ethylene.[24]

1.2 Modeling the ETR1 Active site with Poly(pyrazolyl)borates

1.2.1 Poly(pyrazolyl)Borates

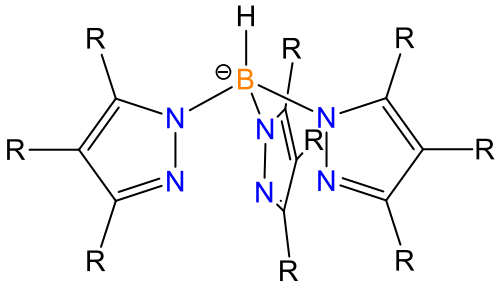

Figure 1.5. Generic Structure of Tris(pyrazolyl)borate (Tp).

Structure-function studies of ETR1 have suggested that the ethylene-binding site is composed from a copper ion ligated by cysteine and histidine residues.[10] There is also some though that the ligands may have tetrahedral

geometry around the metal center. Poly(pyrazolyl)borate ligands such as Tris(pyrazolyl)borate (Tp, Figure 1.5) have been proposed as a model for the ETR1 active site due their tetrahedral geometry around the metal center and the similarities between the histidine chelation sites found in ETR1, and the pyrazole moieties that make up Tp.[1] These are similar in that they are aromatic, five membered rings with two nitrogen atoms incorporated into the ring. Nitrogen is well known as a good σ-donor metal chelation site, and coinage complexes supported by nitrogen based ligands have been well explored in the literature. Copper(I) olefin complexes of poly(pyrazolyl)borates, particularly the ethylene adducts, are of great interest because they serve as models for copper based ethylene receptor sites in plants.[1, 10]

1.2.2 Tris(pyrazolyl)borates

Tp is a particularly attractive ligand because the steric and electronic properties of the ligands can be fine-tuned by changing the number and nature of the substituents on the pyrazolyl moieties and on the boron and thereby modulate the reactivity of the bound metal center. These monoanionic ligands generally form tridentate complexes bound facially through three N σ-donors in C_{3v} geometry.[25] A lot of attention has been paid to Tp ligands decorated with electron withdrawing groups such as F, Br, and NO_2, because these complexes are typically robust and tend to have quite reactive metal centers useful for applications in catalysis.[26-28] The

electron rich analogs are much less explored, perhaps because they do not share the tendency to be robust, but instead tend to be vulnerable to metal oxidation.[1]

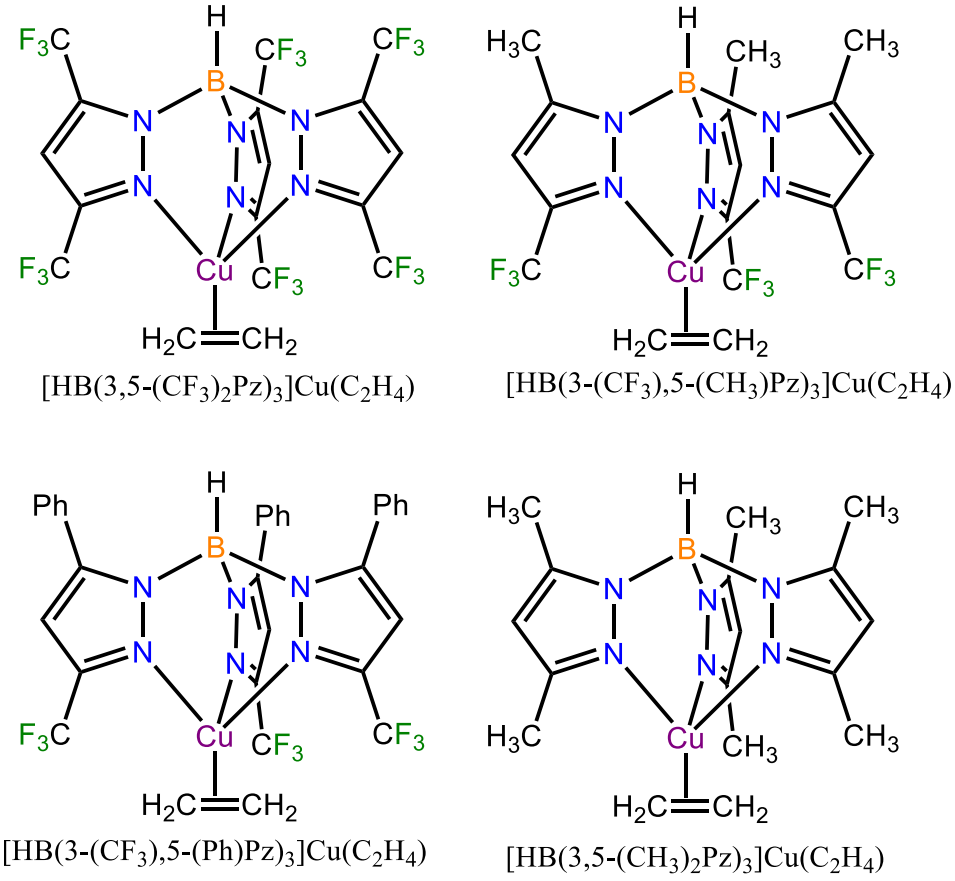

Figure 1.6. Structures of $[HB(3,5\text{-}(CF_3)_2Pz)_3]Cu(C_2H_4)$, $[HB(3\text{-}(CF_3),5\text{-}(CH_3)Pz)_3]Cu(C_2H_4)$, $[HB(3\text{-}(CF_3),5\text{-}(Ph)Pz)_3]Cu(C_2H_4)$, and $[HB(3,5\text{-}(CH_3)_2Pz)_3]Cu(C_2H_4)$.

It has been reported that the copper center in ETR1 sits in an electron rich hydrophobic pocket, and cysteine and histidine do not contain any highly electron withdrawing groups.[10] Based on this information, the copper site in ETR1 is probably more similar to the copper adducts of electron rich ligands, such as $[HB(3,5\text{-}(CH_3)_2Pz)_3]^-$, or $[HB(3,5\text{-}(^iPr)_2Pz)_3]^-$ (Pz = pyrazolyl). However, the stability of these complexes is extremely limiting in our experience. For this purpose we have explored Tp varieties that bridge the gap between the electron rich and electron poor ligands (Figure 1.6). We have synthesized the ethylene adducts $[HB(3\text{-}(CF_3),5\text{-}(CH_3)Pz)_3]M(C_2H_4)$ (where M = Cu, Ag, Au) and the silver adducts $[HB(3\text{-}(CF_3),5\text{-}(Ph)Pz)_3]CuL$ (where L = C_6H_6, CO, and PPh_3). Further details about these studies are covered in the subsequent chapters found herein.

1.2.3 Bis(pyrazolyl)borates and bis(pyrazolyl)methane

Ethylene inhibition studies using long chain cyclopropenes (1-decylcyclopropene, 1-nonylcyclopropene, 1-octylcyclopropene), and larger alkenes (1-dodecene, 1-decene, 1-octene, 1-hexene, 1-pentene, 1-butene) have shown that the active site of the ethylene receptor is not restrictive to these large branched alkenes.[6] A known sulfur-ligated Cu(I)-ethylene complex exhibits very weak Cu-S interaction with a Cu-S bond distance of 2.30 Å. So, it is possible that the cysteine residues form disulfide bonds in situ, rather than coordinating to the copper metal center, and only the histidine residues may chelate the metal.[6, 29] A bis(pyrazolyl)borate may therefore be a closer model for the active site in ETR1.

The closely related bis(pyrazolyl)borates (Bp) (

Figure 1.7) are known and have been moderately explored.[30-32] These ligands are similar to Tp in that they carry a formal negative charge, but they are bidentate, rather than tridentate, and bind in κ^2 fashion. Similarly to Tp, the substituents of the pyrazole moieties can be used to tune the properties of the chelated metal ion. While several copper ethylene complexes are known with tris(pyrazolyl)borates (including their heavier silver and gold counterparts), very few examples of copper-olefin adducts have been reported stabilized by the bidentate bis(pyrazolyl)borate system.[32-34] The fluorinated bis(pyrazolyl)borate complex $[H_2B(3,5\text{-}(CF_3)_2Pz)_2]Cu(PhCH{=}CH_2)$ has been previously reported and is the most relevant alkene adduct of this type.[32]

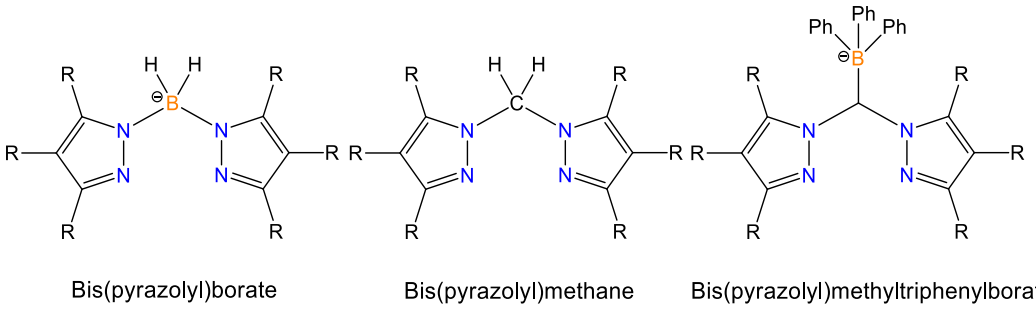

Figure 1.7. General structures of the bidentate ligands bis(pyrazolyl)borate, bis(pyrazolyl)methane, and bis(pyrazolyl)methyltriphenylborate.

The similar bidentate ligand bis(pyrazolyl)methane (

Figure 1.7) is known, and while it is similar in structure to Bp, it does not carry the formal negative charge. These ligands eliminate the sometimes problematic B-H backbone, do not carry a formal negative charge and require counter ions to balance the change of the metal ion. We have synthesized bis(pyrazolyl)methyltriphenylborate (

Figure 1.7), which is based on bis(pyrazolyl)methane, but carries a formal negative charge. Specifically we have synthesized the methylated ligand $[(Ph_3B)CH(3,5\text{-}(CH_3)_2Pz)_2)]Li$ and isolated bidentate copper(I)-olefin complexes, including the ethylene adduct $[(Ph_3B)CH(3,5\text{-}(CH_3)_2Pz)_2)]Cu(C_2H_4)$. Further details can be found in the related chapter herein.

1.3 Research Objectives and Organization

This dissertation focuses on the development of new models of the ethylene receptor found in plants (ETR1) in order to gain further understanding of how ethylene interacts with the active site of ETR1. Each chapter consists of a published manuscript or a manuscript in preparation for submission. The writer of this dissertation has performed the majority of the synthesis and characterization experiments (NMR, IR, Raman, single crystal growth) included in each chapter, and participated in the writing, preparation, and editing of each manuscript. As a co-author of Chapter 2, Dr. Jiang Wu provided the original preparation of [HB(3-(CF_3),5-(CH_3)Pz)$_3$]Au(C_2H_4). The co-author Dr. Naveen Kulkarni provided ligand samples and contributed to the editing of Chapter 2 and Chapter 3. He also provided the original preparation of [(Ph_3B)CH(3,5-(CH_3)$_2$Pz)$_2$]Li·THF in Chapter 4. Prof. Rasika Dias is the principal investigator. He has contributed the collection and crystal structure determination for all of the reported structures, and to the writing and editing of each manuscript. We have chosen to only include completed works for the purpose of confidentiality.

Chapter 1 gives an introduction to ethylene chemistry, and its importance to the agricultural industry. The later part of this chapter gives the known details about the ethylene receptor ETR1 and how polyl(pyrazolyl) ligands may serve as models for the active site in the receptor.

Chapter 2, describes four new coinage metal (Cu, Ag, and Au) ethylene complexes we have synthesized. The complexes reported in this chapter are supported by $[HB(3\text{-}(CF_3),5\text{-}(CH_3)Pz)_3]^-$, and by $[HB(3\text{-}(CF_3),5\text{-}(Ph)Pz)_3]^-$. These ligands help to fill a broad gap in the literature moving from the highly electron deficient coinage metal ethylene complexes and the electron rich adducts. We have reported the characterization of these complexes by NMR spectroscopy and X-ray crystallography. The reported data shows remarkably different characteristics for these complexes, including a trigonal planar Au(I)-ethylene adduct supported by tris(pyrazolyl)borate.

In chapter 3 we have reported three new silver adducts of benzene, carbon monoxide (CO), and triphenylphosphine (PPh_3). These silver(I) complexes are supported by the tris(pyrazolyl)borate $[HB(3\text{-}(CF_3),5\text{-}(Ph)Pz)_3]^-$ and have been characterized by NMR spectroscopy, and by X-ray crystallography. These adducts help to extend the understanding of the interactions between silver(I) and π-acceptors. The benzene adduct is bound in an η^2-bound fashion and the NMR data point to fluxional behavior in solution. The CO adduct reported here exhibits non-classical behavior with a nearly unchanged carbonyl stretch observed by infrared. Interesting F-P coupling is observed for the PPh_3 complex by solution NMR. This chapter contains a detailed analysis of the spectral and structural features of these complexes.

Chapter 4 describes the synthesis and characterization of a brand new bis(pyrazolyl)methyltriphenylborate ligand and three copper complexes. The ligand has the formula $[(Ph_3B)CH(3,5\text{-}(CH_3)_2Pz)_2)]^-$ and serves as a model for a bidentate N-donor based ethylene receptor. This ligand has been used to isolate the complexes $[(Ph_3B)CH(3,5\text{-}(CH_3)_2Pz)_2)]Cu(L)$ (L = ethylene, *cis*-2-butene, and CO). The ethylene adduct reported in this chapter is the first Cu(I)-ethylene adduct supported by a bis(pyrazolyl) based ligand. The *cis*-2-butene adduct helps to probe the steric tolerance of the ligand and extends the known olefin adducts closer to a cyclopropene, (i.e. *cis*-2-butene is similar to an "opened" cyclopropene). Finally, the CO adduct helps to probe the interaction between the ligand and copper(I), and thereby the electron donating ability of the chelated copper center.

Complete experimental and characterization details have been given in chapter 5. A chapter summary is given in the final chapter, chapter 6. The appendices that follow the final chapter present spectral data (Appendix A), and X-ray characterization data (Appendix B) for all new complexes reported in this dissertation.

Chapter 2

Isolable Ethylene Complexes of Copper(I), Silver(I), and Gold(I) Supported by Fluorinated Scorpionates $[HB(3\text{-}(CF_3),5\text{-}(CH_3)Pz)_3]^-$ and $[HB(3\text{-}(CF_3),5\text{-}(Ph)Pz)_3]^-$

Shawn G. Ridlen, Jiang Wu, Naveen V. Kulkarni, and H. V. Rasika Dias*

This work has been published in Eur. J. Inorg. Chem., **2016,** 15-16, 2573-2580[a]

[a] Used with permission of the publisher, 2016

2.1 Abstract

The group 11 metal adducts $[HB(3\text{-}(CF_3),5\text{-}(CH_3)Pz)_3]M(C_2H_4)$ (M = Au, Ag, and Cu; Pz = pyrazolyl) have been synthesized via a metathesis process using $[HB(3\text{-}(CF_3),5\text{-}(CH_3)Pz)_3]Na$ and CF_3SO_3Cu, CF_3SO_3Ag, AuCl and ethylene. The related $[HB(3\text{-}(CF_3),5\text{-}(Ph)Pz)_3]Ag(C_2H_4)$ has also been synthesized using $[HB(3\text{-}(CF_3),5\text{-}(Ph)Pz)_3]Na(THF)$, CF_3SO_3Ag and ethylene. These group 11 metal ethylene complexes are white solids and form colorless crystals. They have been characterized by NMR spectroscopy and X-ray crystallography. The gold-ethylene adduct $[HB(3\text{-}(CF_3),5\text{-}(CH_3)Pz)_3]Au(C_2H_4)$ shows large upfield NMR shifts of the ethylene proton and carbon signals relative to the corresponding peaks of the free ethylene, indicating relatively high Au→ethylene backbonding. NMR chemical shift data suggest that the silver complexes of both the tris(pyrazolyl)borate ligands $[HB(3\text{-}(CF_3),5\text{-}(CH_3)Pz)_3]^-$ and $[HB(3\text{-}(CF_3),5\text{-}(Ph)Pz)_3]^-$ exhibit the weakest interaction with ethylene as compared to the respective copper and gold complexes. X-ray crystal structures reveal that the gold atom in $[HB(3\text{-}(CF_3),5\text{-}(CH_3)Pz)_3]Au(C_2H_4)$ binds to scorpionate in κ^2-fashion while the related silver adduct features a κ^3-bonded scorpionate. $[HB(3\text{-}(CF_3),5\text{-}(CH_3)Pz)_3]Cu(C_2H_4)$ has a scorpionate that binds to copper in essentially κ^2-mode with two short Cu-N bonds and one long Cu-N distance.

2.2 Introduction

Tris(pyrazolyl)borates, which belong to a class of ligands generally referred to as Scorpionates, are excellent, mono-anionic, nitrogen based supporting ligands for most metals of the Periodic Table including d-block elements.[35-39] They are particularly useful because of the ease with which the steric and electronic properties can be modified by varying the substituents on the pyrazolyl moieties and on the boron atom. Our research activities in the field of Scorpionates are mainly focused on the development and applications of fluorinated ligand versions of poly(pyrazolyl)borates[31, 33, 40-43] and other azolyl analogs like tris(triazolyl)borates.[44-45] For example, we have reported the synthesis of [HB(3-(CF_3)Pz)$_3$]$^-$,[41] [HB(3,5-$(CF_3)_2$Pz)$_3$]$^-$,[40-41] [HB(3,4,5-$(CF_3)_3$Pz)$_3$]$^-$,[46] [HB(3,5-$(CF_3)_2$,4-(Cl)Pz)$_3$]$^-$,[28] [HB(3,5-$(CF_3)_2$,4-(NO_2)Pz)$_3$]$^-$,[28] as well as the B-alkylated and B-arylated systems like [MeB(3-(CF_3)Pz)$_3$]$^-$ and [PhB(3-(CF_3)Pz)$_3$]$^-$ (Figure 2.1).[47-48] Tris(pyrazolyl)borate ligands such as [HB(3-(C_3F_7)Pz)$_3$]$^-$ and [PhB(3-(C_2F_5)Pz)$_3$]$^-$ with longer fluoroalkyl substituents are also known.[49-51]

Fluorinated tris(pyrazolyl)borates like [HB(3,5-$(CF_3)_2$Pz)$_3$]$^-$ are significantly weaker donors compared to hydrocarbon counterparts like [HB(3,5-$(CH_3)_2$Pz)$_3$]$^-$.[52] Metal adducts of fluorinated tris(pyrazolyl)borates feature more electrophilic metal sites and display greater catalytic activity in certain reactions like in the C-H and C-halogen bond functionalization chemistry via carbene insertion, compared to the non-fluorinated, electron rich tris(pyrazolyl)borate

analogs.[26-28, 53-58] There are several additional applications involving fluorinated tris(pyrazolyl)borates as well (e.g., model active sites of enzymes and to develop catalysts to mediate other processes like oxidation).[59-68] Fluorinated ligands like $[HB(3,5\text{-}(CF_3)_2Pz)_3]^-$ have also permitted us to isolate a range of rare group 11 metal adducts (e.g., involving CO,[69-71] *1*-azidoadamantane,[72] ethylene oxide,[73] propylene sulfide,[73] dimethyl diazomalonate,[74] Sn(II) and Ge(II) species[75-76]), as well as to prepare compounds with good antimicrobial properties.[77-78] $[HB(3,5\text{-}(CF_3)_2Pz)_3]CuCO$ shows relatively high oxidative stability compared to $[HB(3,5\text{-}(CH_3)_2Pz)_3]CuCO$. The carbonyl stretching frequency of $[HB(3,5\text{-}(CF_3)_2Pz)_3]CuCO$ appears at 2137 cm^{-1}, which is very close to that of the free CO (2143 cm^{-1}) and about 71 cm^{-1} higher than that of $[HB(3,5\text{-}(CH_3)_2Pz)_3]CuCO$.[70, 79] Related silver(I) adduct $[HB(3,5\text{-}(CF_3)_2Pz)_3]AgCO$ displays its carbonyl stretching frequency at 2178 cm^{-1}, which is even higher than that of the free CO.[69, 80]

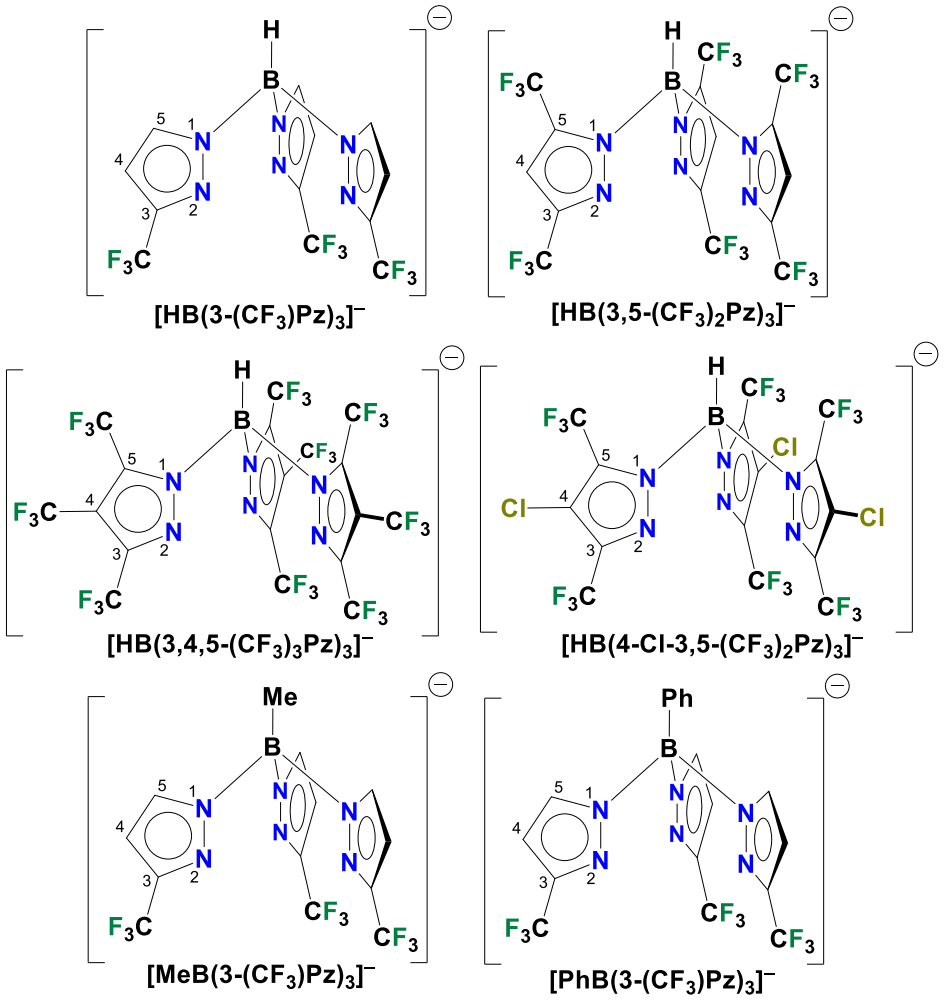

Figure 2.1 Several examples of fluorinated tris(pyrazolyl)borate ligands

Tris(pyrazolyl)borates have played a crucial role in group 11 metal (Cu, Ag, Au) ethylene chemistry. For example, the first structurally authenticated ethylene adducts of copper, $[HB(3,5\text{-}(CH_3)_2Pz)_3]Cu(C_2H_4)$,[1] silver, $[HB(3,5\text{-}(CF_3)_2Pz)_3]Ag(C_2H_4)$,[80] and gold, $[HB(3,5\text{-}(CF_3)_2Pz)_3]Au(C_2H_4)$[81] involve the use of tris(pyrazolyl)borate supporting ligands.[33, 82-85] Fluorinated ligand analog of the

copper-ethylene adduct $[HB(3,5\text{-}(CF_3)_2Pz)_3]Cu(C_2H_4)$ is also known.[65] Such isolable complexes are of significant interest as models for likely intermediates in biochemical[1, 10, 86-91] and industrial and laboratory processes[92-100] involving group 11 metals and ethylene or alkenes. For example, ethylene is an important plant hormone and the ethylene receptor site in plants is believed to be a copper center.[10, 91] Partial oxidation of ethylene to ethylene oxide is a major industrial process and silver is the catalyst of choice.[101-104] Gold is an excellent catalyst for the selective epoxidation of propene and other alkenes.[105-107] Group 11 metal ethylene adducts supported by scorpionates have also been used in other applications such as in catalysis and sensor development.[56, 59, 65]

In this paper, we describe the use of $[HB(3\text{-}(CF_3),5\text{-}(CH_3)Pz)_3]^-$ ligand in copper, silver and gold ethylene chemistry as well as the related metal-ethylene adduct of $[HB(3\text{-}(CF_3),5\text{-}(Ph)Pz)_3]^-$ (Figure 2.2). Group trends of the two isoleptic coinage metal-ethylene adduct series $[HB(3\text{-}(CF_3),5\text{-}(CH_3)Pz)_3]M(C_2H_4)$ and $[HB(3\text{-}(CF_3),5\text{-}(Ph)Pz)_3]M(C_2H_4)$ (M = Cu, Ag, Au) are also described.

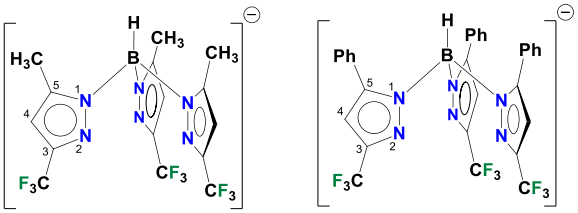

Figure 2.2 Fluorinated tris(pyrazolyl)borate ligands $[HB(3\text{-}(CF_3),5\text{-}(CH_3)Pz)_3]^-$ and $[HB(3\text{-}(CF_3),5\text{-}(Ph)Pz)_3]^-$

2.3 Results and Discussion

The copper(I) adduct $[HB(3\text{-}(CF_3),5\text{-}(CH_3)Pz)_3]Cu(C_2H_4)$ was obtained by treating $[HB(3\text{-}(CF_3),5\text{-}(CH_3)Pz)_3]Na$[108] with CF_3SO_3Cu in THF in the presence of excess ethylene. The analogous Ag(I) and Au(I) adducts $[HB(3\text{-}(CF_3),5\text{-}(CH_3)Pz)_3]Ag(C_2H_4)$ and $[HB(3\text{-}(CF_3),5\text{-}(CH_3)Pz)_3]Au(C_2H_4)$ can also be prepared via a metathesis process using CF_3SO_3Ag in dichloromethane and AuCl in hexane, respectively. These group 11 metal ethylene complexes are white solids and form colorless crystals. Solid samples of $[HB(3\text{-}(CF_3),5\text{-}(Me)Pz)_3]Cu(C_2H_4)$, and $[HB(3\text{-}(CF_3),5\text{-}(Me)Pz)_3]Au(C_2H_4)$ can be exposed to air and indoor lighting for several days without obvious signs of decomposition. Similarly, solid samples of $[HB(3\text{-}(CF_3),5\text{-}(Me)Pz)_3]Ag(C_2H_4)$ can be handled in air for short periods, but decompose after several hours of exposure. In all cases, solid samples of these compounds do not lose ethylene under reduced pressure. Silver and gold adducts show greater solution stability in hexanes compared to chlorinated solvents like dichloromethane.

X-ray analysis of $[HB(3\text{-}(CF_3),5\text{-}(CH_3)Pz)_3]M(C_2H_4)$ (M = Au, Ag, Cu; Table 2.1) revealed that all three coinage metal adducts crystallize in the $P\overline{3}$ space group with crystallographically imposed three fold axis of symmetry containing the B-H group (Figure 2.3, Figure 2.4, Figure 2.5). The $M(C_2H_4)$ moiety sits very close to but slightly away from the three fold axis. As a result, $M(C_2H_4)$ unit is disordered

over three symmetry related sites with equal occupancy. Although we have modeled this disorder satisfactorily, the metrical parameters at M(C_2H_4) should be treated with due caution and are not suitable for detailed bond distance and angle comparisons. Nevertheless, X-ray data show the formation of [HB(3-(CF_3),5-(CH_3)Pz)$_3$]M(C_2H_4) adducts with η^2-bound ethylene molecules. The gold center in [HB(3-(CF_3),5-(CH_3)Pz)$_3$]Au(C_2H_4) adopts a trigonal planar geometry with κ^2-bound scorpionate (Au-N distances of 2.214, 2.247, and long 2.727 Å), while [HB(3-(CF_3),5-(CH_3)Pz)$_3$]Ag(C_2H_4) has a distorted tetrahedral silver atom and κ^3-bound scorpionate (Ag-N distances of 2.222, 2.383, 2.375 Å). The [HB(3-(CF_3),5-(CH_3)Pz)$_3$]Cu(C_2H_4) structure is much closer to that of the gold analog (Cu-N distances of 2.024, 2.040, and long 2.279 Å) with an essentially trigonal planar copper site (sum of angles at copper = 352°). In the absence of other interfering factors like steric constrains (e.g., imposed by the substituents on boron), the κ^2 vs κ^3 bonding of scorpionates in group 11 metal ethylene adducts can be attributable principally to covalent vs. ionic metal-ligand bonding, with the latter type is reflected in symmetrically and κ^3-bound scorpionates and feature close to T-shaped metal-ethylene interaction (rather than metal-ethylene bonding closer to metallacyclopropane regime, with significant σ-bonding and π-backbonding between M and C_2H_4).[82, 109] Computational studies and M-ethylene bond strength data of various related and unrelated group 11 metal ethylene systems indicate that

Au(I) forms the strongest bond with ethylene while Ag(I) forms the weakest bond.[109-113] Indeed, the C=C bond distances of $[HB(3\text{-}(CF_3),5\text{-}(CH_3)Pz)_3]M(C_2H_4)$ adducts in general (despite the uncertainties caused by $M(C_2H_4)$ moiety disorder) show an increase in the order of Ag < Cu < Au, and are in good agreement with bond strength based prediction. In addition, the solution NMR chemical shifts of these compounds (especially ^{13}C NMR values for the ethylene moiety; see Table 2.2) are also consistent with the bonding features reflected in solid state structural data. The Cu-N < Au-N < Ag-N bond distance trend in $[HB(3\text{-}(CF_3),5\text{-}(CH_3)Pz)_3]M(C_2H_4)$ adducts follow the sizes of covalent radii, as silver is the largest atom and copper is the smallest among group 11 metals[114] (e.g., covalent radii of two-coordinate copper(I), gold(I), and silver(I) are 1.13, 1.25, and 1.33 Å, respectively).[115-117] The M-C bond distances also follow the same pattern. It is interesting to note that in addition to κ^2 and κ^3 bonding of scorpionates noted above, distorted κ^1-bonding has also been observed in scorpionate adducts of group 11 like $[HB(3,5\text{-}(CF_3)_2Pz)_3]Au(CN^tBu)$.[71]

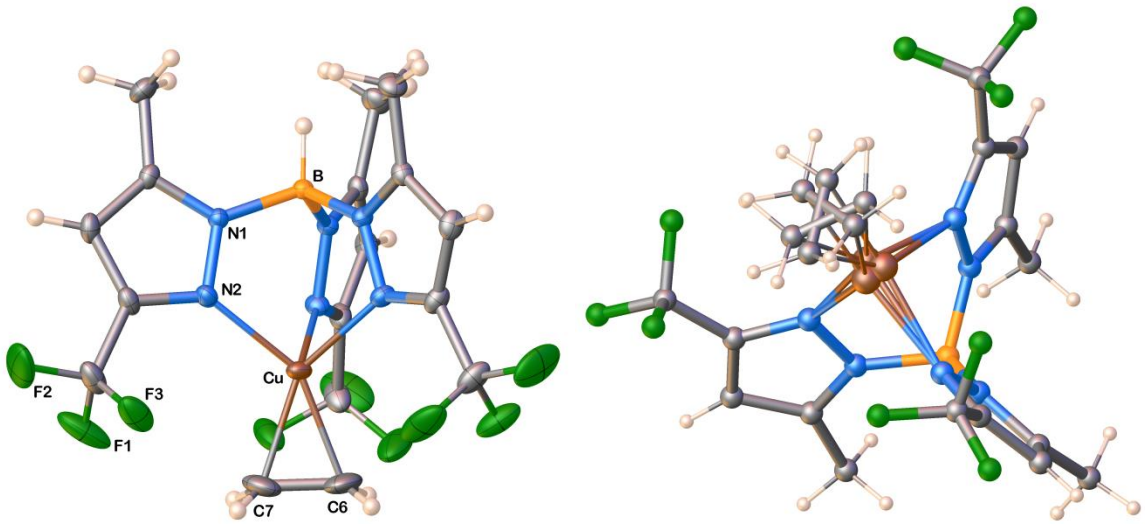

Figure 2.3 ORTEP diagram of [HB(3-(CF_3),5-(CH_3)Pz)$_3$]Cu(C_2H_4) (thermal ellipsoids set at 50% probability) and a view showing the disordered copper-ethylene moiety.

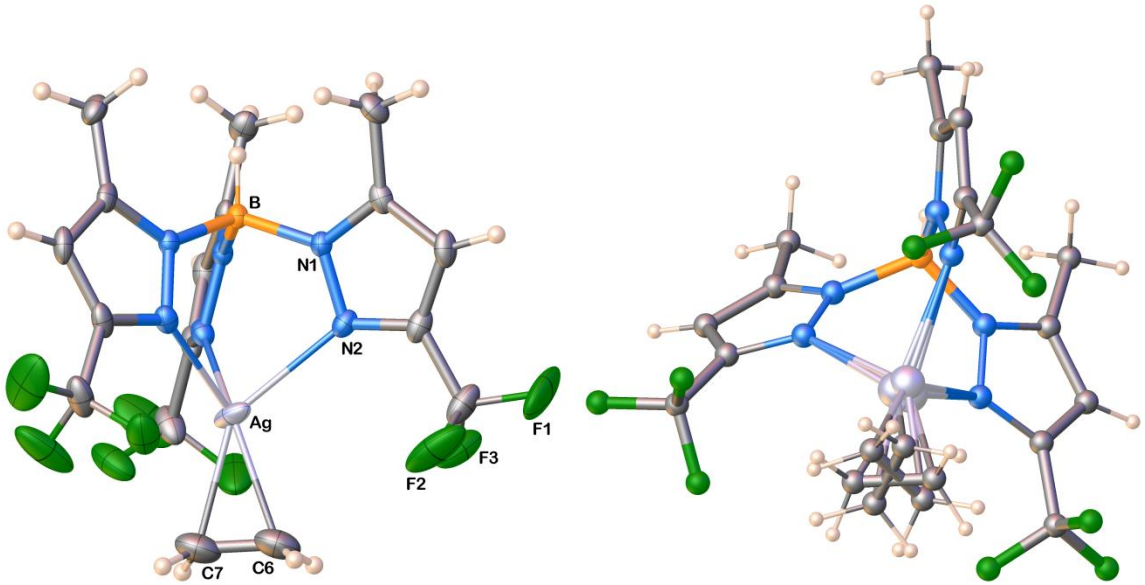

Figure 2.4 ORTEP diagram of [HB(3-(CF_3),5-(CH_3)Pz)$_3$]Ag(C_2H_4) (thermal ellipsoids set at 50% probability) and a view showing the disordered silver-ethylene moiety.

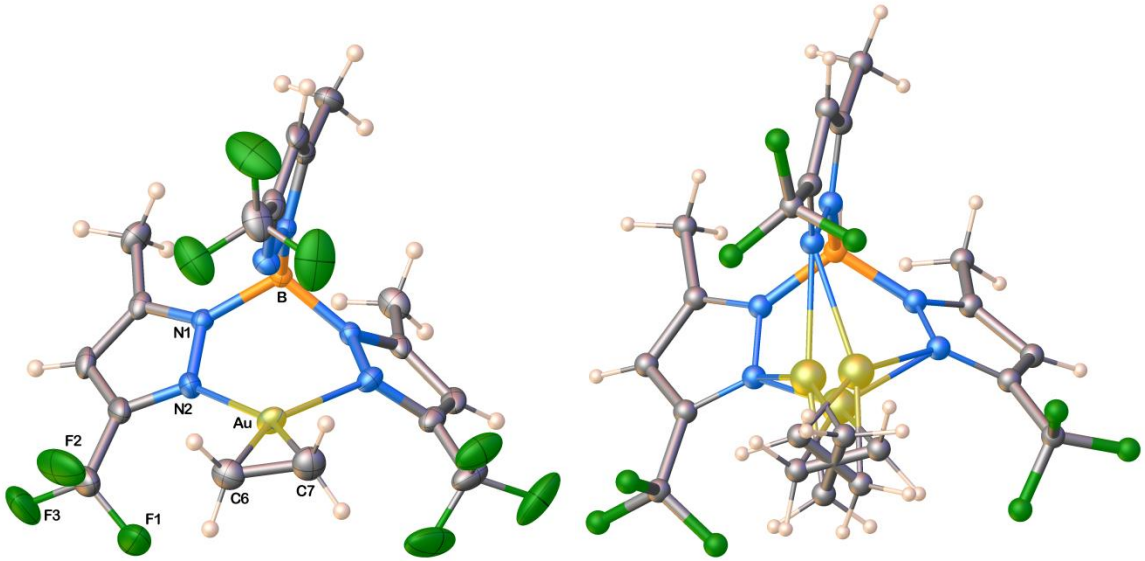

Figure 2.5 ORTEP diagram of [HB(3-(CF_3),5-(CH_3)Pz)$_3$]Au(C_2H_4) (thermal ellipsoids set at 30% probability) and a view showing the disordered gold-ethylene moiety.

.

We have synthesized the silver(I) ethylene adduct [HB(3-(CF_3),5-(Ph)Pz)$_3$]Ag(C_2H_4) using [HB(3-(CF_3),5-(Ph)Pz)$_3$]Na(THF),[79] CF_3SO_3Ag and ethylene. It is a white solid. X-ray crystal structure of [HB(3-(CF_3),5-(Ph)Pz)$_3$]Ag(C_2H_4) shows that it features a κ^3-bonded tris(pyrazolyl)borate and a pseudo-tetrahedral silver site (Figure 2.6). Unfortunately, the Ag(C_2H_4) moiety sits on two different sites at 46% and 54% occupancy, and is disordered. Although we have modeled this disorder satisfactorily, the metrical parameters of Ag(C_2H_4) are not ideal for detailed comparison of bond distances and angles. [HB(3-(CF_3),5-(Ph)Pz)$_3$]Ag(C_2H_4) is the missing member of isoleptic [HB(3-(CF_3),5-(Ph)Pz)$_3$]M(C_2H_4) series as we have reported the copper[65] and gold[81] adducts in previously. [HB(3-(CF_3),5-(Ph)Pz)$_3$]Au(C_2H_4) has a κ^2-bonded scorpionate just like the [HB(3-(CF_3),5-(CH_3)Pz)$_3$]Au(C_2H_4) adduct. The copper adduct [HB(3-(CF_3),5-(Ph)Pz)$_3$]Cu(C_2H_4) in contrast features a pseudo-tetrahedral copper site, and shows disorder at ethylene moiety.

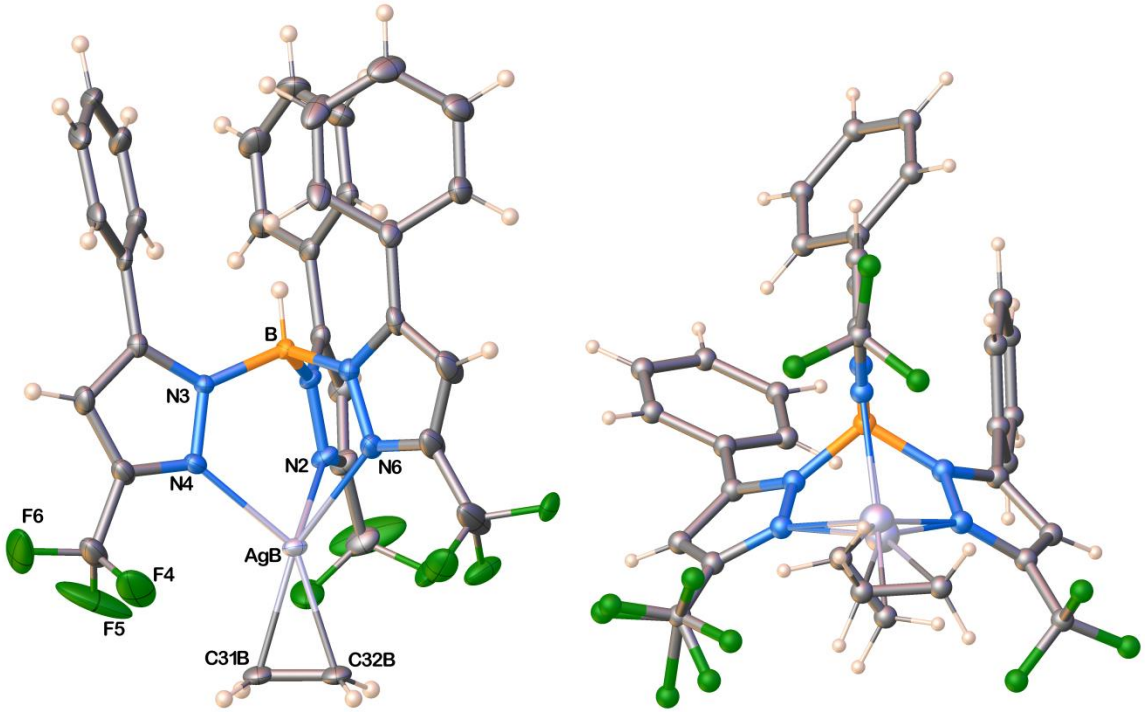

Figure 2.6 ORTEP diagram of [HB(3-(CF_3),5-(Ph)Pz)$_3$]Ag(C_2H_4) (thermal ellipsoids set at 50% probability) and a view showing the disordered silver-ethylene moiety.

`

^{1}H NMR signal corresponding to the coordinated ethylene of [HB(3-(CF_3),5-(CH_3)Pz)$_3$]Cu(C_2H_4) in $CDCl_3$ appears at δ = 4.71 ppm (Table 2.2), while the related silver and gold analogs display this peak at δ = 5.45 and 3.47 ppm, respectively. For comparison, [HB(3,5-(CH_3)$_2$Pz)$_3$]Cu(C_2H_4) and [HB(3,5-(CF_3)$_2$Pz)$_3$]Cu(C_2H_4) ethylene proton signals have been observed at δ 4.41 and 4.96 ppm, respectively. It appears that the upfield shift of ethylene proton signal follows the relative donor-properties of the scorpionate ligand on copper(I).[52, 79] The copper supported by electron rich [HB(3,5-(CH_3)$_2$Pz)$_3$]$^-$ shields the ethylene protons most while the Lewis acidic [HB(3,5-(CF_3)$_2$Pz)$_3$]Cu moiety provides the least amount of shielding. In the isoleptic [HB(3-(CF_3),5-(CH_3)Pz)$_3$]M(C_2H_4) series (M = Cu, Ag, Au), the gold adduct shows the largest upfield shift of the ethylene proton signal from that of free ethylene protons (δ = 5.40 ppm in $CDCl_3$) followed by the copper adduct, while silver adduct shows a small downfield shift. The ^{13}C NMR resonance of the metal bound ethylene carbon of [HB(3-(CF_3),5-(CH_3)Pz)$_3$]M(C_2H_4) appear at δ = 84.8, 103.5, and 58.3 ppm, respectively for M = Cu, Ag, and Au. The upfield shift of the carbon resonance in the gold adduct relative to that of free ethylene (δ = 123.5 ppm) is particularly large. For example, Δδ(C) (where $\Delta\delta(C) = \delta(C)_{complex} - \delta(C)_{ethylene}$) for these Au, Ag, and Cu adducts are −39, −20, −65 ppm, respectively. The upfield shift of the ^{13}C and ^{1}H NMR resonance of ethylene signal has been attributed to the increased metal-to-ethylene π-back-donation contribution.[109, 118-120] Overall, these NMR data point to a significantly higher π-back-donation

component in the gold(I)–ethylene bond than in the lighter members, and are in good agreement with the latest computational work and structural features observed above.

^{1}H and ^{13}C NMR spectra of $[HB(3\text{-}(CF_3),5\text{-}(Ph)Pz)_3]Ag(C_2H_4)$ in CD_2Cl_2 exhibited the resonance attributable to ethylene protons and carbons at δ = 5.56 and 104.0 ppm, respectively. As evident from the data presented in Table 2.2, $[HB(3\text{-}(CF_3),5\text{-}(Ph)Pz)_3]M(C_2H_4)$ adducts also follow trends similar to that of the $[HB(3\text{-}(CF_3),5\text{-}(CH_3)Pz)_3]M(C_2H_4)$ series.

2.4 Conclusions

In summary, we have reported the isolation and characterization of a series of thermally stable, isoleptic group 11 metal–ethylene adducts, $[HB(3\text{-}(CF_3),5\text{-}(CH_3)Pz)_3]M(C_2H_4)$ (M = Au, Ag, and Cu). The related $[HB(3\text{-}(CF_3),5\text{-}(Ph)Pz)_3]Ag(C_2H_4)$ has also been isolated completing a second set of isoleptic group 11 metal ethylene adducts. The gold atoms bind to scorpionates in κ^2-fashion while silver feature essentially κ^3-bonded scorpionates. $[HB(3\text{-}(CF_3),5\text{-}(CH_3)Pz)_3]Cu(C_2H_4)$ shows scorpionate coordination approaching the κ^2-mode. Unfortunately, $M(C_2H_4)$ fragments in $[HB(3\text{-}(CF_3),5\text{-}(CH_3)Pz)_3]M(C_2H_4)$ (M = Au, Ag, and Cu) and $[HB(3\text{-}(CF_3),5\text{-}(Ph)Pz)_3]Ag(C_2H_4)$ are disordered. Nevertheless, M-C and M-N distances of the $[HB(3\text{-}(CF_3),5\text{-}(CH_3)Pz)_3]M(C_2H_4)$ and $[HB(3\text{-}(CF_3),5\text{-}(Ph)Pz)_3]M(C_2H_4)$ complexes show that they follow the same trend as the covalent radii of M(I). The gold-ethylene adducts $[HB(3\text{-}(CF_3),5\text{-}$

$(CH_3)Pz)_3]Au(C_2H_4)$ and $[HB(3\text{-}(CF_3),5\text{-}(Ph)Pz)_3]Au(C_2H_4)$ show large upfield NMR shifts of the ethylene proton and carbon signals, indicating relatively high Au→ethylene backbonding. NMR data suggest that silver complexes of both the tris(pyrazolyl)borate ligands $[HB(3\text{-}(CF_3),5\text{-}(CH_3)Pz)_3]^-$ and $[HB(3\text{-}(CF_3),5\text{-}(Ph)Pz)_3]^-$ exhibit the weakest interaction with ethylene as compared to the respective copper and gold complexes.

2.5 X-ray crystallographic data

A suitable crystal covered with a layer of hydrocarbon/paratone-N oil was selected and mounted on a Cryo-loop, and immediately placed in the low temperature nitrogen stream. The X-ray intensity data for $[HB(3\text{-}(CF_3),5\text{-}(CH_3)Pz)_3]Cu(C_2H_4)$, $[HB(3\text{-}(CF_3),5\text{-}(CH_3)Pz)_3]Ag(C_2H_4)$ and $[HB(3\text{-}(CF_3),5\text{-}(Ph)Pz)_3]Ag(C_2H_4)$ were measured at 100(2) K on a Bruker D8 Quest with a Photon 100 CMOS detector equipped with an Oxford Cryosystems 700 series cooler, a Triumph monochromator, and a Mo Kα fine-focus sealed tube (λ = 0.71073 Å). X-ray intensity data for $[HB(3\text{-}(CF_3),5\text{-}(CH_3)Pz)_3]Au(C_2H_4)$ were measured at 188(2) K (because crystals crack at 100 K) on a SMART APEX II CCD area detector system equipped with an Oxford Cryosystems 700 series cooler, a graphite monochromator, and a Mo Kα fine-focus sealed tube (λ = 0.71073 Å). Intensity data were processed using the Bruker ApexII program suite. All the calculations for the structure determination were carried out using the SHELXTL package (version 6.14). Initial atomic positions were located by direct methods using XS,

and the structures of the compounds were refined by the least-squares method using SHELXL.[121] Absorption corrections were applied by using SADABS. All the non-hydrogen atoms were refined anisotropically. X-ray structural figures were generated using Olex2.[122] Further details are given in Table 2.1. The CCDC 1437975-1437978 contain the supplementary crystallographic data. These data can be obtained free of charge *via* http://www.ccdc.cam.ac.uk/conts/retrieving.html or from the Cambridge Crystallographic Data Centre (CCDC), 12 Union Road, Cambridge, CB2 1EZ, UK).

All three coinage metal compounds $[HB(3\text{-}(CF_3),5\text{-}(CH_3)Pz)_3]M(C_2H_4)$ (M = Cu, Ag, Au) crystallize in the $P\bar{3}$ space group with crystallographically imposed three fold axis of symmetry containing B-H moiety (for a Z value of 2). Unfortunately, M-ethylene fragment lies slightly off three-fold axis in these adducts, and therefore is disordered equally over three symmetry related positions. The disordered M-ethylene units in these adducts were modeled successfully. The $[HB(3\text{-}(CF_3),5\text{-}(Ph)Pz)_3]Ag(C_2H_4)$ crystallizes in *P*bcn space group with a CH_2Cl_2 molecule of crystallization. The Ag-ethylene moiety is also disordered but over two sites, and was modeled satisfactorily and the occupancies were refined to 46% and 54%. The fluorine atoms of one CF_3 group and CH_2Cl_2 also show positional disorder over two sites, and were modeled well. Hydrogen atoms on boron and pyrazolyl ring of $[HB(3\text{-}(CF_3),5\text{-}(CH_3)Pz)_3]Cu(C_2H_4)$ as well as the hydrogen atom on boron of $[HB(3\text{-}(CF_3),5\text{-}(CH_3)Pz)_3]Au(C_2H_4)$ were located from difference

maps and included. All the other hydrogen atoms of the crystal structures reported here including those of the ethylene moieties were placed at calculated positions and refined using a riding model.

Table 2.1 Crystal Data and Summary of Data Collection and Refinement for $[HB(3\text{-}(CF_3),5\text{-}(CH_3)Pz)_3]Cu(C_2H_4)$, $[HB(3\text{-}(CF_3),5\text{-}(CH_3)Pz)_3]Ag(C_2H_4)$, $[HB(3\text{-}(CF_3),5\text{-}(CH_3)Pz)_3]Cu(C_2H_4)$ and $[HB(3\text{-}(CF_3),5\text{-}(Ph)Pz)_3]Ag(C_2H_4)\bullet CH_2Cl_2$

Compound	$[HB(3\text{-}(CF_3),5\text{-}(CH_3)Pz)_3]Cu(C_2H_4)$	$[HB(3\text{-}(CF_3),5\text{-}(CH_3)Pz)_3]Ag(C_2H_4)$	$[HB(3\text{-}(CF_3),5\text{-}(CH_3)Pz)_3]Au(C_2H_4)$	$[HB(3\text{-}(CF_3),5\text{-}(Ph)Pz)_3]Ag(C_2H_4)$
Empirical formula	$C_{17}H_{17}BCuF_9N_6$	$C_{17}H_{17}AgBF_9N_6$	$C_{17}H_{17}BN_6F_9Au$	$C_{33}H_{25}AgBCl_2F_9N_6$
Formula weight	550.71	595.04	684.14	866.17
Temperature	100(2) K	100(2) K	188(2) K	100(2) K
Wavelength	0.71073 Å	0.71073 Å	0.71073 Å	0.71073 Å
Crystal system	Trigonal	Trigonal	Trigonal	Orthorhombic
Space group	P-3	P-3	P-3	Pbcn
Unit-cell dimen.	a = 11.5392(9)	a = 11.3758(10) Å	a = 11.531(2) Å	a = 23.8686(17) Å
	b = 11.5392(9)	b = 11.3758(10) Å	b = 11.531(2) Å	b = 16.8381(12) Å
	c = 9.5646(7)	c = 10.0549(9) Å	c = 9.981(2) Å	c = 16.9675(12) Å
	α= 90°	α= 90°	α= 90°	α= 90°
	β = 90°	β = 90°	β = 90°	β = 90°
	γ = 120°	γ = 120°	γ = 120°	γ = 90°
Volume	1102.93(19)	1126.9(2)	1149.3(5)	6819.3(8)
Z	2	2	2	8
Density (calculated)	1.658 Mg/m^3	1.754 Mg/m^3	1.977 Mg/m^3	1.687 Mg/m^3
Absorption coefficient	1.083 mm^{-1}	0.986 mm^{-1}	6.490 mm^{-1}	0.833 mm^{-1}
Final R indices	$R_1 = 0.0341$	$R_1 = 0.0291$	$R_1 = 0.0461$	$R_1 = 0.0360$
[I>=2σ (I)]	$wR_2 = 0.0975$	$wR_2 = 0.0765$	$wR_2 = 0.1122$	$wR_2 = 0.0835$
Final R indexes	$R_1 = 0.0394$	$R_1 = 0.0316$	$R_1 = 0.0520$	$R_1 = 0.0384$
[all data]	$wR_2 = 0.1011$	$wR_2 = 0.0785$	$wR_2 = 0.1151$	$wR_2 = 0.0853$

Table 2.2 Selected ^{1}H and ^{13}C NMR Spectroscopic data of the ethylene group of the copper, silver and gold ethylene adducts supported by fluorinated scorpionates $LM(C_2H_4)$ (M = Cu, Ag, Au; L = fluorinated scorpionate). Chemical shifts are given in ppm

LM(C₂H₄)	**^{1}H NMR data of C_2H_4 moiety**			**^{13}C NMR data of C_2H_4 moiety**			**Ref.**
Supporting ligand L	**Cu**	**Ag**	**Au**	**Cu**	**Ag**	**Au**	
[HB(3-(CF_3),5-(CH_3)Pz)₃]	4.71 ($CDCl_3$)	5.45 (CD_2Cl_2)	3.47 ($CDCl_3$)	84.8 ($CDCl_3$)	103.5 (CD_2Cl_2)	58.3 ($CDCl_3$)	This work
[HB(3-(CF_3),5-(Ph)Pz)₃]	4.91 ($CDCl_3$)	5.56 (CD_2Cl_2)	3.69 ($CDCl_3$)	85.7 (C_6D_6)	104.0 (CD_2Cl_2)	59.3 ($CDCl_3$)	This work,[33, 65, 81]
[HB(3,5-(CF_3)₂Pz)₃]	4.96 ($CDCl_3$)	5.56 (C_6D_{12})	3.81 ($CDCl_3$)	89.5 (C_6D_{12})	104.9 (C_6D_{12})	63.7 ($CDCl_3$)	33, 65, 81
[HB(3,4,5-(CF_3)₃Pz)₃]	5.06 ($CDCl_3$)	5.65 (CD_2Cl_2)		94.9 ($CDCl_3$)	111.1 (CD_2Cl_2)		46
[HB(3,5-(CF_3)₂Tz)₃]	5.12 ($CDCl_3$)	5.70 ($CDCl_3$)		92.6 (CD_2Cl_2)	109.7 ($CDCl_3$)		45
Free C_2H_4	*5.40 ($CDCl_3$), 5.25 (C_6D_6)*			*123.13 ($CDCl_3$), 122.96 (C_6D_6)*			*123*

2.6 Acknowledgments

This work was supported by the National Science Foundation (CHE-01265807), Robert A. Welch Foundation (Grant Y-1289) and the American Floral Endowment.

Chapter 3

Partially fluorinated Scorpionate $[HB(3\text{-}(CF_3),5\text{-}(Ph)Pz)_3]^-$ as a supporting ligand for silver(I)-benzene, -carbonyl, and $-PPh_3$ complexes

Shawn G. Ridlen, Naveen V. Kulkarni, and H. V. Rasika Dias*

This work has been published in Polyhedron, **2017**, 125, 68-73[b]

[b] Used with permission of the publisher, 2016

3.1 Abstract

The benzene, CO, and PPh_3 adducts [HB(3-(CF_3),5-(Ph)Pz)$_3$]AgL (L = C_6H_6, CO, or PPh_3) have been synthesized by a metathesis process using [HB(3-(CF_3),5-(Ph)Pz)$_3$]Na(THF), CF_3SO_3Ag, and the corresponding co-ligands. These silver(I) adducts have been characterized by NMR spectroscopy, and by X-ray crystallography. In all cases the Scorpionate is bound to silver in typical κ^3-fashion. The X-ray crystallographic data of [HB(3-(CF_3),5-(Ph)Pz)$_3$]Ag(η^2-C_6H_6) show that it has a η^2-bound benzene molecule. NMR data point to fluxional behavior in solution. The ^{13}C NMR resonance corresponding to the CO moiety of [HB(3-(CF_3),5-(Ph)Pz)$_3$]Ag(CO) appears as a single peak at δ 177.4 ppm and the $\bar{\upsilon}_{co}$ is observed at 2148 cm^{-1}. These values indicate the presence of a fairly Lewis acidic silver atom in [HB(3-(CF_3),5-(Ph)Pz)$_3$]Ag(CO) and significantly diminished Ag→CO π-backbonding. Interesting coupling is observed in the solution ^{19}F and ^{19}P NMR spectra of the Ag(I) adduct [HB(3-(CF_3),5-(Ph)Pz)$_3$]Ag(PPh_3). A detailed analysis of the spectral and structural features of these complexes has been described herein.

3.2 Introduction

Poly(pyrazolyl)borates are a very popular class of ligands in coordination chemistry.[35-39] Since some modes of poly(pyrazolyl)borate ligand-metal ion interactions resemble hunting habits of a scorpion, they are often referred to as Scorpionates.[35] Poly(pyrazolyl)borates are also remarkably versatile group of

ligands because, their steric and electronic properties can be modified quite easily by varying the number and type of substituents on the pyrazolyl moieties and on the boron atom. Many Poly(pyrazolyl)borate ligand varieties are known and the majority contain various hydrocarbon substituents (e.g., Me, *i*-Pr, *t*-Bu, Ph, Mesityl) on the pyrazolyl moieties.[36, 39]

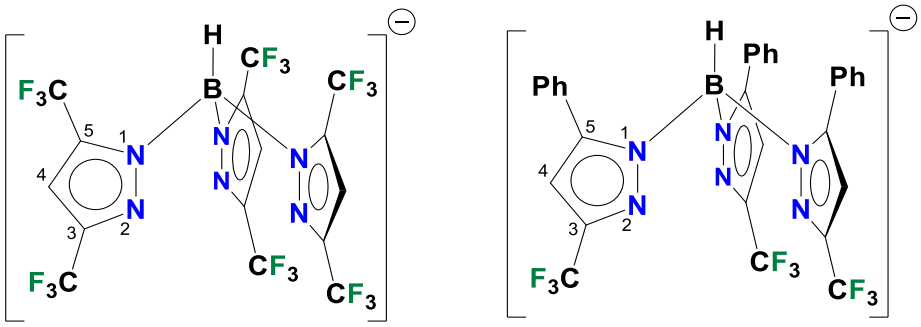

Figure 3.1 Fluorinated tris(pyrazolyl)borate ligands $[HB(3,5\text{-}(CF_3)_2Pz)_3]^-$ and $[HB(3\text{-}(CF_3),5\text{-}(Ph)Pz)_3]^-$

An area of research focus in our laboratory concerns the chemistry of fluorinated poly(pyrazolyl)borates[31, 33, 40-43] and other azolyl analogs like tris(triazolyl)borates.[44-45] For example, we have reported the synthesis of $[HB(3\text{-}(CF_3)Pz)_3]^-$,[41] $[HB(3,5\text{-}(CF_3)_2Pz)_3]^-$ (Figure 3.1),[40-41] $[HB(3,4,5\text{-}(CF_3)_3Pz)_3]^-$,[46] $[HB(3,5\text{-}(CF_3)_2,4\text{-}(Cl)Pz)_3]^-$,[28] $[HB(3,5\text{-}(CF_3)_2,4\text{-}(NO_2)Pz)_3]^-$,[28] $[H_2B(3,5\text{-}(CF_3)_2Pz)_2]^-$,[31] as well as the B-alkylated and B-arylated systems like $[MeB(3\text{-}(CF_3)Pz)_3]^-$ and $[PhB(3\text{-}(CF_3)Pz)_3]^-$.[47-48] Scorpionates bearing longer fluoroalkyl substituents on the pyrazolyl moieties are also known.[49-51]

Ligands such as $[HB(3,5\text{-}(CF_3)_2Pz)_3]^-$ have electron withdrawing fluoroalkyl groups and are significantly less electron-rich and weaker donors compared to the non-fluorinated systems like $[HB(3,5\text{-}(CH_3)_2Pz)_3]^-$.[52] Metal adducts of fluorinated tris(pyrazolyl)borates therefore possess more electrophilic metal sites. They display greater catalytic activity in certain reactions like in the C-H and C-halogen bond functionalization chemistry via carbene insertion, compared to the non-fluorinated, electron rich tris(pyrazolyl)borate analogs.[26-28, 53-58] Fluorinated Scorpionates like $[HB(3,5\text{-}(CF_3)_2Pz)_3]^-$ and $[HB(3\text{-}(CF_3),5\text{-}(CH_3)Pz)_3]^-$ are also of interest because perfluoroalkyl groups at the pyrazolyl moiety 3-positions provide a robust environment around the metal site. The C-F bonds are strong and less prone to intramolecular activation (compared for example, to C-H bonds) when reactive species are generated at the metal site. Fluorinated tris(pyrazolyl)borates are useful as effective supporting ligands in metal mediated oxidation chemistry.[60-61, 124-125] Other fluorinated Scorpionates and Scorpionates bearing other types of electron withdrawing substituents such as nitro groups, cyanides, and halogens have been reported as well.[108, 126-140]

In this paper, we describe the successful use of a mixed aryl-perfluoroalkyl substituent bearing tris(pyrazolyl)borate ligand in silver chemistry. In particular, we report the synthesis and complete characterization of Ag(I)-benzene, Ag(I)-carbonyl, and Ag(I)-PPh_3 adducts supported by $[HB(3\text{-}(CF_3),5\text{-}(Ph)Pz)_3]^-$. Isolation of silver(I) Scorpionates is challenging because they have a tendency to decompose

thermally or photochemically producing metallic silver, especially when reducing borohydride moieties are present on the supporting ligand backbone.

3.3 Results and discussion

The Scorpionate precursor [HB(3-(CF_3),5-(Ph)Pz)$_3$]Na(THF) used in this work has been reported previously.[79] The silver(I)-benzene complex [HB(3-(CF_3),5-(Ph)Pz)$_3$]Ag(η^2-C_6H_6) was obtained by treating [HB(3-(CF_3),5-(Ph)Pz)$_3$]Na(THF) with CF_3SO_3Ag in a dichloromethane-benzene solvent mixture. It is a white solid, and forms very good quality colorless crystals with well-defined faces.

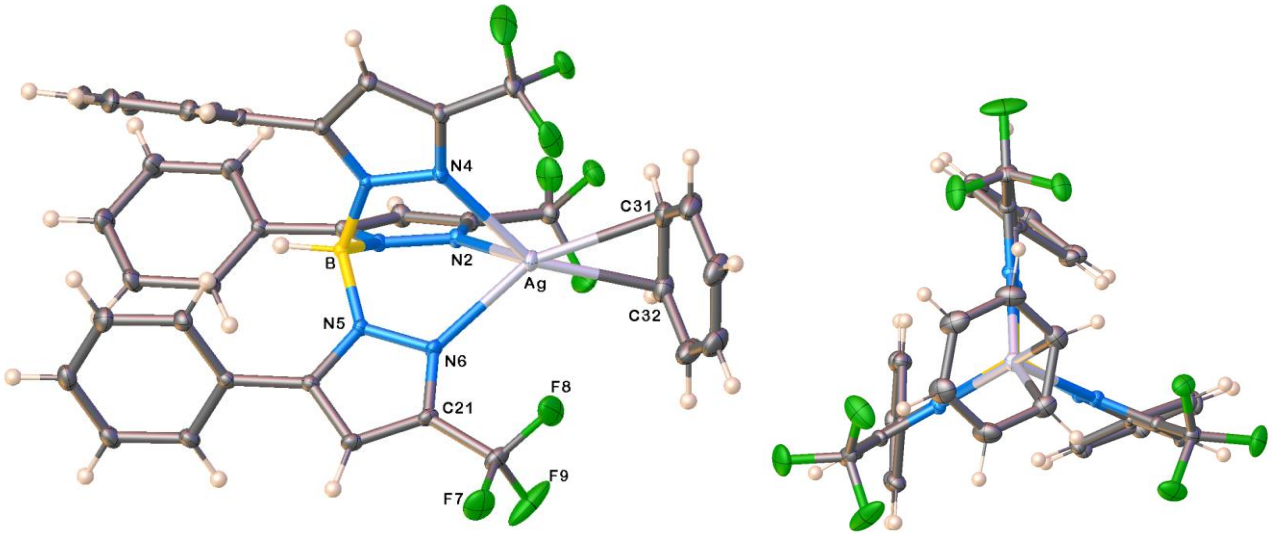

Figure 3.2 Left: ORTEP diagram of [HB(3-(CF_3),5-(Ph)Pz)$_3$]Ag(η^2-C_6H_6) (thermal ellipsoids set at 50% probability). Selected bond distances (Å) and angles (°): Ag-N2 2.4170(9), Ag-N4 2.3505(9), Ag-N6 2.3463(9), Ag-C31 2.4507(12), Ag-C32 2.4480(12), Ag•••(C31-C32 centroid) 2.347, Ag•••B 3.343; N4-Ag-N2 80.61(3), N4-Ag-N6 81.56(3), N2-Ag-N6 84.41(3), C31-Ag-C32 33.29(4), B•••Ag•••(C31-C32 centroid) 161.3. Right: A view down Ag•••B axis

X-ray crystallographic data of [HB(3-(CF_3),5-(Ph)Pz)$_3$]Ag(η^2-C_6H_6) show that is has a η^2-bound benzene molecule (Figure 3.2). The Ag-C31 and Ag-C32 distances are equal. The benzene molecule is tilted relative to the Scorpionate face, and the angle between Ag-C31-C32 plane and benzene ring plane is about 102°. The silver atom adopts a distorted tetrahedral geometry, with the Scorpionate showing κ^3-coordination mode. There are no reports of structurally characterized silver Scorpionates with benzene co-ligands for comparisons.[141] However, related toluene complexes [HB(3,5-(CF_3)$_2$Pz)$_3$]Ag(η^2-toluene) and [HB(3-(CF_3),5-(CH_3)Pz)$_3$]Ag(η^2-toluene) are known and they also have η^2-bound arenes.[80, 142] Interestingly, in contrast to [HB(3-(CF_3),5-(Ph)Pz)$_3$]Ag(η^2-C_6H_6), the silver-arene bonding in [HB(3,5-(CF_3)$_2$Pz)$_3$]Ag(η^2-toluene) which has a very weakly donating Scorpionate, is rather asymmetric with significantly different Ag-C distances (range 2.414-2.505 Å for two molecules in the asymmetric unit). The average Ag-C distances however, do not show a large difference (e.g., av. Ag-C of 2.449, 2.425, 2.448 Å for [HB(3-(CF_3),5-(Ph)Pz)$_3$]Ag(η^2-C_6H_6), [HB(3-(CF_3),5-(CH_3)Pz)$_3$]Ag(η^2-toluene) and [HB(3,5-(CF_3)$_2$Pz)$_3$]Ag(η^2-toluene), respectively). Average Ag-N distances also do not show a major variation (2.371, 2.367, and 2.390 Å, respectively, for the three adducts listed above with the highest value not unexpectedly associated with the more weakly donating Scorpionate).

The solution NMR spectra of [HB(3-(CF_3),5-(Ph)Pz)$_3$]Ag(η^2-C_6H_6) in CD_2Cl_2 at room temperature show only one sharp proton and one carbon signal for the benzene moiety, and one fluorine signal for the Scorpionate. This indicates the presence of a fluxional benzene ligand. The ^{1}H resonance of C_6H_6 in [HB(3-(CF_3),5-(Ph)Pz)$_3$]Ag(η^2-C_6H_6) (δ 7.42 ppm) shows a small down-field shift compared to the corresponding peak of free benzene in the same solvent (δ 7.35 ppm).[123]

The silver(I) carbonyl adduct [HB(3-(CF_3),5-(Ph)Pz)$_3$]Ag(CO) was synthesized by treating a mixture of [HB(3-(CF_3),5-(Ph)Pz)$_3$]Na(THF)[79] and CF_3SO_3Ag in dichloromethane with carbon monoxide (1 atm). It is a white solid. The characteristic $\bar{\upsilon}_{co}$ band of [HB(3-(CF_3),5-(Ph)Pz)$_3$]Ag(CO) can be observed at 2148 cm^{-1} in the IR spectrum, which is higher than the $\bar{\upsilon}_{co}$ of the free CO (2143 cm^{-1}). This is indicative of a significantly high electrostatic component in the Ag-CO interaction and diminished Ag→CO π-backbonding, which is not surprising since the silver(I) atom supported by the fluorinated [HB(3-(CF_3),5-(Ph)Pz)$_3$]$^-$ is expected to be fairly electrophilic.[79] A comparison of $\bar{\upsilon}_{co}$ values to silver carbonyl adducts supported by more weakly and strongly donating Scorpionates [HB(3,5-(CF_3)$_2$Pz)$_3$]Ag(CO) and [MeB(3-(Mes)Pz)$_3$]Ag(CO) show that the CO stretch of [HB(3-(CF_3),5-(Ph)Pz)$_3$]Ag(CO) is in the expected range (Table 3.1). We have also observed the ^{13}C NMR resonance corresponding to the CO moiety of [HB(3-(CF_3),5-(Ph)Pz)$_3$]Ag(CO). It appears as a singlet at δ 177.4 ppm in CD_2Cl_2 at room

temperature. The absence of $^{107/109}$Ag-^{13}C coupling in solution probably an indication for the presence of a labile CO ligand in [HB(3-(CF_3),5-(Ph)Pz)$_3$]Ag(CO) that dissociates-coordinates rapidly in CD_2Cl_2 on the NMR timescale. For comparison, the corresponding signals of [HB(3,5-(CF_3)$_2$Pz)$_3$]Ag(CO) and free CO were reported at δ 175.5 and 184 ppm, respectively. Based on these IR and NMR data, [HB(3-(CF_3),5-(Ph)Pz)$_3$]Ag(CO) can be considered as a non-classical metal carbonyl adduct.[143] The classical metal carbonyls like $Cr(CO)_6$ with significant metal→CO π-backbonding, in contrast, show low CO stretching frequencies (e.g., 2000 cm^{-1})[144] and higher ^{13}C NMR chemical shifts (e.g., δ 212.3 ppm),[145] relative to the corresponding values for the free CO.

The treatment of [HB(3-(CF_3),5-(Ph)Pz)$_3$]Ag(CO) with excess benzene in dichloromethane led to the loss of CO and the formation of [HB(3-(CF_3),5-(Ph)Pz)$_3$]Ag(η^2-C_6H_6). It is also possible to regenerate [HB(3-(CF_3),5-(Ph)Pz)$_3$]Ag(CO) from [HB(3-(CF_3),5-(Ph)Pz)$_3$]Ag(η^2-C_6H_6) by exposing it to CO in dichloromethane. This suggest the presence of rather labile CO and benzene co-ligands in these two silver Scorpionate adducts.

Table 3.1 Selected spectroscopic and structural data for tris(pyrazolyl)borato-silver(I) carbonyls

Scorpionate	$\delta(^{13}CO)$ (NMR, ppm)	$\bar{\upsilon}(CO)$ (IR, cm^{-1})	Ag-C (Å)	Ref.
$[HB(3\text{-}(CF_3),5\text{-}(Ph)Pz)_3]^-$	177.4 (CD_2Cl_2)	2148 (neat)	2.019(2)	This work
$[HB(3,5\text{-}(CF_3)Pz)_3]^-$	175.5 (CD_2Cl_2)	2178 (nujol)	2.037(5)	[80]
$[HB(3,4,5\text{-}(CF_3)Pz)_3]^-$		2177 (KBr)	2.083(3)	[46]
$[HB(3,5\text{-}(CF_3),4\text{-}BrPz)_3]^-$		2167 (soln.)		[146]
$[HB(3,4,5\text{-}(Br)_3Pz)_3]^-$		2153 (THF)		[129]
$[MeB(3\text{-}(C_2F_5)Pz)_3]^-$	176.1 ($CDCl_3$)	2153 (KBr)	2.030(4)	[50]
$[MeB(3\text{-}(CF_3)Pz)_3]^-$		2152 (hexane)		[56]
$[MeB(3\text{-}(Mes)Pz)_3]^-$		2128 (hexane)	1.994(3)	[147]
Free CO	*184*	*2143*		[33, 143]

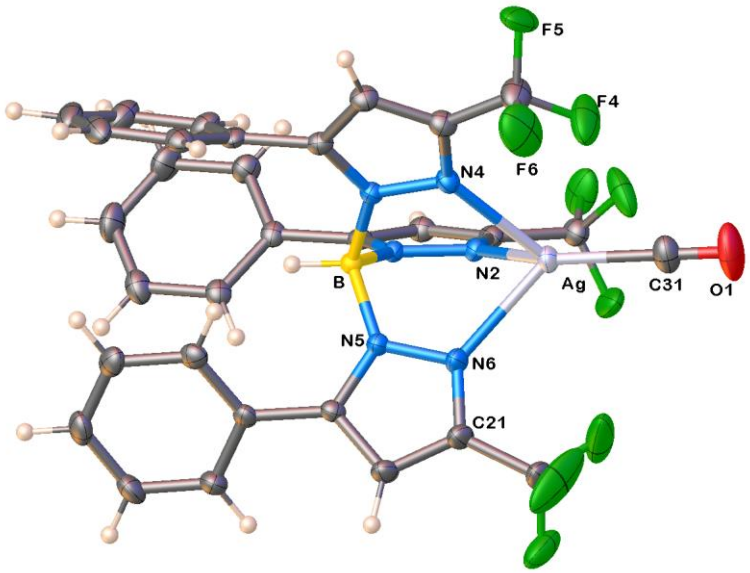

Figure 3.3 Top: ORTEP diagram of [HB(3-(CF_3),5-(Ph)Pz)$_3$]Ag(CO) (thermal ellipsoids set at 50% probability). Selected bond distances (Å) and angles (°): Ag-N2 2.2931(18), Ag-N4 2.3197(18), Ag-N6 2.3051(18), Ag-C31 2.019(2), O1-C31 1.110(3), Ag•••B 3.317; N4-Ag-N2 85.13(6), N4-Ag-N6 82.74(6), N2-Ag-N6 80.34(6), O1-C31-Ag 177.1(3), B•••Ag-C31 176.5.

X-ray crystal structure of [HB(3-(CF_3),5-(Ph)Pz)$_3$]Ag(CO) shows that it features a κ^3-bonded tris(pyrazolyl)borate and a pseudo-tetrahedral silver site (Figure 3.3). The Ag-CO moiety is essentially linear. Isolable silver(I) adducts are rare. Search of Cambridge Structural Database show that there are only four structurally characterized tris(pyrazolyl)boratosilver(I) carbonyl complexes in the literature. Some of their structural and spectroscopic features are summarized in

Table 3.1 with several other related adducts observed spectroscopically. The Ag-C bond distances of these adducts range from 2.083(3) to 1.994(3) Å. The corresponding distance of 2.019(2) Å observed for the [HB(3-(CF_3),5-(Ph)Pz)$_3$]Ag(CO) lies closer to the shorter end of the spectrum. For comparison, the copper(I) analog [HB(3-(CF_3),5-(Ph)Pz)$_3$]Cu(CO)[79] is known and it has a much shorter Cu-C distance (1.773(5) Å), consistent with the smaller atomic radius of copper.[115-117] The characteristic $\bar{\upsilon}_{co}$ band of the copper analog appears at 2103 cm^{-1} in the IR spectrum, which is lower than the $\bar{\upsilon}_{co}$ of free CO.[79]

The reaction between [HB(3-(CF_3),5-(Ph)Pz)$_3$]Na(THF) and CF_3SO_3Ag in the presence of PPh_3 afforded [HB(3-(CF_3),5-(Ph)Pz)$_3$]Ag(PPh_3), which was isolated as a white solid in 80% yield. It was characterized by ^1H, ^{13}C, ^{19}F and ^{31}P NMR spectroscopy. The ^{19}F and ^{31}P NMR spectra are the most interesting as they not only show coupling to each other but also to spin active silver nuclei (I = ½; ^{109}Ag (48.2%) and ^{107}Ag (51.8%)). For example, the ^{19}F resonance corresponding to the CF_3 groups at pyrazolyl moiety 3-positions appear as a doublet of doublet at

δ -60.27 ppm due to coupling to ^{31}P and $^{107/109}Ag$ nuclei (Figure 3.4). For comparison, the corresponding signal in $[HB(3,5\text{-}(CF_3)_2Pz)_3]Ag(PPh_3)$ also appears as a doublet of doublet, whereas in the copper adduct $[HB(3,5\text{-}(CF_3)_2Pz)_3]Cu(PPh_3)$, it shows up as a doublet.[41] The ^{31}P NMR spectrum of $[HB(3\text{-}(CF_3),5\text{-}(Ph)Pz)_3]Ag(PPh_3)$ is equally informative as the phosphorus signal of silver bound PPh_3 appears as a doublet of doublet of multiplet centered at δ 17.8 ppm (Figure 3.4). The coupling of ^{31}P to the two silver isotopes is well resolved with $^1J(^{31}P\text{-}^{107}Ag)$ = 634 Hz and $^1J(^{31}P,^{109}Ag)$ = 732 Hz. The $^1J(^{31}P,^{109}Ag)/\,^1J(^{31}P\text{-}^{107}Ag)$ ratio is consistent with the $^{109}Ag/^{107}Ag$ gyromagnetic ratio of 1.149. The magnitude of $^1J(Ag\text{-}P)$ coupling is at the higher end of four-coordinate silver phosphine complexes.[148] Each of these signals also shows spin-spin coupling to nine fluorine atoms of the CF_3 groups. Such long range coupling has been observed in the ^{31}P NMR spectra of $[HB(3,5\text{-}(CF_3)_2Pz)_3]Ag(PPh_3)$ and $[HB(3\text{-}(CF_3),5\text{-}(CH_3)Pz)_3]Ag(PPh_3)$ adducts.[149-151] The well resolved coupling in $[HB(3\text{-}(CF_3),5\text{-}(Ph)Pz)_3]Ag(PPh_3)$ points to the lack of Scorpionate and PPh_3 ligand dissociation (even $\kappa^3 \leftrightarrow \kappa^2$ interconversion) on the NMR timescale.

Although further studies are needed to ascertain whether these "long-range" $^5J(P\text{-}F)$ couplings are a result of through bond or through-space interaction between phosphorous and fluorine spins, we note that the closest nonbonded intramolecular P•••F distance in crystalline $[HB(3\text{-}(CF_3),5\text{-}(Ph)Pz)_3]Ag(PPh_3)$ is short at 3.62 Å, and may be close enough to permit through-space, Fermi-contact spin-spin

coupling by the interaction between phosphorus with fluorines of the CF_3 groups. In fact, the closest separation in solution would be even less and estimated to be about 3.2-3.3 Å (which is near the sum of the P and F van der Waals radii of 3.27 or 3.36 Å according to Bondi or Alvarez),[152] because in the crystal structure, Ag and P atoms lie on a plane which dissects the F-C-F angle of CF_3 groups. It is also noteworthy that very large (>800 Hz), long-range Tl-F coupling has been reported in fluorinated Scorpionate complexes of thallium such as [HB(3-(CF_3),5-(2-thienyl)Pz)$_3$]Tl and [MeB(3-(CF_3)Pz)$_3$]Tl.[47, 135]

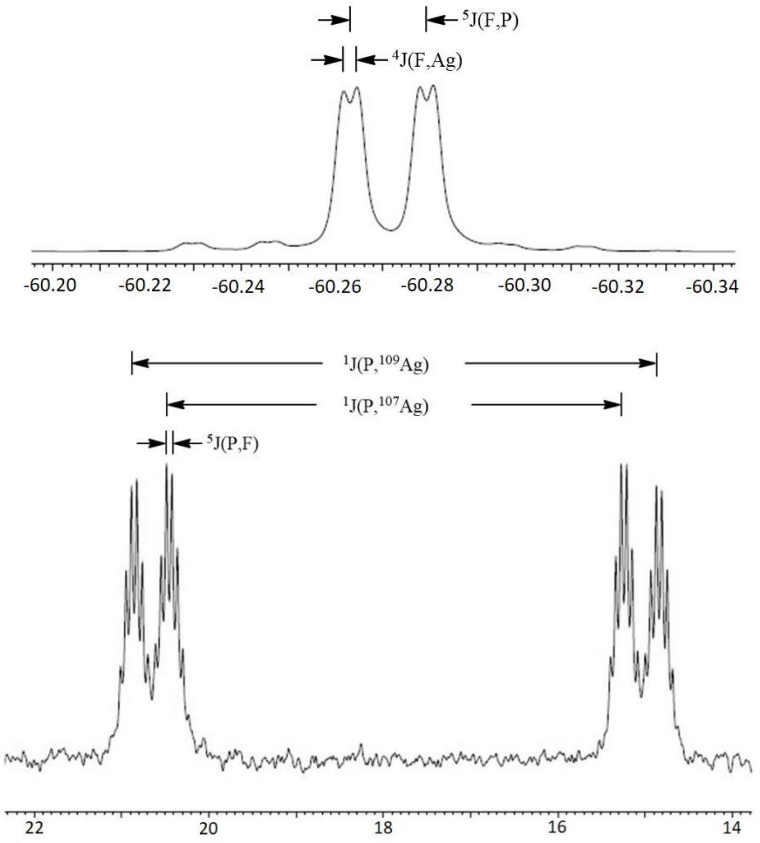

Figure 3.4 Top: ^{19}F NMR spectrum of $[HB(3\text{-}(CF_3),5\text{-}(Ph)Pz)_3]Ag(PPh_3)$, Bottom: $^{31}P\{^1H\}$ NMR spectrum of $[HB(3\text{-}(CF_3),5\text{-}(Ph)Pz)_3]Ag(PPh_3)$

The X-ray crystal structure of $[HB(3\text{-}(CF_3),5\text{-}(Ph)Pz)_3]Ag(PPh_3)$ is illustrated in Figure 3.5. The Scorpionate is bonded to the silver atom in a typical κ^3-fashion. The Ag-P and average Ag-N bond distances are within the normal range observed for silver-Scorpionates with phosphine co-ligands (Table 3.2). In general, they are closer in value to the corresponding distances reported for $[HB(3\text{-}(CF_3),5\text{-}(CH_3)Pz)_3]Ag(PPh_3)$.

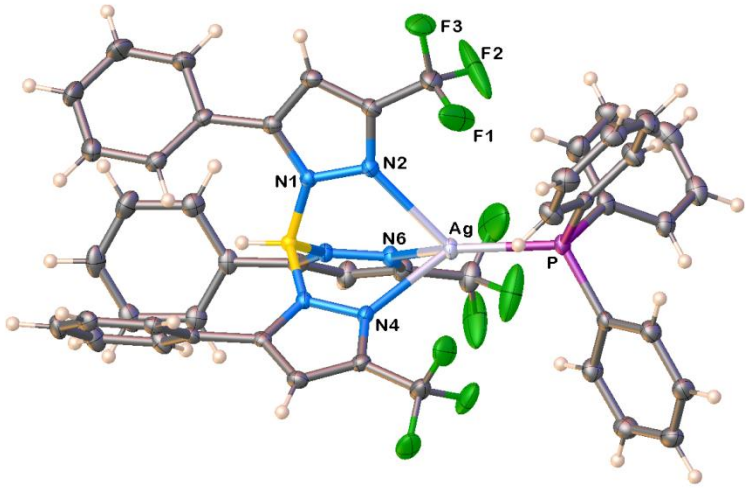

Figure 3.5 Top: ORTEP diagram of $[HB(3\text{-}(CF_3),5\text{-}(Ph)Pz)_3]Ag(PPh_3)$ (thermal ellipsoids set at 50% probability). Selected bond distances (Å) and angles (°): Ag-P 2.3690(7), Ag-N2 2.410(2), Ag-N4 2.349(2), Ag-N6 2.415(2), P-C31 1.831(3), P-C37 1.831(3), P-C43 1.830(3), Ag•••B 3.420; N4-Ag-N2 80.43(7), N4-Ag-N6 79.56(7), N2-Ag-N6 80.40(7), B•••Ag-P 176.1.

Table 3.2 Selected spectroscopic and structural data for tris(pyrazolyl)borato-silver(I) PPh_3 complexes

Scorpionate	$\delta(^{31}P)$ (NMR, ppm)	Ag-P (Å)	Ave Ag-N (Å)	$^1J(^{31}P\text{-}^{107}Ag)$	$^1J(^{31}P\text{-}^{109}Ag)$	Ref.
$[HB(3\text{-}(CF_3),5\text{-}(Ph)Pz)_3]^-$	17.9 (C_6D_6)	2.3690(7)	2.391	633.9	732.4	This work
$[HB(3\text{-}(CF_3),5\text{-}(CH_3)Pz)_3]^-$	16.53 ($CDCl_3$)	2.3642(5)	2.386	631.8	729.0	142
$[HB(3,5\text{-}(CF_3)_2Pz)_3]^-$	17.8 (C_6D_6)	2.376(1)	2.432	657.5	758.8	41
$[HB(3,5\text{-}(CH_3)_2Pz)_3]^-$	17.9 ($CDCl_3$)	2.347(6)	2.345	576	665	148, 153
$[HB(4\text{-}BrPz)_3]^-$	16.9 ($CDCl_3$)	2.345(3)	2.374	613	707	148
$[HB(Pz)_3]^-$	17.0 ($CDCl_3$)	2.337(3)	2.341	607	700	148
$[HB(3,5\text{-}(Ph)_2Pz)_3]^-$	13.4 ($CDCl_3$)	2.360(1)	2.370	600	693	154
$[HB\{3,5\text{-}(Me),4\text{-}(C_5H_4N)Pz\}_3]^-$	18.2 ($CDCl_3$)	2.3403(6)	2.338	584	675	155
Free PPh_3	*-6.0*					*156*

Solid samples of C_6H_6, CO, and PPh_3 adducts [HB(3-(CF_3),5-(Ph)Pz)$_3$]AgL (L = C_6H_6, CO, or PPh_3) can be exposed to air and indoor lighting at room temperature for several minutes without obvious signs of decomposition and do not lose co-ligands under reduced pressure. Although they are moderately air stable, these complexes should be kept under nitrogen and protected from light for long term storage. The complex [HB(3-(CF_3),5-(Ph)Pz)$_3$]Ag(PPh_3) shows excellent solution stability and does not decompose after being exposed to air and ambient light for several days. Conversely, [HB(3-(CF_3),5-(Ph)Pz)$_3$]Ag(C_6H_6) and [HB(3-(CF_3),5-(Ph)Pz)$_3$]Ag(CO) slowly form black precipitates over several hours when dissolved in chlorinated solvents, even when protected from exposure to air and indoor lighting.

3.4 Conclusions

In summary, we have reported the isolation and characterization of three new silver(I) complexes supported by [HB(3-(CF_3),5-(Ph)Pz)$_3$]$^-$ ligand. The benzene and carbonyl adducts of silver Scorpionates are particularly rare. [HB(3-(CF_3),5-(Ph)Pz)$_3$]Ag(η^2-C_6H_6) has an η^2-bound benzene on silver(I). The $\bar{\upsilon}_{co}$ of [HB(3-(CF_3),5-(Ph)Pz)$_3$]Ag(CO) appear at 2148 cm^{-1} and can be considered as a non-classical metal carbonyl complex. The phosphine adduct [HB(3-(CF_3),5-(Ph)Pz)$_3$]Ag(PPh_3) shows interesting ^{19}F and ^{19}P NMR spectra with coupling to each other and spin active silver. Silver Scorpionates supported by weakly coordinating ligands are useful in catalysis and are good ligand transfer agents. We

are currently exploring the coordination chemistry of [HB(3-(CF_3),5-(Ph)Pz)$_3$]Ag with various other co-ligands.

3.5 X-ray crystallographic data

A suitable crystal covered with a layer of hydrocarbon/paratone-N oil was selected and mounted on a Cryo-loop, and immediately placed in the low temperature nitrogen stream. The X-ray intensity data for [HB(3-(CF_3),5-(Ph)Pz)$_3$]Ag(C_6H_6), [HB(3-(CF_3),5-(Ph)Pz)$_3$]Ag(CO) and [HB(3-(CF_3),5-(Ph)Pz)$_3$]Ag(PPh_3) were measured at 100(2) K or at 106(2) K on a Bruker D8 Quest with a Photon 100 CMOS detector equipped with an Oxford Cryosystems 700 series cooler, a Triumph monochromator, and a Mo Kα fine-focus sealed tube (λ = 0.71073 Å). Intensity data were processed using the Bruker ApexII program suite. All the calculations for the structure determination were carried out using the SHELXTL package (version 6.14). Initial atomic positions were located by direct methods using XS, and the structures of the compounds were refined by the least-squares method using SHELXL.[121] Absorption corrections were applied by using SADABS. All the non-hydrogen atoms were refined anisotropically. X-ray structural figures were generated using Olex2.[122] The hydrogen atom on boron and hydrogen atoms of benzene carbons (C31 and C32) bonded to silver in [HB(3-(CF_3),5-(Ph)Pz)$_3$]Ag(C_6H_6) were located in a Fourier difference synthesis and refined satisfactorily. All the remaining hydrogen atoms of [HB(3-(CF_3),5-(Ph)Pz)$_3$]Ag(C_6H_6) as well as hydrogens of [HB(3-(CF_3),5-(Ph)Pz)$_3$]Ag(CO) and

[HB(3-(CF_3),5-(Ph)Pz)$_3$]Ag(PPh_3) were placed at calculated positions and refined using a riding model. [HB(3-(CF_3),5-(Ph)Pz)$_3$]Ag(CO) crystallizes with a molecule of CH_2Cl_2 in the asymmetric unit. The fluorine atoms of one CF_3 group in [HB(3-(CF_3),5-(Ph)Pz)$_3$]Ag(CO) and the CH_2Cl_2 show positional disorder over two sites, but these disorders were modeled satisfactorily. Further details are given in Table 3.3. The CCDC 1495609, 1495610, 1495611 contain the supplementary crystallographic data for [HB(3-(CF_3),5-(Ph)Pz)$_3$]Ag(C_6H_6), [HB(3-(CF_3),5-(Ph)Pz)$_3$]Ag(CO) and [HB(3-(CF_3),5-(Ph)Pz)$_3$]Ag(PPh_3), respectively. These data can be obtained free of charge *via* http://www.ccdc.cam.ac.uk/conts/retrieving.html or from the Cambridge Crystallographic Data Centre (CCDC), 12 Union Road, Cambridge, CB2 1EZ, UK).

Table 3.3 Crystal Data and Summary of Data Collection and Refinement for $[HB(3\text{-}(CF_3),5\text{-}(Ph)Pz)_3]Ag(\eta^2\text{-}C_6H_6)$, $[HB(3\text{-}(CF_3),5\text{-}(Ph)Pz)_3]Ag(CO)\bullet CH_2Cl_2$ and $[HB(3\text{-}(CF_3),5\text{-}(Ph)Pz)_3]Ag(PPh_3)$

Compound	$[HB(3\text{-}(CF_3),5\text{-}(Ph)Pz)_3]Ag(\eta^2\text{-}C_6H_6)$	$[HB(3\text{-}(CF_3),5\text{-}(Ph)Pz)_3]Ag(CO)\bullet CH_2Cl_2$	$[HB(3\text{-}(CF_3),5\text{-}(Ph)Pz)_3]Ag(PPh_3)$
Empirical formula	$C_{36}H_{25}AgBF_9N_6$	$C_{32}H_{21}AgBCl_2F_9N_6O$	$C_{48}H_{34}AgBF_9N_6P$
Formula weight	831.30	866.13	1015.46
Temperature	100.01 K	99.99 K	106.78 K
Wavelength	0.71073 Å	0.71073 Å	0.71073 Å
Crystal system	Monoclinic	Orthorhombic	Monoclinic
Space group	P2(1)/n	Pbcn	P2(1)/n
Unit-cell dimensions	a = 13.3013(5) Å	a = 23.8118(17) Å	a = 13.1909(9) Å
	b = 12.7215(4) Å	b = 16.7916(12) Å	b = 18.2128(12) Å
	c = 20.7889(7) Å	c = 17.0571(12) Å	c = 18.3172(12) Å
	α = 90°	α= 90°	α= 90°
	β = 104.6960(10)°	β = 90°	β = 94.006(2)°
	γ = 90°	γ = 90°	γ = 90°
Volume	3402.7(2) $Å^3$	6820.1(8) $Å^3$	4389.8(5) $Å^3$
Z	4	8	4
Density (calculated)	1.623 Mg/m^3	1.687 Mg/m^3	1.536 Mg/m^3
Absorption coefficient	0.679 mm^{-1}	0.835 mm^{-1}	0.577 mm^{-1}
Final R indices [I>2sigma(I)]	R1 = 0.0316, wR2 = 0.0644	R1 = 0.0322, wR2 = 0.0759	R1 = 0.0343, wR2 = 0.0824
R indices (all data)	R1 = 0.0473, wR2 = 0.0689	R1 = 0.0392, wR2 = 0.0805	R1 = 0.0455, wR2 = 0.0929

3.6 Acknowledgments

This work was supported by the National Science Foundation (CHE-01265807) and the Robert A. Welch Foundation (Grant Y-1289).

Chapter 4

Monoanionic, bis(pyrazolyl)methylborate $[(Ph_3B)CH(3,5\text{-}(CH_3)_2Pz)_2)]^-$ as a supporting ligand for copper(I)-ethylene, *cis*-2-butene, and carbonyl complexes[c]

Shawn G. Ridlen, Naveen V. Kulkarni, and H. V. Rasika Dias*

Department of Chemistry and Biochemistry, The University of Texas at Arlington, Arlington, Texas 76019. E-mail: dias@uta.edu

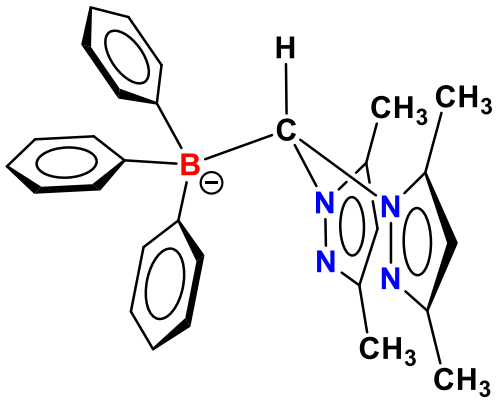

[c] This work has submitted to Inorganic Chemistry

4.1 Abstract

The monoanionic bidentate ligand $[(Ph_3B)CH(3,5\text{-}(CH_3)_2Pz)_2)]^-$ has been prepared from lithium bis(pyrazolyl)methanide and triphenylborane. This useful new ligand is closely related to the well-established bis(pyrazolyl)borate and bis(pyrazolyl)methane ligands but has key differences to both analogs as well. The ethylene, *cis*-2-butene, and carbon monoxide adducts $[(Ph_3B)CH(3,5\text{-}(CH_3)_2Pz)_2]Cu(L)$ (where L = C_2H_4, *cis*-$CH_3HC{=}CHCH_3$, and CO) have been prepared from $[(Ph_3B)CH(3,5\text{-}(CH_3)_2Pz)_2)]Li(THF)$, copper(I) triflate, and the corresponding co-ligand. These complexes have been characterized by NMR spectroscopy and X-ray crystallography. In all cases the bis(pyrazolyl) moiety is bound in κ^2*N* fashion with the BPh_3 group rotated to sit over the metal center, sometimes coordinating to the metal via phenyl carbons as in $[(Ph_3B)CH(3,5\text{-}(CH_3)_2Pz)_2)]Li(THF)$ and $[(Ph_3B)CH(3,5\text{-}(CH_3)_2Pz)_2]Cu(CO)$ or simply hovering above the metal site as in $[(Ph_3B)CH(3,5\text{-}(CH_3)_2Pz)_2)]Cu(C_2H_4)$ and $[(Ph_3B)CH(3,5\text{-}(CH_3)_2Pz)_2)]Cu(cis\text{-}CH_3HC{=}CHCH_3)$. The ^{13}C and ^1H resonances of the ethylene carbon and protons of $[(Ph_3B)CH(3,5\text{-}(CH_3)_2Pz)_2)]Cu(C_2H_4)$ appear at δ 80.4 and 3.68 ppm in CD_2Cl_2, respectively. The characteristic CO frequency for $[(Ph_3B)CH(3,5\text{-}(CH_3)_2Pz)_2]Cu(CO)$ has been observed at $\bar{\upsilon}$ 2092 cm^{-1} by infrared spectroscopy, and is lower than that of free CO suggesting moderate M→CO π-back-donation. A detailed analysis of these complexes has been presented herein.

4.2 Introduction

Poly(pyrazolyl)borates have been widely explored by inorganic, organometallic, and coordination chemists since their discovery in 1966.[35-39, 157] These monoanionic nitrogen based ligands are particularly attractive due to the ability to fine tune their steric and electronic properties and thereby modulate the reactivity of the bound metal center by changing the number and nature of the substituents on the pyrazolyl moieties and on the boron. The bulk of the attention in these ligands has been paid to tris(pyrazolyl)borates (Tp; e.g., $[HB(3,5\text{-}(CH_3)_2Pz)_3]^-$, Figure 1).[35-39, 147, 157] The closely related bis(pyrazolyl)borates (Bp; $[H_2B(3,5\text{-}(CH_3)_2Pz)_2]^-$) are also known and found to be useful, but have only been moderately explored.[30-32, 37] Most of the common tris- and bis-(pyrazolyl)borates feature somewhat reactive, and reducing B-H functionality which interferes with certain processes, especially involving easily reducible metal ions.[50, 158]

Poly(pyrazolyl)methanes like tris(pyrazolyl)methanes (e.g., $HC(3,5\text{-}(CH_3)_2Pz)_3$) and bis(pyrazolyl)methanes (e.g., $H_2C(3,5\text{-}(CH_3)_2Pz)_2$; Figure 1) were first reported in the late 1950's, and are similar in structure to the tris- and bis-(pyrazolyl)borate except that they do not share the borate backbone or carry the formal negative charge (e.g., $H_2C(3,5\text{-}(CH_3)_2Pz)_2$; Figure 1).[37, 39, 159-164] Poly(pyrazolyl)borates are also widely used in metal coordination chemistry as a supporting ligand. Here we report the design and synthesis of a bidentate ligand analog of bis(pyrazolyl)borate using the closely related bis(pyrazolyl)methane

precursor and triarylboron. These monoanionic, bis(pyrazolyl)methylborate ligands allow the synthesis of neutral metal adducts with M(I) salts including those of copper(I). In particular, we describe the preparation of $[(Ph_3B)CH(3,5\text{-}(CH_3)_2Pz)_2)]^-$ (Figure 4.1) and its utility in the synthesis of $[(Ph_3B)CH(3,5\text{-}(CH_3)_2Pz)_2)]CuL$ complexes containing L = ethylene, carbon monoxide, and cis-2-butene. This bis(pyrazolyl)methylborate ligand does not have the sometimes problematic and reactive B-H moiety found in common bis(pyrazolyl)borates.[158, 165] It features a negatively charged third arm that is significantly less prone to coordination in contrast to previously reported monoanionic bis(pyrazolyl)methane versions containing third arms like $-CO_2^-$, $-CS_2^-$, $-CPh_2(C_5H_4)^-$, $-CH_2NDipp^-$ fragments that coordinate readily to metal ions.[30, 162] Synthesis of $[(F_3B)C(Pz)_3)]Li$ and its tungsten adducts like $[(F_3B)C(Pz)_3)]W(CMe)(CO)_2$ have been described by Stone *et al.*[166] It is the only report on a related poly(pyrazolyl)methylborate to our knowledge. There is no structural data available on these $[(F_3B)C(Pz)_3)]^-$ adducts.

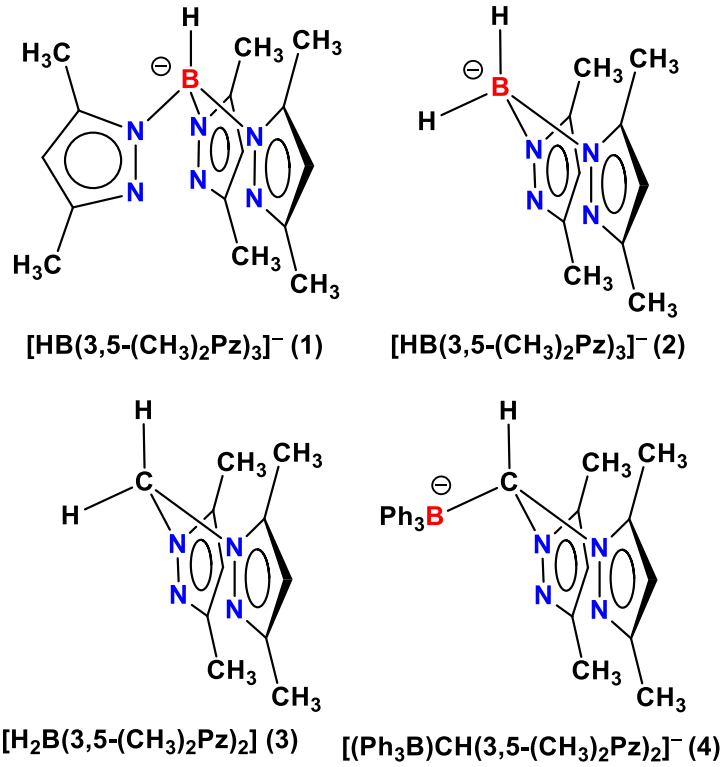

Figure 4.1 Examples of tris(pyrazolyl)borate (**1**), bis(pyrazolyl)borate (**2**), bis(pyrazolyl)methane (**3**), and bis(pyrazolyl)methyltriphenylborate (**4**) ligands.

We have focused on the isolation of copper complexes of small, carbon based molecules because they are of significant fundamental interest and technological importance. For example, copper(I) olefin complexes of ethylene adducts, are serve as models for copper(I) based ethylene receptor sites in plants,[1, 10] and as reaction intermediates in copper mediated alkene chemistry.[33, 82, 167] Copper(I) carbonyl complexes have also attracted similar interest due to their importance in biochemistry, organic synthesis, and several industrial catalytic processes.[33, 167-171] Notably, the oxychlorination of ethylene, the synthesis of methanol from syngas, and the selective removal of CO from gas mixtures are a few processes in which copper plays a key role.[172-174] While several copper ethylene and carbonyl complexes are known with tris(pyrazolyl)borates (including their heavier silver and gold counterparts),[33, 80-81, 127] and tris(pyrazolyl)methanes,[175-181] only a very few examples of copper-alkene or –carbonyl adducts have been successfully stabilized and structurally characterized using bidentate bis(pyrazolyl)borate and bis(pyrazolyl)methane system.[32-34] For example, the fluorinated bis(pyrazolyl)borate ligand supported copper(I) alkene complexes $[H_2B(3,5\text{-}(CF_3)_2Pz)_2]CuL$ (L = styrene, cyclooctene, 4-vinylanisole, triethylvinylstyrene) and $\{[H_2B(3,5\text{-}(CF_3)_2Pz)_2]Cu\}_2$(1,5-COD), as well as cationic copper(I) olefin complex $\{[CH_2(3,5\text{-}(CH_3)_2Pz)_2]Cu(cyclooctene)\}OTf$ of bis(pyrazolyl)methane have been reported in the literature.[32, 182-183] Copper carbonyl complexes of bis(pyrazolyl)borate and bis(pyrazolyl)methane are also less

numerous and include $[CH_2(3,5\text{-}(CF_3)_2Pz)_2]Cu(CO)(OTf)$, $[CH_2(3\text{-}(CF_3)Pz)_2]Cu(CO)(OTf)$, $[CH_2(3,5\text{-}(CH_3)_2Pz)_2]Cu(CO)(OClO_3)$, and $[\{[CH_2(3,5\text{-}(CH_3)_2Pz)_2]Cu(CO)\}_2(\mu\text{-pyrazine})](ClO_4)$ as the structurally well authenticated adducts of this type.[182, 184]

4.3 Results and Discussion

The lithium salt of bis(3,5-dimethylpyrazolyl)methyltriphenylborate, $[(Ph_3B)CH(3,5\text{-}(CH_3)_2Pz)_2)]Li$ is obtained in two steps by first treating the bis(3,5-dimethylpyrazolyl)methane with n-BuLi in THF at -78 °C for 15 minutes, followed by the addition of triphenylborane to the resulting methanide. After stirring at room temperature overnight, the final product was isolated as a colorless crystalline solid from the concentrated reaction medium layered with hexanes and characterized by ^1H, ^{13}C, and ^{11}B NMR spectroscopy, CHN analysis, and X-ray crystallography. $[(Ph_3B)CH(3,5\text{-}(CH_3)_2Pz)_2]Li(THF)$ is a white solid that melts around 142 °C. The complex should be stored under a nitrogen atmosphere to prevent decomposition.

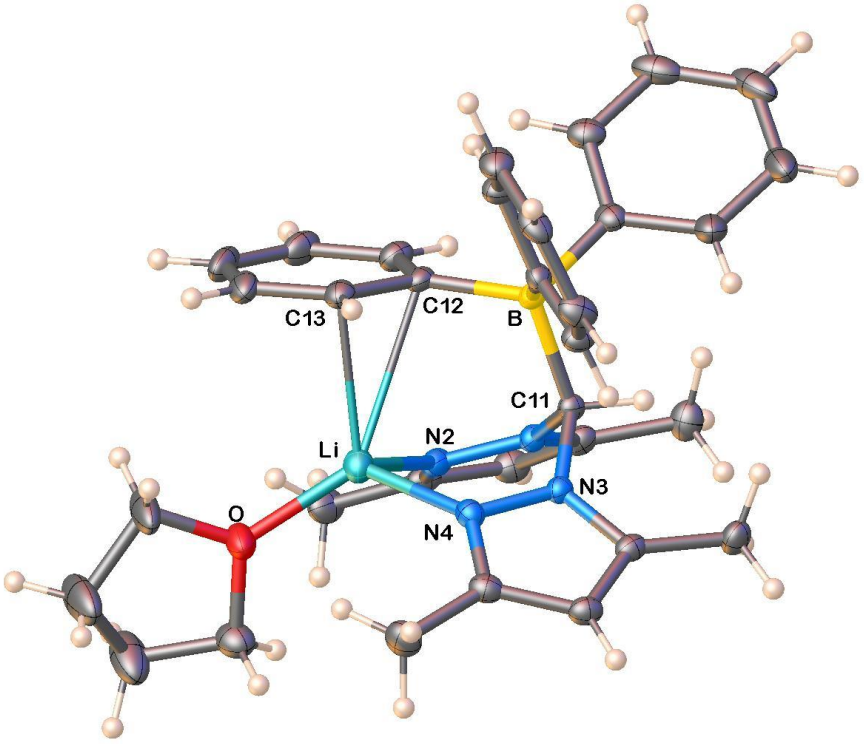

Figure 4.2 ORTEP diagram of $[(Ph_3B)CH(3,5\text{-}(CH_3)_2Pz)_2]Li(THF)$ (thermal ellipsoids set at 50% probability). Selected bond distances (Å) and angles (°): Li-N2 2.004(3), Li-N4 2.032(3), Li-O 1.927(3), Li-C12 2.709(3), Li-C13 2.455(3), Li-B 3.52, Li-C11 3.042, C11-B 1.7021(18), N2-Li-N4 94.82(10), O-Li-N2 121.55(12), O-Li-N4 114.73(12), N3-C11-N1 107.00(9), N1-C11-B 114.39(9), N3-C11-B 118.35(10), N3-C11-N1 107.00(9).

The ^{1}H NMR spectrum of [(Ph$_3$B)CH(3,5-(CH$_3$)$_2$Pz)$_2$]Li(THF) in CDCl$_3$ displayed a singlet ^{1}H resonance at δ 5.68 ppm assigned to the pyrazolyl ring C-H protons. This resonance is shifted upfield from the corresponding peak at δ 5.78 ppm observed for the neutral ligand H$_2$C(3,5-(CH$_3$)$_2$Pz)$_2$ in CDCl$_3$. The methyl groups of the pyrazolyl motifs are observed as two singlets at δ 2.13 and 1.99 ppm, that are shifted only slightly downfield from the parent molecule bis(3,5-dimethylpyrazolyl)methane (δ 2.41 and 2.18 ppm). The pyrazolyl ^{13}C peaks are relatively unchanged, however there are few features in the ^{13}C spectrum that indicate the formation of [(Ph$_3$B)CH(3,5-(CH$_3$)$_2$Pz)$_2$]Li(THF). For example, the *C*BPh$_3$ carbon resonance is observed as a broad peak at δ 71.2 ppm in CDCl$_3$ and is shifted significantly downfield from the original CH$_2$ backbone resonance observed at δ 60.5 ppm in CDCl$_3$. The single broad ^{11}B resonance observed at δ -8.52 ppm in CDCl$_3$ is indicative of a four coordinate boron center, and is shifted dramatically compared to that of the triphenylborane starting material which is observed at δ 60.2 ppm.[185] The CHN analysis is in good agreement with the expected molecule and confirmed by X-ray crystallography.

[(Ph$_3$B)CH(3,5-(CH$_3$)$_2$Pz)$_2$]Li(THF) crystallizes in the *P*2$_1$/n space group and is monomeric (Figure 4.2). The lithium atom displays distorted tetrahedral geometry, and is coordinated to the two nitrogen atoms of the two pyrazolyl groups, the oxygen of THF, and one of the aryl groups attached to boron asymmetrically, essentially in η^1-fashion (with Li-C distances of 2.455(3) and 2.709(3) Å).

Although there are no bis(pyrazolyl)methylborate systems for direct comparisons, there are very few lithium adducts like $[(C_5H_4)(Ph)_2CCH(3,5\text{-}(CH_3)_2Pz)_2]Li(THF)$ and $[(C_5H_4)(Bu^t)CHCH(3,5\text{-}(CH_3)_2Pz)_2]Li(THF)$ that exist with *NNOC* coordination at lithium.[186-187] The geometry of these compounds can be described as distorted tetrahedrons with the lithium coordinated to two pyrazolyl ring nitrogens, cyclopentadienyl ring, and a THF. Cyclopentadienyl groups are bonded to lithium in η^5-fashion somewhat asymmetrically with Li-C bond lengths ranging from 2.25(1) – 2.50(6) Å. The Li-C bond lengths of the nearest cyclopentadienyl ring carbon of each complex are 2.25(1) and 2.321(5) Å, and are significantly shorter than that of $[(Ph_3B)CH(3,5\text{-}(CH_3)_2Pz)_2]Li(THF)$ (2.455(3) Å). This is perhaps due to the better donor ability of anionic cyclopentadienyl groups of the former systems compared to neutral B-phenyl groups of the latter. The Li-N bond distances of $[(Ph_3B)CH(3,5\text{-}(CH_3)_2Pz)_2]Li(THF)$ are however, significantly shorter at just 2.004(3) and 2.032(3) Å compared to those of $[(C_5H_4)(Ph)_2CCH(3,5\text{-}(CH_3)_2Pz)_2]Li(THF)$ (2.13(1) and 2.37(1) Å) and $[(C_5H_4)(Bu^t)CHCH(3,5\text{-}(CH_3)_2Pz)_2]Li(THF)$ (2.131(5) and 2.131(5) Å).

The copper(I)-L adducts $[(Ph_3B)CH(3,5\text{-}(CH_3)_2Pz)_2)]CuL$ (L = C_2H_4, and *cis*-$CH_3HC{=}CHCH_3$) were obtained by treating $[(Ph_3B)CH(3,5\text{-}(CH_3)_2Pz)_2]Li(THF)$ with CF_3SO_3Cu in a solution of dichloromethane containing the corresponding co-ligand, alkene. X-ray quality crystals were obtained from a concentrated dichloromethane solution containing excess alkene and the products

were isolated as white solids. Solid samples of these complexes can be exposed to laboratory atmosphere for several days without obvious signs of decomposition, but should be stored under nitrogen to prevent decomposition during long term storage. Solid samples of these compounds do not lose the coordinated olefin even under reduced pressure.

The ^{13}C NMR spectrum of $[(Ph_3B)CH(3,5\text{-}(CH_3)_2Pz)_2]Cu(C_2H_4)$ in CD_2Cl_2 exhibited one singlet resonance at δ 80.4 ppm in CD_2Cl_2, corresponding to the carbons of coordinated ethylene. The proton signals of ethylene were observed at δ 3.68 ppm in CD_2Cl_2. These resonances are shifted significantly upfield from the ^{13}C and ^{1}H signals of free ethylene, which are observed at δ 123.2 and 5.40 ppm in CD_2Cl_2, respectively.[123] The upfield shift of the ethylene carbon resonances is typical for metal-ethylene complexes, and has been linked to the metal-to-ligand π-backbonding to the π^* orbital of ethylene.[109, 119, 188-189] The ^{13}C resonances of the structurally authenticated monoethylene adducts, including the cationic species, range from δ 89.5-73.0 ppm.[82] The ^{13}C resonance at δ 80.4 ppm indicates mid-level of metal-to-ligand backbonding between copper and ethylene compared to related complexes. For instance, the ethylene carbon signals of neutral, copper(I) complexes $[HC\{C(CH_3)N(2,6\text{-}(CH_3)_2C_6H_3)\}_2]Cu(C_2H_4)$ and $[N\{(C_3F_7)C(C_6F_5)N\}_2]Cu(C_2H_4)$ are observed at δ 74.74 (C_6D_6) and 86.1 ($CDCl_3$) ppm, respectively, (Table 4.1).[190-191] The ^{1}H resonances of the structurally authenticated mono-ethylene copper(I) adducts, including the cationic species,

range from δ 5.22-2.91 ppm.[33, 82] The ethylene carbon and proton resonances of [(Ph_3B)CH(3,5-(CH_3)$_2$Pz)$_2$]Cu(C_2H_4) therefore appear at a normal region expected for copper(I)-ethylene compounds, but analogous bis(pyrazolyl)methane or bis(pyrazolyl)borate adducts are not available for a comparison of more closely related systems.

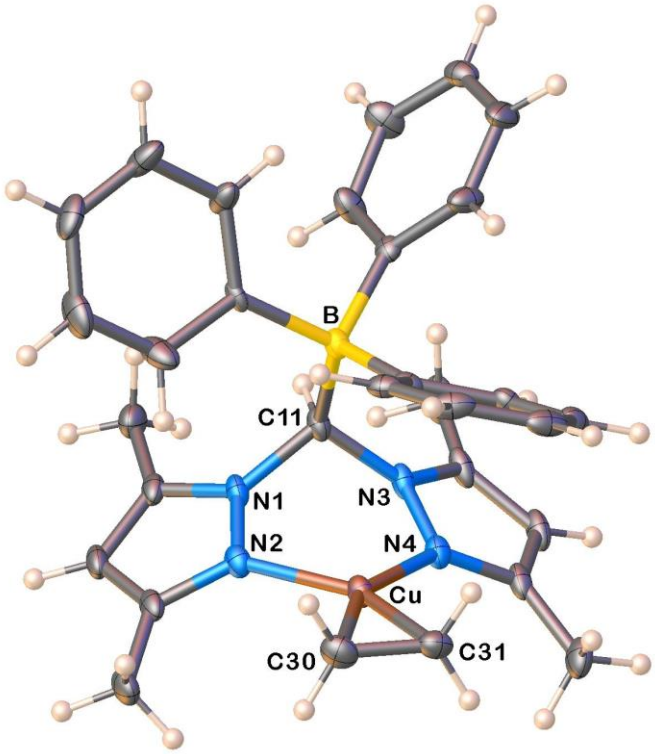

Figure 4.3 ORTEP diagram of $[(Ph_3B)CH(3,5\text{-}(CH_3)_2Pz)_2]Cu(C_2H_4)$ (thermal ellipsoids set at 50% probability). Selected bond distances (Å) and angles (°): Cu-N2 1.9541(14), Cu-N4 1.9647(13), Cu-C30 2.0023(18), Cu-C31 2.0025(18), Cu-C11 3.090, Cu···(C30-C31 centroid) 1.882, C30-C31 1.365(3), Cu-B 3.530, C30-Cu-C31 39.87(8), C11-B 1.703(2), N2-Cu···(C30-C31 centroid) 134.52, N4-Cu···(C30-C31 centroid) 131.24, C11···Cu···(C30-C31 centroid) 155.91, N2-Cu-N4 94.04, N1-C11-B 107.58(12), N3-C11-B 116.11(12), N1-C11-N3 107.49(12).

The solid state structure of $[(Ph_3B)CH(3,5\text{-}(CH_3)_2Pz)_2]Cu(C_2H_4)$ shows a trigonal planar copper ion coordinated to nitrogens and single ethylene molecule (Figure 4.3). The $[(Ph_3B)CH(3,5\text{-}(CH_3)_2Pz)_2]^-$, which is bonded to copper in κ^2N fashion via the nitrogen atoms of the pyrazolyl arms, adopts a boat configuration with the BPh_3 moiety rotated toward the metal center. The Cu-ethylene moiety is well behaved and shows that the ethylene molecule coordinated in typical η^2-fashion. The C=C bond length of the coordinate ethylene is 1.365(3) Å, which is slightly longer than that reported for free ethylene (1.3369(16) Å).[192] Based on a recent search of the Cambridge Structural Database,[193] the Cu-N, and Cu-C bond lengths for three coordinate copper-ethylene complexes range from 1.913-2.046, and 1.959-2.046 Å, respectively. The Cu-N bond distances of $[(Ph_3B)CH(3,5\text{-}(CH_3)_2Pz)_2]Cu(C_2H_4)$ are 1.9541(14), and 1.9647(13) Å, and the Cu-C bond lengths are 2.0023(18), and 2.0025(18) Å are in the mid-range of the typical Cu-N and Cu-C distances.

We have synthesized and characterized the *cis*-2-butene adduct $[(Ph_3B)CH(3,5\text{-}(CH_3)_2Pz)_2]Cu(\textit{cis}\text{-}CH_3HC{=}CHCH_3)$ to further explore the natures of these complexes. The olefinic ^1H resonances appear as broad peaks at δ 4.90 ppm in $CDCl_3$, and at δ 4.79 ppm in CD_2Cl_2. The corresponding signals for free *cis*-2-butene appear at δ 5.46 ppm in $CDCl_3$. The ^{13}C resonance of the olefinic carbons of $[(Ph_3B)CH(3,5\text{-}(CH_3)_2Pz)_2]Cu(\textit{cis}\text{-}CH_3HC{=}CHCH_3)$ could not be observed at the room temperature, but appears as a broad peak at δ 95.0 ppm in

CD_2Cl_2 at -20 °C. This peak shifts upfield, comparably to that observed for the ethylene complex, relative to the free ligand which appears at δ 124.8 ppm in $CDCl_3$. The corresponding peak for example in [Cu((S,S)-L)(*cis*-$CH_3HC{=}CHCH_3$)]ClO_4 (L = (1S,2S)-N,N'-Bis-(mesitylmethyl)-1,2-diphenyl-1,2-ethanediamine)[164] and [K(18-crown-6)][$PtCl_3$(*cis*-$CH_3HC{=}CHCH_3$)][194] has been observed at δ 96.4 and 82.7 ppm, respectively. The ^1H and ^{13}C resonances corresponding to the methyl groups of *cis*-2-butene in [(Ph_3B)CH(3,5-$(CH_3)_2Pz)_2$]Cu(*cis*-$CH_3HC{=}CHCH_3$) are only marginally shifted from those of the free ligand. For example, the methyl protons of the coordinated *cis*-2-butene appear as a doublet centered at δ 1.49 ppm in $CDCl_3$ and the similar peak observed for the free ligand at δ 1.61 ppm in $CDCl_3$. The carbon resonance appears at δ 13.5 ppm in $CDCl_3$ compared to the free ligand at δ 12.5 ppm in $CDCl_3$).

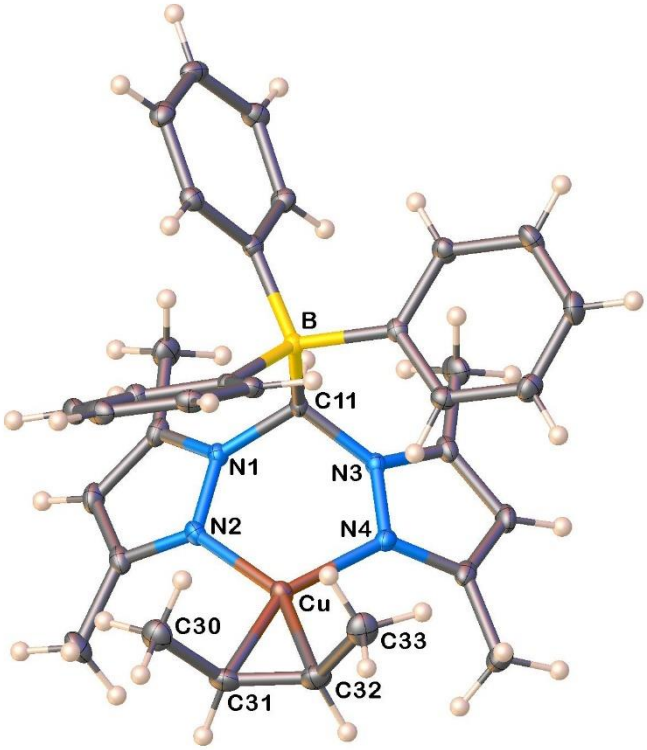

Figure 4.4 ORTEP diagram of $[(Ph_3B)CH(3,5\text{-}(CH_3)_2Pz)_2]Cu(\textit{cis}\text{-}CH_3HC{=}CHCH_3)$ (thermal ellipsoids set at 50% probability). Selected bond distances (Å) and angles (°): Cu-N2 1.9745(13), Cu-N4 1.9569(13), Cu-C31 2.0315(16), Cu-C32 2.0296(17), Cu···(C31-C32 centroid) 1.909, C31-C32 1.382(2), Cu-C11 3.167, Cu-B 3.765, C11-B 1.700(2), C31-Cu-C32 39.78(7), N4-Cu···(C31-C32 centroid) 131.83, N2-Cu···(C31-C32 centroid) 133.68, N2-Cu-N4 94.40(5), N3-C11-N1 107.86(12), N1-C11-B 117.58(12), N3-C11-B 118.15(12), C11-Cu···(C31-C32 centroid) 158.68.

X-ray analysis of [(Ph_3B)CH(3,5-(CH_3)$_2$Pz)$_2$]Cu(*cis*-CH_3HC=$CHCH_3$) revealed that it has a similar structure to that of the corresponding ethylene analog (Figure 4.4). The ligand [(Ph_3B)CH(3,5-(CH_3)$_2$Pz)$_2$]$^-$ coordinates to copper in κ^2*N* fashion via the nitrogen atoms of the pyrazolyl arms and adopts a boat configuration with the BPh_3 moiety rotated toward the metal center. Methyl groups of the butene moiety of [(Ph_3B)CH(3,5-(CH_3)$_2$Pz)$_2$]Cu(*cis*-CH_3HC=$CHCH_3$) point toward the BPh_3 moiety (see Figure 4.4) perhaps to avoid the adverse steric interactions with the methyl groups of pyrazolyl moiety at 3-position. This also significantly reduces the encroachment of the nearby B-phenyl group towards copper. The Cu-C distance to nearest B-phenyl ipso carbon is 3.49 Å, compared to that of 3.01 Å in [(Ph_3B)CH(3,5-(CH_3)$_2$Pz)$_2$]Cu(C_2H_4). The sum of the angles at the metal center in [(Ph_3B)CH(3,5-(CH_3)$_2$Pz)$_2$]Cu(C_2H_4) and [(Ph_3B)CH(3,5-(CH_3)$_2$Pz)$_2$]Cu(*cis*-CH_3HC=$CHCH_3$) total 360°, and indicate that the B-phenyl groups do not interact with copper significantly in these alkene adducts to distort the trigonal planar geometry at copper. The degree of curl-like distortion of the "boat-shaped" bis(pyrazolyl)methyl fragment is reflected in the Cu•••B separation, which increases from the ethylene adduct to the *cis*-2-butene adduct (3.53 and 3.77 Å). Selected metrical and spectroscopic data of structurally characterized copper-alkene complexes of bis(pyrazolyl)borate and bis(pyrazolyl)methane ligands are presented in Table 4.2. [CH_2(3,5-(CH_3)$_2$Pz)$_2$]Cu(cyclooctene)][OTf] is the closest analog of [(Ph_3B)CH(3,5-(CH_3)$_2$Pz)$_2$]Cu(*cis*-CH_3HC=$CHCH_3$) among the reported

compounds for a comparison. $[(Ph_3B)CH(3,5\text{-}(CH_3)_2Pz)_2]Cu(cis\text{-}CH_3HC{=}CHCH_3)$ has shorter Cu-N distances suggesting that it has somewhat better donating Scorpionate.

There are a fair number of well characterized copper carbonyl adducts presently known in the literature including a few involving tris(pyrazoyl)borate supporting ligands.[33, 168] In contrast, copper carbonyl complexes of bis(pyrazolyl)borate and bis(pyrazolyl)methane ligands are much less common. The $[CH_2(3,5\text{-}(CF_3)_2Pz)_2]Cu(CO)(OTf)$, $[CH_2(3\text{-}(CF_3)Pz)_2]Cu(CO)(OTf)$, $[CH_2(3,5\text{-}(CH_3)_2Pz)_2]Cu(CO)(OClO_3)$, and $[\{[CH_2(3,5\text{-}(CH_3)_2Pz)_2]Cu(CO)\}_2(\mu\text{-pyrazine})](ClO_4)$ represent well authenticated copper-carbonyl adducts of this type (Table 4.3).[182, 184] In these systems, the CO stretching frequency of metal carbonyl adducts serves as a good measure of relative electron density at a metal site (or the electron acceptor/back-donation ability of a metal ion). It also provides information about the donor properties of the auxiliary ligands coordinated to a metal ion. Considering these reasons, we also explored the copper(I) carbonyl chemistry of $[(Ph_3B)CH(3,5\text{-}(CH_3)_2Pz)_2]^-$.

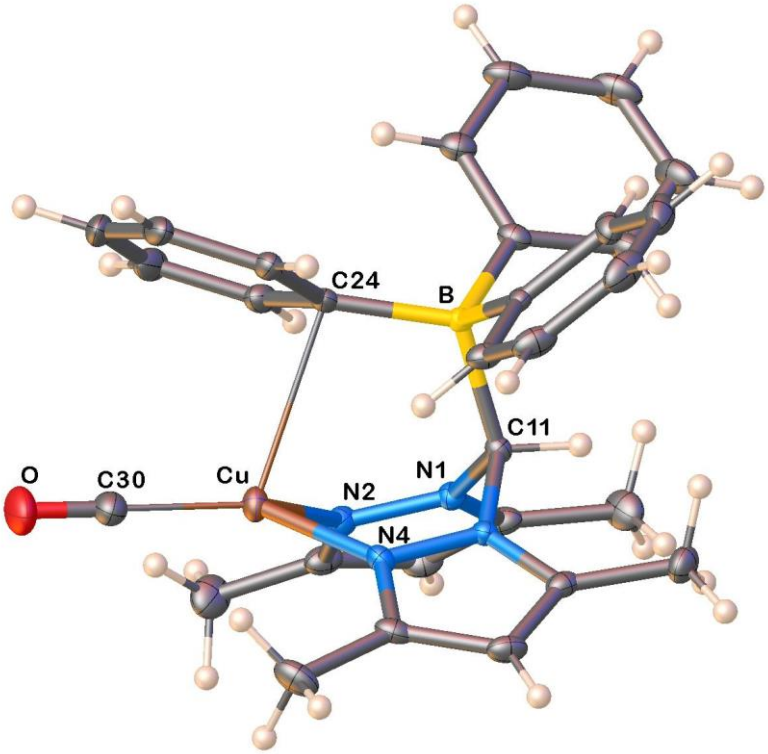

Figure 4.5 ORTEP diagram of $[(Ph_3B)CH(3,5\text{-}(CH_3)_2Pz)_2]Cu(CO)$ (thermal ellipsoids set at 50% probability). Selected bond distances (Å) and angles (°): Cu-N2 1.9939(14), Cu-N4 1.9827(13), Cu-C30 1.8055(18), O-C30 1.123(2), Cu-C24 2.609, Cu-B 3.334, Cu-C11 3.309, C11-B 1.692(2), N4-Cu-N2 91.68(6), C30-Cu-N2 134.53(7), C30-Cu-N4 127.55(7), O-C30-Cu 177.77(19), C11-Cu-C30 167.57, N1-C11-B 118.24(12), N3-C11-B 114.67(12), N3-C11-N1 106.99(12).

The carbonyl adduct was obtained by treating [(Ph_3B)CH(3,5-(CH_3)$_2$Pz)$_2$]Li(THF) with CF_3SO_3Cu in a solution of dichloromethane saturated with carbon monoxide. X-ray quality crystals were obtained from a concentrated dichloromethane solution containing the CO and the product was isolated as colorless crystals. [(Ph_3B)CH(3,5-(CH_3)$_2$Pz)$_2$]Cu(CO) can be handled in air for several days without obvious signs of decomposition and solid samples do not lose CO under reduced pressure. However, samples should be stored under nitrogen for long term storage. The ^{13}C and ^{1}H NMR spectra of [(Ph_3B)CH(3,5-(CH_3)$_2$Pz)$_2$]Cu(CO) is similar to that of the analogous ethylene and *cis*-2-btuene analogs. The ^{13}C resonance of copper bound CO was not observed, which is not uncommon in copper adducts.[127, 178]

X-ray analysis of [(Ph_3B)CH(3,5-(CH_3)$_2$Pz)$_2$]Cu(CO) revealed that this Cu-CO adduct has the deepest Cu(N-N)$_2$C boat with a Cu•••B distance of 3.33 Å and the nearest Cu-C_{Phenyl} distance at just 2.61 Å (Figure 4.5). The trigonal-planar geometry of the Cu-CO adduct is distorted, and the sum of the angles around the copper center is 354°. The geometry around copper can better be described as trigonally distorted tetrahedron, with the approaching B-phenyl group as the fourth electron domain. This is further evident from the (N2/N4 centroid)-Cu-CO angle of 160°. For comparison, (N2/N4 centroid)-Cu-(C30/C31 centroid) angle of [(Ph_3B)CH(3,5-(CH_3)$_2$Pz)$_2$]Cu(C_2H_4) is essentially linear at 176°. The Cu-C bond distance of the reported three coordinate copper(I)-carbonyl complexes chelated by

nitrogen range from 1.749-1.813 Å while the Cu-C bond distance of $[(Ph_3B)CH(3,5\text{-}(CH_3)_2Pz)_2]Cu(CO)$ is 1.8055(18) Å. The cationic copper-carbonyl complex based on bis(pyrazolyl)methane ligand $[CH_2(3,5\text{-}(CH_3)_2Pz)_2]Cu(CO)(OClO_3)$[184] is perhaps the most closely related to $[(Ph_3B)CH(3,5\text{-}(CH_3)_2Pz)_2]Cu(CO)$. It also features a pseudo-tetrahedral copper site as a result of the Cu-O interaction with weakly coordinating $OClO_3^-$ counter ion. The Cu-N and Cu-C bond distances of these two adducts are similar (e.g., the Cu-C and Cu-N distances of $[(Ph_3B)CH(3,5\text{-}(CH_3)_2Pz)_2]Cu(CO)$ are 1.80555(18) (Cu-C), 1.9939(14) (Cu-N), and 1.9827(13) Å (Cu-N), and the Cu-C and Cu-N distances of $[CH_2(3,5\text{-}(CH_3)_2Pz)_2]Cu(CO)(OClO_3)$ are 1.806(5) (Cu-C), 2.001(3) (Cu-N), and 2.007(3) Å (Cu-N)).

The CO frequency of $[(Ph_3B)CH(3,5\text{-}(CH_3)_2Pz)_2]Cu(CO)$ was observed at 2092 cm^{-1} by infrared spectroscopy, which is lower than that of the free CO ($\bar{\upsilon}$ 2143 cm^{-1}). For comparison, the CO absorptions for the pseudo-four coordinate and closely related complexes $[CH_2(3,5\text{-}(CF_3)_2Pz)_2]Cu(CO)(OTf)$[182] and $[CH_2(3,5\text{-}(CH_3)_2Pz)_2]Cu(CO)(OClO_3)$[184] appear at 2127 and 2108 cm^{-1}, respectively. These data indicate that $[(Ph_3B)CH(3,5\text{-}(CH_3)_2Pz)_2]Cu(CO)$ has a somewhat electron rich, and better back-donating copper site. The CO band of $(Ph_3B)CH(3,5\text{-}(CH_3)_2Pz)_2]Cu(CO)$ was observed at 2091 cm^{-1} by Raman spectroscopy and is good agreement with the infrared data.

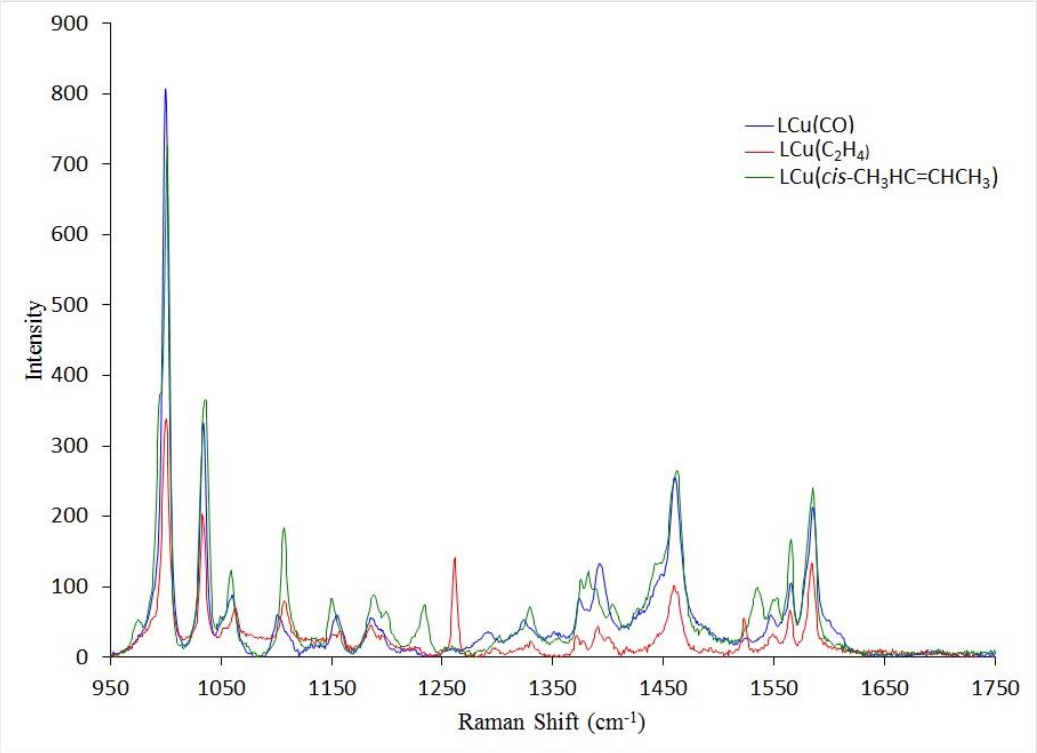

Figure 4.6 Raman spectra for $[(Ph_3B)CH(3,5\text{-}(CH_3)_2Pz)_2]Cu(CO)$, $[(Ph_3B)CH(3,5\text{-}(CH_3)_2Pz)_2]Cu(C_2H_4)$, and $[(Ph_3B)CH(3,5\text{-}(CH_3)_2Pz)_2]Cu(cis\text{-}CH_3HC{=}CHCH_3)$.

A comparison of Raman spectra of $[(Ph_3B)CH(3,5\text{-}(CH_3)_2Pz)_2]CuL$ (L = CO, ethylene and *cis*-$CH_3HC{=}CHCH_3$) show that two copper-alkene adducts have an extra peak in the 1500-1650 cm^{-1} region (Figure 4.6). These bands, observed at 1523 and 1535 cm^{-1} respectively, for $[(Ph_3B)CH(3,5\text{-}(CH_3)_2Pz)_2]Cu(C_2H_4)$ and $[(Ph_3B)CH(3,5\text{-}(CH_3)_2Pz)_2]Cu$(*cis*-$CH_3HC{=}CHCH_3$), may correspond to the alkene C=C stretching frequency. For comparison, free ethylene ($\tilde{\upsilon}$ 1623 cm^{-1}) and for free *cis*-2-butene ($\tilde{\upsilon}$ 1660 cm^{-1}) have higher C=C stretching frequencies.[195] The lowering of the C=C stretching frequency upon coordination to copper(I) is expected because of the ethylene→Cu and Cu→ethylene σ-donor/π-acceptor interactions. The $\tilde{\upsilon}$(C=C) value observed for $[(Ph_3B)CH(3,5\text{-}(CH_3)_2Pz)_2]Cu(C_2H_4)$ is slightly lower than the values observed for $[Cu(Ph_2bpm)(C_2H_4)]^+$ ($\tilde{\upsilon}$ 1529-1531 cm^{-1}, for various counter ions; Ph_2bpm = 6,6-diphenyl-4,4-bipyrimidine) and in the same range as typical, trigonal planar, mono(ethylene) complexes of copper(I) ($\tilde{\upsilon}$ 1515-1537 cm^{-1}).[196] The lower C=C stretching frequency in $[(Ph_3B)CH(3,5\text{-}(CH_3)_2Pz)_2]Cu(C_2H_4)$ relative to $[Cu(Ph_2bpm)(C_2H_4)]^+$ is understandable as latter adducts feature more Lewis acidic, cationic copper(I) sites that would show relatively less Cu→ethylene backbonding. It has been noted that the C=C stretch and the metal-ethylene bonding relationship is not straightforward, as the ethylene CH_2 scissoring action couples with the C=C stretch.[82, 197-198] It is advisable to consider these vibrational data in combination with other supporting evidence such

as those from ^{13}C NMR spectroscopy and X-ray crystallography for the analysis of metal-ethylene bonding.

In summary we have described the preparation and characterization of the ligand $[(Ph_3B)CH(3,5\text{-}(CH_3)_2Pz)_2)]^-$, as well as its value in the stabilization of the copper(I) ethylene, *cis*-2-butene, and carbon monoxide adducts $[(Ph_3B)CH(3,5\text{-}(CH_3)_2Pz)_2]Cu(L)$ (where L = C_2H_4, *cis*-$CH_3HC{=}CHCH_3$, and CO). In the case of the copper-olefin adducts, the Scorpionate ligand is bound in κ^2 fashion with the BPh_3 moiety rotated to sit over the metal center. Isolable ethylene adducts like $[(Ph_3B)CH(3,5\text{-}(CH_3)_2Pz)_2)]Cu(C_2H_4)$ have not been reported using closely related bis(pyrazolyl)borate and bis(pyrazolyl)methane ligands. The ^{13}C resonance of ethylene carbons of $[(Ph_3B)CH(3,5\text{-}(CH_3)_2Pz)_2]Cu(C_2H_4)$ and CO frequency for $[(Ph_3B)CH(3,5\text{-}(CH_3)_2Pz)_2]Cu(CO)$ indicate moderately strong M→L π-back-donation for these copper adducts. We are continuing to explore the various other metal complexes of bis(pyrazolyl)methyltriphenylborate ligands as well as the effects of ligand steric-electronic properties on coordinated metal site and chemistry.

.

Table 4.1 Spectroscopic and bond distances for selected, three-coordinate copper-ethylene complexes with κ^2*N*Cu(ethylene) moiety.

Compound	$\delta(^{13}C)$ (ppm)	$\delta(^{1}H)$ (ppm)	C=C (Å)	Cu-C (Å)	Cu-N (Å)	ref
$[(Ph_3B)CH(3,5\text{-}(CH_3)_2Pz)_2]Cu(C_2H_4)$	80.4 (CD_2Cl_2)	3.68 (CD_2Cl_2)	1.365(3)	2.0023(18) 2.0025(18)	1.9541(14) 1.9647(13)	This work
$[HC\{C(CH_3)N(2,6\text{-}(CH_3)_2C_6H_3)\}_2]Cu(C_2H_4)$	74.74 (C_6D_6)	2.91 (C_6D_6)	1.365(3)	1.986(2) 1.992(2)	1.917(2) 1.908(1)	190
$[Bu^t_2P(NSiMe_3)_2N]Cu(C_2H_4)$	73.0 (C_6D_6)	3.48 (C_6D_6)	1.362(6)	1.987(3) 1.987(3)	2.0140(16) 2.0140(16)	199
κ^2-$[PhB(3\text{-}(C_2F_5)Pz)_3]Cu(C_2H_4)$	85.5 (C_6D_{12})	3.70 ($CDCl_3$)	1.354(7)	2.033(4) 2.027(4)	2.009(3) 2.008(3)	51
$[N\{(C_3F_7)C((2,6\text{-}(i\text{Pr})_2C_6H_3)N\}_2]Cu(C_2H_4)$	86.0 ($CDCl_3$)	3.37 ($CDCl_3$)	1.3518(14)	2.0006(11) 1.9974(11)	1.9406(9) 1.9403(9)	200
$[N\{(C_3F_7)C(4\text{-}(NO_2)C_6H_4)N\}_2]Cu(C_2H_4)$	87.6 ($CDCl_3$)	3.68 ($CDCl_3$)	1.332(12)	2.027(8) 1.997(8)	1.955(5) 1.958(6)	201
$[N\{(C_3F_7)C(C_6F_5)N\}_2]Cu(C_2H_4)$	86.1 ($CDCl_3$)	3.86 ($CDCl_3$)	1.364(4)	2.018(3) 2.010(3)	1.946(2) 1.955(2)	191
$[N\{(C_3F_7)C(2,6\text{-}Cl_2C_6H_3)N\}_2]Cu(C_2H_4)$	84.20 ($CDCl_3$)	3.53 ($CDCl_3$)	1.364(9)	2.004(6) 2.004(6)	1.958(5) 1.946(5)	118
Free ethylene	123.20 (CD_2Cl_2)	5.40 (CD_2Cl_2)	1.313(1) (X-ray) 1.3369(16) (electr. diff.)			123, 192, 202

Table 4.2 Spectroscopic and bond distances for selected copper-olefin complexes.

Compound	$\delta(^{13}C)$ (ppm)	$\delta(^{1}H)$ (ppm)	C=C (Å)	Cu-C (Å)	Cu-N (Å)	Ref
$[(Ph_3B)CH(3,5\text{-}(CH_3)_2Pz)_2]Cu(cis\text{-}CH_3HC{=}CHCH_3)$	95.0 (CD_2Cl_2)	4.79 (CD_2Cl_2)	1.382(2)	2.0315(16), 2.0296(17)	1.9745(13), 1.9569(13)	This work
$[H_2B(3,5\text{-}(CF_3)_2Pz)_2]Cu$(cyclooctene)	102.6 (C_6D_6)	4.90 (C_6D_6)	1.338(5)	2.035(3), 2.046(3)	1.998(3), 1.995(3)	183
$[H_2B(3,5\text{-}(CF_3)_2Pz)_2]Cu(PhCH{=}CH_2)$	76.0, 105.0 ($CDCl_3$)	4.61, 4.98 ($CDCl_3$)	1.368(5)	2.055(3), 2.020(3)	1.993(3), 2.000(3)	32
$\{[H_2B(3,5\text{-}(CF_3)_2Pz)_2]Cu\}_2$(1,5-COD)		5.01 (C_6D_6)	1.370(4)	2.030(3), 2.021(3)	1.989(3), 1.994(3)	32
			1.374(4)	2.023(3), 2.025(3)	1.989(3), 1.985(2)	
$[CH_2(3,5\text{-}(CH_3)_2Pz)_2]Cu$(cyclooctene)][OTf]	103.5 ($CDCl_3$)	5.28 ($CDCl_3$)	1.362(3)	2.072(2), 2.050(2)	2.009(2), 2.007(2)	203

Table 4.3 Infrared spectroscopy data and selected bond distances for copper CO complexes.

Cu(CO) Complex	$\tilde{\upsilon}$(CO) (IR, cm^{-1})	Cu-C (Å)	C-O (Å)	Cu-N (Å)	Reference
$[(Ph_3B)CH(3,5\text{-}(CH_3)_2Pz)_2]Cu(CO)$	2092 (neat)	1.8055(18)	1.123(2)	1.9939(14) 1.9827(13)	This work
$[CH_2(3,5\text{-}(CF_3)_2Pz)_2]Cu(CO)(OTf)$	2127 (neat)	1.803(7)	1.144(7)	2.064(4) 2.075(4)	[182]
$[CH_2(3\text{-}(CF_3)Pz)_2]Cu(CO)(OTf)$	2120 (neat)	1.812(5)	1.117(6)	2.067(2)	[182]
$[CH_2(3,5\text{-}(CH_3)_2Pz)_2]Cu(CO)(OClO_3)$	2108 (neat)	1.806(5)	1.124(6)	2.001(3) 2.007(3)	[184]
$\{[CH_2(3,5\text{-}(CH_3)_2Pz)_2]Cu(CO)(OClO_3)\}_2(\mu$-pyrazine)	2119 (Nujol)	1.835(8)	1.121(8)	2.043(6) 2.046(6) 2.056(5)	[184]
$[CH(3,5\text{-}(CH_3)_2Pz)_3]Cu(CO)(PF_6)$	2113 (Nujol)				[175]
$[CH(3\text{-}(t\text{-}Bu)Pz)_3]Cu(CO)(PF_6)$	2100 (Nujol)	1.778(10)	1.133(9)	2.076(6) 2.075(5) 2.088(5)	[175]
Free CO	2143		1.12822(7)		143

4.5 X-ray crystallography

A suitable crystal covered with a layer of hydrocarbon/paratone-N oil was selected and mounted on a Cryo-loop, and immediately placed in the low temperature nitrogen stream. The X-ray intensity data for [(Ph_3B)CH(3,5-(CH_3)$_2$Pz)$_2$)]Li(THF), [(Ph_3B)CH(3,5-(CH_3)$_2$Pz)$_2$)]Cu(C_2H_4), [(Ph_3B)CH(3,5-(CH_3)$_2$Pz)$_2$)]Cu(*cis*-CH_3HC=$CHCH_3$) and [(Ph_3B)CH(3,5-(CH_3)$_2$Pz)$_2$)]Cu(CO) were collected at 100(2) K on a Bruker D8 Quest with a Photon 100 CMOS detector equipped with an Oxford Cryosystems 700 series cooler, a Triumph monochromator, and a Mo Kα fine-focus sealed tube (λ = 0.71073 Å). Intensity data were processed using the Bruker ApexII program suite. All the calculations for the structure determination were carried out using the SHELXTL package (version 6.14). Initial atomic positions were located by direct methods using XS, and the structures of the compounds were refined by the least-squares method using SHELXL.[121] Absorption corrections were applied by using SADABS. All the non-hydrogen atoms were refined anisotropically. X-ray structural figures were generated using Olex2.[122]

The hydrogen atom of ethylene moiety in [(Ph_3B)CH(3,5-(CH_3)$_2$Pz)$_2$)]Cu(C_2H_4) were located in a Fourier difference synthesis and refined satisfactorily. All the remaining hydrogen atoms of [(Ph_3B)CH(3,5-(CH_3)$_2$Pz)$_2$)]Cu(C_2H_4) and hydrogen atoms of [(Ph_3B)CH(3,5-(CH_3)$_2$Pz)$_2$)]Li(THF), [(Ph_3B)CH(3,5-(CH_3)$_2$Pz)$_2$)]Cu(*cis*-CH_3HC=$CHCH_3$) and

[(Ph_3B)CH(3,5-(CH_3)$_2$Pz)$_2$)]Cu(CO) were placed at calculated positions and refined using a riding model. Carbon atoms of THF in [(Ph_3B)CH(3,5-(CH_3)$_2$Pz)$_2$)]Li(THF) and one of the phenyl groups of [(Ph_3B)CH(3,5-(CH_3)$_2$Pz)$_2$)]Cu(C_2H_4) were disordered over two sites. These positional disorders were modeled quite well. [(Ph_3B)CH(3,5-(CH_3)$_2$Pz)$_2$)]Cu(CO) crystallizes with a molecule of CH_2Cl_2 in the asymmetric unit. The CH_2Cl_2 shows positional disorder over two sites, which was treated satisfactorily. Additional data collection, structure solution and refinement data are presented in Table 4.4 and supporting information (in cif format). Figures showing disordered atoms are given in Supporting Information.

Table 4.4 Crystal data and summary of data collection and refinement for $[(Ph_3B)CH(3,5\text{-}(CH_3)Pz)_2]Li(THF)$, $[(Ph_3B)CH(3,5\text{-}(CH_3)Pz)_2]Cu(C_2H_4)$, $[(Ph_3B)CH(3,5\text{-}(CH_3)Pz)_2]Cu(cis\text{-}CH_3HC{=}CHCH_3)$, and $[(Ph_3B)CH(3,5\text{-}(CH_3)Pz)_2]Cu(CO)$.

Compound	$[(Ph_3B)CH(3,5\text{-}(CH_3)Pz)_2]Li(THF)$	$[(Ph_3B)CH(3,5\text{-}(CH_3)Pz)_2]Cu(C_2H_4)$	$[(Ph_3B)CH(3,5\text{-}(CH_3)Pz)_2]Cu(cis\text{-}CH_3HC{=}CHCH_3)$	$[(Ph_3B)CH(3,5\text{-}(CH_3)Pz)_2]Cu(CO)\bullet CH_2Cl_2$
Empirical formula	$C_{33}H_{38}BLiN_4O$	$C_{28}H_{34}BN_4Cu$	$C_{33}H_{38}BCuN_4$	$C_{31}H_{32}BCl_2CuN_4O$
Formula weight	524.42	500.94	565.02	621.85
Temperature	100 K	99.96 K	101.73 K	101.53 K
Wavelength	0.71073 Å	0.71073 Å	0.71073 Å	0.71073 Å
Crystal system	Monoclinic	Triclinic	Triclinic	Monoclinic
Space group	P2(1)/n	P-1	P-1	P2(1)/n
Unit-cell dimensions	a = 12.0600(5) Å	a = 8.3862(12) Å	a = 8.6761(5) Å	a = 10.1293(5) Å
	b = 14.1103(6) Å	b = 10.5732(15) Å	b = 10.7866(7) Å	b = 19.1290(9) Å
	c = 17.3524(8) Å	c = 16.695(2) Å	c = 16.3429(10) Å	c = 16.0586(7) Å
	α = 90°	α = 77.206(2)°	α= 92.498(2)°	α= 90°
	β = 98.9860(11) °	β = 84.276(2)°	β = 104.506(2)°	β = 104.024(2)°
	γ = 90°	γ = 68.071(2)°	γ = 104.528(2)°	γ = 90°
Volume	2916.6(2) $Å^3$	1338.9(3) $Å^3$	1424.09(15) $Å^3$	3018.8(2) $Å^3$
Z	4	2	2	4
Density (calculated)	1.194 Mg/m^3	1.243 Mg/m^3	1.318 Mg/m^3	1.368 Mg/m^3
Absorption coefficient	0.072 mm^{-1}	0.838 mm^{-1}	0.796 mm^{-1}	0.931 mm^{-1}
Final R indices [$I>2\sigma(I)$]	R1 = 0.0424 wR2 = 0.1090	R1 = 0.0283, wR2 = 0.0702	R1 = 0.0304, wR2 = 0.0732	R1 = 0.0352, wR2 = 0.0965
R indices (all data)	R1 = 0.0485 wR2 = 0.1137	R1 = 0.0338, wR2 = 0.0725	R1 = 0.0339, wR2 = 0.0750	R1 = 0.0371, wR2 = 0.0981

4.6 Acknowledgments

This work was supported by the Robert A. Welch Foundation (Grant Y-1289).

4.7 Supporting Information Available

X-ray crystallographic data (CIF) for $[(Ph_3B)CH(3,5\text{-}(CH_3)_2Pz)_2]Li(THF)$, $[(Ph_3B)CH(3,5\text{-}(CH_3)_2Pz)_2]Cu(C_2H_4)$, $[(Ph_3B)CH(3,5\text{-}(CH_3)_2Pz)_2]Cu(cis\text{-}CH_3HC{=}CHCH_3)$, and $[(Ph_3B)CH(3,5\text{-}(CH_3)_2Pz)_2]Cu(CO)$, additional figures**.** This material is available free of charge via the Internet at http://pubs.acs.org.

.

Chapter 5

Experimental Details

5.1 General Methods

All manipulations were carried out under an atmosphere of purified nitrogen using standard Schlenk techniques or in a Vacuum Atmosphere single-station glovebox equipped with a -25 °C refrigerator. Solvents were purchased from commercial sources and purified prior to use. Glassware was oven-dried at 150 °C overnight. NMR spectra were recorded at 25 °C on a JEOL Eclipse 500 and JEOL Eclipse 300 spectrometer (^{1}H, 500.16 MHz and 300.53 MHz; ^{13}C, 125.78 MHz, and 75.59 MHz; ^{19}F, 470.62 MHz, and 282.78 MHz; ^{11}B, 96.42 MHz, ^{31}P, 121.66 MHz). Proton and carbon chemical shifts are referenced using the residual proton or carbon signals of the deuterated solvent and ^{19}F NMR values were referenced to external $CFCl_3$. ^{11}B NMR values were referenced to external BF_3OEt_2 and ^{31}P NMR values were referenced to external H_3PO_4 (85%). Melting points were obtained on a Mel-Temp II apparatus. Elemental analyses were performed at Intertek Pharmaceutical Services. IR spectra were collected at room temperature on a Shimadzu IRPrestige-21 FTIR containing an ATR attachment. Raman spectra were collected on a HORIBA Jobin Yvon LabRam ARAMIS. Silver(I) triflate, and AuCl were purchased from Aldrich. $[HB(3\text{-}(CF_3),5\text{-}(CH_3)Pz)_3]Na$,[108] $[HB(3\text{-}(CF_3),5\text{-}(Ph)Pz)_3]Na(THF)$,[79] bis(3,5-dimethylpyrazolyl)methane,[204] and $[CF_3SO_3Cu]_2 \bullet C_6H_6$[205206] were prepared via reported procedures. Carbon monoxide

gas was purchased from Airgas, ethylene gas was purchased from Matheson, and cis-2-butene was purchased from sigma-aldrich.

5.2 Experimental for Chapter 2

Synthesis of [HB(3-(CF_3),5-(CH_3)Pz)$_3$]Cu(C_2H_4)

[HB(3-(CF_3),5-(CH_3)Pz)$_3$]Na (0.100 g, 0.207 mmol) was dissolved in THF (10 mL) and the solution was saturated with ethylene. This solution was slowly added to solid $[CF_3SO_3Cu]_2$•C_6H_6 (0.054 g, 0.107) via syringe under a flow of ethylene. The resulting mixture was allowed to stir overnight under an ethylene atmosphere at room temperature. The solvent was removed under reduced pressure and the residue was dissolved in dichloromethane. Na(CF_3SO_3) was removed by filtration through a bed of Celite and the pale green filtrate was concentrated by bubbling ethylene and stored at -20 °C under an ethylene atmosphere for crystallization. Yield: 0.195 g, 86%; m.p. 147 °C (decomposition). ^{1}H NMR ($CDCl_3$, 500.16 MHz, 298 K) δ (ppm): 6.27 (s, 3H, *CH*), 4.71 (s, 4H, C*H*$_2$=C*H*$_2$), 2.45 (s, 9H, *CH*$_3$). ^{13}C NMR ($CDCl_3$, 125.77 MHz, 298 K): 145.0 (s, *C*CH_3), 142.4 (q, ^{2}J = 38 Hz, *C*CF_3) 121.3 (q, ^{1}J = 277 Hz, *C*F_3), 104.9 (s, *C*H), 84.8 (s, *C*H$_2$=*C*H$_2$), 13.0 (s, *C*H$_3$) ^{19}F NMR ($CDCl_3$, 470.62 MHz, 298 K) δ (ppm): -60.5 (s). ATR-FTIR (Selected peak, cm^{-1}) 2562 (B-H). Anal. Calcd. for $C_{17}H_{17}BCuF_9N_6$: C, 37.08; H, 3.11; N, 15.26. Found: C, 37.01; H, 3.01; N, 15.11.

Synthesis of [HB(3-(CF_3),5-(CH_3)Pz)$_3$]Ag(C_2H_4)

CF_3SO_3Ag (0.108 g, 0.420 mmol), and [HB(3-(CF_3),5-(CH_3)Pz)$_3$]Na (0.200 g, 0.415 mmol) were dissolved in dichloromethane (10 mL) under a flow of ethylene. The resulting mixture was wrapped in aluminum foil to protect it from light and stirred overnight under an ethylene atmosphere at room temperature. Over the course of the reaction a black precipitate formed and was removed by filtration. The resulting clear colorless filtrate was concentrated by bubbling ethylene and stored at -20 °C under an ethylene atmosphere for crystallization. Yield: 0.098 g, 80%; m.p. 105 °C (decomposition). ^{1}H NMR (CD_2Cl_2, 500.16 MHz, 298 K) δ (ppm): 6.29 (s, 3H, C*H*), 5.45 (s, 4H, CH_2=CH_2), 2.47 (s, 9H, CH_3). ^{13}C NMR (CD_2Cl_2, 125.77 MHz, 298 K) δ (ppm): 146.8 (s, *C*CH_3), 142.7 (q, ^{2}J = 38 Hz, *C*CF_3), 122.2 (q, ^{1}J = 250 Hz, *C*F_3), 104.4 (s, *C*H), 103.5 (s, *C*H_2=*C*H_2), 13.4 (s, *C*H_3). ^{19}F NMR (CD_2Cl_2, 470.62 MHz, 298 K) δ (ppm): -61.5 (s). ATR-FTIR (Selected peak, cm^{-1}): 2540 (B-H). Anal. Calc. for $C_{17}H_{17}AgBF_9N_6$: C, 34.32; H, 2.88; N, 14.12. Found: C, 34.38; H, 2.77; N, 13.74.

Synthesis of [HB(3-(CF_3),5-(CH_3)Pz)$_3$]Au(C_2H_4)

AuCl (0.062 g, 0.270 mmol) and freshly sublimed [HB(3-(CF_3),5-(CH_3)Pz)$_3$]Na (0.13 g, 0.270 mmol) were dissolved in ethylene saturated hexane at room temperature. The mixture was protected from light using aluminum foil, and stirred at room temperature for 4 h while periodically passing ethylene through the solution. Over the course of the reaction the yellow solution became gray with an

off white precipitate. The mixture was filtered through a bed of Celite, and the clear colorless filtrate was dried under reduced pressure to obtain [HB(3-(CF_3),5-(CH_3)Pz)$_3$]Au(C_2H_4) as a white solid. X-ray quality crystals were obtained from a hexane solution saturated with ethylene at -20 °C. Yield: 0.110 g, 80%; m.p. 130 °C (decomposition). ^{1}H NMR ($CDCl_3$, 500.16 MHz, 298 K) δ (ppm): 6.31 (s, 3H, C*H*), 3.47 (s, 4H, CH_2=CH_2), 2.42 (s, 9H, CH_3). ^{13}C NMR ($CDCl_3$, 125.77 MHz, 298 K) δ (ppm, selected peak): 58.3 (br, CH_2=*C*H_2). ^{19}F NMR ($CDCl_3$, 470.62 MHz, 298 K) δ (ppm): -61.3 (s). Anal. Calc. for $C_{17}H_{17}AuBF_9N_6$: C, 29.85; H, 2.50 N, 12.28. Found: C, 29.66; H, 3.01; N, 12.11.

Synthesis of [HB(3-(CF_3),5-(Ph)Pz)$_3$]Ag(C_2H_4)

CF_3SO_3Ag (0.036 g, 0.140 mmol), and [HB(3-(CF_3),5-(Ph)Pz)$_3$]Na(THF) (0.100 g, 0.135 mmol) were dissolved in hexanes (10 mL) under a flow of ethylene. The resulting mixture was covered with aluminium foil to protect it from light and stirred overnight under an ethylene atmosphere at room temperature. Over the course of the reaction a white precipitate formed and was removed by filtration. The resulting clear colorless filtrate was concentrated by bubbling ethylene and stored at -20 °C under an ethylene atmosphere for crystallization. Yield: 0.078 g, 72%; m.p. 124 °C (decomposition). ^{1}H NMR (500.16 MHz, C_6D_{12}) δ (ppm): 7.10 (br, 3H, Ph-*H*), 6.84 (br, 12H, Ph-*H*), 6.40 (s, 3H, C*H*), 5.55 (s, 4H, CH_2=CH_2). ^{13}C NMR (C_6D_{12}, 125.77 MHz, 298 K) δ (ppm): 151.7 (s, *C*CH_3), 143.7 (q, ^{2}J = 38 Hz, *C*CF_3), 132.3 (s, Ph), 130.4 (s, Ph), 128.3 (s, Ph), 122.4 (q, ^{1}J = 264 Hz, *C*F_3),

105.0 (s, *C*H), 102.4 (s, *C*H_2=*C*H_2). ^{19}F NMR (CD_2Cl_2, 470.62 MHz, 298 K) δ (ppm): -62.1 (s). ^{1}H NMR (500.16 MHz, CD_2Cl_2) δ (ppm): 7.23 (t, 3H, Ph-*H*, $^3J_{HH}$ = 5.0 Hz), 6.94 (t, 6H, Ph-*H*, $^3J_{HH}$ = 10.0 Hz), 6.89 (d, 6H, Ph-*H*, $^3J_{HH}$ = 10.0 Hz), 6.57 (s, 3H, C*H*), 5.56 (s, 4H, C*H*$_2$=C*H*$_2$). ^{13}C NMR (CD_2Cl_2, 125.76 MHz, 298 K) δ (ppm, selected peak): 104.0 (s, *CH*$_2$=*CH*$_2$). ^{19}F NMR (CD_2Cl_2, 470.62 MHz, 298 K) δ (ppm): -61.4 (s). ATR-FTIR (Selected peak, cm^{-1}) 2626 (B-H). Anal. Calc. for $C_{32}H_{23}AgBF_9N_6 \cdot 0.5CH_2Cl_2$: C, 47.39; H, 2.94; N, 10.20. Found: C, 47.26; H, 2.84; N, 9.92.

5.3 Experimental Chapter 3

[HB(3-(CF$_3$),5-(Ph)Pz)$_3$]Ag(η^2-C$_6$H$_6$)

[HB(3-(CF$_3$),5-(Ph)Pz)$_3$]Na(THF) (0.25 g, 0.34 mmol) and CF_3SO_3Ag (0.095 g, 0.37 mmol) were placed in a Schlenk flask under nitrogen atmosphere and the flask was covered aluminum foil to protect it from light. Dichloromethane (20 mL) and benzene (2.0 mL) were combined in a separate Schlenk flask and slowly added via syringe. The resulting solution was stirred overnight at room temperature and filtered through a bed of Celite to remove the insoluble material. The filtrate was concentrated under reduced pressure and placed in a freezer maintained at -20 °C. X-ray quality crystals of [HB(3-(CF$_3$),5-(Ph)Pz)$_3$]Ag(□^{2}-C$_6$H$_6$) were obtained after several days at -20 °C. Yield: 0.234 g, 83%; m.p. 83-120 °C (slowly decomposes over this wide temperature range with a final melting point of the residue at 211 °C). ^{1}H NMR (CD_2Cl_2, 500.16 MHz, 298 K) δ (ppm): 7.42 (s,

6H, C_6H_6), 7.23 (t, 3H, Ph-*H*, $^3J_{HH}$ = 7.25 Hz), 6.95 (t, 6H, Ph-*H*, $^3J_{HH}$ = 8.00 Hz), 6.90 (d, 6H, Ph-*H*, $^3J_{HH}$ = 6.6 Hz), 6.57 (s, 3H, Pz-C*H*). $^{13}C\{^1H\}$ NMR (CD_2Cl_2, 125.77 MHz, 298 K) δ (ppm): 152.2 (s, *C*(C_6H_5)), 143.0 (q, $^2J(C,F)$ = 37 Hz, *C*CF_3), 131.6 (s, Ph), 130.2 (s, Ph), 128.5 (s, Ph), 128.5 (s, *C*$_6H_6$), 128.2 (s, Ph), 121.1 (q, $^1J(C,F)$ = 269 Hz, *C*F_3), 105.0 (s, *C*H). ^{19}F NMR (CD_2Cl_2, 470.62 MHz, 298 K) δ(ppm): -61.98 (s, 9F). ATR-FTIR (Selected peak, cm^{-1}): $\bar{\upsilon}$ = 2628 (B-H). Analysis Calcd. for $C_{36}H_{25}AgBF_9N_6 \cdot 0.5CH_2Cl_2$: C, 50.17; H, 3.00; N, 9.62%. Found. C, 50.38; H, 2.99; N, 9.86%.

[HB(3-(CF_3),5-(Ph)Pz)$_3$]Ag(CO)

[HB(3-(CF_3),5-(Ph)Pz)$_3$]Na(THF) (0.25 g, 0.34 mmol) and CF_3SO_3Ag (0.087 g, 0.34 mmol) were placed in a Schlenk flask under a nitrogen atmosphere and the flask was covered aluminum foil to protect it from light. An atmosphere of CO was established and dichloromethane (25 mL) was added to the flask. The resulting mixture was stirred at RT for 1 h while gently bubbling CO, to obtain a solution with some black precipitate. It was filtered through a bed of Celite to obtain a clear colorless solution. The solution was concentrated by bubbling CO and placed in a freezer maintained at -20 °C overnight under a positive pressure of CO to obtain x-ray quality colorless crystals. Yield 0.197 g, 75%; m.p. 106-192 °C (slowly decomposes over this wide temperature range and finally melts 192 °C). ^1H NMR (CD_2Cl_2, 500.16 MHz, 298 K) δ (ppm): 7.24 (t, 3H, Ph), 6.90 (m, 12H, Ph), 6.56 (s, 3H). $^{13}C\{^1H\}$ NMR (CD_2Cl_2, 125.77 MHz, 298 K) δ (ppm): 177.4 (s,

*C*O), 151.2 (s, *C*(C6H5)), 143.2 (q, ^{2}J(C,F) = 36 Hz, *C*CF_3), 131.2 (s, Ph), 130.2 (s, Ph), 128.9 (s, Ph), 128.3 (s, Ph), 121.9 (q, ^{1}J(C,F) = 269 Hz, *C*F_3), 105.0 (s, *C*H). ^{19}F NMR (CD_2Cl_2, 470.62 MHz, 298 K) δ (ppm): -61.68 (s, 9F). ATR-FTIR (Selected peak, cm^{-1}): $\bar{\upsilon}$ = 2629 (B-H), 2148 (CO). Analysis Calcd. for $C_{31}H_{19}AgBF_9N_6O$: C, 47.66; H, 2.45; N, 10.76%. Found. C, 47.27; H, 2.07; N, 10.67%.

[HB(3-(CF_3),5-(Ph)Pz)$_3$]Ag(PPh_3)

[HB(3-(CF_3),5-(Ph)Pz)$_3$]Na(THF) (0.25 g, 0.34 mmol) and PPh_3 (0.089 g, 0.34 mmol) were dissolved in THF (10 mL) and this mixture was slowly added to a stirring solution of CF_3SO_3Ag (0.087 g, 0.33 mmol) in THF (10 mL) at 0 °C under an atmosphere of nitrogen. The flask was covered aluminum foil to protect it from light. After 1 h, the solution was allowed to warm to room temperature and stirred for additional 30 min. The reaction solvent was removed under vacuum, and the residue was extracted into toluene. The resulting mixture was filtered through bed of Celite and the solvent was removed under reduced pressure to obtain a white solid, which was thoroughly washed with hexanes and dried under vacuum. X-ray quality crystals were obtained from a dichloromethane solution stored at -20 ^{o}C. Yield: 0.274 g, 80%; m.p. 96-154 °C (slowly decomposes over this wide temperature range with a final melting point of the residue at 224 °C). ^{1}H NMR (C_6D_6, 500.16 MHz, 298 K) δ (ppm): 7.89 (m, 6H, Ph), 7.18, (m, 12H, Ph), 7.12 (m, 3H, Ph), 6.99 (m, 3H, Ph), 6.78 (m, 12H, Ph), 6.34 (s, 3H, Pz-C*H*). ^{13}C{^{1}H}

NMR (C_6D_6, 125.77 MHz, 298 K) δ (ppm): 151.8 (s, *C*Ph), 144.1 (q, ^{2}J(C,F) = 36 Hz, *C*CF_3), 135.0 (d, ^{2}J(C,P) = 17 Hz, PPh_3), 133.3 (dd, ^{1}J = 34, ^{2}J = 5 Hz, PPh_3), 132.2 (s, PPh_3), 130.9 (s, Ph), 130.5 (s, Ph), 129.3 (d, ^{3}J(C,P) = 11 Hz, PPh_3), 122.4 (q, ^{1}J(C,F) = 268 Hz, *C*F_3), 105.8 (s, *C*H). ^{19}F NMR (C_6D_6, 470.62 MHz, 298 K) δ (ppm): -60.27 (dd, ^{5}J(F,P) = 7.8 Hz, ^{4}J(F,Ag) = 1.3 Hz. ^{31}P{^{1}H} NMR (C_6D_6, 121.65 MHz, 298 K) δ (ppm): 17.8 (^{1}J(P,^{107}Ag) = 633.9 Hz, ^{1}J(P,^{109}Ag) = 732.4 Hz, ^{5}J(F,P) = 7.6 Hz). ATR-FTIR (Selected peak, cm^{-1}): $\bar{\upsilon}$ = 2623 (B-H). Analysis Calcd. for $C_{48}H_{34}AgBF_9N_6P$: C, 56.77; H, 3.37; N, 8.28%. Found. C, 56.12; H, 3.30; N, 8.25%

5.3 Experimental for Chapter 4

[(Ph_3B)CH(3,5-(CH_3)$_2$Pz)$_2$]Li(THF)

Bis(3,5-dimethylpyrazolyl)methane (0.204 g, 1.0 mmol) was added to a Schlenk flask and dissolved in THF (10 mL, dry). The solution was cooled to -78 ^{o}C using a dry ice-acetone bath and 1.6 M ethereal solution of n-BuLi (1.1 eq) was added dropwise via syringe. The contents were vigorously stirred while maintaining the reaction temperature below -70 ^{o}C for 15 minutes and triphenylborane (0.242 g, 1.0 mmol) of was added at once using a solid addition funnel. The mixture was slowly allowed to attain room temperature and stirred overnight. The solution was concentrated under vacuum, layered with hexanes and kept in -20 ^{o}C freezer to obtain the colorless crystals. Yield: 0.419 g, 80 %; m.p. 142 ^{o}C (melts at this temperature and begins to decompose at 170 ^{o}C). ^{1}H NMR

($CDCl_3$, 500.16 MHz) δ (ppm): 7.10 (m, 13H, aromatic (BPh_3), 7.09 (m, 2H, aromatic (BPh_3)), 6.43 (s, 1H, C*H*-BPh_3), 5.68 (s, 2H, Pz-*H*), 3.56 (m, 4H, THF), 2.13 (s, 6H, CH_3), 1.99 (s, 6H, CH_3), 1.81 (m, 4H, THF). $^{13}C\{^1H\}$ NMR ($CDCl_3$, 125.76 MHz) δ (ppm): 145.7 (*C*CH_3), 139.6 (*C*CH_3), 136.7 (BPh_3), 126.0(BPh_3), 123.8 (BPh_3), 104.3 (*C*H-Pz), 71.2 (*C*H-BPh_3) 68.4 (THF), 25.41 (THF), 13.2 (CH_3), 11.8 (*C*H_3). ^{11}B NMR ($CDCl_3$, 96.42 MHz) δ (ppm): -8.52. ^1H NMR (C_6D_6, 500.16 MHz) δ (ppm): 7.58 (d, 6H, Ph, $^3J_{HH}$ = 7.15 Hz), 7.25 (t, 6H, Ph, $^3J_{HH}$ = 7.45 Hz), 6.65 (s, 1H, C*H*-BPh_3), 5.57 (s, 2H, Pz-*H*), 3.18 (m, 4H, THF), 1.94 (s, C*H*$_3$), 1.80 (s, CH3), 1.20 (m, 4H, THF). $^{13}C\{^1H\}$ NMR (C_6D_6, 125.76 MHz) δ (ppm): 145.7 (s, *C*CH3), 140.0 (s, *C*CH_3), 137.4 (s, BPh_3), 126.6 (s, BPh_3), 124.3 (s, BPh_3), 104.6 (s, CH-Pz), 72.0 (*C*H-BPh_3), 68.1 (THF), 25.4 (THF) 13.3 (*C*H_3), 11.7 (*C*H_3). Anal.Calcd. for $C_{33}H_{38}BLiN_4O$: C, 75.58; H, 7.30; N, 10.68. Found: C, 75.13; H, 7.01; N, 10.52.

[(Ph_3B)CH(3,5-(CH_3)$_2$Pz)$_2$]Cu(C_2H_4)

[(Ph_3B)CH(3,5-(CH_3)$_2$Pz)$_2$]Li(THF) (0.262 g, 0.5 mmol) and (CF_3SO_3Cu)$_2$•C_6H_6 (0.125, 0.5 mmol) were added to Schlenk flask and dissolved in DCM (10 mL, dry) saturated with the C_2H_4. The mixture was stirred under positive pressure of C_2H_4 for 2h. The resulting white precipitate (LiOTf) was removed by filtration through a bed of Celite and the colorless filtrate was concentrated by bubbling C_2H_4. The concentrated solution was stored under C_2H_4 atmosphere in a -20 ^oC freezer to obtain x-ray quality crystals. Yield: 0.188 g, 70%,

m.p. 125 ^{o}C (slowly starts to turn brown at this temperature and completely decomposes at 138 ^{o}C). ^{1}H NMR (CD_2Cl_2, 500.16 MHz) δ (ppm): 6.99 (m, 10H, (BPh_3), 6.83 (m, 5H, BPh_3), 6.63 (s, 1H, C*H*-BPh_3), 5.79 (s, 2H, Pz-*H*), 3.68 (s, 4H, C_2H_4), 2.12 (s, 6H, CH_3), 2.03 (s, 6H, CH_3). ^{13}C{^{1}H} NMR (CD_2Cl_2, 125.76 MHz) δ (ppm): 147.7 (*C*CH_3), 140.8 (*C*CH_3), 136.7 (BPh_3), 125.8 (BPh_3), 123.8 (BPh_3), 105.6 (*C*H-Pz), 80.4 (C_2H_4), 68.6 (*C*H-BPh_3), 13.8 (*C*H_3), 11.8 (*C*H_3). ^{11}B NMR (CD_2Cl_2, 96.42 MHz) δ (ppm): -8.19. ^{1}H NMR ($CDCl_3$, 500.16 MHz) δ (ppm): 6.98 (m, 15H, BPh_3), 6.68 (s, 1H, C*H*-BPh_3), 5.78 (s, 2H, Pz-*H*), 3.69 (s, 4H, C_2H_4), 2.16 (s, 6H, C*H*$_3$), 2.05 (s, 6H, C*H*$_3$). ^{13}C{^{1}H} NMR ($CDCl_3$, 125.76 MHz) δ (ppm): 147.4 (*C*CH_3), 140.9 (*C*CH_3), 137.0 (BPh_3), 126.0 (BPh_3), 124.0 (BPh_3), 105.8 (*C*H-Pz), 80.3 (C_2H_4), 14.3 (*C*H_3), 12.1 (*C*H_3). Raman (Selected peak, cm^{-1}): ῡ = 1523 (C=C). Anal.Calcd. for $C_{31}H_{32}BCuN_4$: C, 69.60; H, 6.03; N, 10.47%. Found: C, 69.32; H, 5.63; N, 10.17%.

[(Ph_3B)CH(3,5-(CH_3)$_2$Pz)$_2$]Cu(*cis*-CH_3HC=$CHCH_3$)

[(Ph_3B)CH(3,5-(CH_3)$_2$Pz)$_2$]Li(THF) (0.100 g, 0.191 mmol) and (CF_3SO_3Cu)$_2$•C_6H_6 (0.048 g, 0.095 mmol) were added to Schlenk flask under a nitrogen atmosphere and *cis*-2-butene was gently bubbled through dichloromethane (10 mL, dry) in a separate flask for ~2 min. and the resulting solution was slowly added via syringe. After the addition, 2-butene was gently bubbled for ~2 min. and the mixture was stirred for 2 h. The resulting white precipitate (LiOTf) was removed by filtration through a bed of Celite and the filtrate was concentrated under

reduced pressure. The concentrated solution was stored at -20 ^{o}C freezer after bubbling 2-butene for ~1 min. to obtain x-ray quality crystals. Yield: 0.085 g, 79%, m.p. 134 ^{o}C (slowly starts to melt at this temperature and completely decomposes at 146 ^{o}C). ^{1}H NMR ($CDCl_3$, 500.16 MHz) δ (ppm): 7.02 (m, 10H, BPh_3, 6.90 (m, 5H, BPh_3), 6.76 (s, 1H, C*H*-BPh_3), 5.72 (s, 2H, Pz-*H*), 4.90 (br, 2H, $(CH_3)_2C_2H_2$), 2.23 (s, 6H, CH_3), 2.01 (s, 6H, CH_3) 1.49 (d, 6H, $(CH_3)_2C_2H_2$, $^{3}J_{HH}$ = 4.60). ^{13}C{^{1}H} NMR ($CDCl_3$, 125.77 MHz) δ (ppm): 146.9 (CCH_3), 140.8 (CCH_3), 136.6 (BPh_3), 126.1 (BPh_3), 123.8 (BPh_3), 105.7 (*C*H-Pz), 14.0 (CH_3), 13.5 (($CH_3)_2C_2H_2$), 12.3 (CH_3). ^{11}B NMR ($CDCl_3$, 96.42 MHz): δ -7.96. ^{1}H NMR (CD_2Cl_2, 500.16 MHz, 253 K) δ (ppm): 7.01 (m, 10H, BPh_3, 6.88 (m, 5H, BPh_3), 6.73 (s, 1H, C*H*-BPh_3), 5.76 (s, 2H, Pz-*H*), 4.79 (br, 2H, $(CH_3)_2C_2H_2$), 2.23 (s, 6H, CH_3), 2.01 (s, 6H, CH_3) 1.46 (d, 6H, $(CH_3)_2C_2H_2$, $^{3}J_{HH}$ = 4.00). ^{13}C{^{1}H} NMR (CD_2Cl_2, 125.77 MHz, 253 K): δ 147.7 (CCH_3), 141.1 (CCH_3), 136.6 (BPh_3), 126.8, 126.5 (BPh_3), 124.2 (BPh_3), 105.9 (*C*H-Pz), 95.0 (br, $(CH_3)_2C_2H_2$), 74.4 (br, *C*H-BPh_3), 14.1 (CH_3), 13.9 (($CH_3)_2C_2H_2$), 12.5 (CH_3), 12.3 (CH_3). ^{11}B NMR ($CDCl_3$, 96.42 MHz): δ -7.97. Raman (Selected peak, cm^{-1}): ῡ = 1535 (C=C). Anal.Calcd. for $C_{33}H_{38}BCuN_4$•0.1CH_2Cl_2: C, 69.32; H, 6.71; N, 9.77%. Found: C, 69.96; H, 6.53; N, 8.56%.

[(Ph_3B)CH(3,5-$(CH_3)_2$Pz)$_2$]Cu(CO)

[(Ph_3B)CH(3,5-$(CH_3)_2$Pz)$_2$]Li(THF) (0.250 g, 0.477 mmol) and $(CF_3SO_3Cu)_2$•C_6H_6 (0.075, 0.238 mmol) were added to Schlenk flask and dissolved

in DCM (10 mL, dry) saturated with carbon monoxide (CO). The mixture was stirred under positive pressure of CO for 2h. The resulting white precipitate (LiOTf) was removed by filtration through a bed of Celite and the filtrate was concentrated by bubbling CO. The concentrated solution was stored under a CO atmosphere in a -20 ^{o}C freezer to obtain x-ray quality crystals. Yield: 0.190 g, 74%, m.p. 105 - 118 ^{o}C (slowly melts over this wide range and decomposes at 172 ^{o}C). ^{1}H NMR ($CDCl_3$, 500.16 MHz) δ (ppm): 7.12 – 7.01 (m, 15H, BPh_3), 6.31 (s, 1H, C*H*-BPh_3), 5.80 (s, 2H, Pz-*H*), 2.15 (s, 6H, CH_3), 2.12 (s, 6H, CH_3). ^{13}C{^{1}H} NMR ($CDCl_3$, 125.76 MHz) δ (ppm): 146.4 (s, *C*CH_3), 140.3 (s, *C*CH_3), 136.9 (BPh_3), 126.4 (BPh_3), 124.2 (BPh_3), 105.0 (*C*H-Pz), 13.8 (*C*H_3), 11.7 (*C*H_3). ^{11}B NMR ($CDCl_3$, 96.42 MHz) δ (ppm): -8.46. ATR-FTIR (Selected peak, cm^{-1}): ῡ = 2092 (CO)**.** Anal.Calcd. for $C_{30}H_{30}BCuN_4O$•0.3CH_2Cl_2: C, 64.71; H, 5.48; N, 9.96%. Found: C, 65.07; H, 5.00; N, 8.72%.

Chapter 6

General Summary

6.1 Chapter 2 Summary

The synthesis and complete characterization of [HB(3-(CF_3),5-(CH_3)Pz)$_3$]M(C_2H_4) (M = Au, Ag, and Cu) and the related silver complex [HB(3-(CF_3),5-(Ph)Pz)$_3$]Ag(C_2H_4) have been reported. These isoleptic group 11 metal-ethylene adducts are thermally stable and show moderate stability in air. The silver complex completes a second set of previously reported isoleptic complexes. Additional M→ethylene backbonding is observed in the ^{1}H and ^{13}C NMR spectra for the complexes supported by [HB(3-(CF_3),5-(CH_3)Pz)$_3$]$^-$ compared to those supported by [HB(3,5-(CF_3)$_2$Pz)$_3$]$^-$, or [HB(3-(CF_3),5-(Ph)Pz)$_3$]$^-$.

These complexes also show interesting properties in the NMR moving down the group from Cu to Au. This is most pronounced for the complexes supported by [HB(3-(CF_3),5-(CH_3)Pz)$_3$]$^-$. The gold adduct shows the strongest M-ethylene interaction with the ^{13}C and ^{1}H resonances of ethylene shift upfield from free ethylene by 64.8, and 1.93 ppm, respectively. The copper adduct shows moderately strong M-ethylene interaction with the ethylene resonances shift upfield by 38.3 ppm (^{13}C), and by 0.69 ppm (^{1}H). The silver adducts show the weakest M-ethylene interaction and have the smallest upfield shift for the ^{13}C resonance for

ethylene of just 19.6 ppm and shows a downfield shift of the ^{1}H resonances of 0.05 ppm.

Examining the x-ray structures confirms these observations. The gold atoms bind to the scorpionate in κ^2-fashion, displacing one arm of the ligand. The gold atoms have trigonal planar geometry and are ligated by two arms of the Tp ligand and ethylene. The silver atoms show weak interaction with the scorpionate and ethylene, and feature essentially κ^3-bonded scorpionates. The copper adducts show moderately strong interactions with both Tp and ethylene, and show scorpionate coordination approaching the κ^2-mode. Unfortunately, the $M(C_2H_4)$ fragments in these complexes are disordered. Nevertheless, the M-C and M-N bond distances of the $[HB(3\text{-}(CF_3),5\text{-}(CH_3)Pz)_3]M(C_2H_4)$ and $[HB(3\text{-}(CF_3),5\text{-}(Ph)Pz)_3]M(C_2H_4)$ complexes show that they follow the same trend as the corresponding covalent radii of M(I).

These data support the hypothesis that the M→ethylene backbonding, and ethylene disassociation are essential to the ethylene response in plants. Silver ions are well-known inhibitors of the ethylene response, however gold ions do not block ethylene perception, but do limit the response compared to copper ions.[11, 207] As presented above, silver adducts of Tp bind ethylene, but exhibit weak Ag→ethylene backbonding. This likely reduces the effects felt by the surrounding metal chelating ligands in the receptor, preventing the ethylene response. Conversely, the gold adducts of Tp bind tightly to ethylene and this interaction may prevent the loss of

ethylene in the receptor and hinder the rearrangement necessary for the receptor to signal downfield. Copper then must exhibit the right balance to allow for both Cu→Ethylene backbonding and the displacement of ethylene and therefore cause the ethylene response.

6.2 Chapter 3 Summary

We have reported the isolation and characterization of the three new silver(I) complexes [HB(3-(CF_3),5-(Ph)Pz)$_3$]Ag(L) (L = benzene (C_6H_6), carbon monoxide (CO), and triphenylborane (PPh_3)). These silver(I) adducts can be obtained by the reaction of AgOTf and [HB(3-(CF_3),5-(Ph)Pz)$_3$]Na(THF) in dichloromethane containing the corresponding co-ligand. Solid samples of these compounds can be handled briefly in air and do not show any apparent signs of decomposition if briefly exposed to fluorescent lighting. The benzene and carbonyl adducts of silver Scorpionates are particularly rare in the literature.

The x-ray crystallographic data for [HB(3-(CF_3),5-(Ph)Pz)$_3$]Ag(η^2-C_6H_6) shows an η^2-bound benzene on silver(I) with equal Ag-C bond distances. The benzene molecule is tilted slightly away from the face of silver and the angle between the Ag-C31-C32 plane and the plane of the benzene ring about 102°. The ^{13}C and ^{1}H NMR spectra in CD_2Cl_2 at room temperature show a single carbon signal and one sharp proton peak corresponding to the benzene moiety, and only one fluorine peak corresponding to the scorpionate ligand. This indicates the

presence of a fluxional benzene ligand in solution. The ^{1}H resonance of C_6H_6 is observed at δ 7.42 ppm in CD_2Cl_2 and shows a small down-field shift compared to the corresponding peak at δ 7.35 ppm for free benzene in the same solvent.[123]

The infrared spectrum of [HB(3-(CF_3),5-(Ph)Pz)$_3$]Ag(CO) shows the characteristic $\bar{\upsilon}_{co}$ band at 2148 cm^{-1}. This complex exhibits nonclassical metal carbonyl behavior and the increased stretching frequency of CO is indicative of a significantly diminished Ag→CO π-backbonding. $^{107/109}$Ag-^{13}C coupling is not observed for this compound in solution indicating the presence of a labile CO ligand that dissociates-coordinates rapidly in CD_2Cl_2 on the NMR timescale. The Ag-C bond distance for [HB(3-(CF_3),5-(Ph)Pz)$_3$]Ag(CO) is observed to be 2.019(2) Å and lies closer to the shorter end of the spectrum for all known Ag-CO compounds. The CO and C_6H_6 compounds can be readily converted in the presence of an excess of the opposite co-ligand, further supporting the labial nature of these CO and benzene moieties.

The ^{19}F and ^{19}P NMR spectra of the phosphine adduct [HB(3-(CF_3),5-(Ph)Pz)$_3$]Ag(PPh_3) show interesting coupling between the ^{19}F and ^{31}P nuclei and to the spin active silver.

The ^{19}F and ^{31}P NMR spectra are the most interesting as they not only show coupling to each other but also to spin active silver nuclei (I = ½; ^{109}Ag (48.2%) and ^{107}Ag (51.8%)). For example, the ^{19}F resonance corresponding to the CF_3 groups at pyrazolyl moiety 3-positions appear as a doublet of doublet and the ^{31}P

NMR spectrum appears as a doublet of doublet of multiplet. These couplings are well resolved. The 31P signal shows coupling to the spin active silver and shows spin-spin coupling to nine fluorine atoms of the CF_3 groups. The well resolved coupling in [HB(3-(CF_3),5-(Ph)Pz)$_3$]Ag(PPh_3) points to the lack of Scorpionate and PPh_3 ligand dissociation (even $\kappa^3 \leftrightarrow \kappa^2$ interconversion) on the NMR timescale. Further investigation is needed to determine these observed "long-range" couplings are a results of through-bond or through-space coupling.

The examples presented here show that silver forms complexes with weakly coordinating ligands. These weak interactions show that it plausible that silver can occupy the coordinating pocket in ETR1 and bind ethylene without causing a downfield signal from the receptor. These complexes also show that silver may be good for applications involving the capture of small molecule ligands and gases such as ethylene, CO, and benzene. Additionally, silver Scorpionates supported by weakly coordinating ligands are useful in catalysis and as ligand transfer agents.

6.3 Chapter 4 Summary

The design of a new monoionic bidentate analog of bis(pyrazolyl)borate has been described using closely related bis(pyrazolyl)methane and triarylboron. Specifically, we have described the preparation of [(Ph_3B)CH(3,5-(CH_3)$_2$Pz)$_2$)]Li(THF) from bis(pyrazolyl)methane, n-butyllithium, and triphenylborane. [(Ph_3B)CH(3,5-(CH_3)$_2$Pz)$_2$]Li(THF) is a white solid that melts around 142 °C. It is evident that the CH_2 backbone has been deprotonated due to

the downfield shift of the ^{1}H resonance of the C-H moiety related to the backbone observed and was confirmed by the relative integration values comparing to the protons of the pyrazolyl moieties. The single broad ^{11}B resonance is observed at δ -8.52 ppm in $CDCl_3$ is indicative of a four coordinate boron center, and is shifted dramatically compared to that of the triphenylborane starting material which is observed at δ 60.2 ppm.[185] The ligand structure was confirmed by CHN analysis and by x-ray crystallography.

The copper(I) adducts $[(Ph_3B)CH(3,5\text{-}(CH_3)_2Pz)_2]Cu(L)$ (where L = C_2H_4, *cis*-$CH_3HC{=}CHCH_3$, and CO) were prepared from $[(Ph_3B)CH(3,5\text{-}(CH_3)_2Pz)_2]Li(THF)$, copper triflate, and the corresponding co-ligand in dichloromethane. Analysis of the X-ray crystallographic data revealed that the ligand binds in κ^2N-fashion with the BPh_3 fragment rotated around such that one phenyl group sits over the metal center. These complexes have been characterized by NMR spectroscopy, and X-ray crystallography.

The ethylene adduct $[(Ph_3B)CH(3,5\text{-}(CH_3)_2Pz)_2)]Cu(C_2H_4)$ is the first of its ethylene adduct isolated from bidentate pyrazole based ligand system. The carbon and proton signals of ethylene are shifted moderately upfield from free ethylene (δ 123.2 and 5.40 ppm) and appear at δ 80.4 and 3.68 ppm in CD_2Cl_2. The upfield shift of the ethylene carbon resonances is typical for metal-ethylene complexes, and the ethylene carbon and proton resonances of $[(Ph_3B)CH(3,5\text{-}$

$(CH_3)_2Pz)_2]Cu(C_2H_4)$ appear at a normal region expected for copper(I)-ethylene compounds.

X-ray crystallographic characterization of $[(Ph_3B)CH(3,5-(CH_3)_2Pz)_2]Cu(cis\text{-}CH_3HC{=}CHCH_3)$ show that the methyl groups of *cis*-2-btuene extend toward the BPh_3 moiety and limit the encroachment of the BPh_3 fragment. ^1H resonances of the protons near the π system of *cis*-2-butene appear as broad peaks at δ 4.90 ppm. The ^1H resonances of the protons near the π system appear as a broad peak at δ 4.79 ppm in CD_2Cl_2 and is shifted upfield from the corresponding signals for free *cis*-2-butene, which appear as a well-defined quartet at δ 5.46 ppm in $CDCl_3$. The ^{13}C resonance of the sp^2 carbons shift upfield comparably to that observed for the ethylene complex and appears as a broad singlet at δ 74.3 ppm in CD_2Cl_2.

X-ray analysis of $[(Ph_3B)CH(3,5\text{-}(CH_3)_2Pz)_2]Cu(CO)$ revealed that this adduct has the deepest $Cu(N\text{-}N)_2C$ boat with a Cu•••B distance of 3.33 Å and the nearest $Cu\text{-}C_{Phenyl}$ distance at just 2.61 Å. The geometry around copper can better be described as trigonally distorted tetrahedron, with the approaching B-phenyl group as the fourth electron domain. The characteristic CO frequency for $[(Ph_3B)CH(3,5\text{-}(CH_3)_2Pz)_2]Cu(CO)$ was observed at $\bar{\upsilon}$ 2092 cm^{-1}, and is lower than that of free CO ($\bar{\upsilon}$ 2143 cm^{-1}). This CO stretching frequency indicates moderately strong M→CO π-back-donation. The CO frequency of $[(Ph_3B)CH(3,5\text{-}(CH_3)_2Pz)_2]Cu(CO)$ was observed at 2092 cm^{-1} by infrared spectroscopy, which is

lower than that of the free CO ($\bar{\upsilon}$ 2143 cm^{-1}). The CO band of $(Ph_3B)CH(3,5\text{-}(CH_3)_2Pz)_2]Cu(CO)$ was observed at 2091 cm^{-1} by Raman spectroscopy and is in good agreeance with the infrared data. The ^{13}C resonance of CO was not observed in $CDCl_3$.

The bidentate complexes presented here represent an active site in ETR1 coordinated by the nitrogen of two histidine residues. $[(Ph_3B)CH(3,5\text{-}(CH_3)_2Pz)_2]^-$ is more electron rich than the similar bis(pyrazolyl)borate analogs and exhibits strong interactions between the copper center and coordinated olefin. The ethylene and cis-2-butene complexes presented here are the first small olefin adducts reported for a bidentate pyrazole based ligand system.

6.4 Future Work

The research that was performed during these studies have advanced the general knowledge of tri(pyrazoyl)borate and bis(pyrazoyl)methane based models of ETR1 and have added to the known coinage metal adducts in the literature. However, the ultimate goal of isolating a copper-cyclopropene adducts has not yet been accomplished. The silver Scorpionates can be explored for applications in catalysis and as ligand transfer agents. The $[(Ph_3B)CH(3,5\text{-}(CH_3)_2Pz)_2]^-$ ligand has shown to be particularly useful for the isolation of electron rich metal adducts and the chemistries of this ligand and complexes will continued to be explored. The versatile complexes presented in this work can be explored in various avenues and

the direction of the continued research will ultimately depend on the continued research interests moving forward.

Appendix A

Spectral Data for Selected Compounds

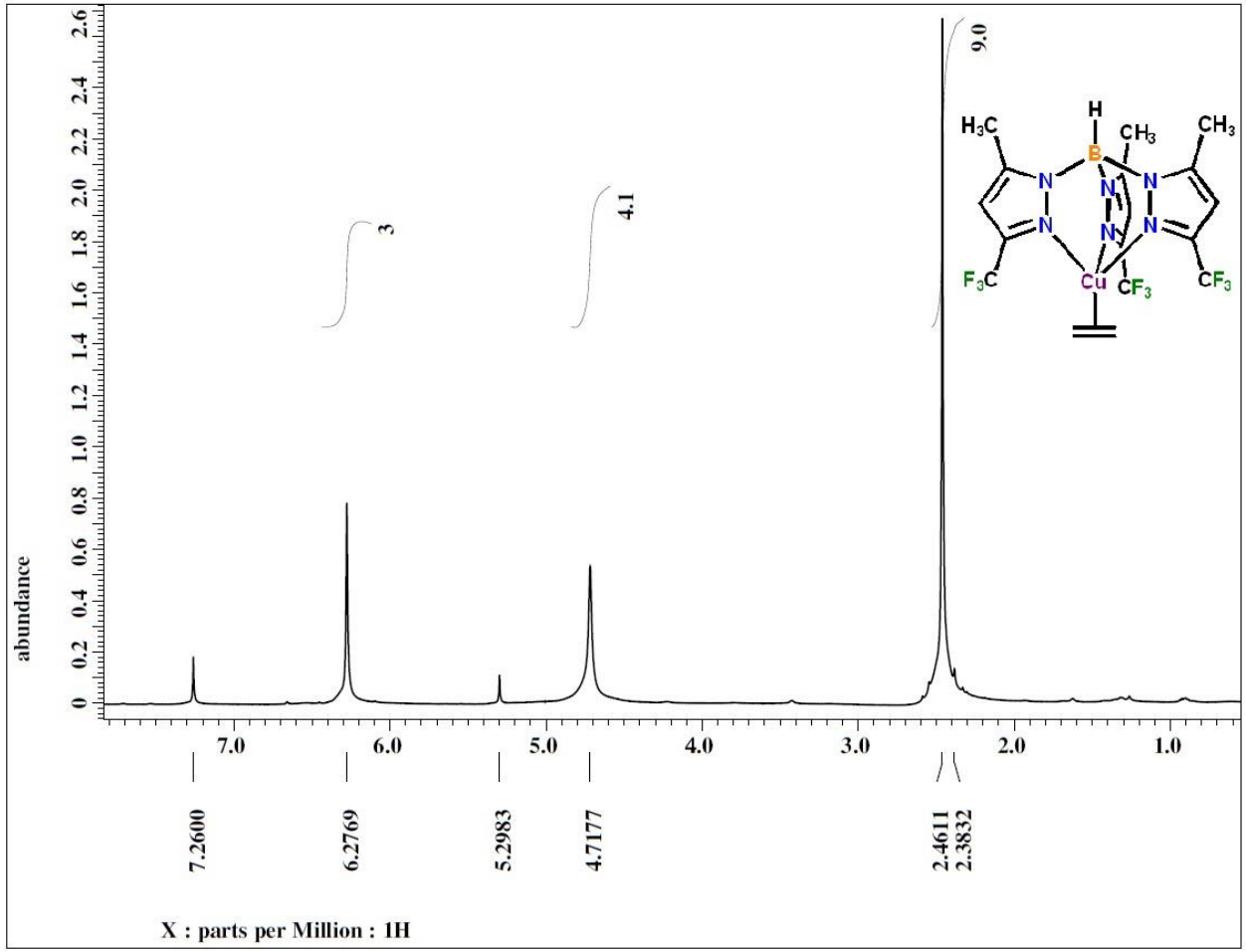

^{1}H NMR Spectrum of [HB(3-(CF_3),5-(CH_3)Pz)$_3$]Cu(C_2H_4) in $CDCl_3$

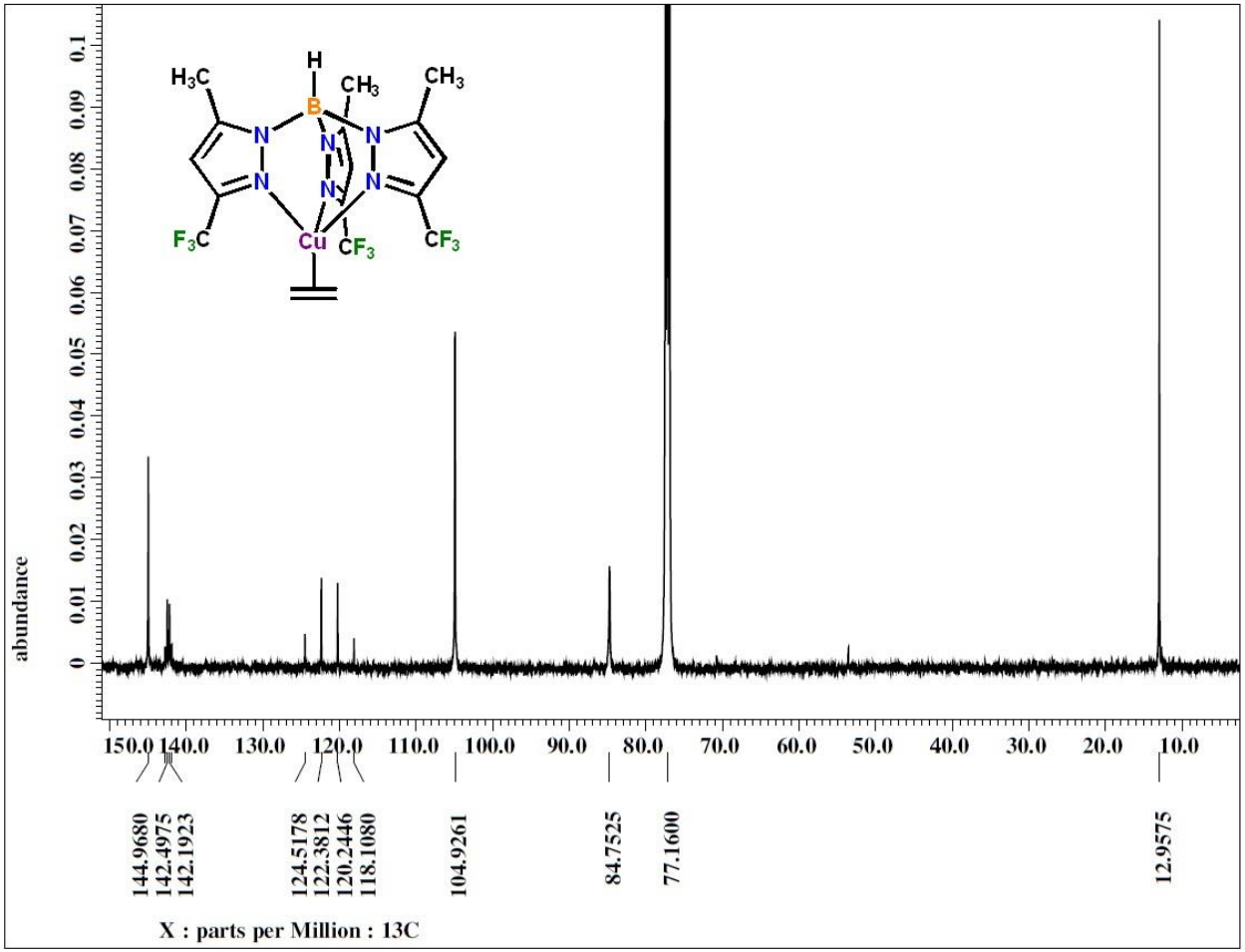

^{13}C NMR Spectrum of $[HB(3\text{-}(CF_3),5\text{-}(CH_3)Pz)_3Cu(C_2H_4)$ in $CDCl_3$

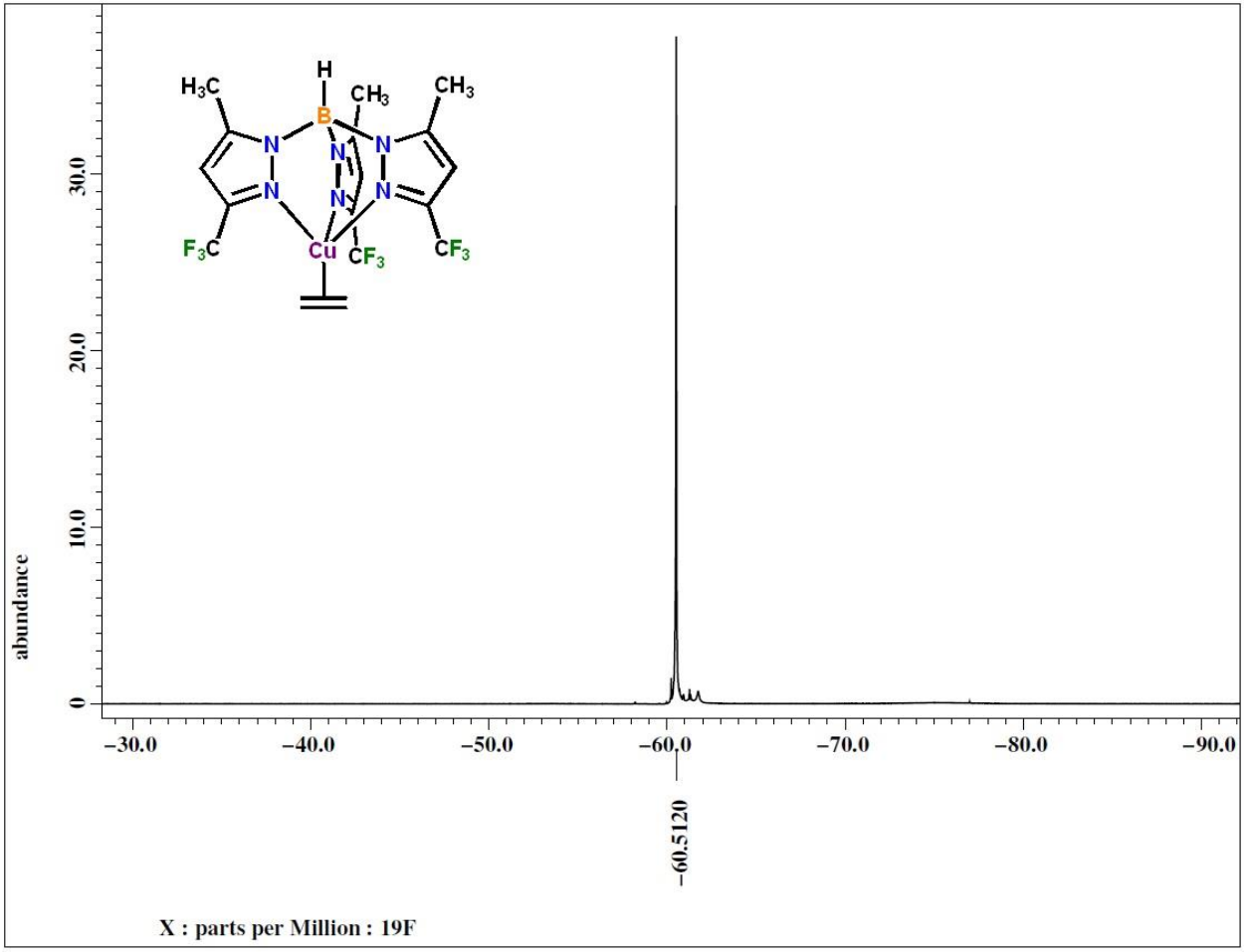

^{19}F NMR Spectrum of [HB(3-(CF_3),5-(CH_3)Pz)$_3$]Cu(C_2H_4) in $CDCl_3$

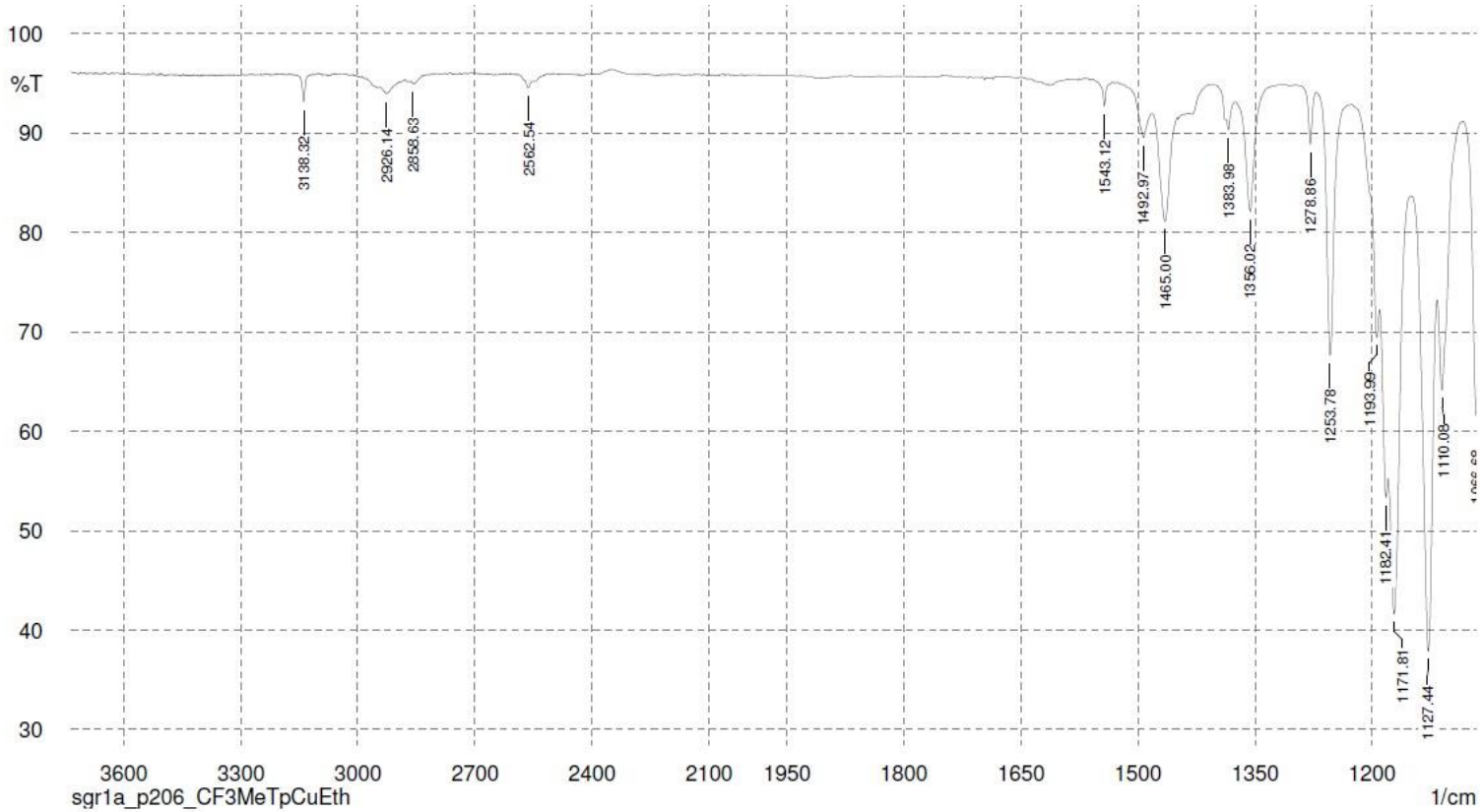

Infrared spectrum of $[HB(3\text{-}(CF_3),5\text{-}(CH_3)Pz)_3]Cu(C_2H_4)$ (neat)

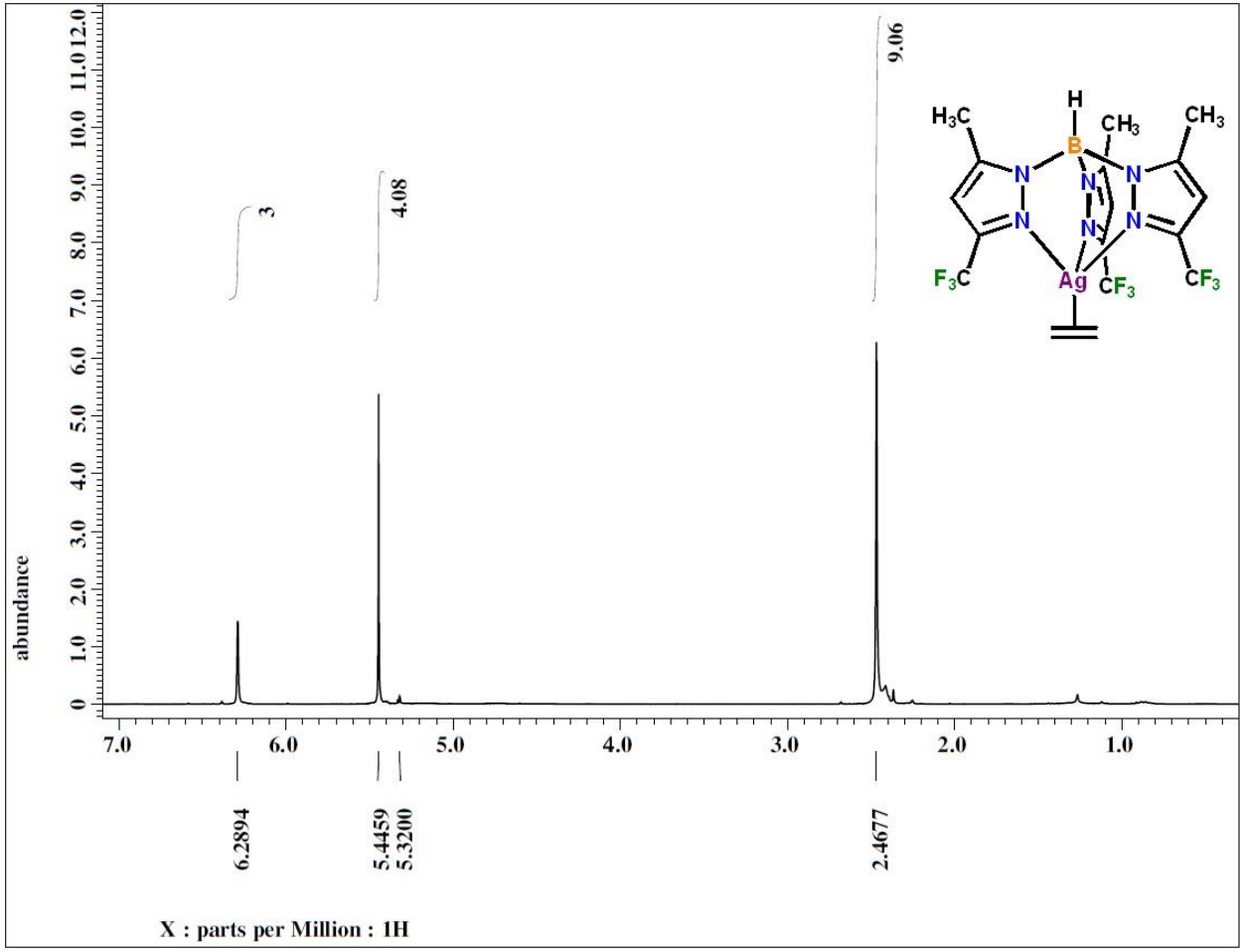

^{1}H NMR Spectrum of [HB(3-(CF_3),5-(CH_3)Pz)$_3$]Ag(C_2H_4) in CD_2Cl_2

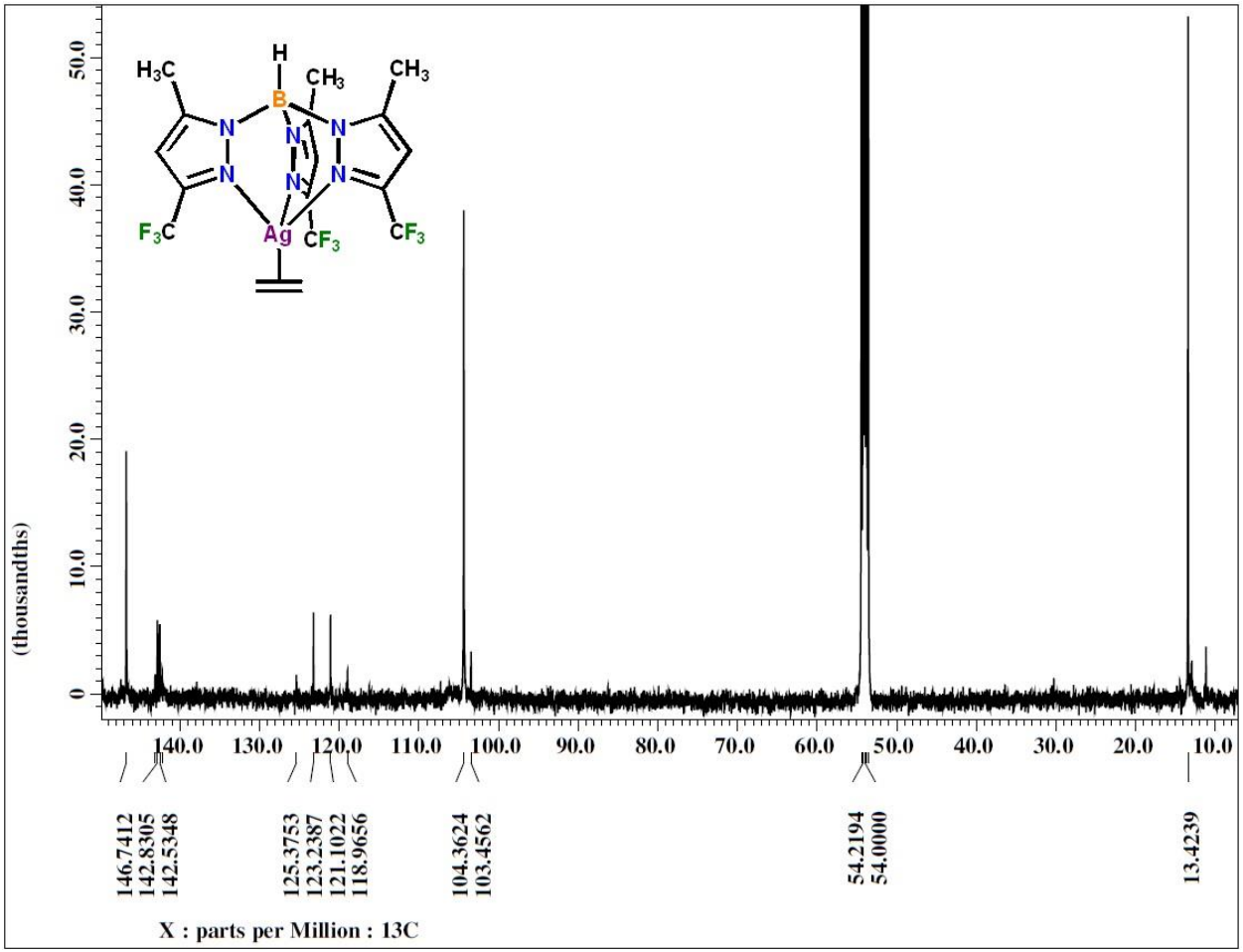

^{13}C NMR Spectrum of $[HB(3\text{-}(CF_3),5\text{-}(CH_3)Pz)_3]Ag(C_2H_4)$ in CD_2Cl_2

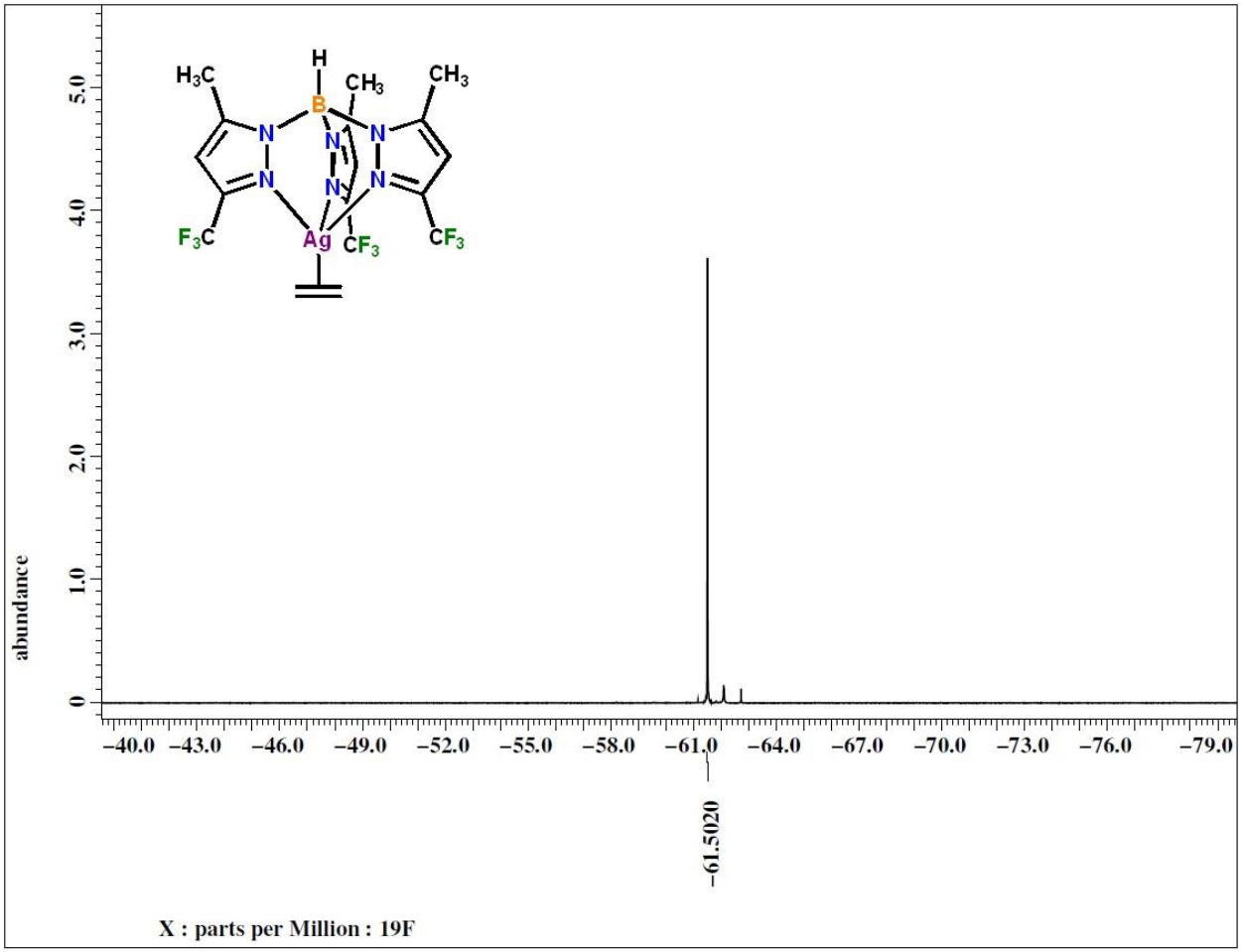

^{19}F NMR Spectrum of [HB(3-(CF_3),5-(CH_3)Pz)$_3$]Ag(C_2H_4) in CD_2Cl_2

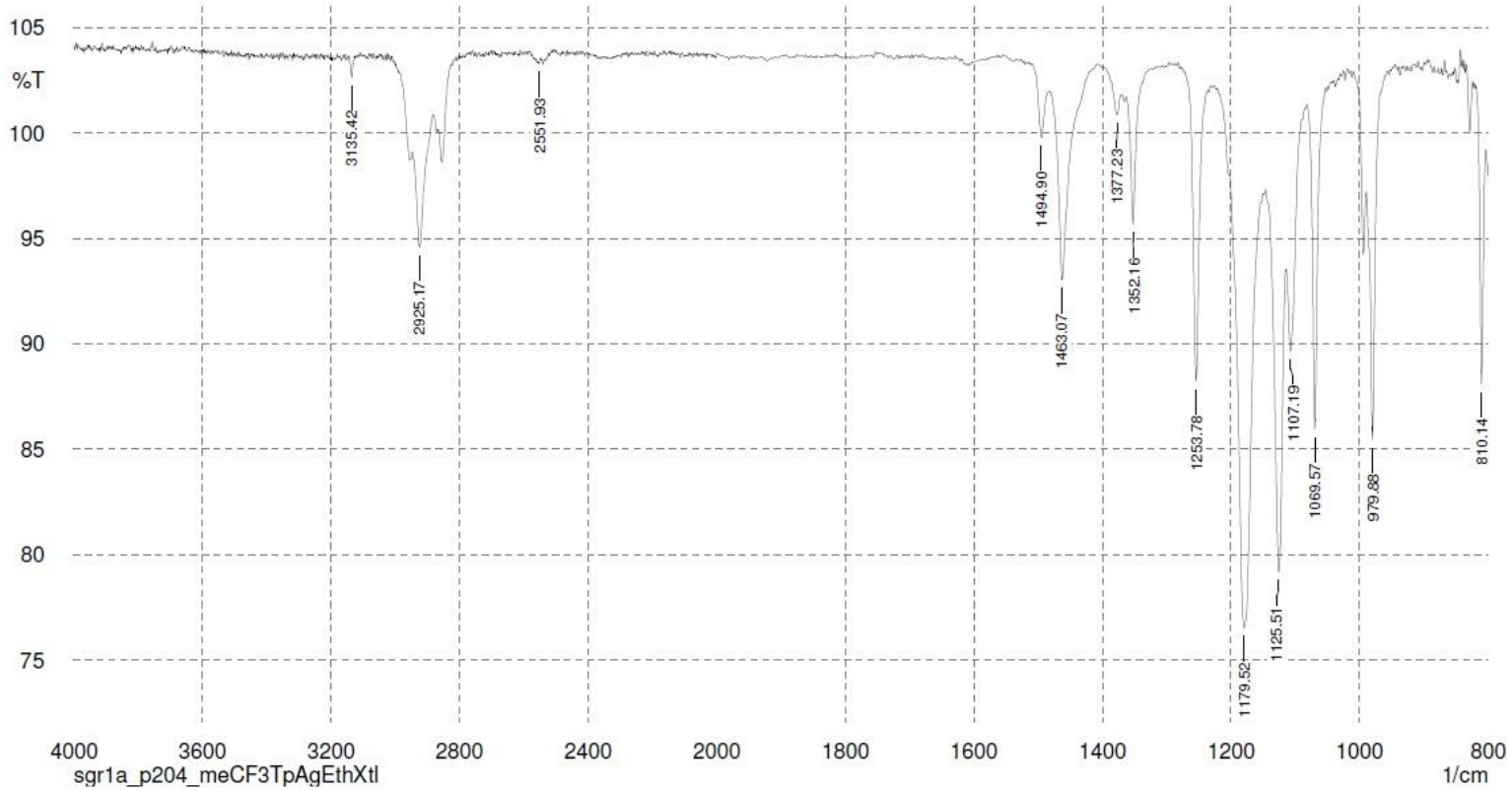

Infrared spectrum of $[HB(3\text{-}(CF_3),5\text{-}(CH_3)Pz)_3]Ag(C_2H_4)$ (neat)

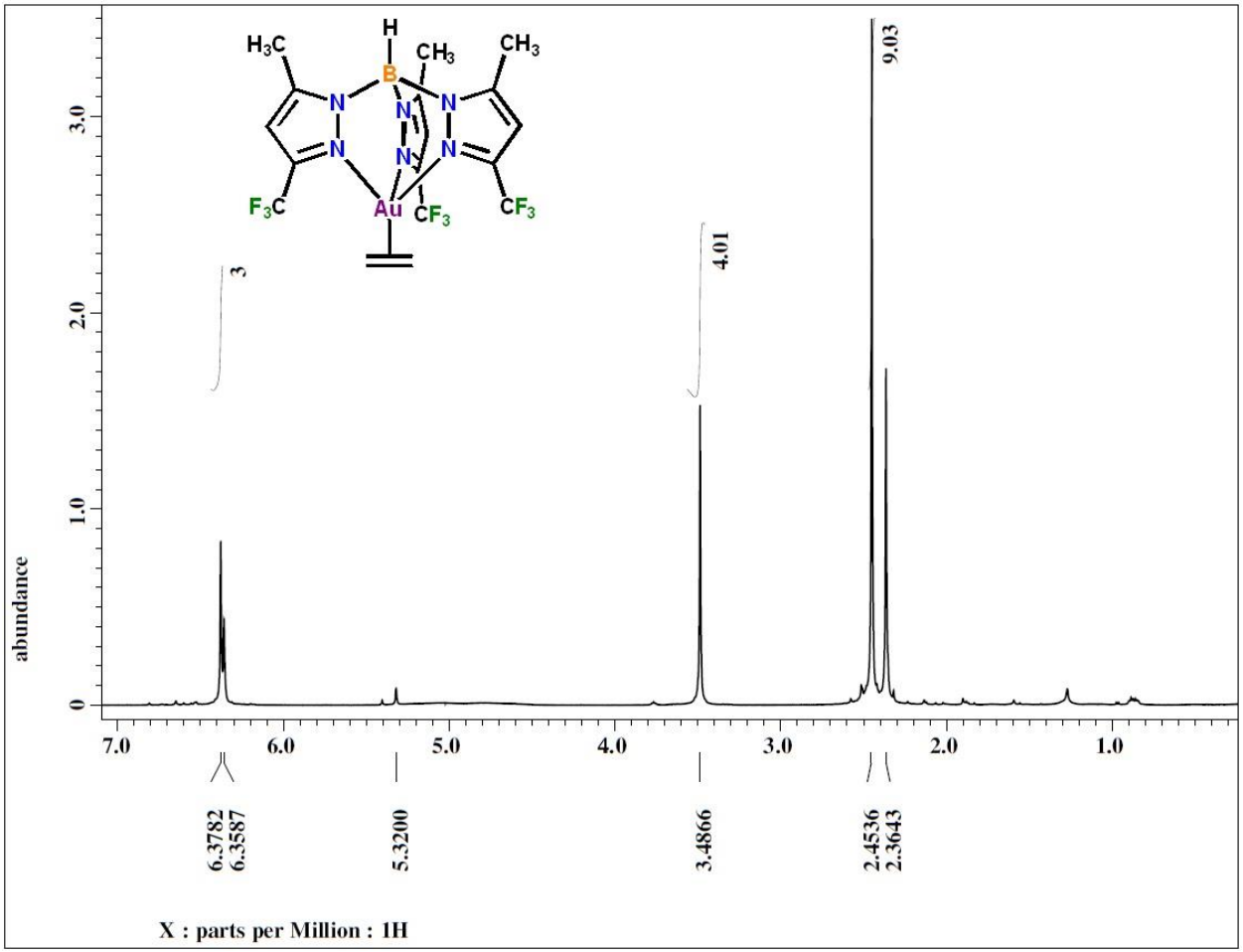

^{1}H NMR Spectrum of [HB(3-(CF_3),5-(CH_3)Pz)$_3$]Au(C_2H_4) in CD_2Cl_2

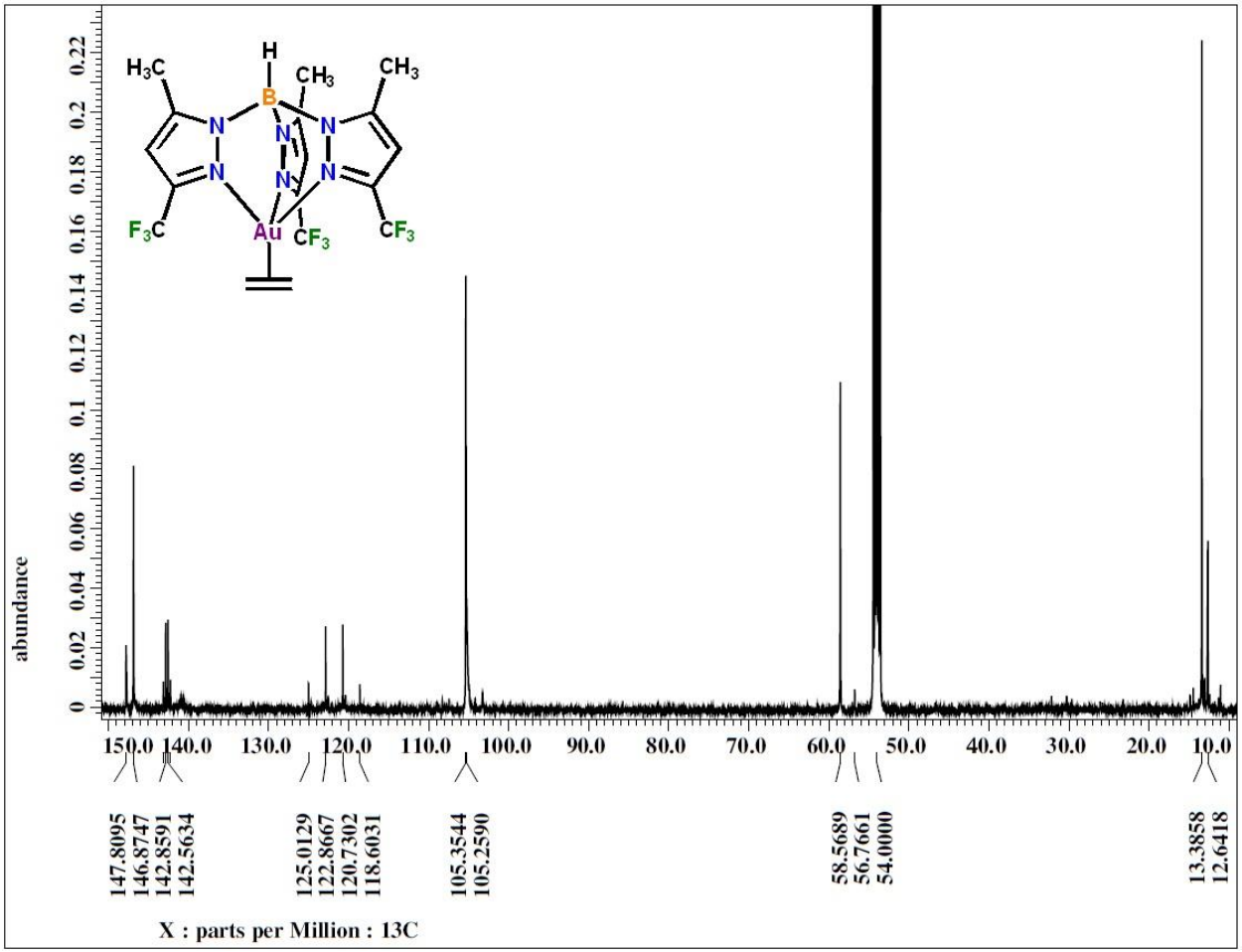

^{13}C NMR Spectrum of $[HB(3\text{-}(CF_3),5\text{-}(CH_3)Pz)_3]Au(C_2H_4)$ in CD_2Cl_2

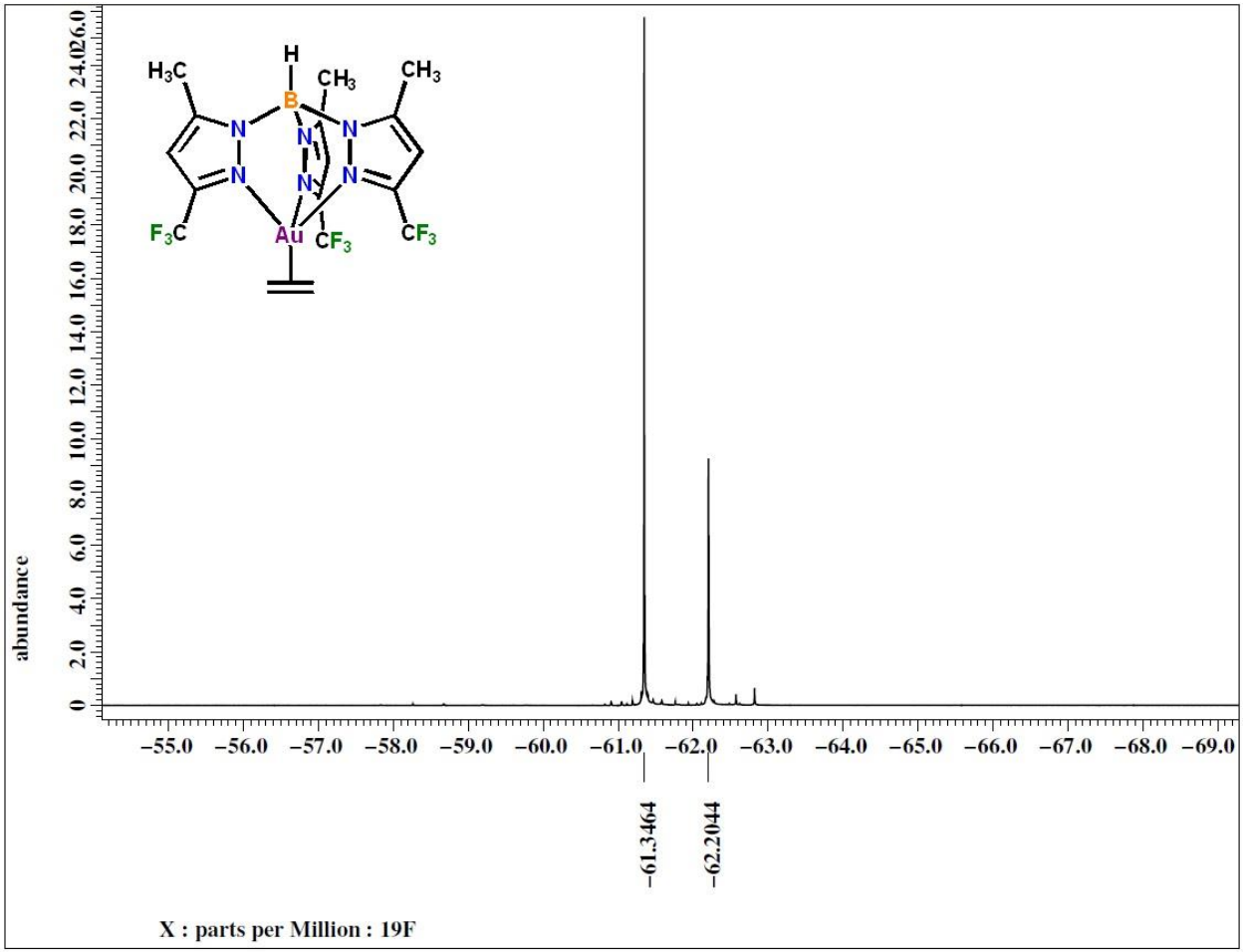

^{19}F NMR Spectrum of $[HB(3\text{-}(CF_3),5\text{-}(CH_3)Pz)_3]Au(C_2H_4)$ in CD_2Cl_2

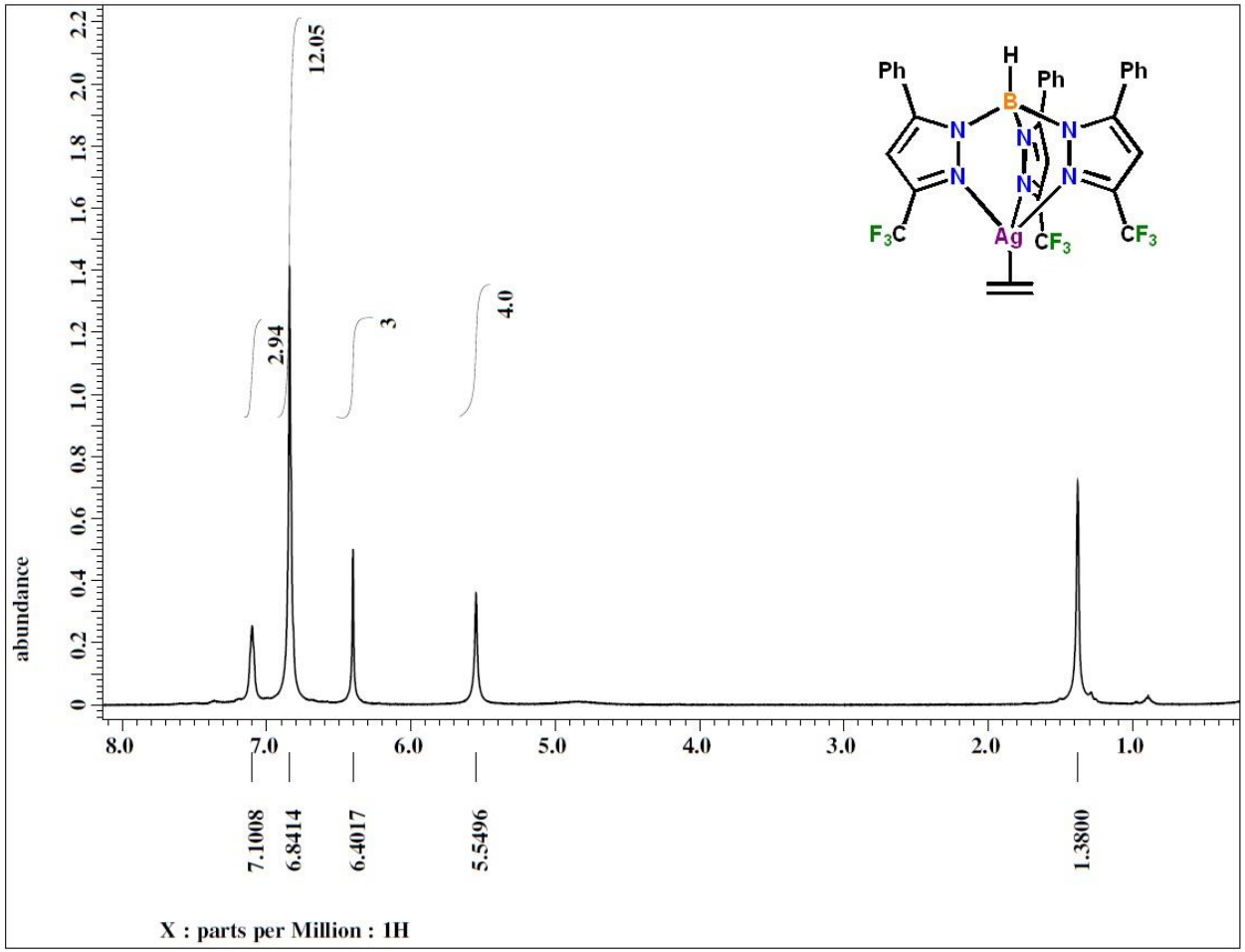

^{1}H NMR Spectrum of [HB(3-(CF_3),5-(Ph)Pz)$_3$]Ag(C_2H_4) in C_6D_{12}

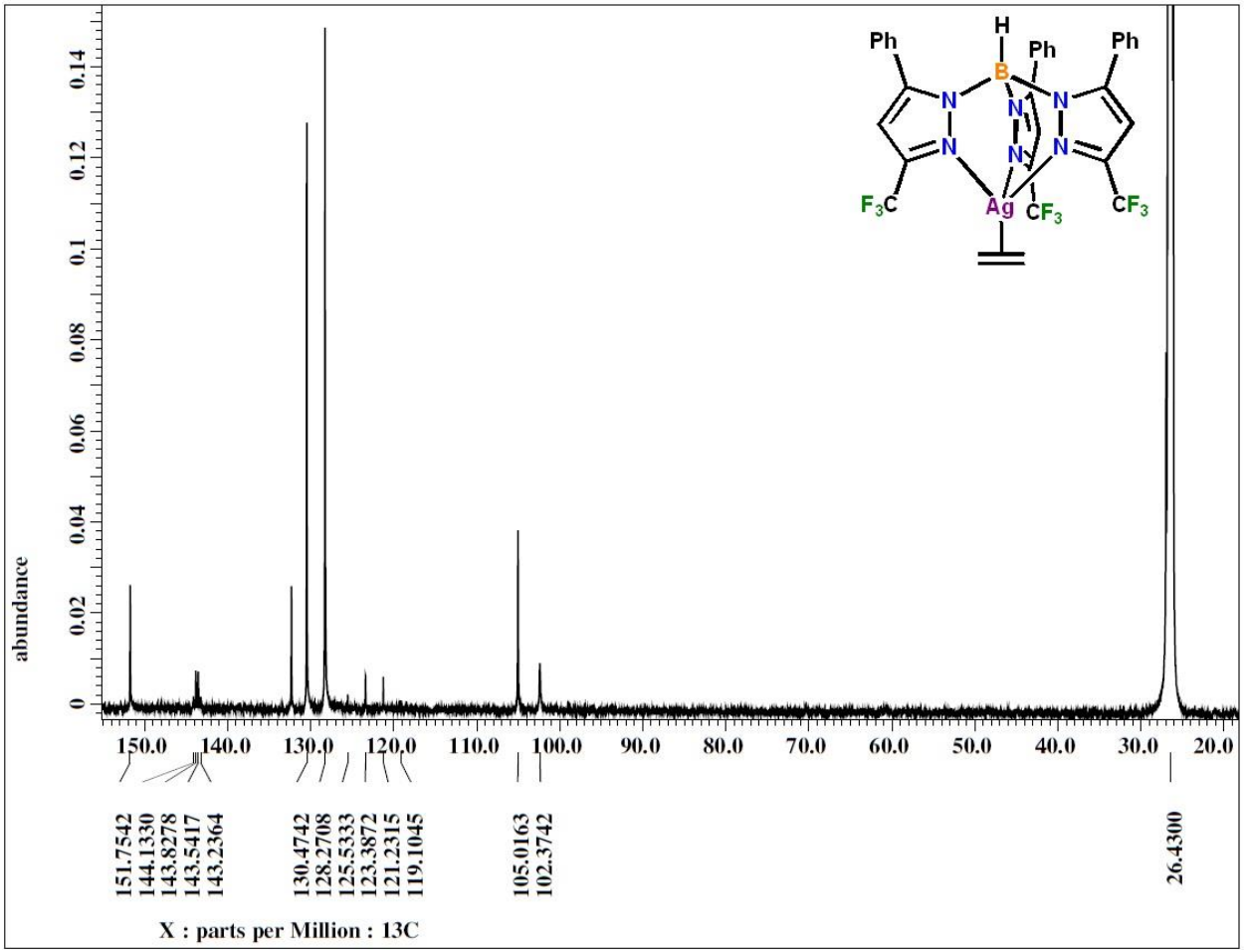

^{13}C NMR Spectrum of $[HB(3\text{-}(CF_3),5\text{-}(Ph)Pz)_3]Ag(C_2H_4)$ in C_6D_{12}

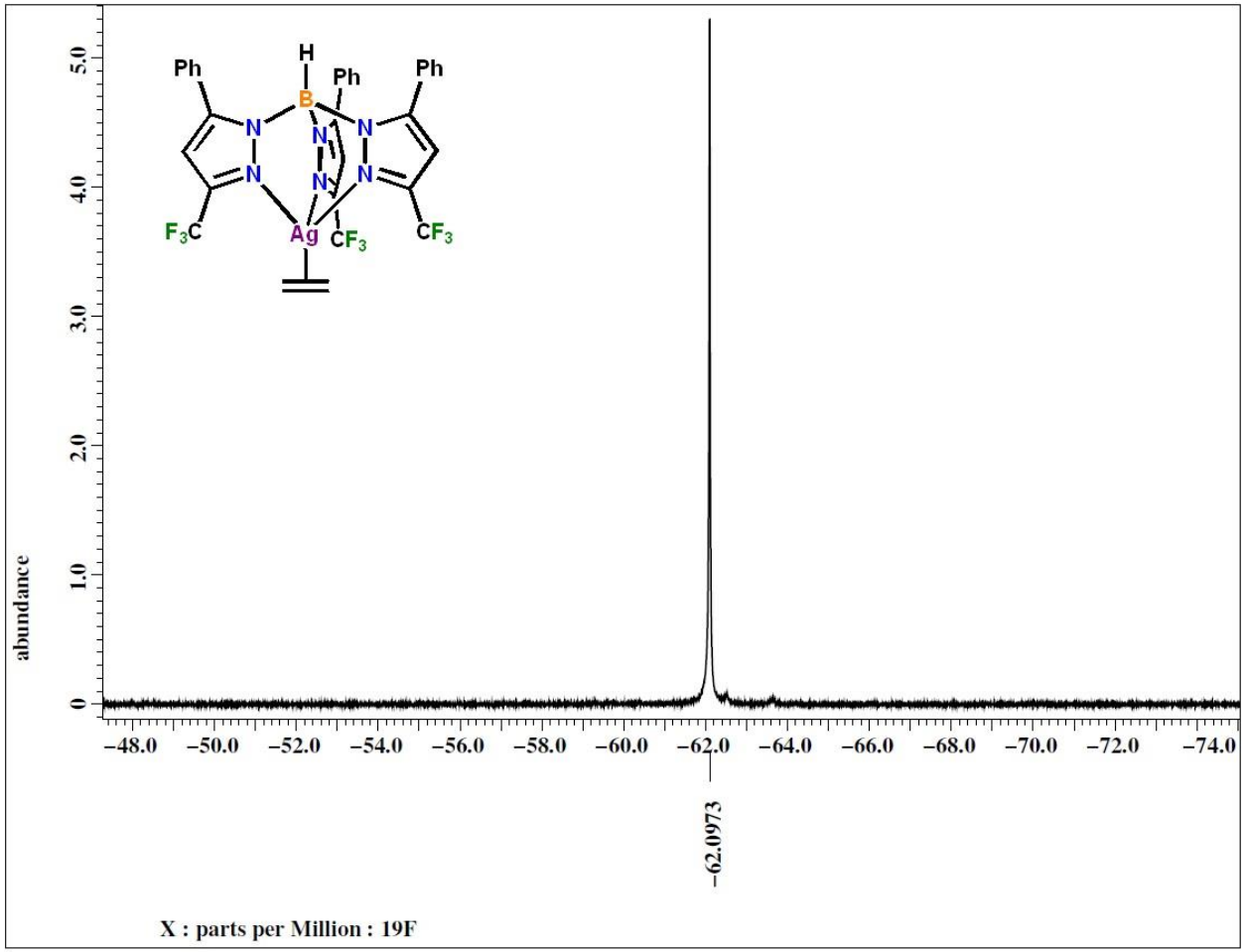

^{19}F NMR Spectrum of $[HB(3\text{-}(CF_3),5\text{-}(Ph)Pz)_3]Ag(C_2H_4)$ in C_6D_{12}

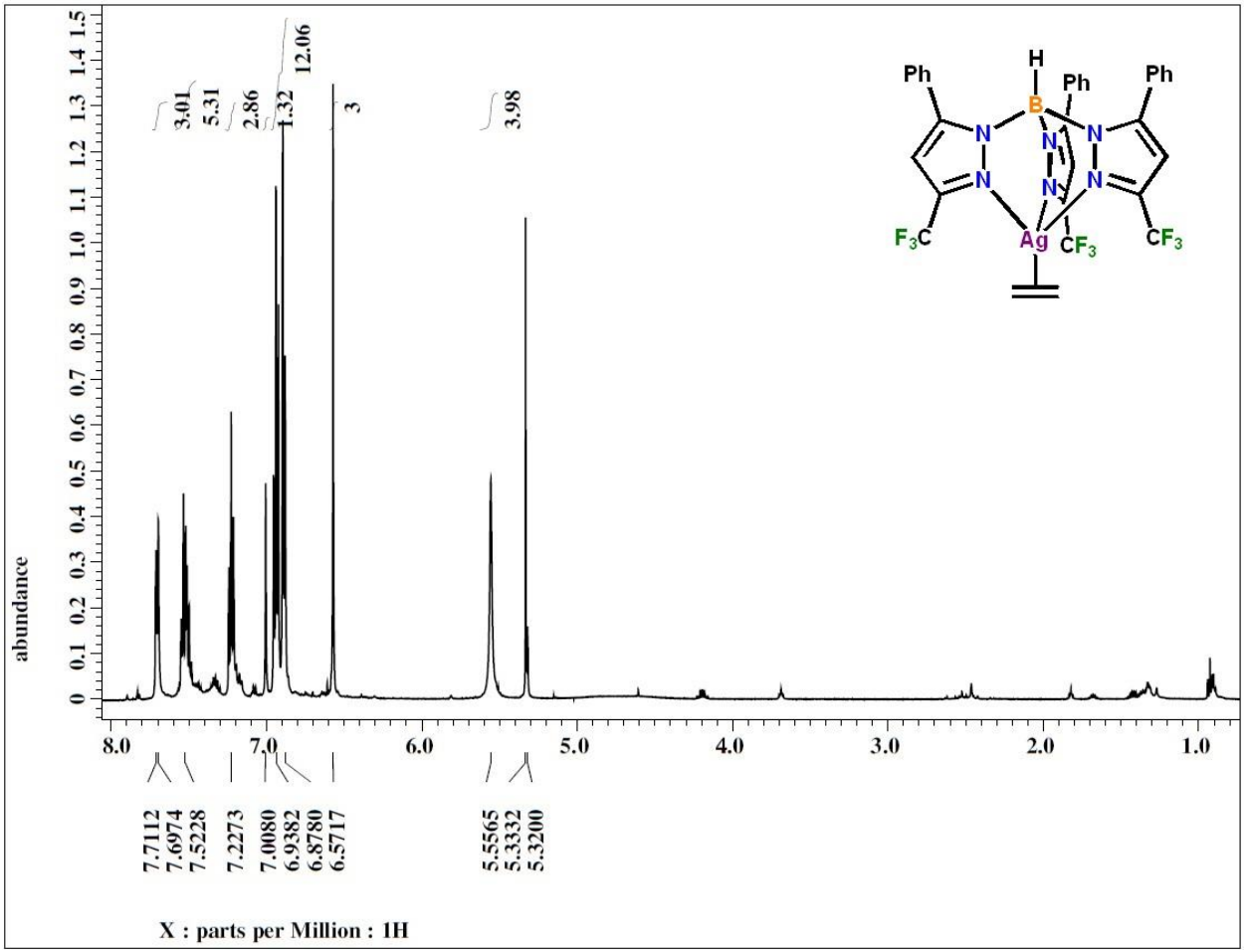

^{1}H NMR Spectrum of [HB(3-(CF_3),5-(Ph)Pz)$_3$]Ag(C_2H_4) in CD_2Cl_2

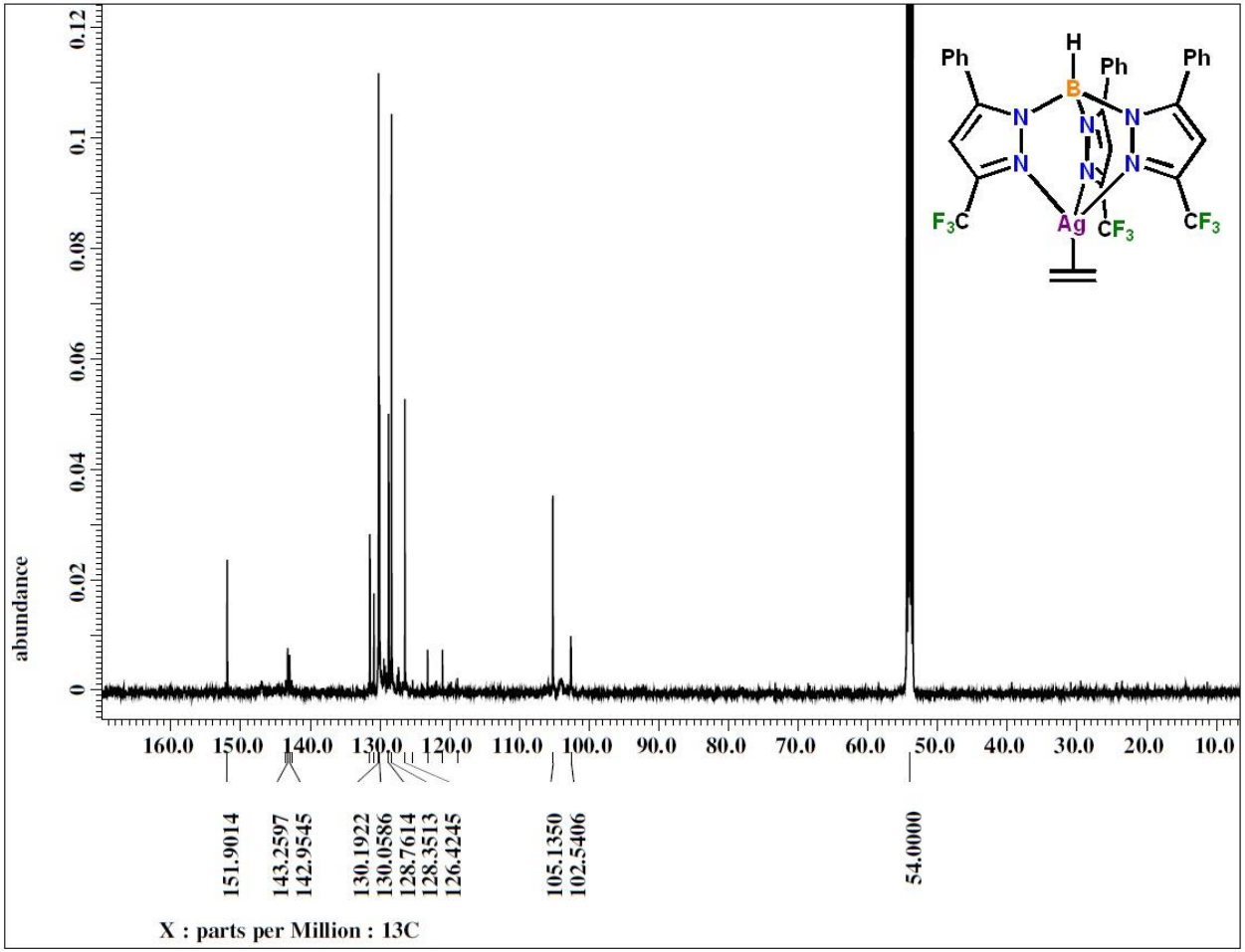

^{13}C NMR Spectrum of $[HB(3\text{-}(CF_3),5\text{-}(Ph)Pz)_3]Ag(C_2H_4)$ in CD_2Cl_2

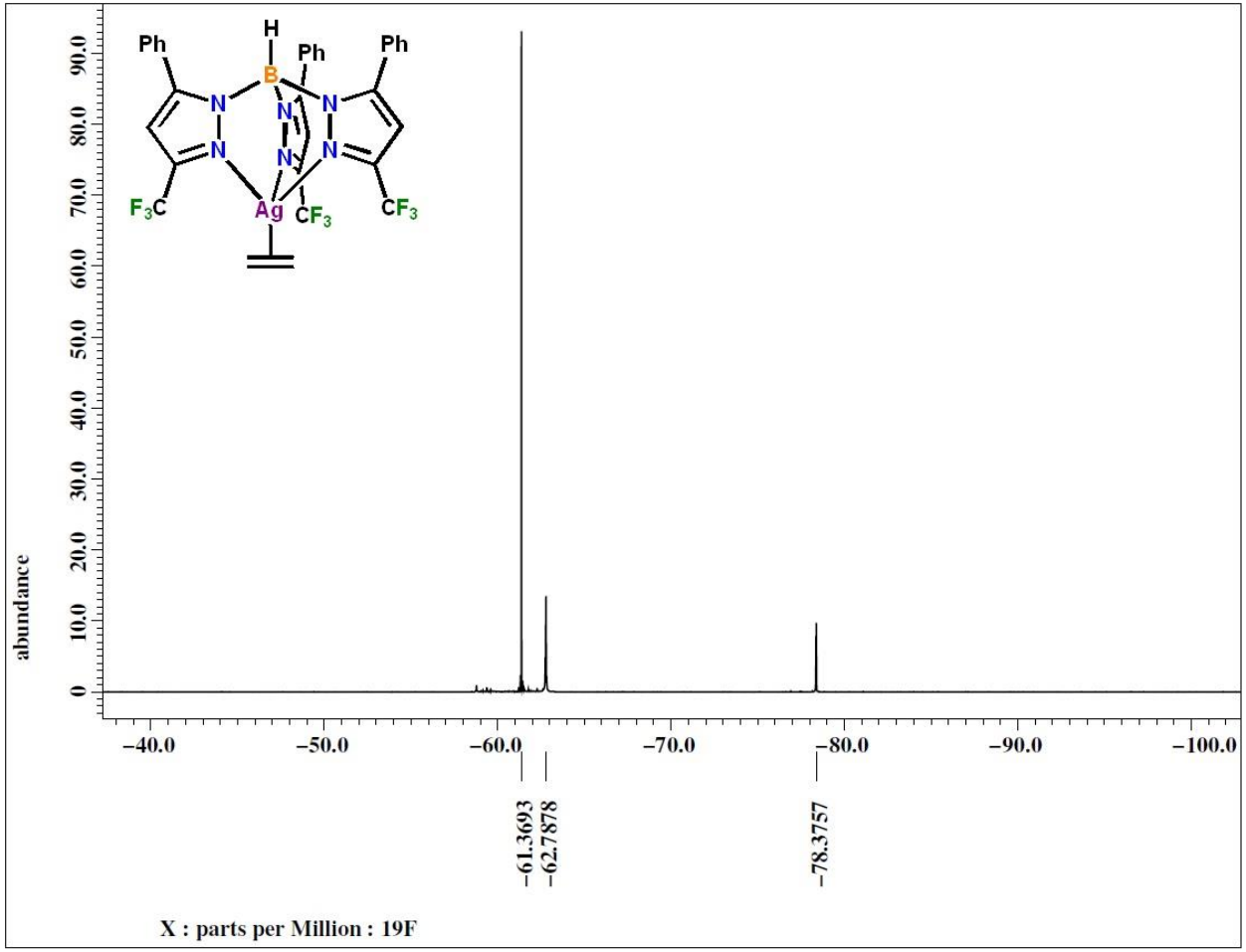

^{19}F NMR Spectrum of [HB(3-(CF_3),5-(Ph)Pz)$_3$]Ag(C_2H_4) in CD_2Cl_2

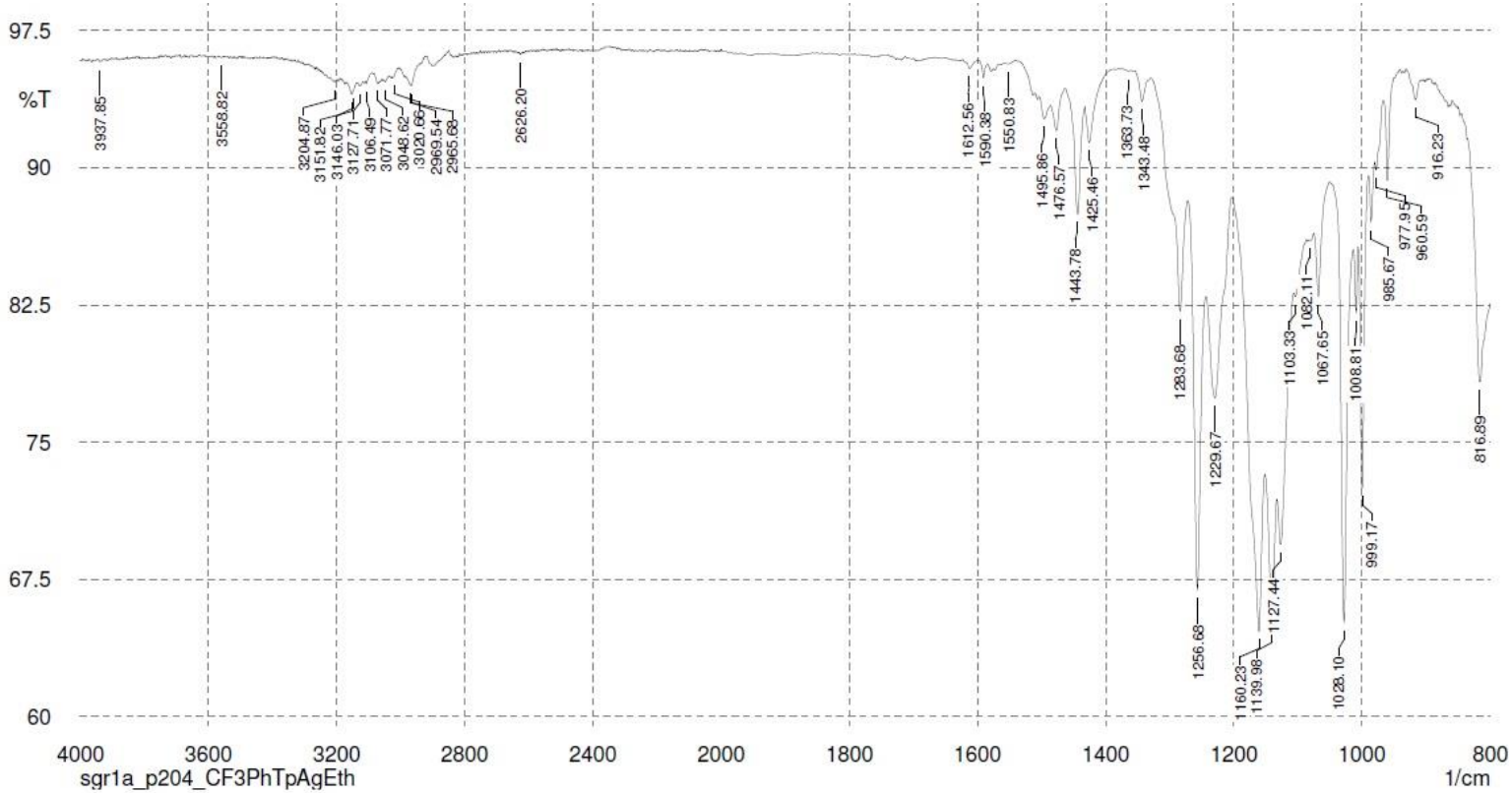

Infrared spectrum of $[HB(3\text{-}(CF_3),5\text{-}(Ph)Pz)_3]Ag(C_2H_4)$ (neat)

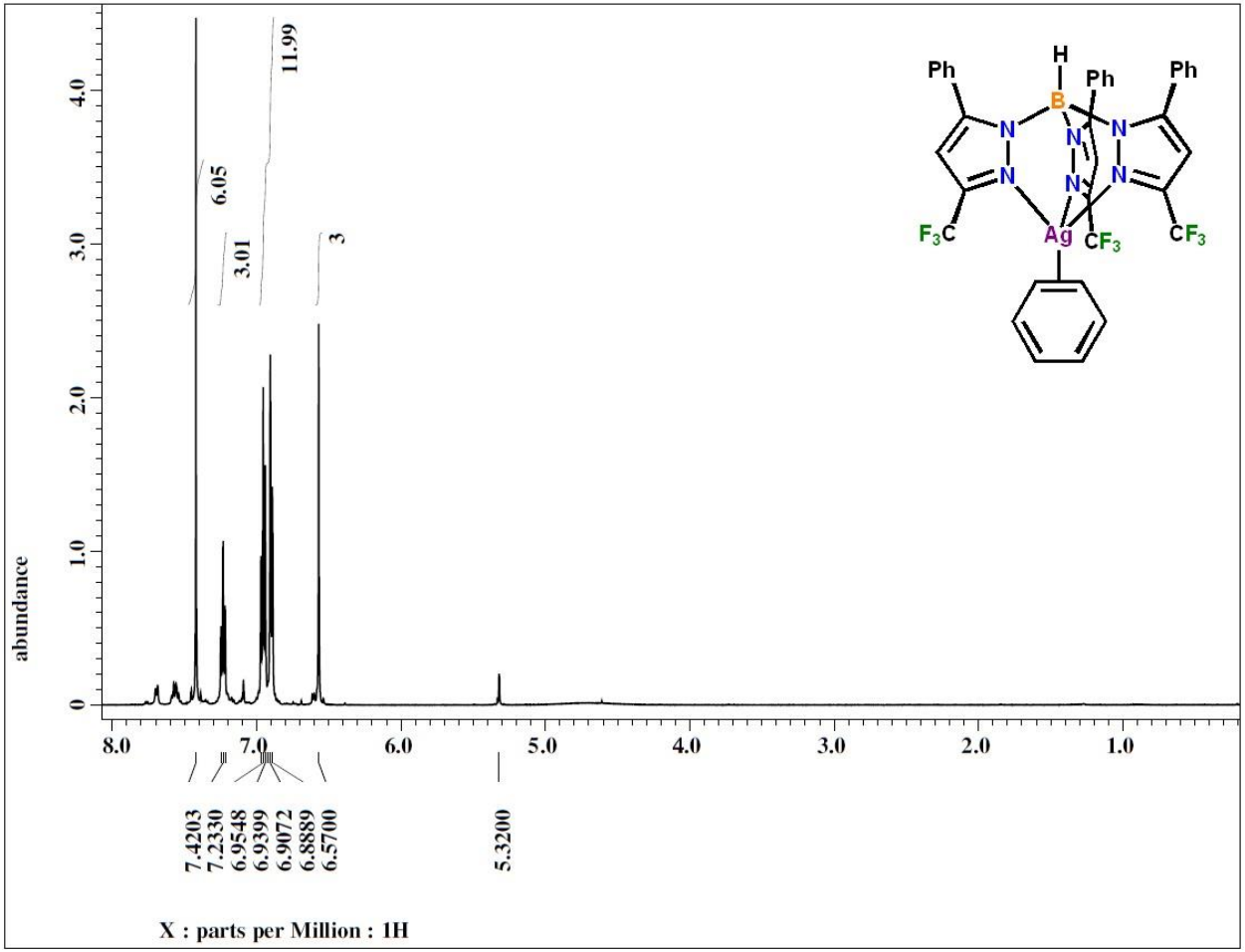

^{1}H NMR Spectrum of [HB(3-(CF_3),5-(Ph)Pz)$_3$]Ag(C_6H_6) in CD_2Cl_2

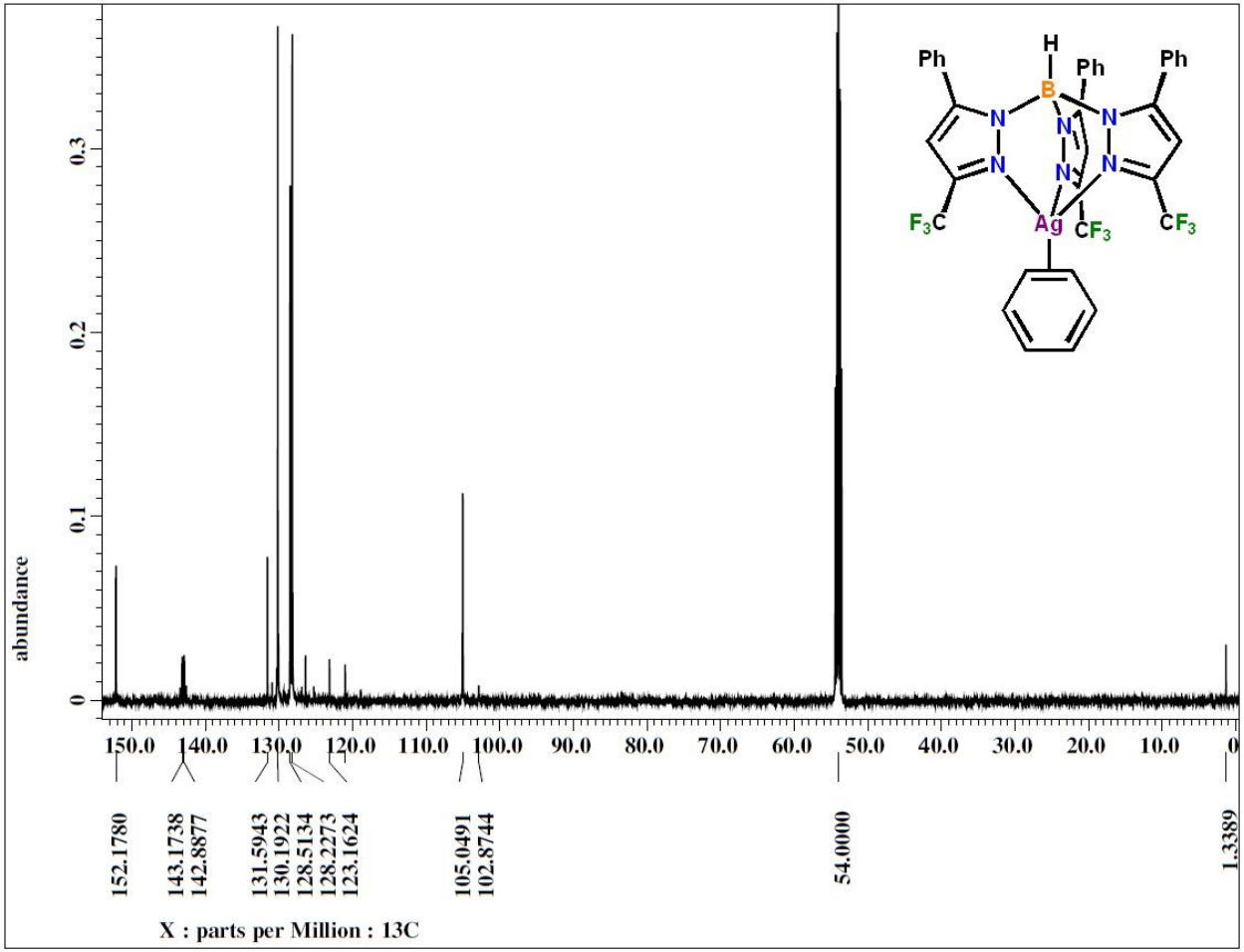

^{13}C NMR Spectrum of $[HB(3\text{-}(CF_3),5\text{-}(Ph)Pz)_3]Ag(C_6H_6)$ in CD_2Cl_2

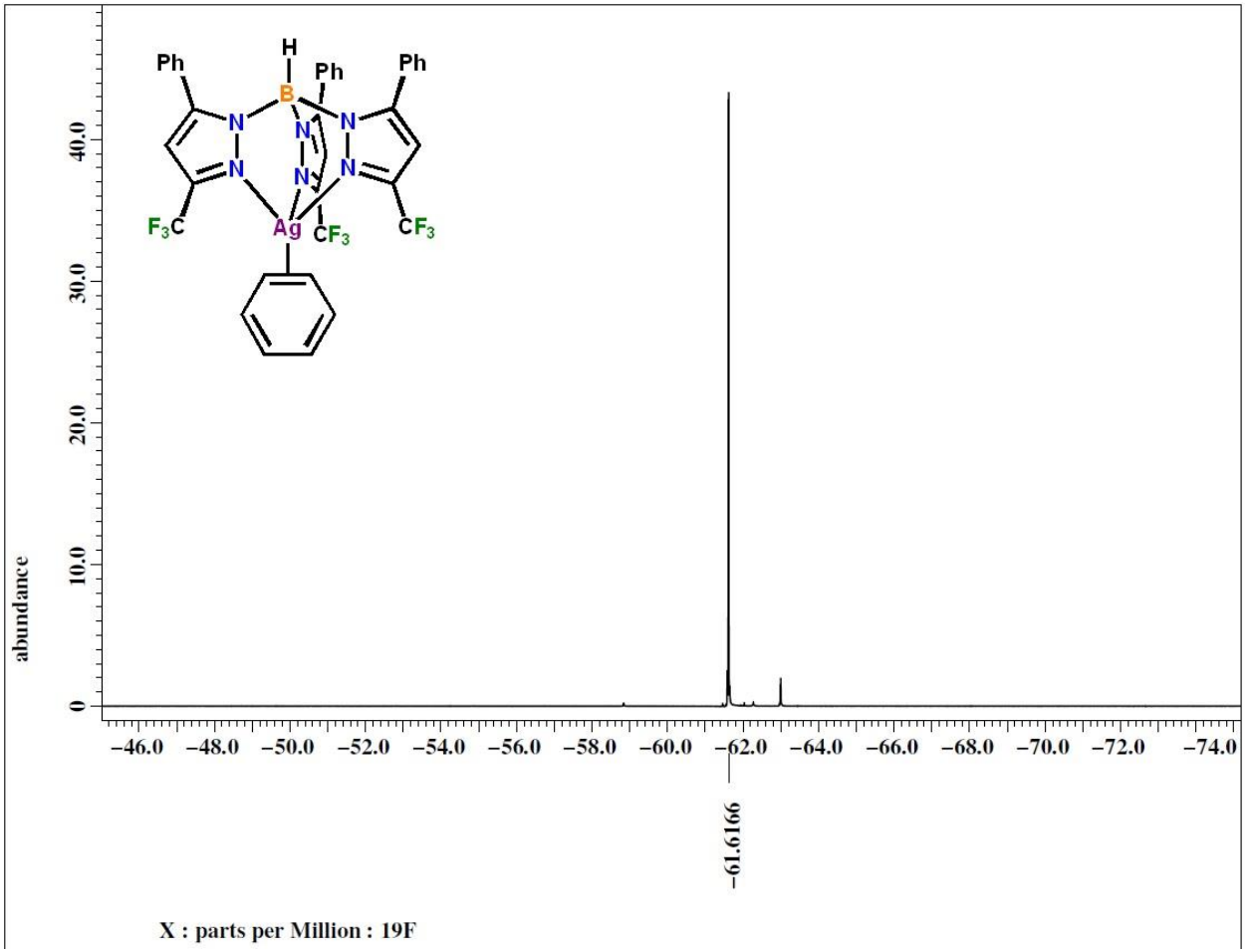

^{19}F NMR Spectrum of [HB(3-(CF_3),5-(Ph)Pz)$_3$]Ag(C_6H_6) in CD_2Cl_2

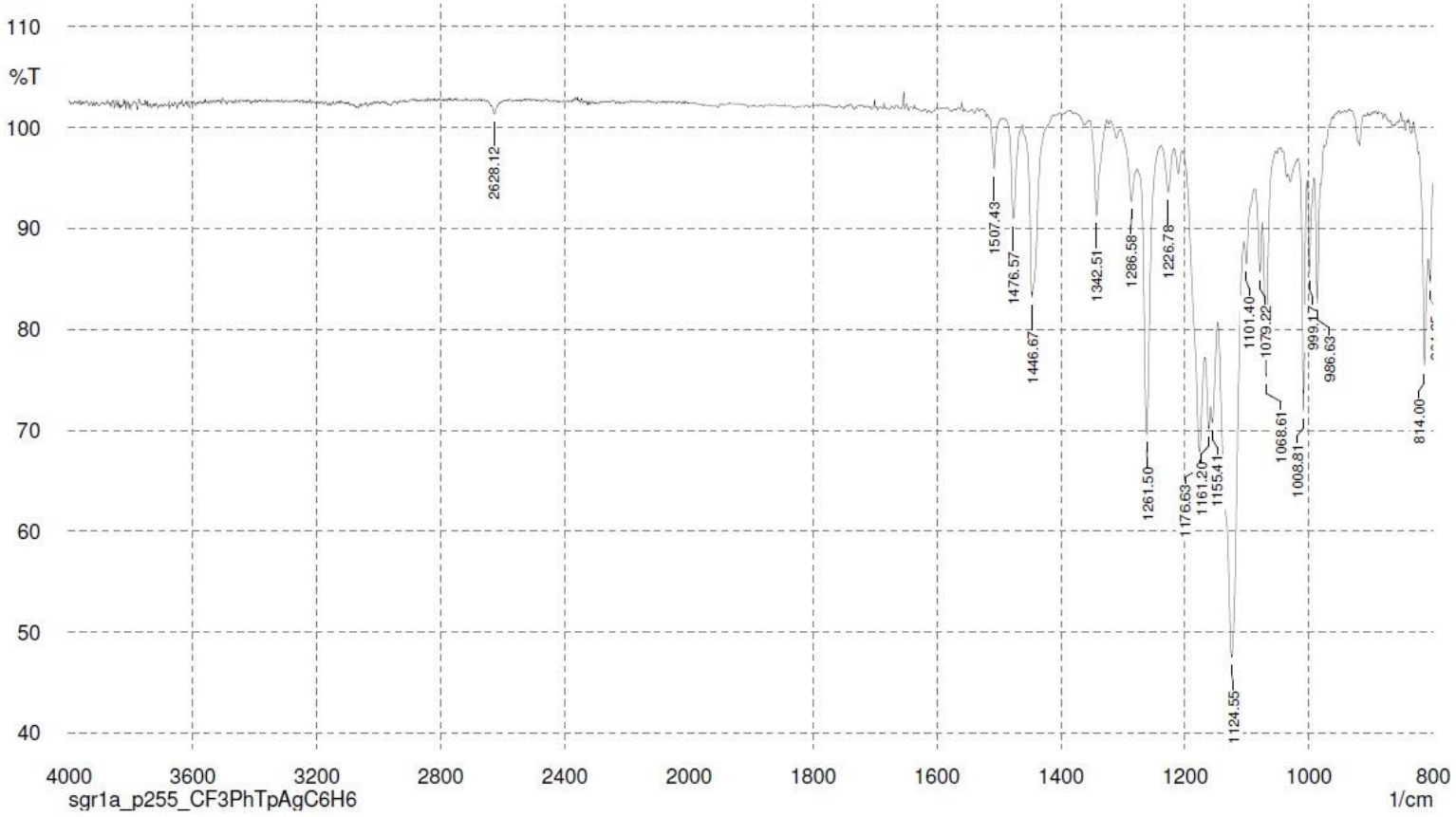

Infrared spectrum of [HB(3-(CF_3),5-(Ph)Pz)$_3$]Ag(C_6H_6) (neat)

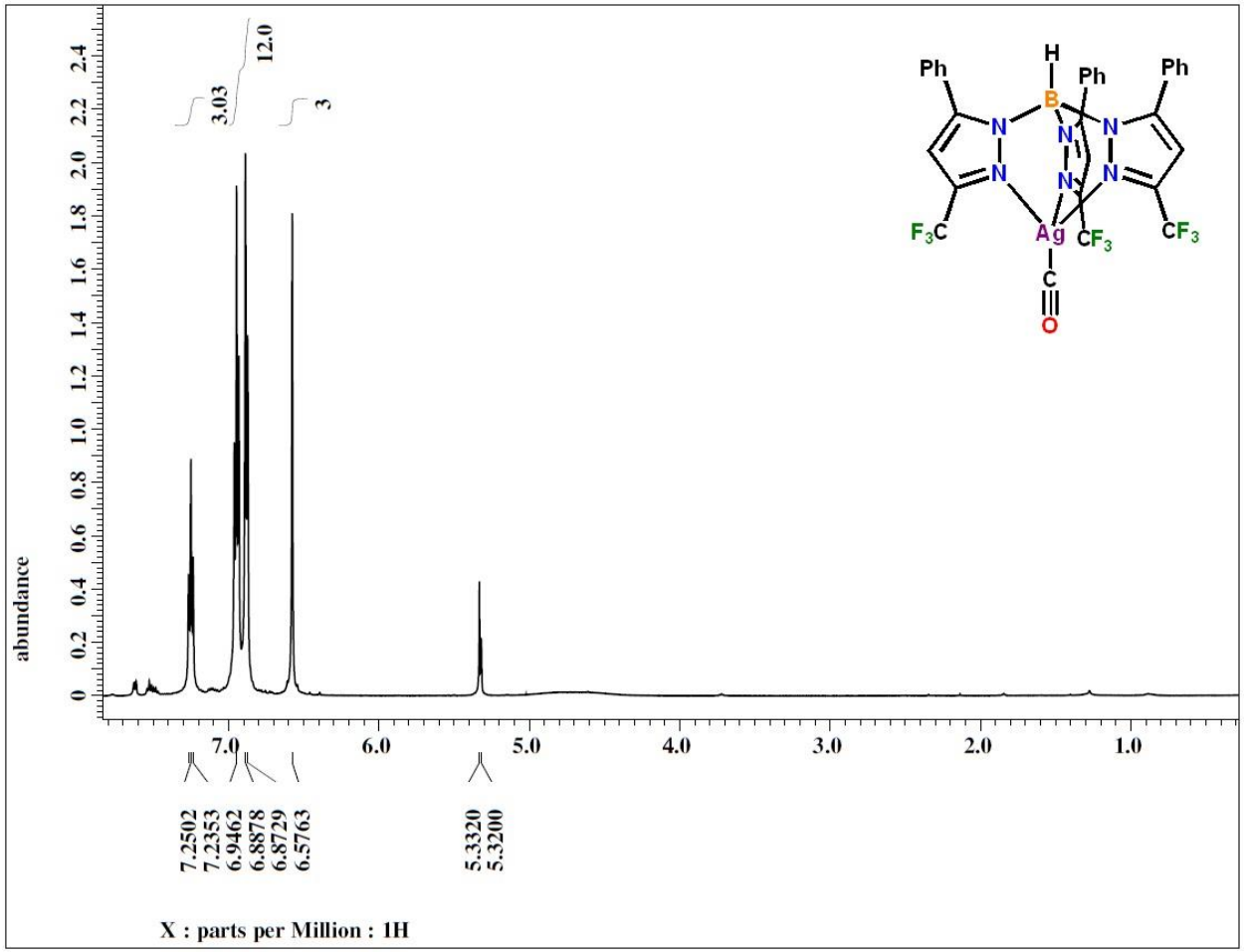

^{1}H NMR Spectrum of [HB(3-(CF_3),5-(Ph)Pz)$_3$]Ag(CO) in CD_2Cl_2

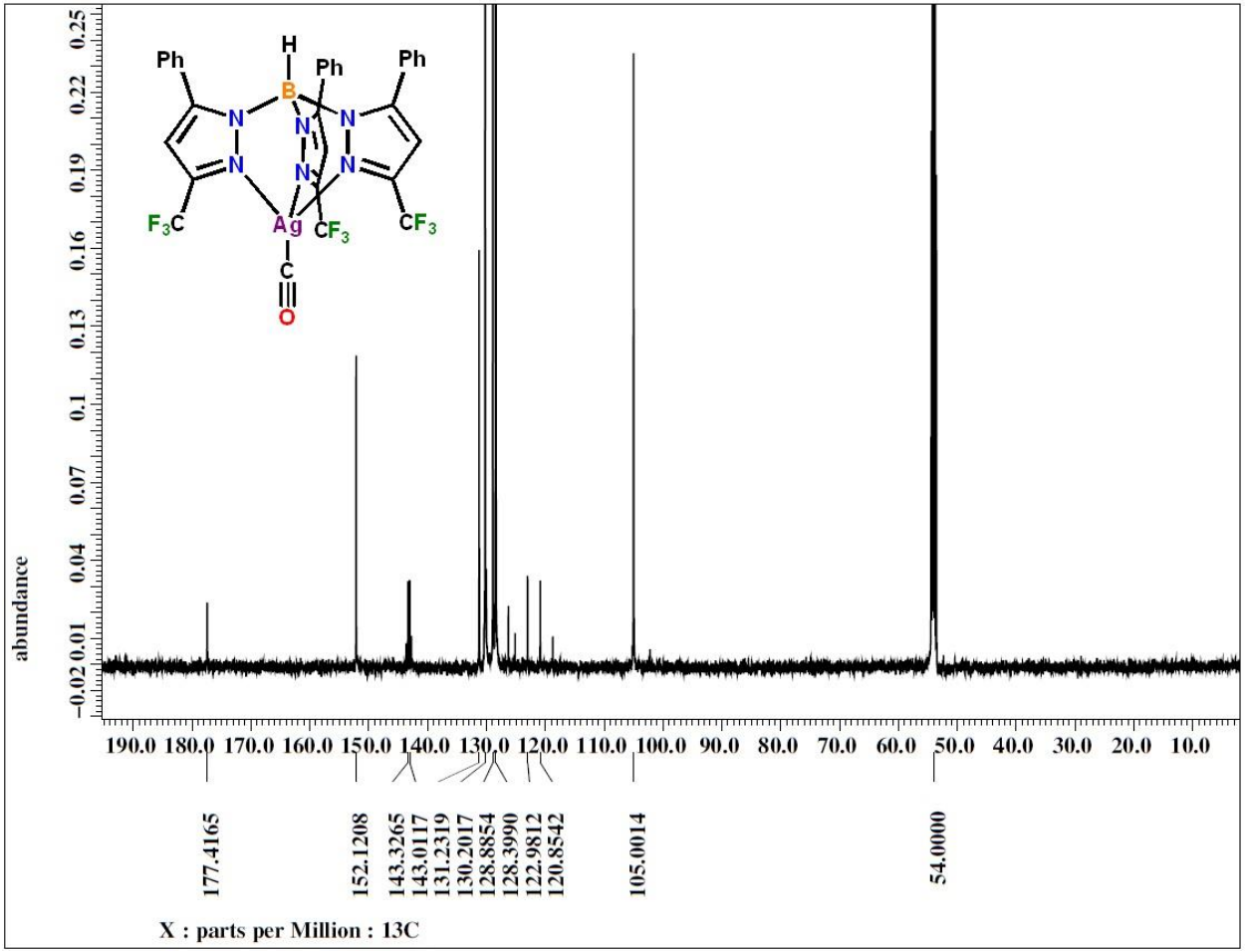

^{13}C NMR Spectrum of $[HB(3\text{-}(CF_3),5\text{-}(Ph)Pz)_3]Ag(CO)$ in CD_2Cl_2

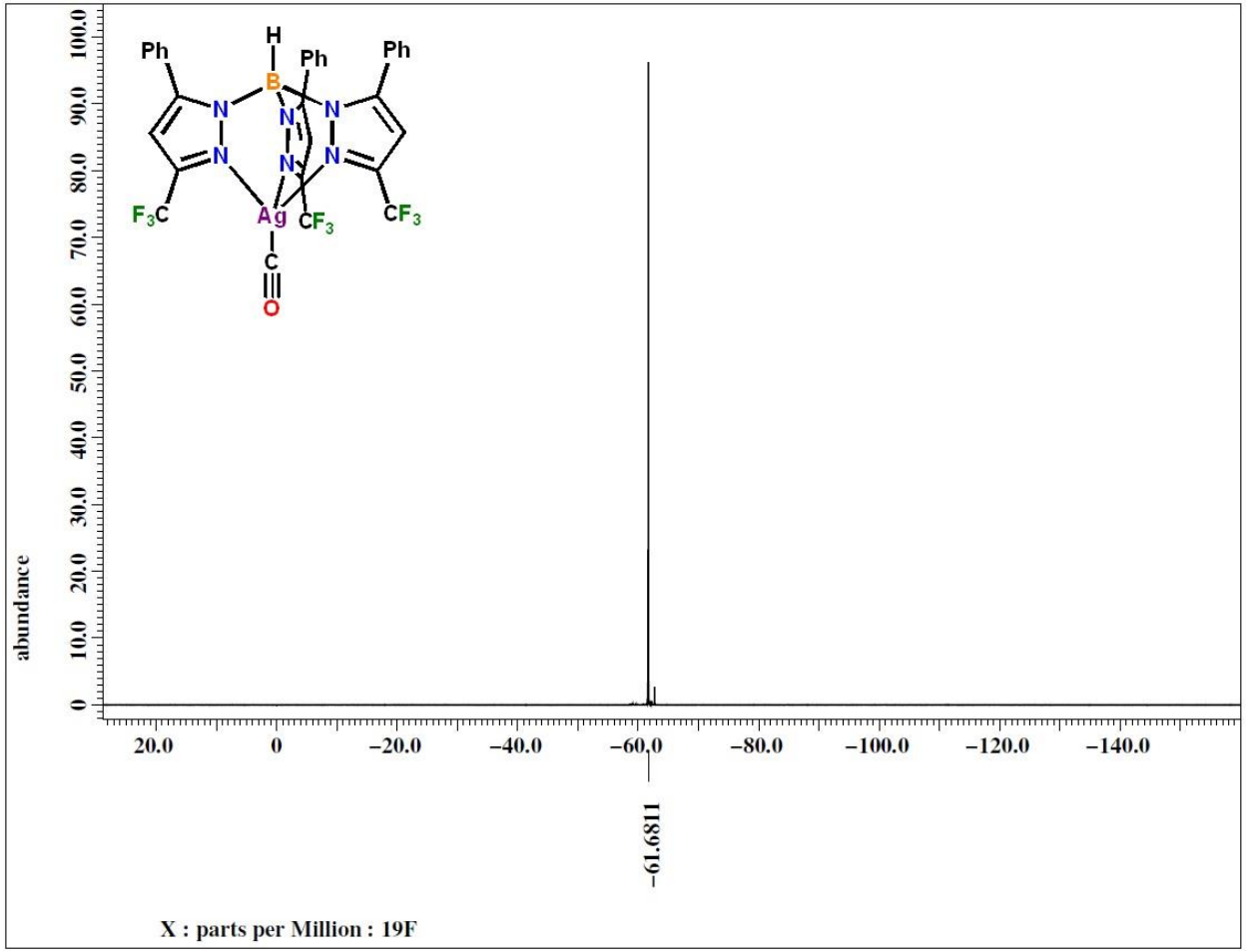

^{19}F NMR Spectrum of [HB(3-(CF_3),5-(Ph)Pz)$_3$]Ag(CO) in CD_2Cl_2

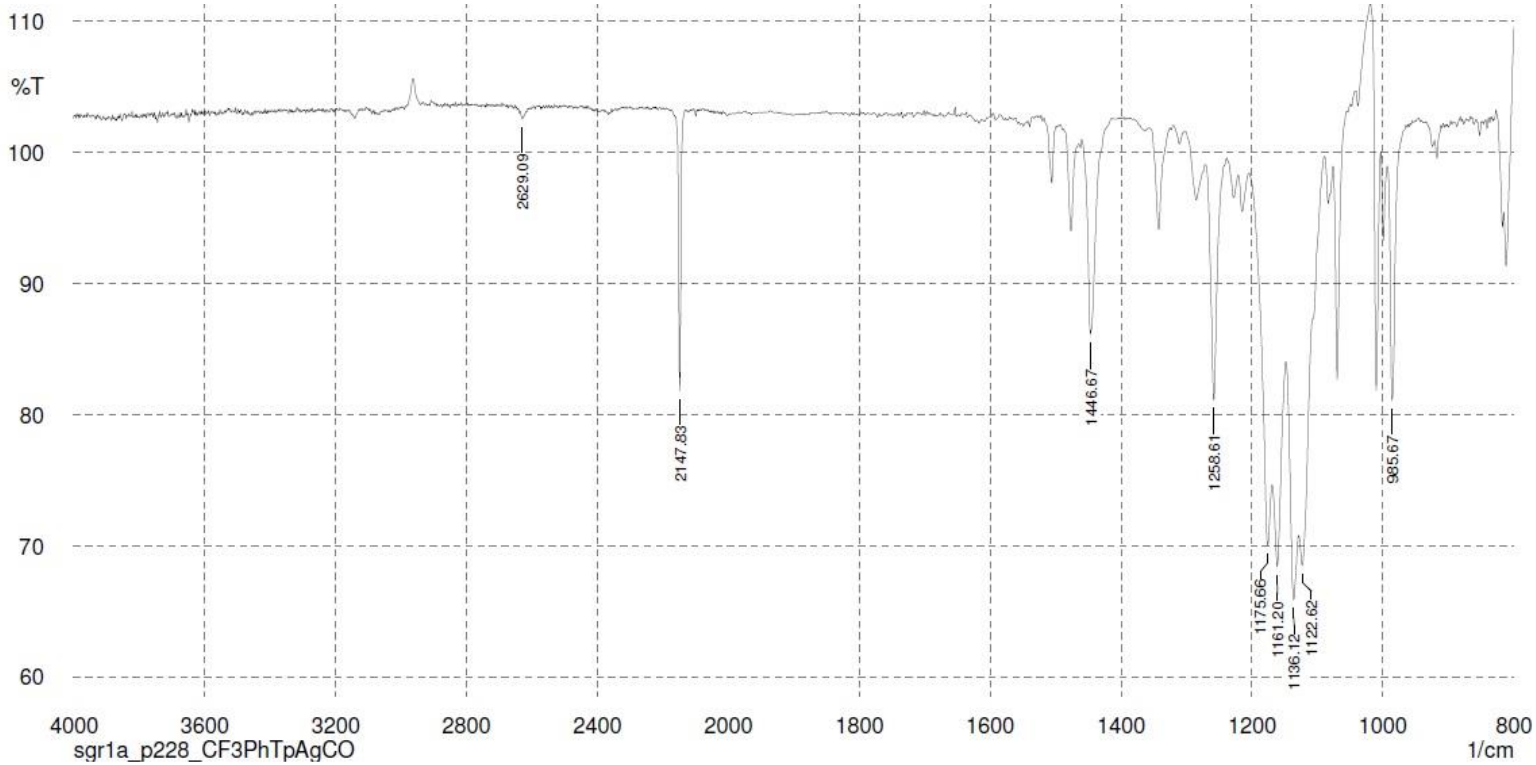

Infrared spectrum of [HB(3-(CF_3),5-(Ph)Pz)$_3$]Ag(CO) (neat)

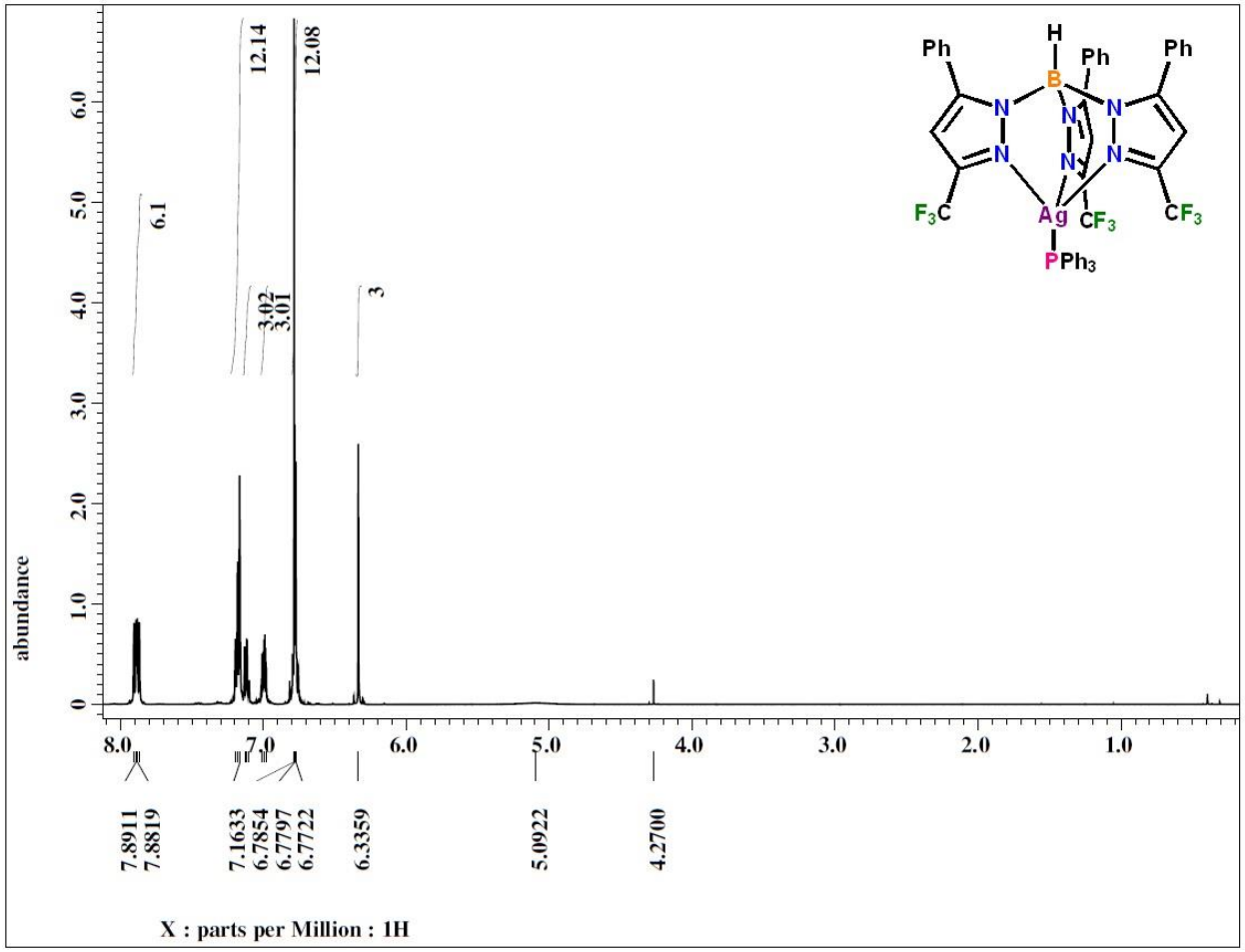

^{1}H NMR Spectrum of [HB(3-(CF_3),5-(Ph)Pz)$_3$]Ag(PPh_3) in C_6D_6

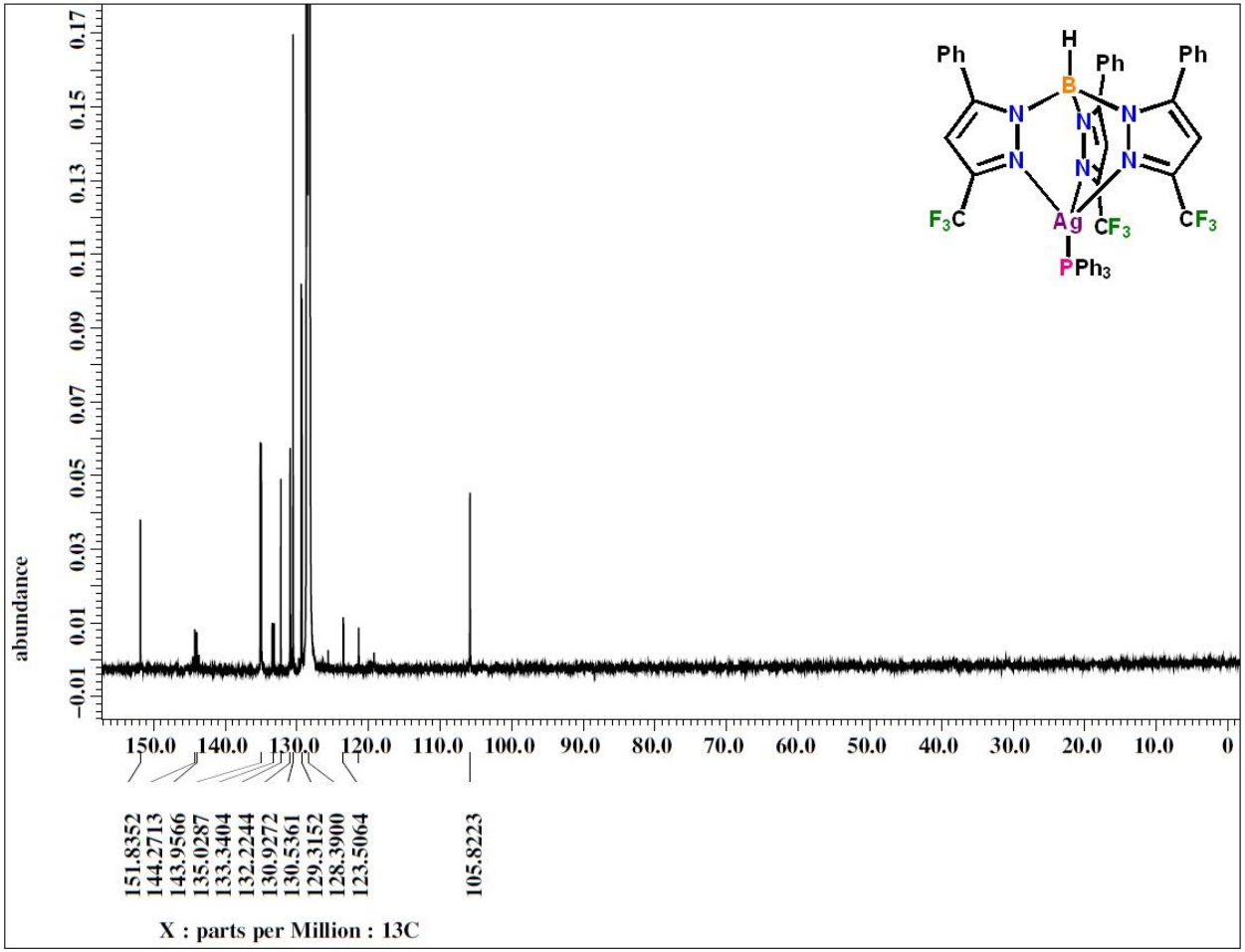

^{13}C NMR Spectrum of [HB(3-(CF_3),5-(Ph)Pz)$_3$]Ag(PPh_3) in C_6D_6

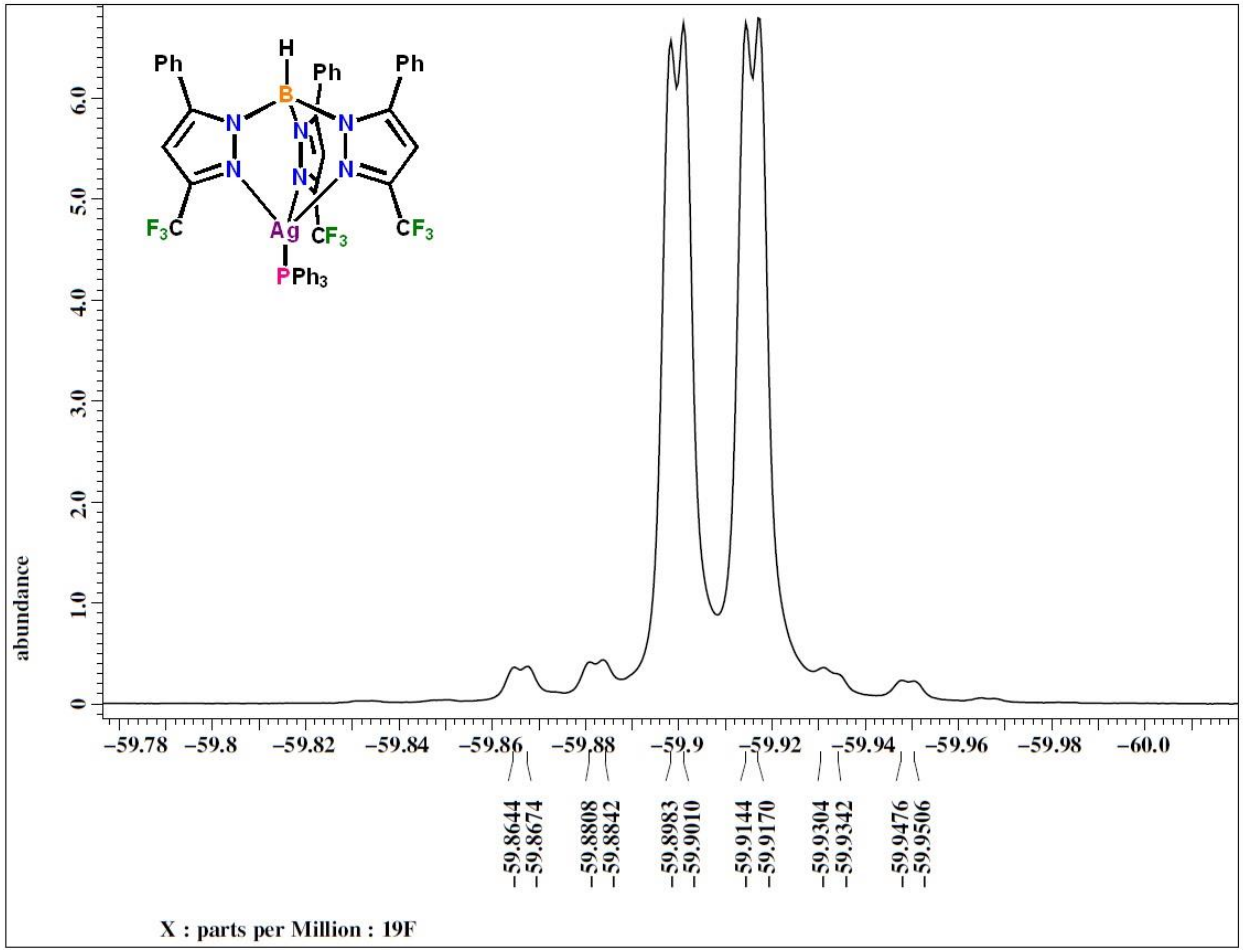

^{13}C NMR Spectrum of [HB(3-(CF_3),5-(Ph)Pz)$_3$]Ag(PPh_3) in C_6D_6

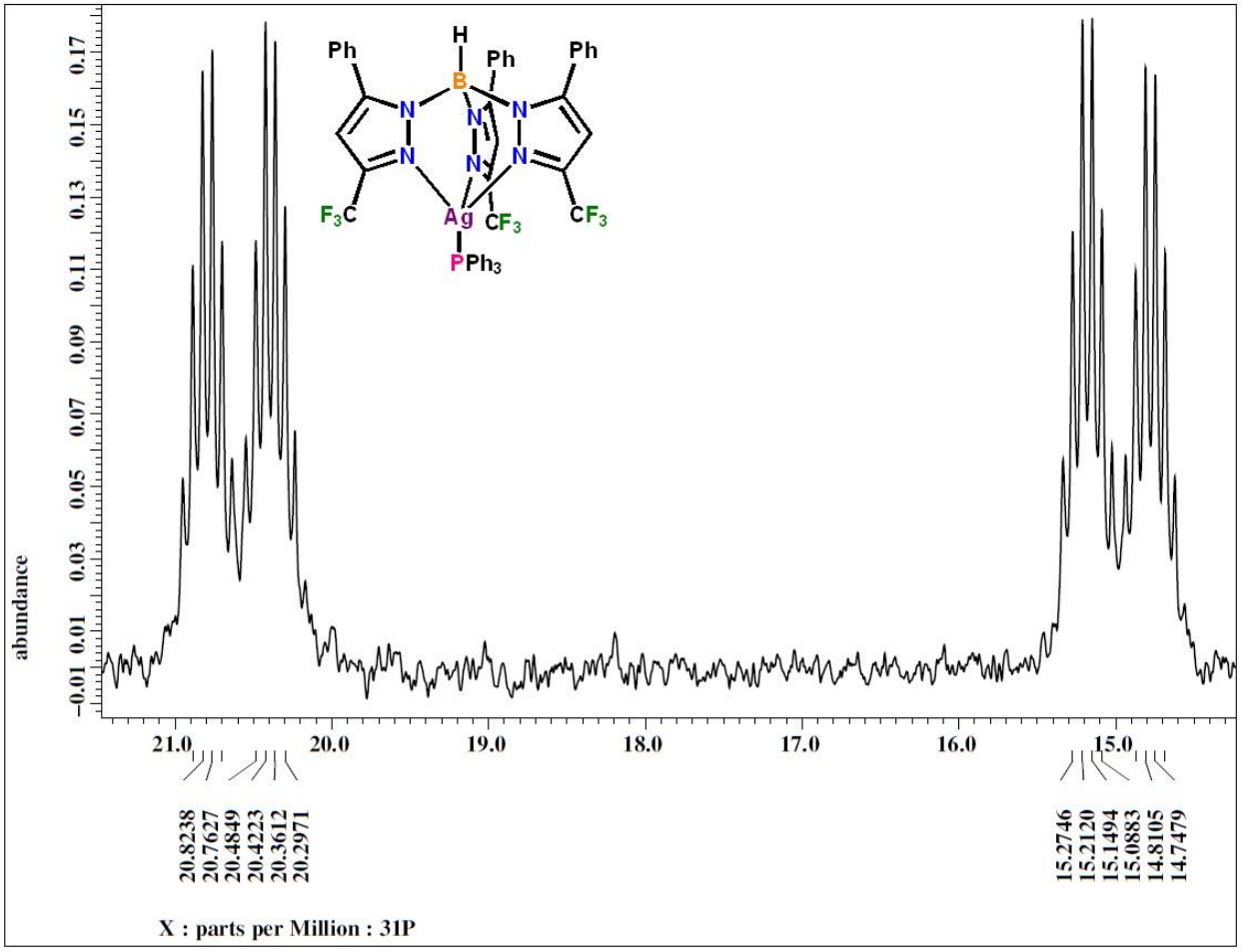

^{31}P NMR Spectrum of [HB(3-(CF_3),5-(Ph)Pz)$_3$]Ag(PPh_3) in C_6D_6

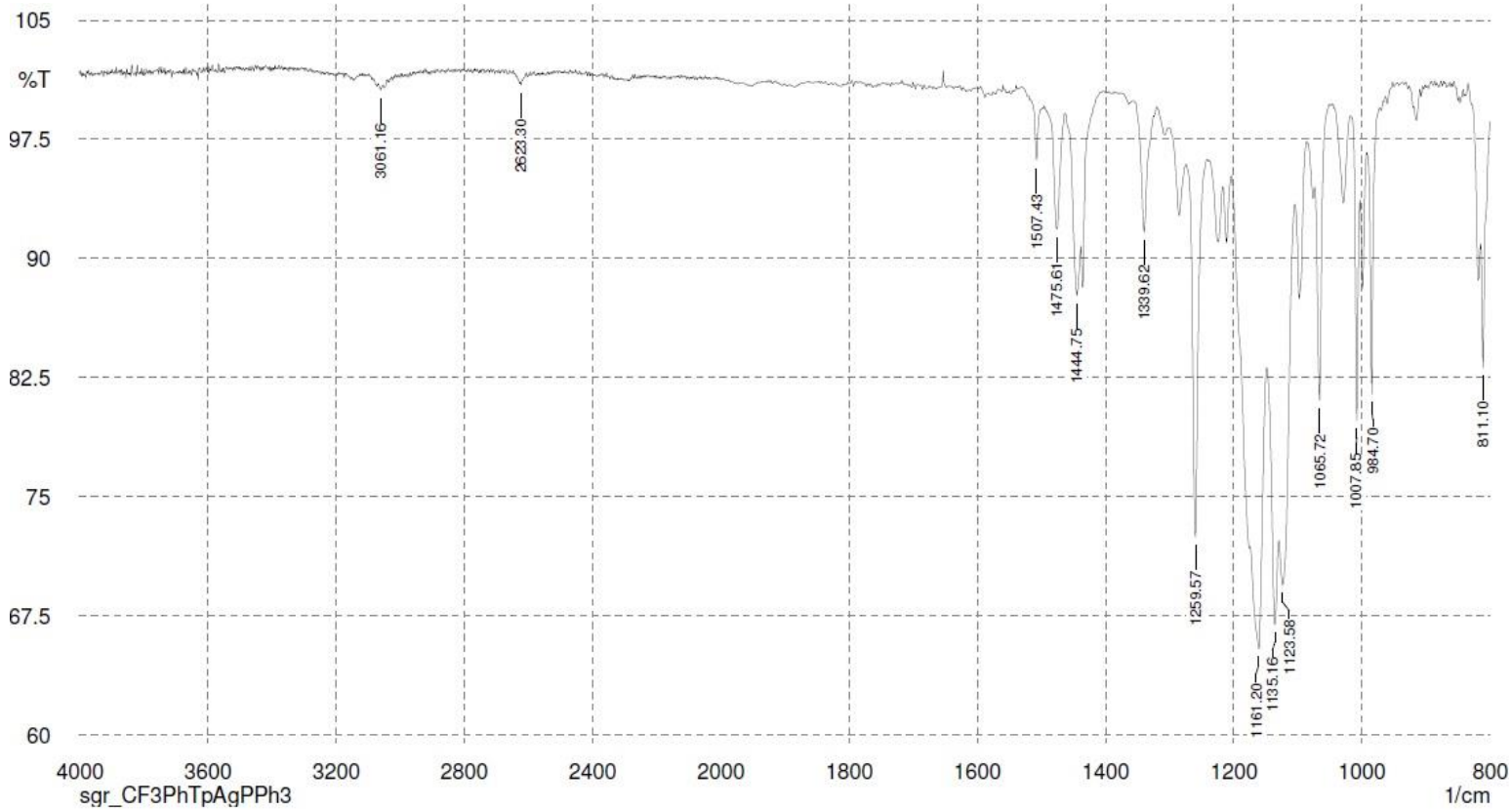

Infrared spectrum of [HB(3-(CF_3),5-(Ph)Pz)$_3$]Ag(PPh_3) (neat)

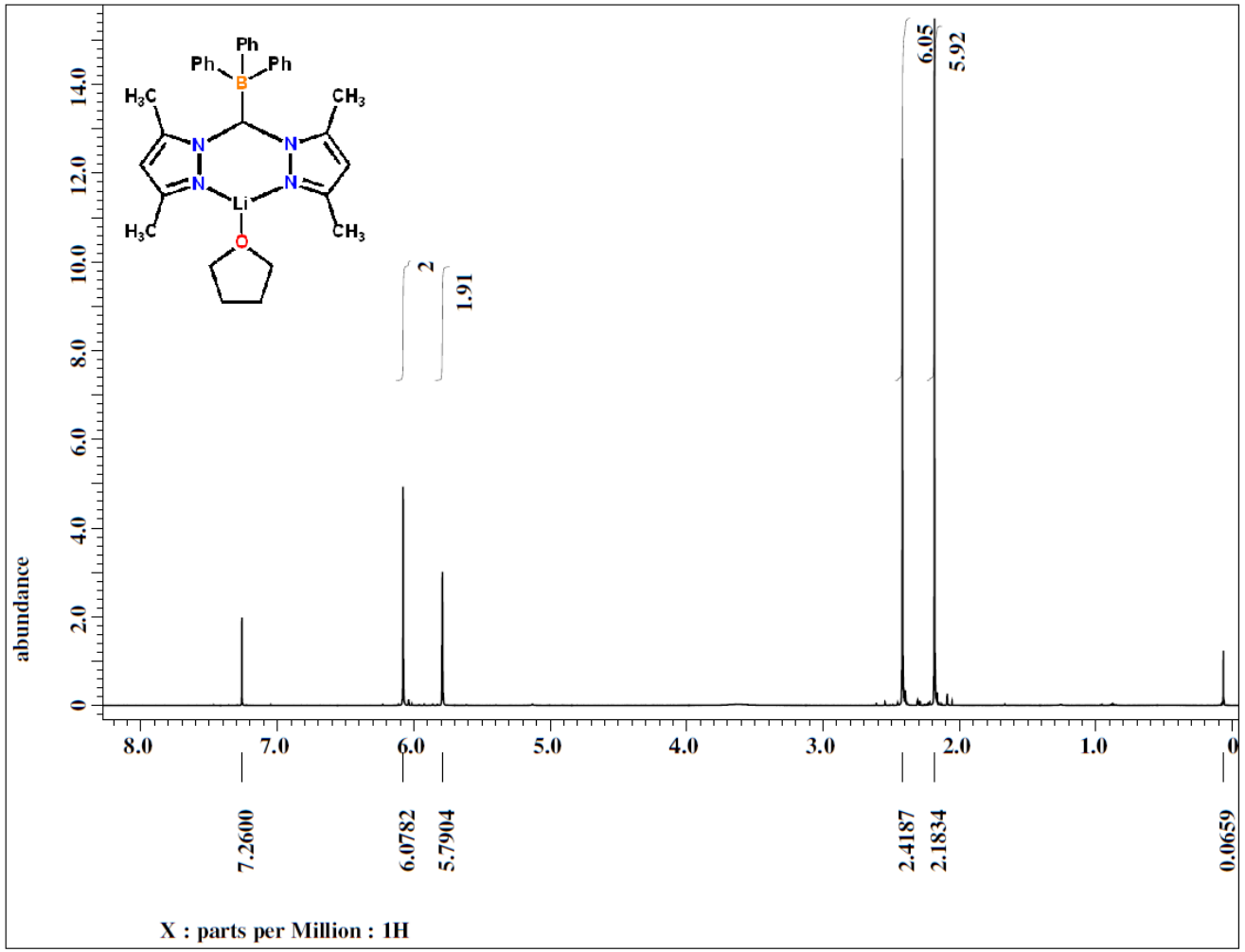

^{1}H NMR Spectrum of [$(Ph_3B)CH(3,5\text{-}(CH_3)_2Pz)_2$]Li(THF) in $CDCl_3$

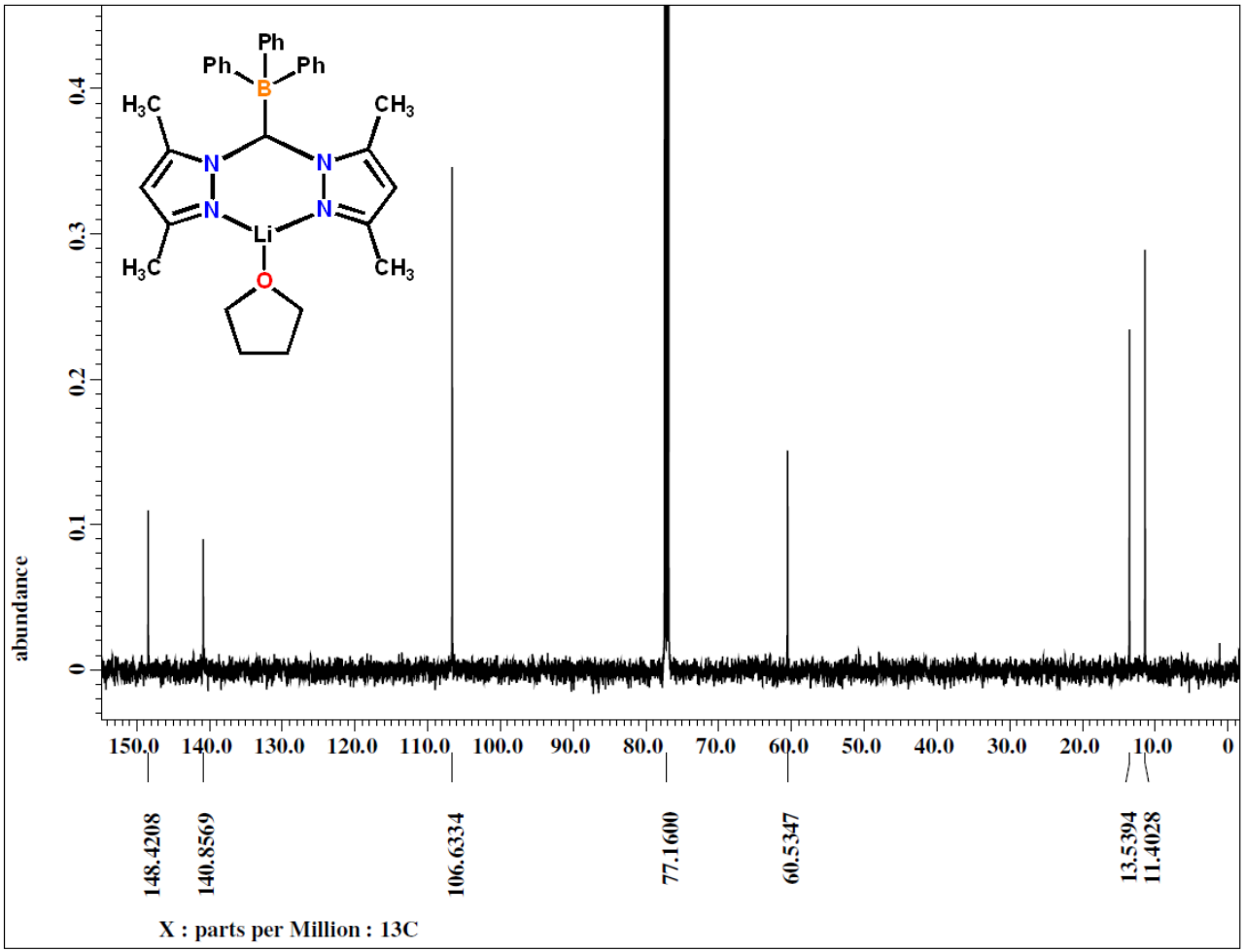

^{13}C NMR Spectrum of [(Ph$_3$B)CH(3,5-(CH$_3$)$_2$Pz)$_2$]Li(THF) in CDCl$_3$

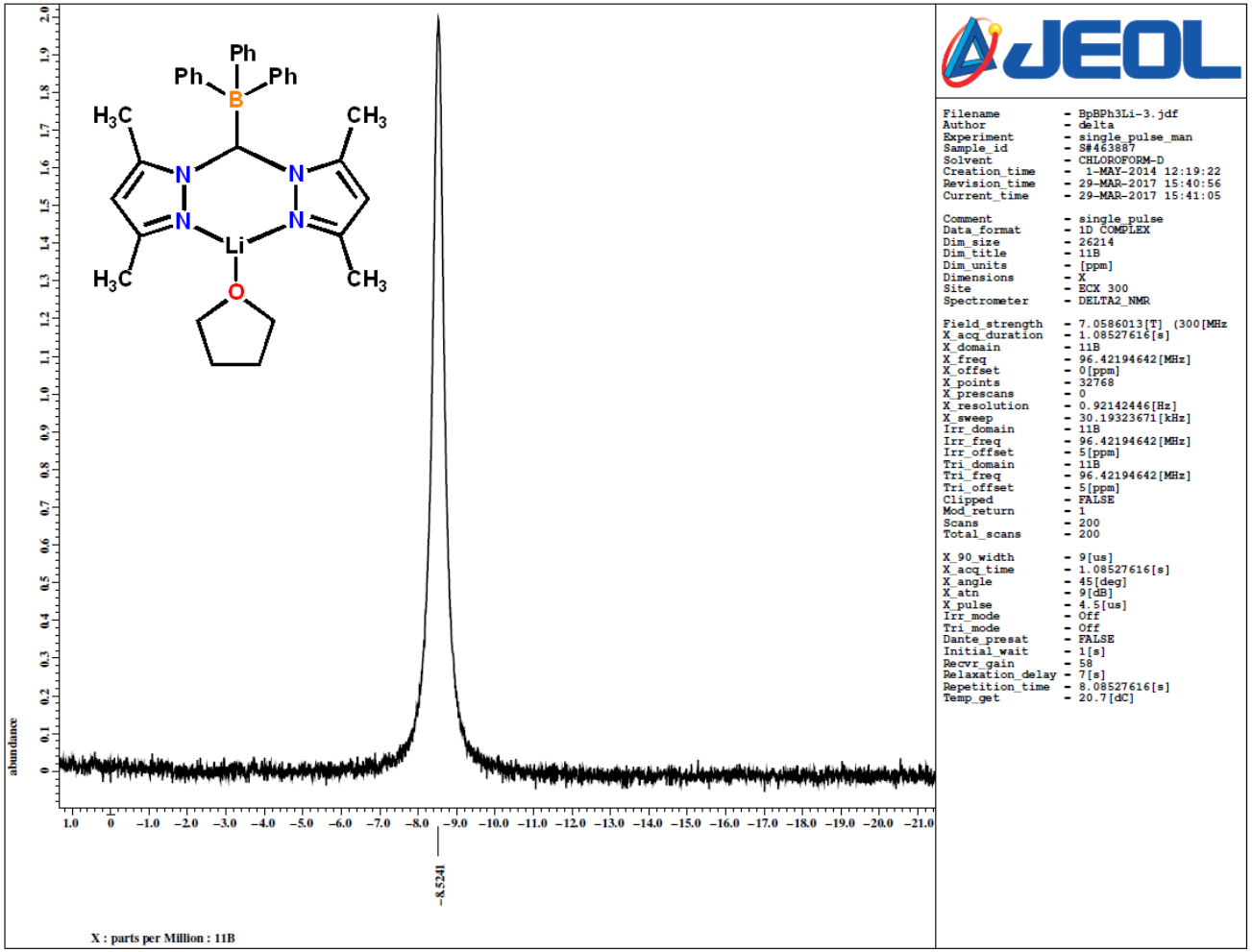

^{11}B NMR Spectrum of $[(Ph_3B)CH(3,5\text{-}(CH_3)_2Pz)_2]Li(THF)$ in $CDCl_3$

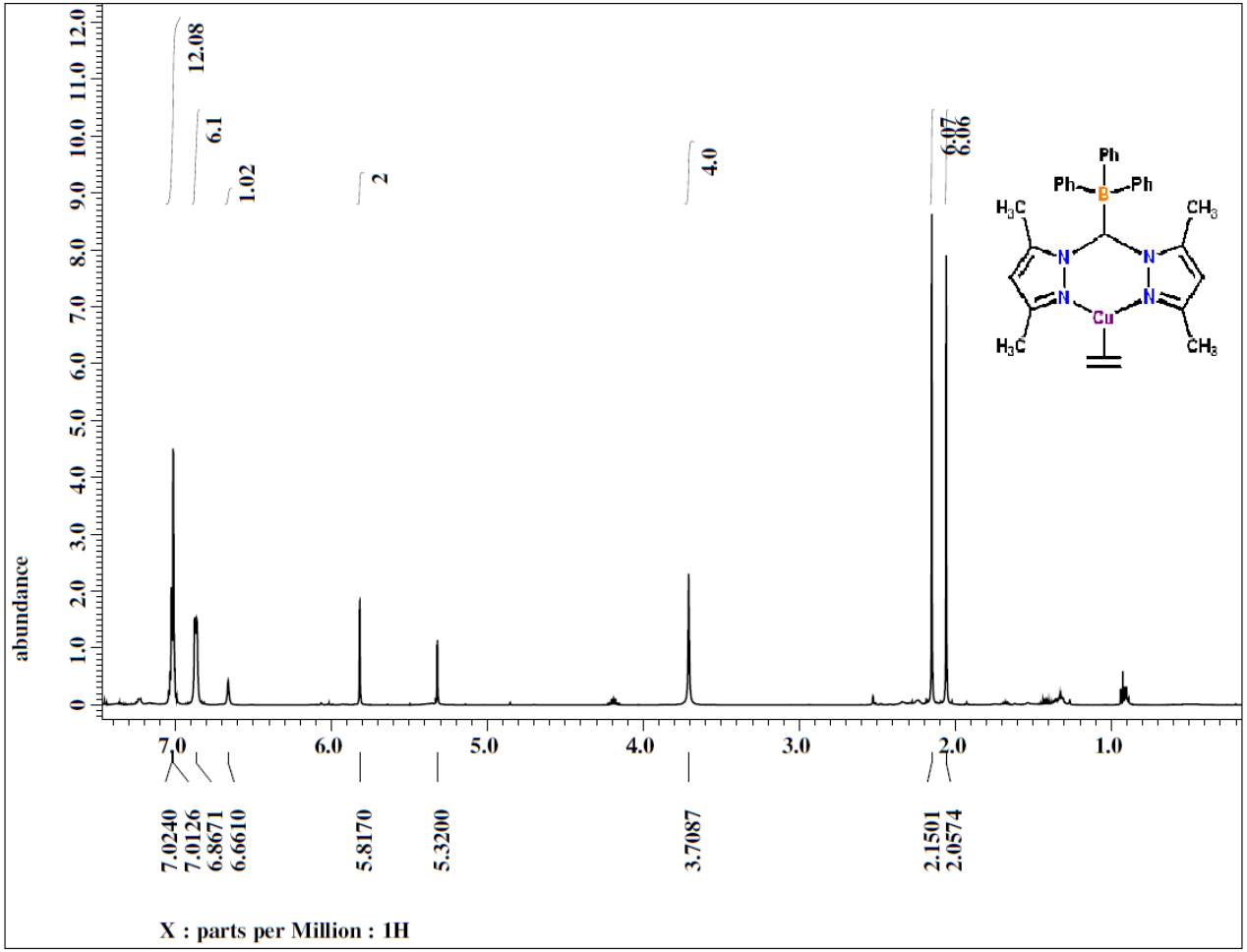

^{1}H NMR Spectrum of [(Ph$_3$B)CH(3,5-(CH$_3$)$_2$Pz)$_2$]Li(C$_2$H$_4$) in CD$_2$Cl$_2$

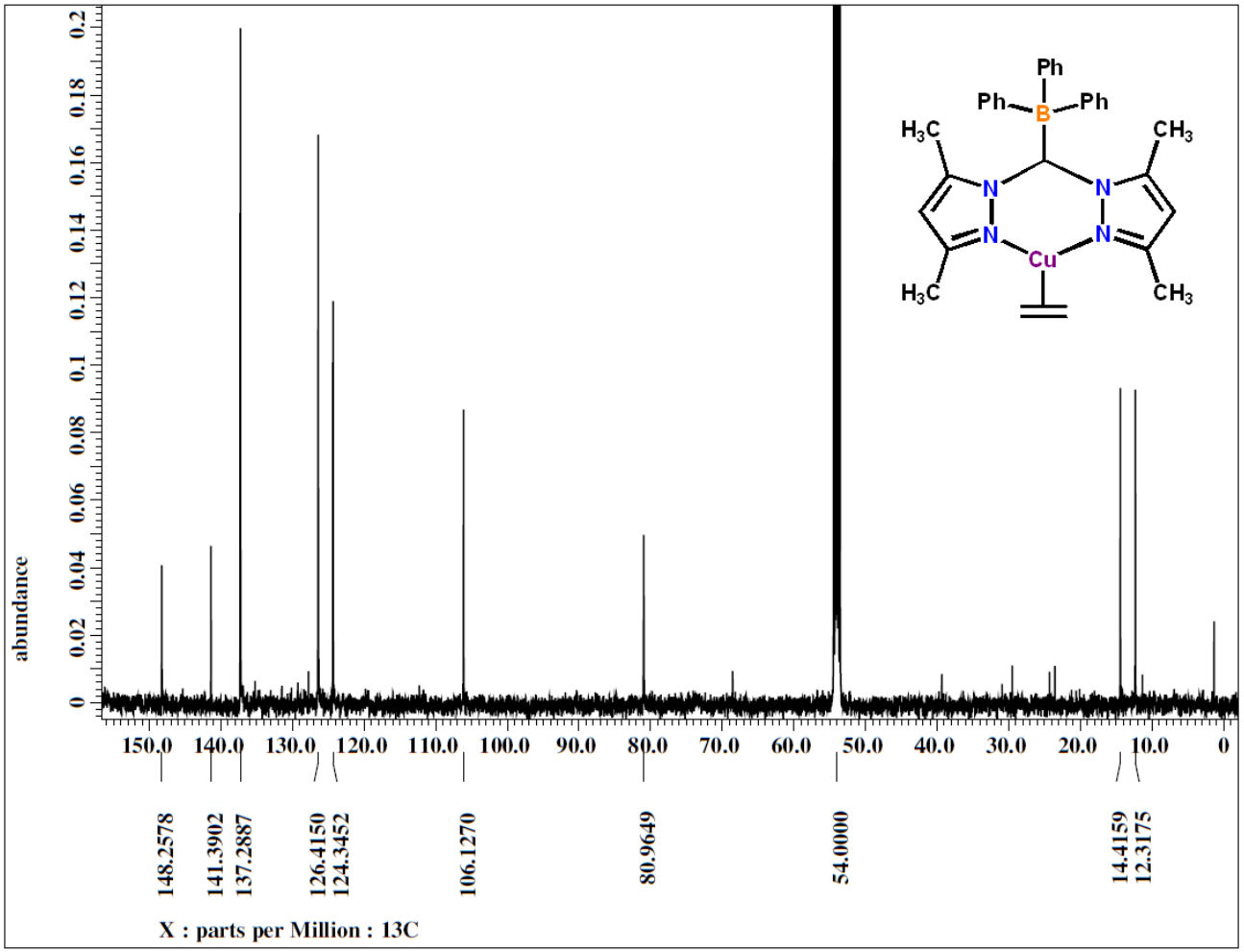

^{1}H NMR Spectrum of [(Ph$_3$B)CH(3,5-(CH$_3$)$_2$Pz)$_2$]Li(C$_2$H$_4$) in CD$_2$Cl$_2$

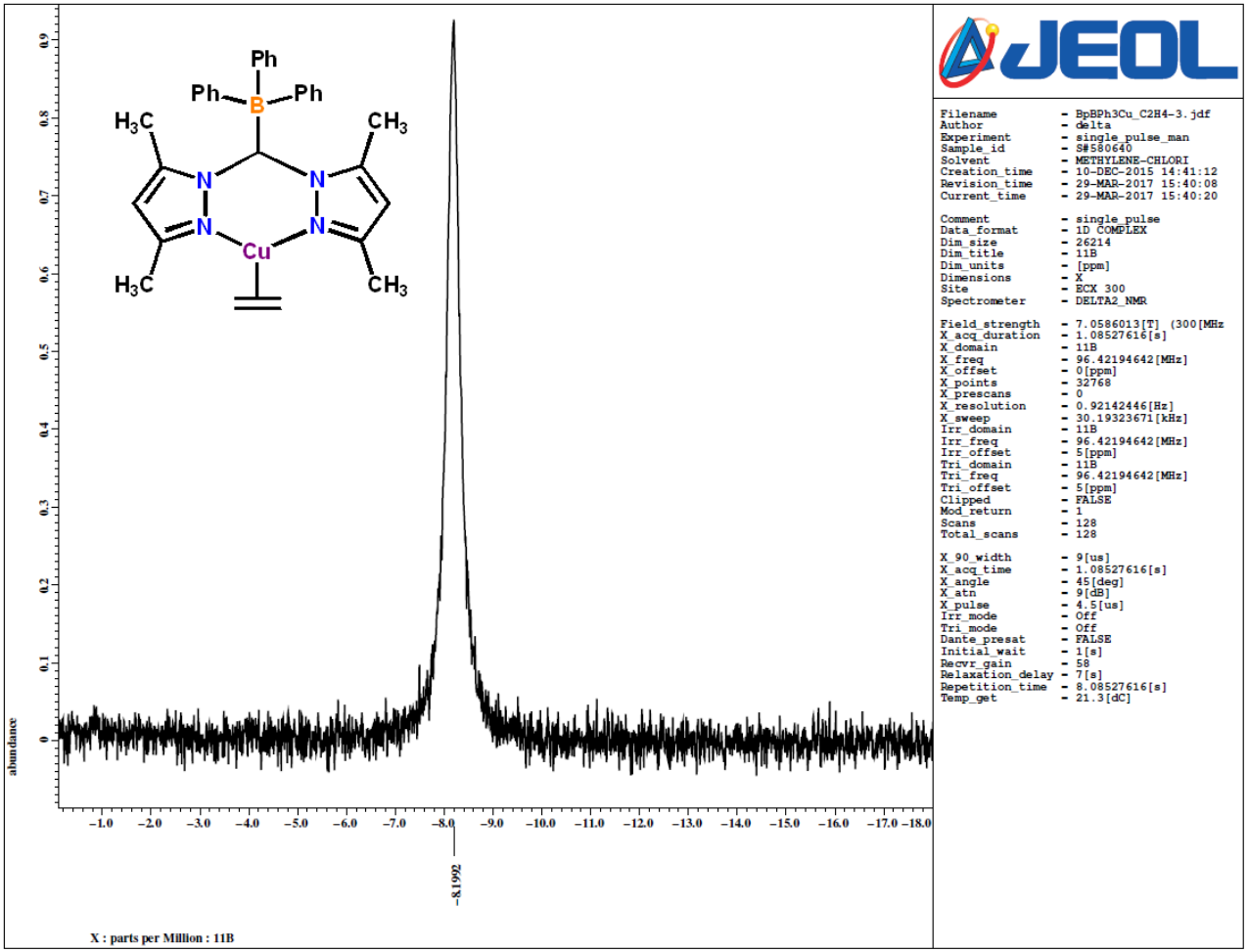

^{11}B NMR Spectrum of [(Ph$_3$B)CH(3,5-(CH$_3$)$_2$Pz)$_2$]Li(C$_2$H$_4$) in CD$_2$Cl$_2$

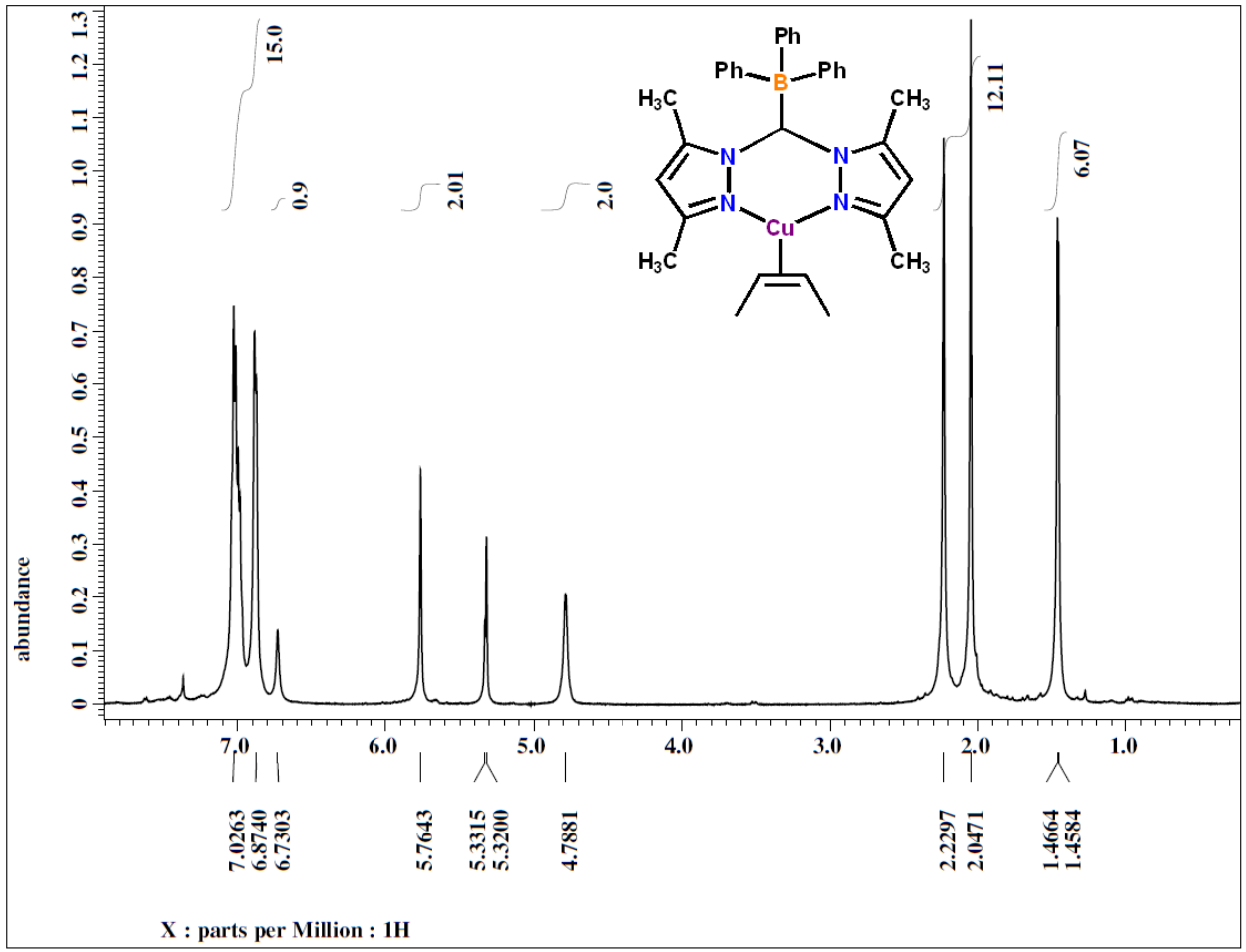

^{1}H NMR Spectrum of [$(Ph_3B)CH(3,5\text{-}(CH_3)_2Pz)_2$]Cu(*cis*-$CH_3HC{=}CHCH_3$)in CD_2Cl_2

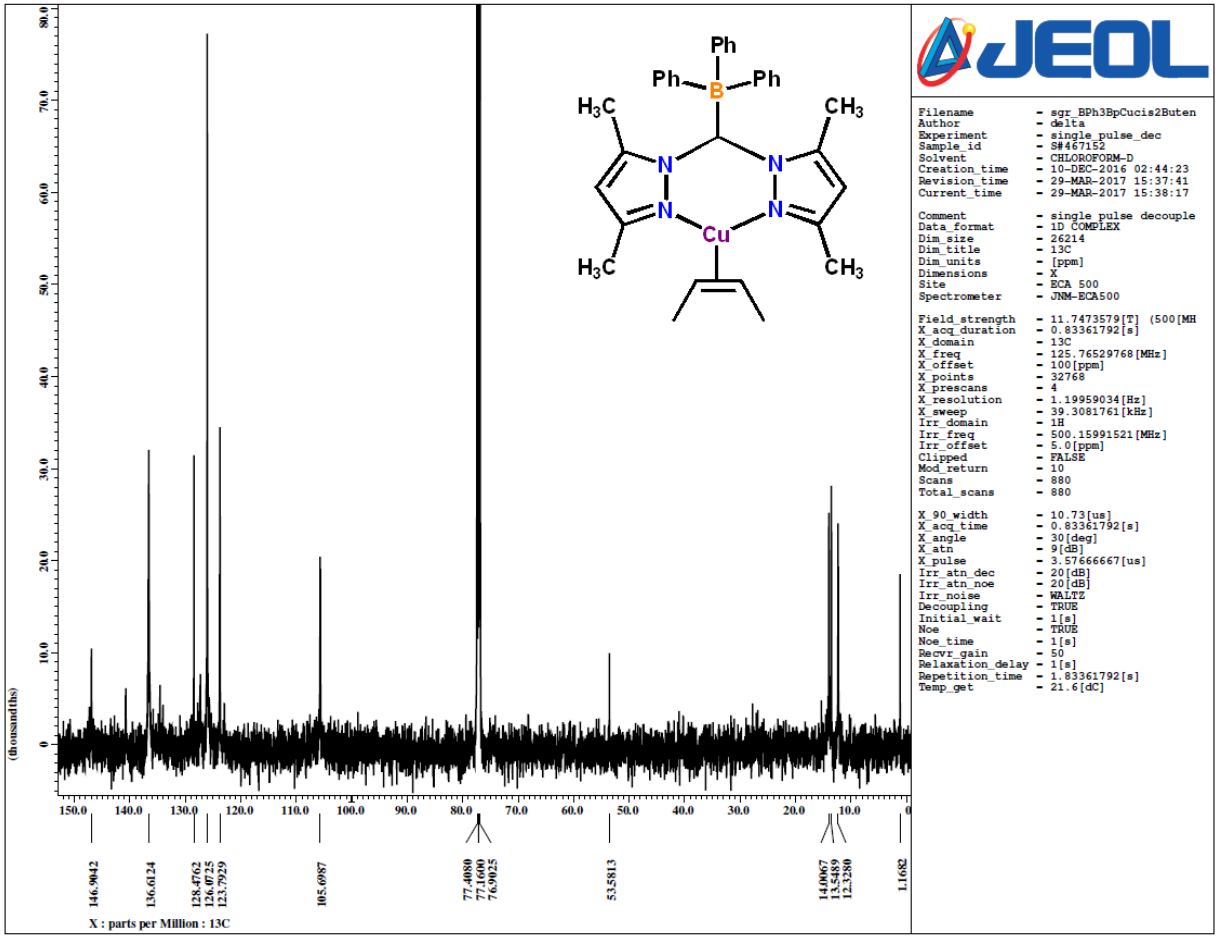

^{13}C NMR Spectrum of [(Ph$_3$B)CH(3,5-(CH$_3$)$_2$Pz)$_2$]Cu(*cis*-CH$_3$HC=CHCH$_3$)in CDCl$_3$

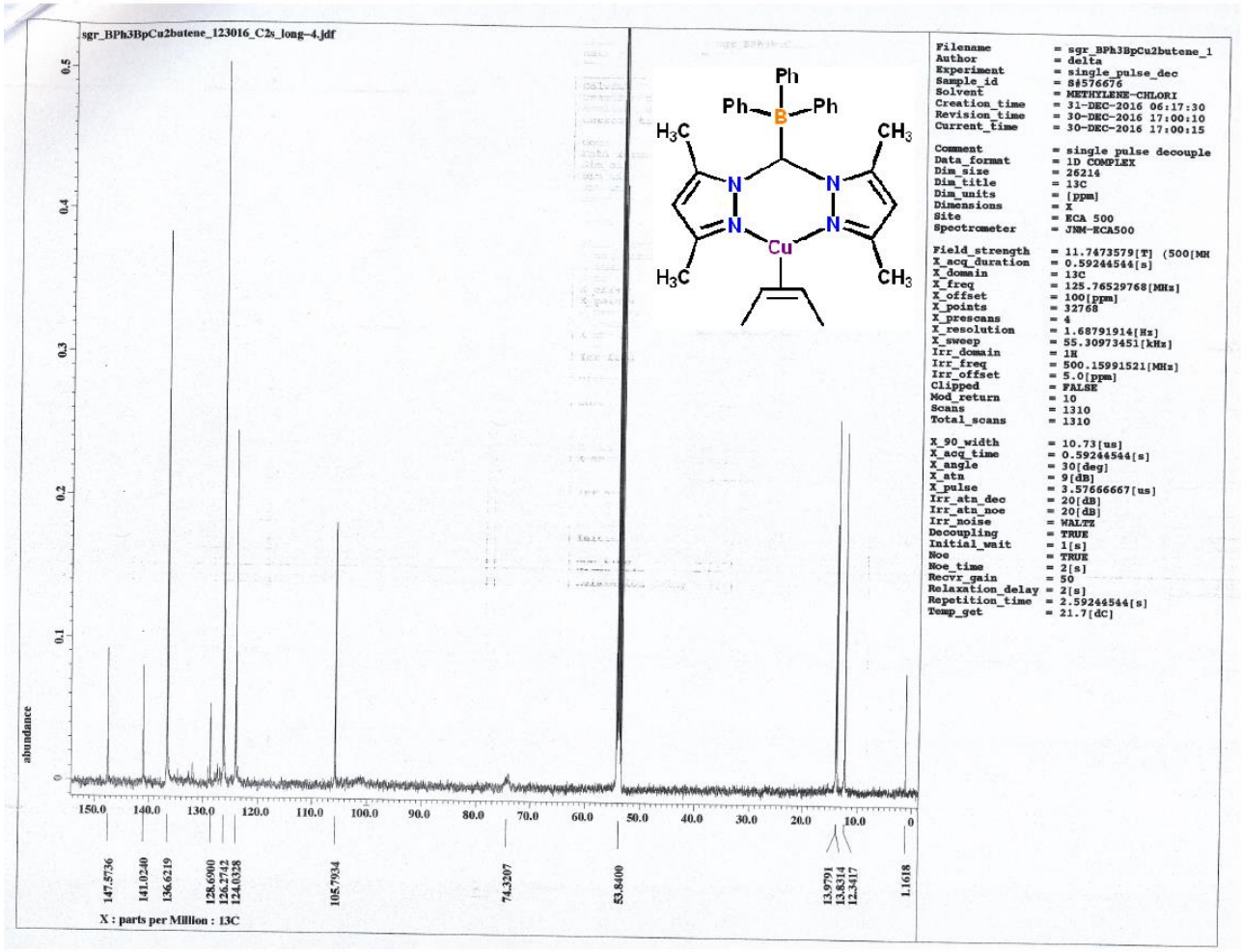

^{13}C NMR Spectrum of [(Ph$_3$B)CH(3,5-(CH$_3$)$_2$Pz)$_2$]Cu(*cis*-CH$_3$HC=CHCH$_3$)in C$_2$DCl$_2$

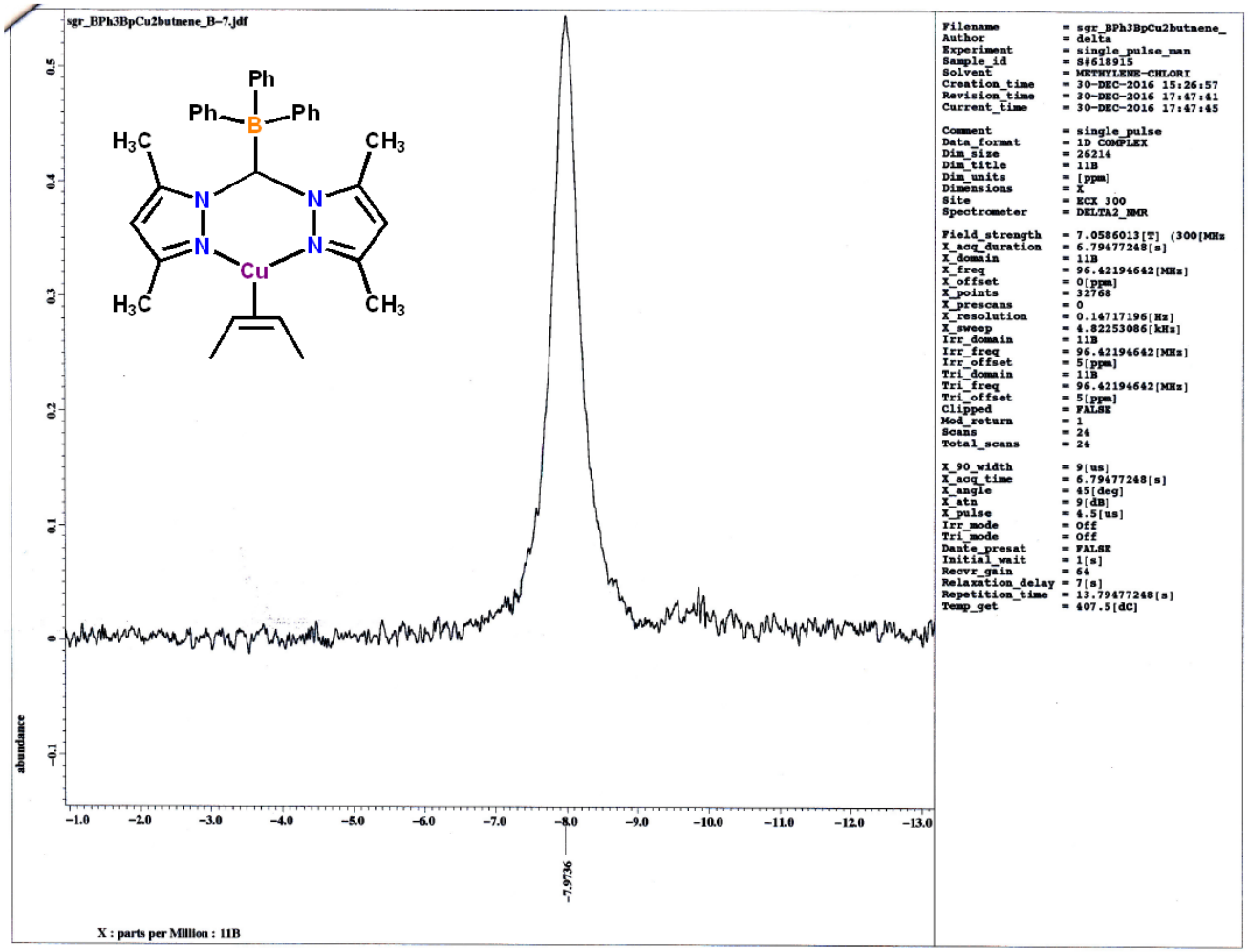

^{11}B NMR Spectrum of [(Ph$_3$B)CH(3,5-(CH$_3$)$_2$Pz)$_2$]Cu(*cis*-CH$_3$HC=CHCH$_3$)in CD$_2$Cl$_2$

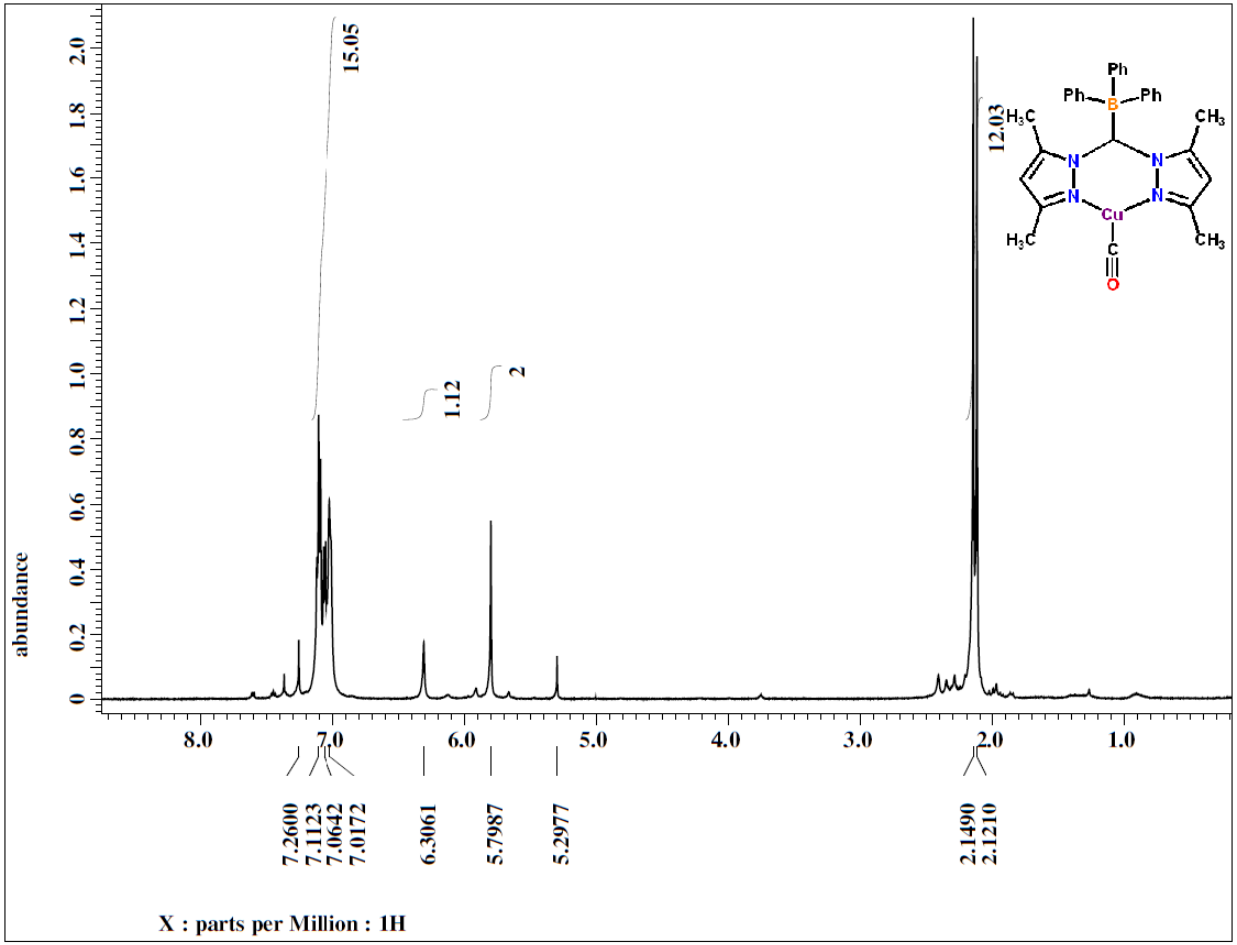

^{1}H NMR Spectrum of [(Ph$_3$B)CH(3,5-(CH$_3$)$_2$Pz)$_2$]Cu(CO)in CDCl$_3$

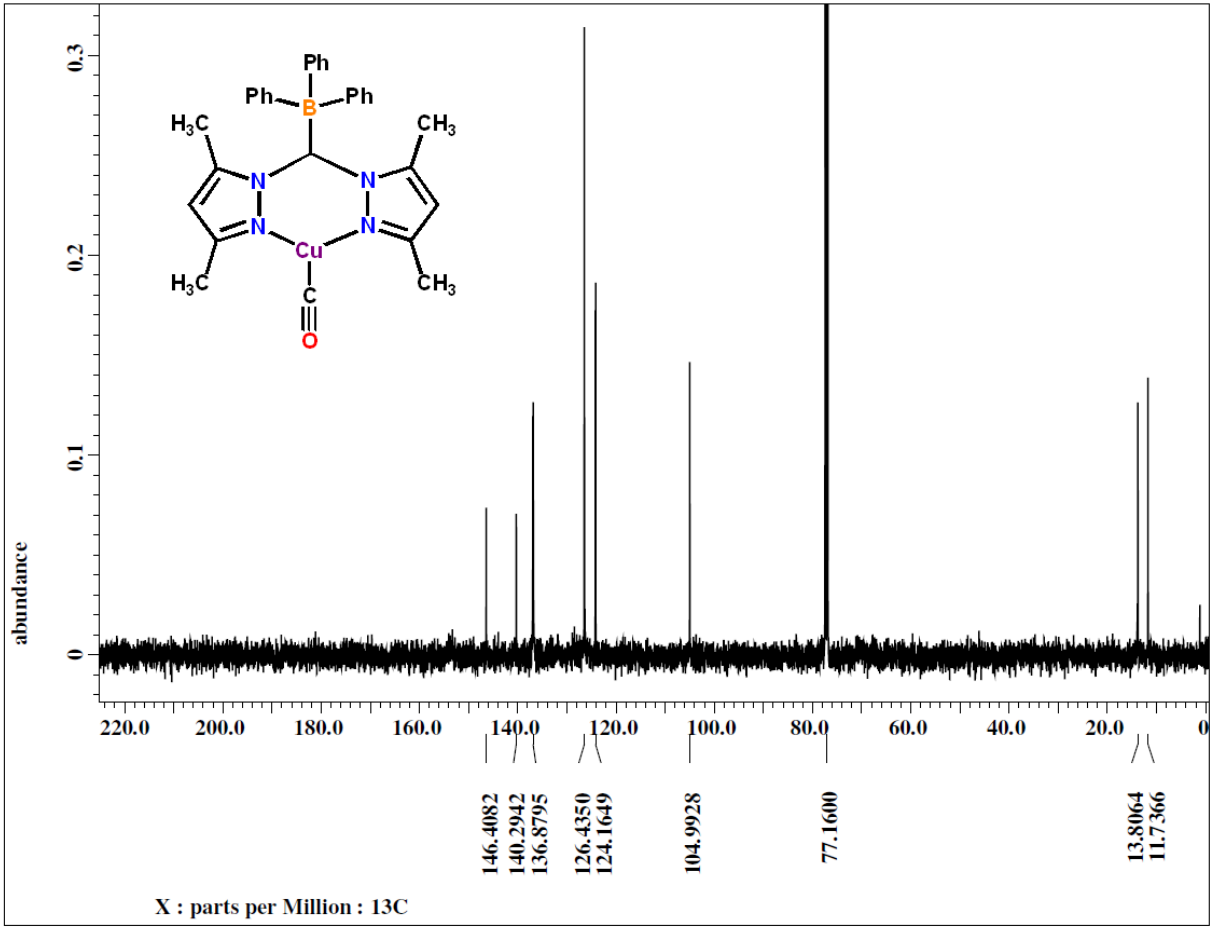

^{13}C NMR Spectrum of [(Ph_3B)CH(3,5-(CH_3)$_2$Pz)$_2$]Cu(CO)in $CDCl_3$

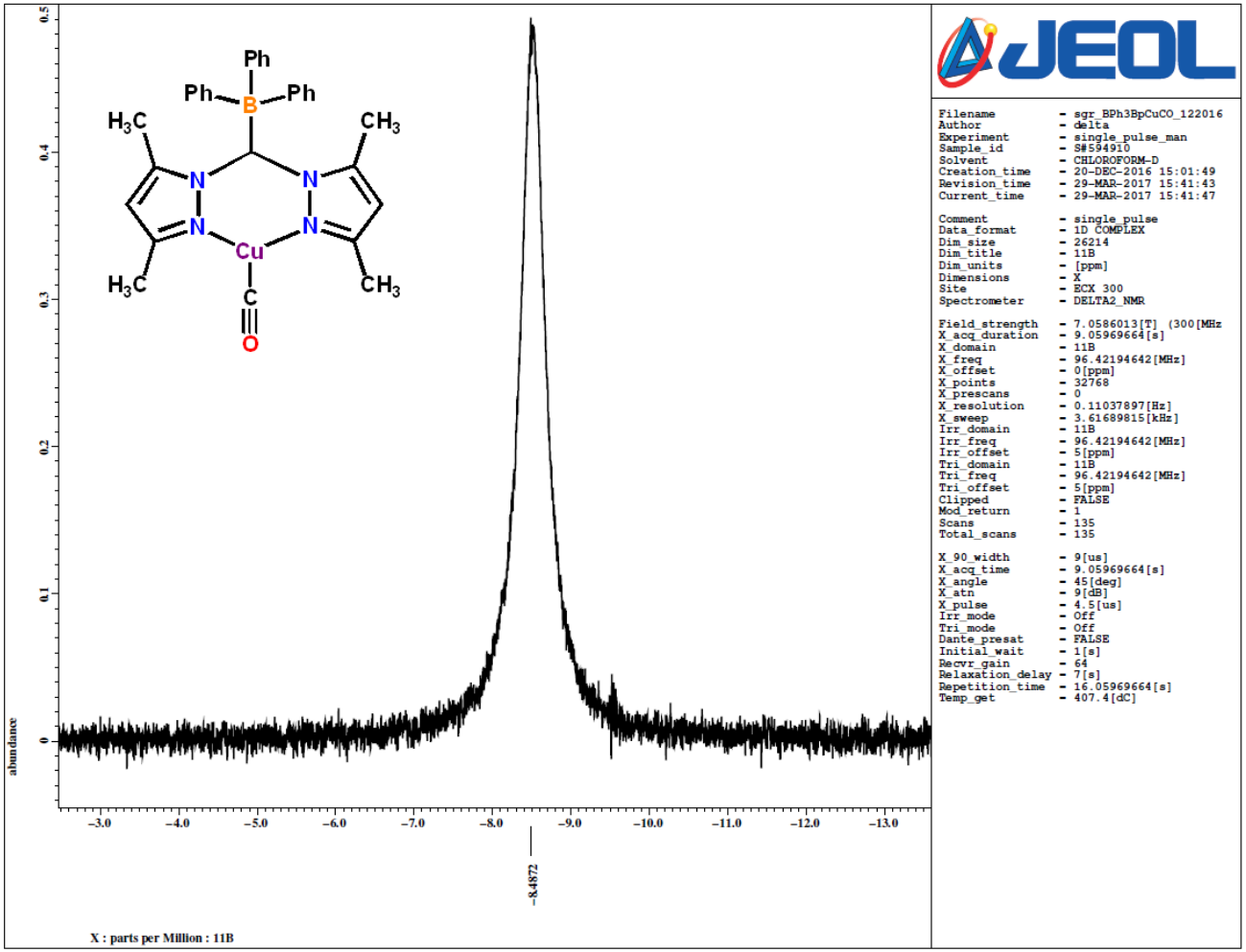

^{11}B NMR Spectrum of [(Ph$_3$B)CH(3,5-(CH$_3$)$_2$Pz)$_2$]Cu(CO)in CDCl$_3$

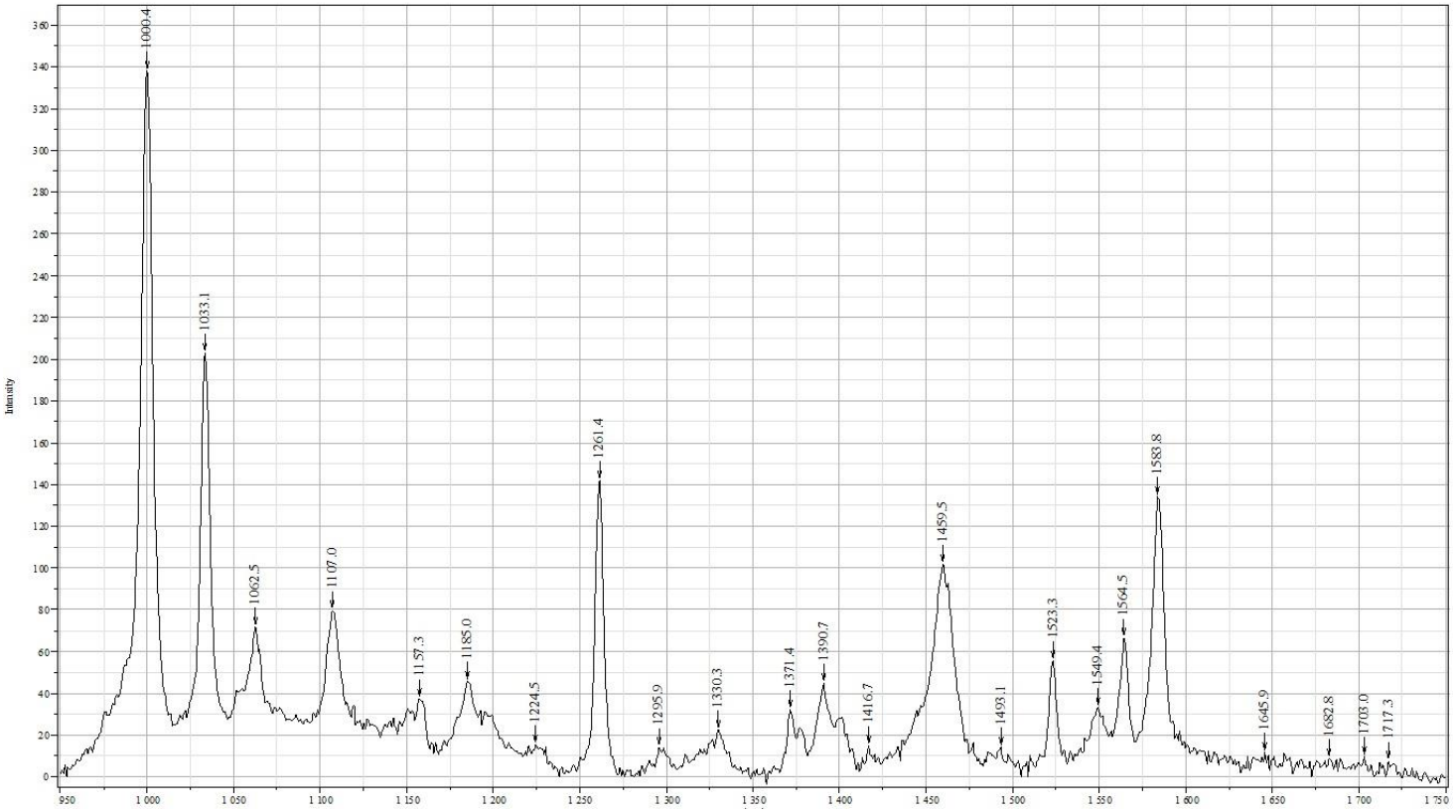

Raman spectrum of $[(Ph_3B)CH(3,5\text{-}(CH_3)_2Pz)_2]Cu(C_2H_4)$

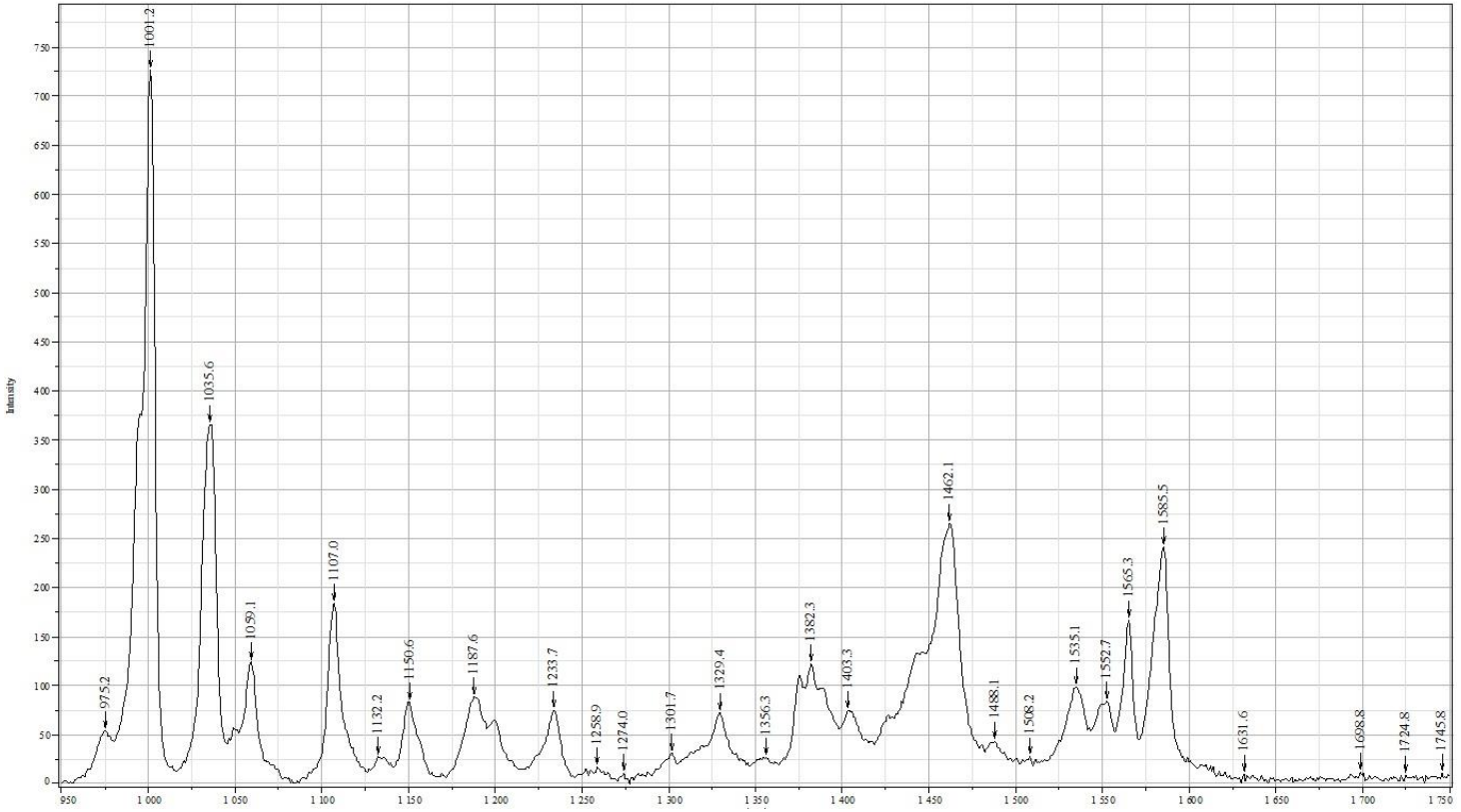

Raman spectrum of $[(Ph_3B)CH(3,5\text{-}(CH_3)_2Pz)_2]Cu(\textit{cis}\text{-}CH_3HC{=}CHCH_3)$

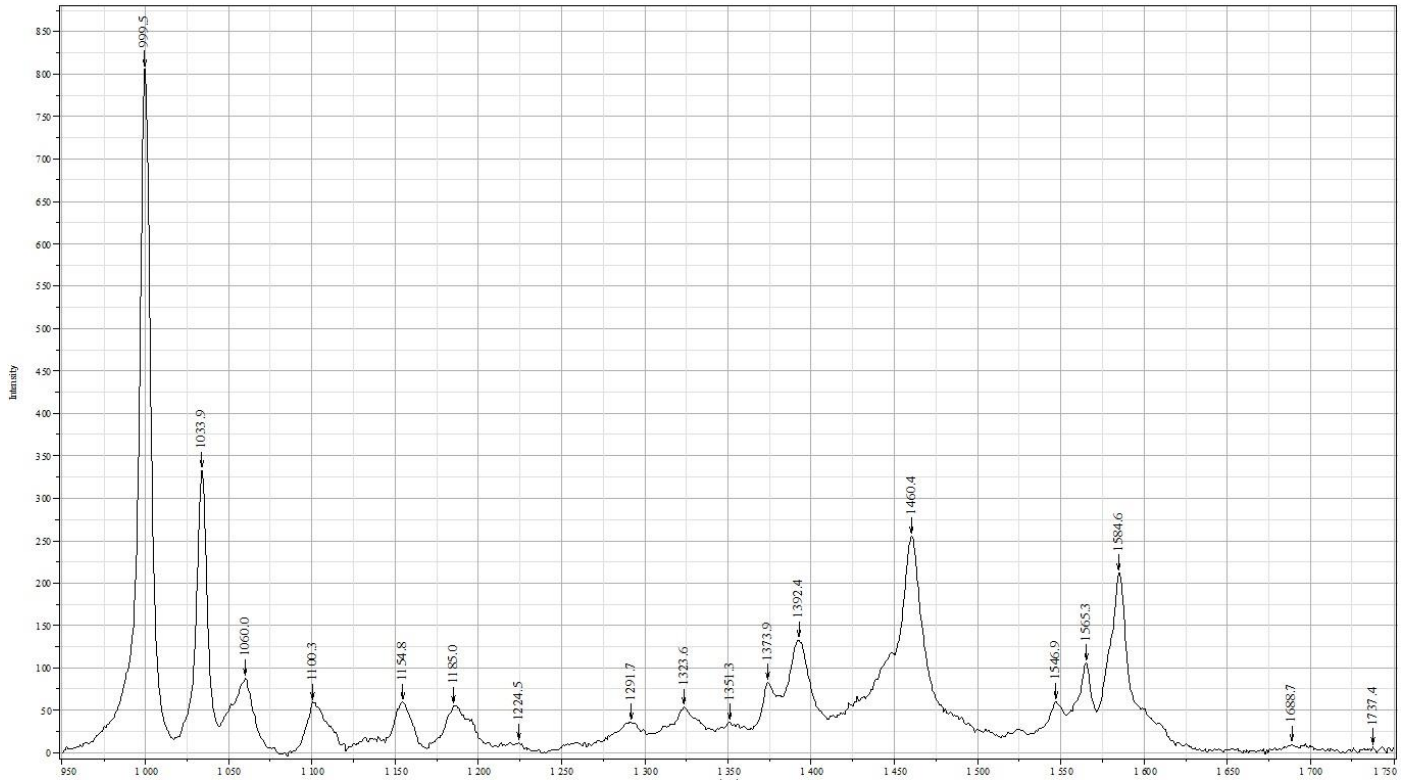

Raman spectrum of $[(Ph_3B)CH(3,5\text{-}(CH_3)_2Pz)_2]Cu(CO)$

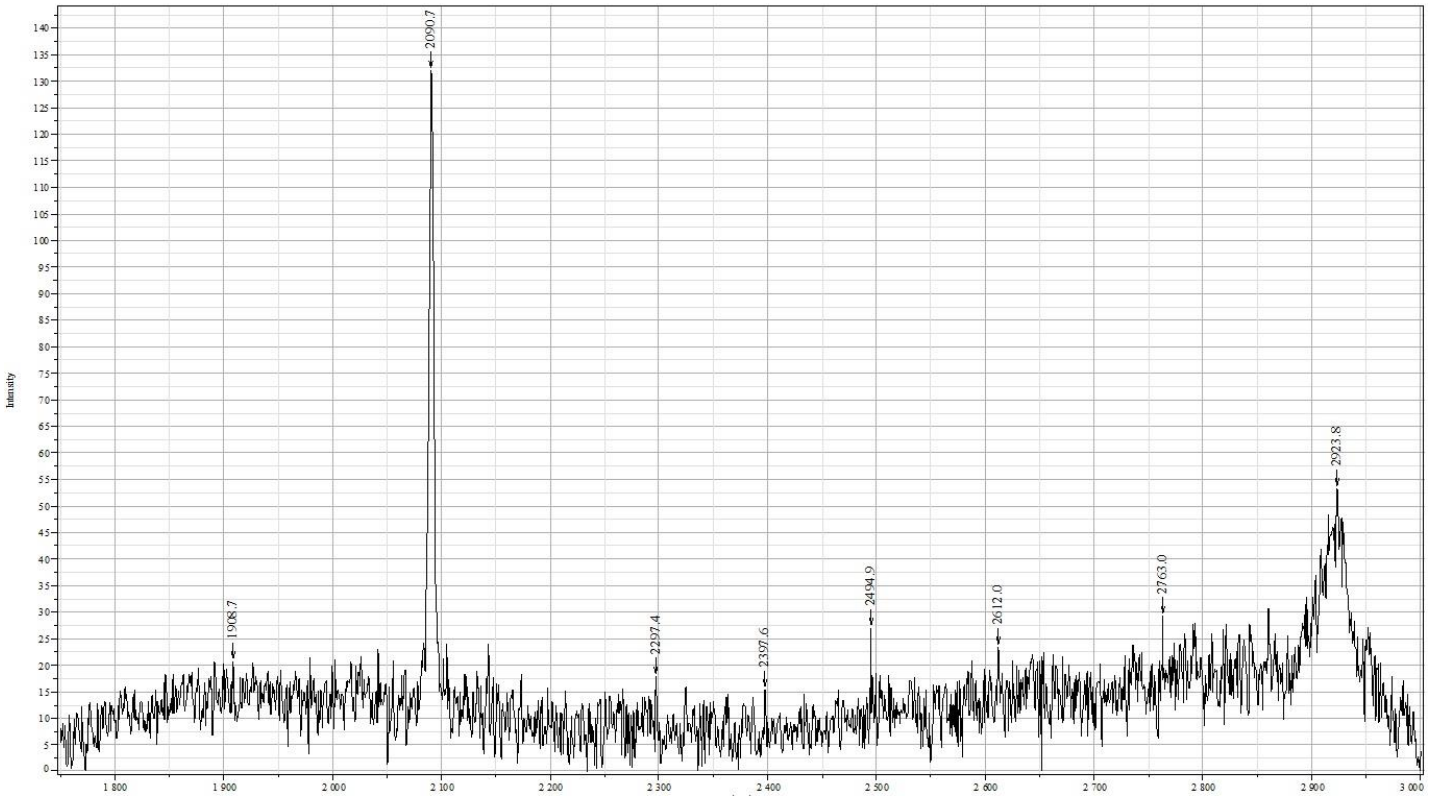

Raman spectrum of $[(Ph_3B)CH(3,5\text{-}(CH_3)_2Pz)_2]Cu(CO)$ showing the CO stretch

Appendix B

X-Ray Crystallographic Data for Selected Compounds

Bond lengths [Å] and angles [deg] for [HB(3-(CF_3),5-(CH_3)Pz)$_3$]Cu(C_2H_4)

Atom	Atom	Length/Å
Cu	C6	2.041(8)
Cu	C7	2.037(7)
Cu	N2^1	2.040(4)
Cu	N2^2	2.2790(10)
Cu	N2	2.024(4)
C6	C7	1.362(6)
F3	C4	1.3240(12)
F1	C4	1.3348(14)
N1	N2	1.3637(9)
N1	C3	1.3559(9)
N1	B	1.5490(8)
F2	C4	1.3328(13)
N2	C1	1.3385(10)
C3	C2	1.3880(11)
C3	C5	1.4923(12)
C1	C2	1.3945(12)
C1	C4	1.4926(12)
B	N1^1	1.5490(8)
B	N1^2	1.5490(8)

Atom	Atom	Atom	Angle/°
C6	Cu	N2^1	107.1(3)
C7	Cu	C6	39.02(18)
C7	Cu	N2^1	114.4(3)
C7	Cu	N2^2	145.8(4)
N2	Cu	C6	150.1(4)
N2^2	Cu	C6	111.3(4)
N2	Cu	C7	111.4(4)
N2	Cu	N2^2	94.67(3)
N2	Cu	N2^1	87.77(10)
N2^2	Cu	N2^1	87.39(11)
C7	C6	Cu	70.3(6)
C6	C7	Cu	70.6(6)
N2	N1	B	119.92(7)
C3	N1	N2	111.00(6)
C3	N1	B	129.04(7)
N1	N2	Cu	115.19(9)
C1	N2	Cu	138.42(11)
C1	N2	N1	105.22(6)
N1	C3	C2	107.48(7)
N1	C3	C5	123.39(7)
C2	C3	C5	129.14(7)
N2	C1	C2	111.72(7)
N2	C1	C4	121.10(8)
C2	C1	C4	127.18(8)
C3	C2	C1	104.58(7)
F3	C4	F1	106.95(10)
F3	C4	F2	107.01(9)
F3	C4	C1	113.17(7)
F1	C4	C1	112.43(8)
F2	C4	F1	106.12(10)
F2	C4	C1	110.74(10)
N1	B	N1^2	109.20(5)
N1	B	N1^1	109.20(5)
N1^2	B	N1^1	109.20(5)

Bond lengths [Å] and angles [deg] for $[HB(3\text{-}(CF_3),5\text{-}(CH_3)Pz)_3]Ag(C_2H_4)$

Atom	Atom	Length/Å
Ag	N2	2.221(4)
Ag	$N2^1$	2.383(7)
Ag	$N2^2$	2.375(7)
Ag	C6	2.256(5)
Ag	C7	2.252(5)
F1	C4	1.324(3)
F2	C4	1.322(3)
F3	C4	1.310(3)
N1	N2	1.359(2)
N1	C3	1.354(3)
N1	B	1.547(2)
N2	C1	1.328(3)
C1	C2	1.384(3)
C1	C4	1.486(3)
C2	C3	1.371(3)
C3	C5	1.491(3)
C6	C7	1.330(13)
B	$N1^2$	1.547(2)
B	$N1^1$	1.547(2)

Atom	Atom	Atom	Angle/°
N2	Ag	$N2^1$	84.56(16)
N2	Ag	$N2^2$	84.36(17)
$N2^1$	Ag	$N2^2$	81.13(10)
N2	Ag	C6	139.7(5)
N2	Ag	C7	124.1(5)
C6	Ag	$N2^2$	109.4(4)
C6	Ag	$N2^1$	134.0(5)
C7	Ag	$N2^2$	143.6(5)
C7	Ag	$N2^1$	120.2(5)
C7	Ag	C6	34.3(3)
N2	N1	B	121.11(19)
C3	N1	N2	110.43(16)
C3	N1	B	128.4(2)
N1	N2	Ag	116.73(16)
C1	N2	Ag	133.87(18)
C1	N2	N1	105.26(17)
N2	C1	C2	111.9(2)
N2	C1	C4	119.5(2)
C2	C1	C4	128.6(2)
C3	C2	C1	104.68(18)
N1	C3	C2	107.75(19)
N1	C3	C5	123.02(19)
C2	C3	C5	129.2(2)
F1	C4	C1	111.1(2)
F2	C4	F1	105.6(2)
F2	C4	C1	111.9(2)
F3	C4	F1	107.1(2)
F3	C4	F2	107.5(3)
F3	C4	C1	113.4(2)
C7	C6	Ag	72.7(3)
C6	C7	Ag	73.0(3)
$N1^2$	B	$N1^1$	110.08(15)
$N1^2$	B	N1	110.08(15)
$N1^1$	B	N1	110.08(15)

Bond lengths [Å] and angles [deg] for $[HB(3\text{-}(CF_3),5\text{-}(CH_3)Pz)_3]Ag(C_2H_4)$

Atom	Atom	Length/Å
Au	N2	2.247(4)
Au	$N2^1$	2.215(4)
Au	C6	2.084(11)
Au	C7	2.088(11)
F1	C4	1.296(7)
F2	C4	1.322(8)
F3	C4	1.318(8)
N1	N2	1.358(5)
N1	C3	1.346(5)
N1	B	1.545(4)
N2	C1	1.324(6)
C1	C2	1.378(7)
C1	C4	1.484(8)
C2	C3	1.368(7)
C3	C5	1.499(7)
C6	C7	1.40(2)
B	$N1^2$	1.545(4)
B	$N1^1$	1.545(4)

Atom	Atom	Atom	Angle/°
$N2^1$	Au	N2	87.72(16)
C6	Au	$N2^1$	119.8(5)
C6	Au	N2	152.3(6)
C6	Au	C7	39.1(6)
C7	Au	$N2^1$	158.8(6)
C7	Au	N2	113.5(6)
N2	N1	B	120.5(4)
C3	N1	N2	110.3(3)
C3	N1	B	129.2(4)
N1	N2	Au	116.9(2)
C1	N2	Au	128.0(3)
C1	N2	N1	105.5(4)
N2	C1	C2	111.5(4)
N2	C1	C4	120.3(5)
C2	C1	C4	128.2(5)
C3	C2	C1	105.0(4)
N1	C3	C2	107.8(4)
N1	C3	C5	123.1(4)
C2	C3	C5	129.2(4)
F1	C4	F2	106.3(6)
F1	C4	F3	108.1(5)
F1	C4	C1	114.6(4)
F2	C4	C1	112.2(5)
F3	C4	F2	103.5(5)
F3	C4	C1	111.4(6)
C7	C6	Au	70.6(5)
C6	C7	Au	70.3(5)
$N1^2$	B	N1	110.5(3)
$N1^1$	B	N1	110.5(3)
$N1^2$	B	$N1^1$	110.5(3)

Bond lengths [Å] and angles [deg] for [HB(3-(CF_3),5-(Ph)Pz)$_3$]Ag(η^2-C_6H_6)

Atom	Atom	Length/Å	Atom	Atom	Length/Å
Ag01	N2	2.4170(9)	C5	C10	1.3979(14)
Ag01	N4	2.3505(9)	C6	C7	1.3964(15)
Ag01	N6	2.3463(9)	C7	C8	1.3896(17)
Ag01	C31	2.4507(12)	C8	C9	1.3937(16)
Ag01	C32	2.4480(12)	C9	C10	1.3934(14)
F1	C4	1.3390(13)	C11	C12	1.3915(14)
F2	C4	1.3439(13)	C11	C14	1.4901(14)
F3	C4	1.3449(13)	C12	C13	1.3902(13)
F4	C14	1.3333(14)	C13	C15	1.4723(13)
F5	C14	1.3442(14)	C15	C16	1.3984(14)
F6	C14	1.3364(15)	C15	C20	1.3960(14)
F7	C24	1.3405(14)	C16	C17	1.3939(15)
F8	C24	1.3335(15)	C17	C18	1.388(2)
F9	C24	1.3336(14)	C18	C19	1.3929(19)
N1	N2	1.3605(11)	C19	C20	1.3924(15)
N1	C3	1.3685(12)	C21	C22	1.3958(14)
N1	B01H	1.5479(13)	C21	C24	1.4867(14)
N2	C1	1.3309(13)	C22	C23	1.3860(14)
N3	N4	1.3604(11)	C23	C25	1.4753(13)
N3	C13	1.3638(12)	C25	C26	1.3999(13)
N3	B01H	1.5591(13)	C25	C30	1.3981(14)
N4	C11	1.3353(13)	C26	C27	1.3954(15)
N5	N6	1.3610(11)	C27	C28	1.3883(18)
N5	C23	1.3678(12)	C28	C29	1.3919(17)
N5	B01H	1.5545(13)	C29	C30	1.3889(15)
N6	C21	1.3355(13)	C31	C32	1.4032(18)
C1	C2	1.3962(14)	C31	C36	1.4008(19)
C1	C4	1.4879(14)	C32	C33	1.3976(19)
C2	C3	1.3878(14)	C33	C34	1.389(2)
C3	C5	1.4765(13)	C34	C35	1.392(2)
C5	C6	1.3984(14)	C35	C36	1.383(2)

Atom	Atom	Atom	Angle/°	Atom	Atom	Atom	Angle/°
N2	Ag01	C31	115.51(4)	C13	C12	C11	103.98(8)
N2	Ag01	C32	108.27(4)	N3	C13	C12	107.96(8)
N4	Ag01	N2	80.61(3)	N3	C13	C15	124.30(8)
N4	Ag01	C31	115.79(4)	C12	C13	C15	127.73(9)
N4	Ag01	C32	148.97(4)	F4	C14	F5	106.88(11)
N6	Ag01	N2	84.41(3)	F4	C14	F6	107.93(11)
N6	Ag01	N4	81.56(3)	F4	C14	C11	111.14(10)
N6	Ag01	C31	154.56(4)	F5	C14	C11	111.72(9)
N6	Ag01	C32	128.08(4)	F6	C14	F5	105.38(10)
C32	Ag01	C31	33.29(4)	F6	C14	C11	113.40(10)
N2	N1	C3	110.20(8)	C16	C15	C13	119.56(9)
N2	N1	B01H	120.52(8)	C20	C15	C13	121.28(9)
C3	N1	B01H	128.66(8)	C20	C15	C16	119.12(9)
N1	N2	Ag01	116.57(6)	C17	C16	C15	120.36(11)
C1	N2	Ag01	137.65(7)	C18	C17	C16	120.12(11)
C1	N2	N1	105.77(8)	C17	C18	C19	119.91(10)
N4	N3	C13	110.24(8)	C20	C19	C18	120.08(11)
N4	N3	B01H	121.63(8)	C19	C20	C15	120.40(11)
C13	N3	B01H	128.00(8)	N6	C21	C22	112.06(9)
N3	N4	Ag01	117.14(6)	N6	C21	C24	120.94(10)
C11	N4	Ag01	137.22(6)	C22	C21	C24	126.99(10)
C11	N4	N3	105.62(8)	C23	C22	C21	104.21(9)
N6	N5	C23	110.36(8)	N5	C23	C22	107.80(9)
N6	N5	B01H	122.57(8)	N5	C23	C25	125.09(9)
C23	N5	B01H	127.07(8)	C22	C23	C25	127.10(9)
N5	N6	Ag01	116.60(6)	F7	C24	C21	111.08(10)
C21	N6	Ag01	137.81(7)	F8	C24	F7	106.22(10)
C21	N6	N5	105.56(8)	F8	C24	C21	112.72(10)
N2	C1	C2	112.14(9)	F9	C24	F7	105.56(11)
N2	C1	C4	120.76(9)	F9	C24	F8	107.38(12)
C2	C1	C4	127.10(9)	F9	C24	C21	113.36(9)
C3	C2	C1	104.08(9)	C26	C25	C23	119.21(9)
N1	C3	C2	107.80(8)	C30	C25	C23	121.62(9)
N1	C3	C5	126.46(9)	C30	C25	C26	119.14(9)
C2	C3	C5	125.73(9)	C27	C26	C25	120.15(10)
F1	C4	F2	107.05(10)	C28	C27	C26	120.20(10)
F1	C4	F3	106.91(9)	C27	C28	C29	119.90(10)
F1	C4	C1	111.11(9)	C30	C29	C28	120.16(11)

F2	C4	F3	105.99(10)	C29	C30	C25	120.46(10)
F2	C4	C1	112.86(9)	C32	C31	Ag01	73.25(7)
F3	C4	C1	112.52(9)	C36	C31	Ag01	108.60(9)
C6	C5	C3	117.83(9)	C36	C31	C32	119.56(12)
C10	C5	C3	123.00(9)	C31	C32	Ag01	73.46(7)
C10	C5	C6	119.13(9)	C33	C32	Ag01	108.17(9)
C7	C6	C5	120.74(10)	C33	C32	C31	119.89(12)
C8	C7	C6	119.70(10)	C34	C33	C32	119.98(13)
C7	C8	C9	119.91(10)	C33	C34	C35	120.01(13)
C10	C9	C8	120.45(10)	C36	C35	C34	120.62(13)
C9	C10	C5	120.04(10)	C35	C36	C31	119.93(13)
N4	C11	C12	112.20(8)	N1	B01H	N3	110.44(8)
N4	C11	C14	119.44(9)	N1	B01H	N5	112.20(8)
C12	C11	C14	128.25(9)	N5	B01H	N3	110.13(7)

Bond lengths [Å] and angles [deg] for [HB(3-(CF_3),5-(Ph)Pz)$_3$]Ag(CO)

Atom	Atom	Length/Å
Ag	N2	2.2933(17)
Ag	N4	2.3199(18)
Ag	N6	2.3052(18)
Ag	C31	2.019(2)
F1	C4	1.317(3)
F2	C4	1.334(3)
F3	C4	1.331(3)
F4	C14	1.312(3)
F4A	C14	1.357(3)
F5	C14	1.299(4)
F5A	C14	1.312(3)
F6	C14	1.365(4)
F6A	C14	1.282(3)
F7	C24	1.307(3)
F8	C24	1.307(3)
F9	C24	1.312(3)
O1	C31	1.110(3)
N1	N2	1.361(2)
N1	C3	1.364(3)
N1	B1	1.552(3)
N2	C1	1.329(3)
N3	N4	1.360(2)
N3	C13	1.364(3)
N3	B1	1.556(3)
N4	C11	1.336(3)
N5	N6	1.362(2)
N5	C23	1.368(3)
N5	B1	1.557(3)
N6	C21	1.329(3)
C1	C2	1.387(3)
C1	C4	1.491(3)
C2	C3	1.384(3)
C3	C5	1.482(3)
C5	C6	1.398(3)
C5	C10	1.396(3)
C6	C7	1.393(3)
C7	C8	1.384(4)
C8	C9	1.384(4)
C9	C10	1.391(3)
C11	C12	1.389(3)
C11	C14	1.478(3)
C12	C13	1.383(3)
C13	C15	1.477(3)
C15	C16	1.394(3)
C15	C20	1.394(3)
C16	C17	1.392(3)
C17	C18	1.377(4)
C18	C19	1.381(4)
C19	C20	1.388(3)
C21	C22	1.389(3)
C21	C24	1.498(3)
C22	C23	1.385(3)
C23	C25	1.476(3)
C25	C26	1.396(3)
C25	C30	1.392(3)
C26	C27	1.392(3)
C27	C28	1.379(4)
C28	C29	1.386(4)
C29	C30	1.388(3)
Cl1A	C32A	1.739(3)
Cl1B	C32B	1.738(3)
Cl2A	C32A	1.739(3)
Cl2B	C32B	1.738(3)

Atom	Atom	Atom	Angle/°	Atom	Atom	Atom	Angle/°
N2	Ag	N4	85.13(6)	N3	C13	C15	124.45(18)
N2	Ag	N6	80.34(6)	C12	C13	C15	127.60(19)
N6	Ag	N4	82.74(6)	F4	C14	F6	97.4(4)
C31	Ag	N2	133.29(9)	F4	C14	C11	117.9(3)
C31	Ag	N4	127.17(9)	F4A	C14	C11	109.6(2)
C31	Ag	N6	130.24(9)	F5	C14	F4	111.3(4)
N2	N1	C3	109.91(16)	F5	C14	F6	101.0(5)
N2	N1	B1	121.11(16)	F5	C14	C11	117.5(4)
C3	N1	B1	128.94(17)	F5A	C14	F4A	102.5(3)
N1	N2	Ag	118.09(12)	F5A	C14	C11	111.3(3)
C1	N2	Ag	135.80(14)	F6	C14	C11	108.1(3)
C1	N2	N1	105.94(17)	F6A	C14	F4A	105.4(4)
N4	N3	C13	110.25(16)	F6A	C14	F5A	111.1(4)
N4	N3	B1	120.83(16)	F6A	C14	C11	115.9(2)
C13	N3	B1	128.39(17)	C16	C15	C13	119.5(2)
N3	N4	Ag	117.60(12)	C20	C15	C13	121.19(19)
C11	N4	Ag	136.86(15)	C20	C15	C16	119.2(2)
C11	N4	N3	105.52(17)	C17	C16	C15	120.2(2)
N6	N5	C23	109.58(16)	C18	C17	C16	120.1(2)
N6	N5	B1	120.52(16)	C17	C18	C19	120.0(2)
C23	N5	B1	129.47(17)	C18	C19	C20	120.6(2)
N5	N6	Ag	118.01(13)	C19	C20	C15	119.8(2)
C21	N6	Ag	135.85(15)	N6	C21	C22	111.96(19)
C21	N6	N5	106.14(17)	N6	C21	C24	120.2(2)
N2	C1	C2	111.90(18)	C22	C21	C24	127.8(2)
N2	C1	C4	119.74(19)	C23	C22	C21	104.28(19)
C2	C1	C4	128.4(2)	N5	C23	C22	108.03(18)
C3	C2	C1	104.44(18)	N5	C23	C25	124.17(18)
N1	C3	C2	107.80(18)	C22	C23	C25	127.70(19)
N1	C3	C5	125.63(18)	F7	C24	F9	106.9(3)
C2	C3	C5	126.55(19)	F7	C24	C21	112.9(2)
F1	C4	F2	106.80(19)	F8	C24	F7	105.7(2)
F1	C4	F3	107.0(2)	F8	C24	F9	106.1(3)
F1	C4	C1	113.84(19)	F8	C24	C21	111.6(2)
F2	C4	C1	111.04(19)	F9	C24	C21	113.1(2)
F3	C4	F2	105.3(2)	C26	C25	C23	118.43(19)
F3	C4	C1	112.30(18)	C30	C25	C23	122.36(19)
C6	C5	C3	117.59(19)	C30	C25	C26	119.2(2)

C10	C5	C3	123.12(19)	C27	C26	C25	120.0(2)
C10	C5	C6	119.2(2)	C28	C27	C26	120.3(2)
C7	C6	C5	120.3(2)	C27	C28	C29	119.9(2)
C8	C7	C6	119.9(2)	C28	C29	C30	120.2(2)
C7	C8	C9	120.3(2)	C29	C30	C25	120.2(2)
C8	C9	C10	120.1(2)	O1	C31	Ag	177.0(3)
C9	C10	C5	120.2(2)	N1	B1	N3	110.89(16)
N4	C11	C12	112.00(19)	N1	B1	N5	109.88(16)
N4	C11	C14	119.72(19)	N3	B1	N5	109.86(16)
C12	C11	C14	128.3(2)	Cl2A	C32A	Cl1A	113.5(4)
C13	C12	C11	104.36(19)	Cl2B	C32B	Cl1B	111.2(4)
N3	C13	C12	107.87(18)				

Bond lengths [Å] and angles [deg] for [HB(3-(CF_3),5-(Ph)Pz)$_3$]Ag(PPh_3)

Atom	Atom	Length/Å	Atom	Atom	Length/Å
Ag	P	2.3690(7)	C11	C12	1.385(4)
Ag	N2	2.410(2)	C11	C14	1.491(4)
Ag	N4	2.349(2)	C12	C13	1.381(4)
Ag	N6	2.415(2)	C13	C15	1.478(3)
P	C31	1.831(3)	C15	C16	1.396(4)
P	C37	1.831(3)	C15	C20	1.394(4)
P	C43	1.830(3)	C16	C17	1.387(4)
F1	C4	1.316(4)	C17	C18	1.384(4)
F2	C4	1.307(4)	C18	C19	1.385(4)
F3	C4	1.318(3)	C19	C20	1.381(4)
F4	C14	1.330(3)	C21	C22	1.391(4)
F5	C14	1.351(4)	C21	C24	1.486(4)
F6	C14	1.337(3)	C22	C23	1.382(4)
F7	C24	1.316(4)	C23	C25	1.473(4)
F8	C24	1.301(4)	C25	C26	1.393(4)
F9	C24	1.310(4)	C25	C30	1.387(4)
N1	N2	1.367(3)	C26	C27	1.383(4)
N1	C3	1.366(3)	C27	C28	1.381(4)
N1	B	1.547(3)	C28	C29	1.382(5)
N2	C1	1.326(3)	C29	C30	1.390(4)
N3	N4	1.363(3)	C31	C32	1.389(4)
N3	C13	1.365(3)	C31	C36	1.396(4)
N3	B	1.556(3)	C32	C33	1.389(4)
N4	C11	1.329(3)	C33	C34	1.381(4)
N5	N6	1.362(3)	C34	C35	1.388(4)
N5	C23	1.364(3)	C35	C36	1.383(4)
N5	B	1.550(3)	C37	C38	1.387(4)
N6	C21	1.328(3)	C37	C42	1.392(4)
C1	C2	1.386(4)	C38	C39	1.393(4)
C1	C4	1.490(4)	C39	C40	1.380(5)
C2	C3	1.384(4)	C40	C41	1.379(5)
C3	C5	1.478(4)	C41	C42	1.388(4)
C5	C6	1.393(4)	C43	C44	1.387(4)
C5	C10	1.395(4)	C43	C48	1.390(4)
C6	C7	1.386(4)	C44	C45	1.392(4)

C7	C8	1.379(5)	C45	C46	1.380(4)
C8	C9	1.386(4)	C46	C47	1.380(4)
C9	C10	1.386(4)	C47	C48	1.383(4)

Atom	Atom	Atom	Angle/°	Atom	Atom	Atom	Angle/°
P	Ag	N2	128.74(5)	F4	C14	C11	113.1(2)
P	Ag	N6	131.93(5)	F5	C14	C11	112.5(2)
N2	Ag	N6	80.40(7)	F6	C14	F5	106.4(2)
N4	Ag	P	135.19(5)	F6	C14	C11	110.8(2)
N4	Ag	N2	80.43(7)	C16	C15	C13	119.6(2)
N4	Ag	N6	79.56(7)	C20	C15	C13	121.7(2)
C31	P	Ag	117.55(8)	C20	C15	C16	118.6(2)
C37	P	Ag	111.88(9)	C17	C16	C15	120.7(2)
C37	P	C31	103.60(12)	C18	C17	C16	120.0(2)
C43	P	Ag	114.65(9)	C17	C18	C19	119.8(3)
C43	P	C31	103.39(12)	C20	C19	C18	120.4(3)
C43	P	C37	104.30(12)	C19	C20	C15	120.5(2)
N2	N1	B	120.6(2)	N6	C21	C22	112.1(2)
C3	N1	N2	110.2(2)	N6	C21	C24	121.0(2)
C3	N1	B	129.1(2)	C22	C21	C24	126.9(2)
N1	N2	Ag	119.27(15)	C23	C22	C21	104.5(2)
C1	N2	Ag	134.92(17)	N5	C23	C22	107.5(2)
C1	N2	N1	105.6(2)	N5	C23	C25	123.3(2)
N4	N3	C13	109.9(2)	C22	C23	C25	129.2(2)
N4	N3	B	121.09(19)	F7	C24	C21	114.3(2)
C13	N3	B	128.8(2)	F8	C24	F7	106.4(3)
N3	N4	Ag	120.11(15)	F8	C24	F9	106.5(3)
C11	N4	Ag	133.54(17)	F8	C24	C21	112.3(3)
C11	N4	N3	105.6(2)	F9	C24	F7	103.4(3)
N6	N5	C23	110.5(2)	F9	C24	C21	113.1(3)
N6	N5	B	122.8(2)	C26	C25	C23	119.8(2)
C23	N5	B	126.6(2)	C30	C25	C23	121.2(2)
N5	N6	Ag	117.47(15)	C30	C25	C26	118.9(2)
C21	N6	Ag	136.85(18)	C27	C26	C25	120.7(3)
C21	N6	N5	105.4(2)	C28	C27	C26	119.9(3)
N2	C1	C2	112.1(2)	C27	C28	C29	120.1(3)
N2	C1	C4	120.3(2)	C28	C29	C30	119.9(3)

C2	C1	C4	127.5(2)	C25	C30	C29	120.4(3)
C3	C2	C1	104.8(2)	C32	C31	P	122.3(2)
N1	C3	C2	107.3(2)	C32	C31	C36	119.0(3)
N1	C3	C5	126.2(2)	C36	C31	P	118.7(2)
C2	C3	C5	126.5(2)	C33	C32	C31	120.4(3)
F1	C4	F3	105.5(3)	C34	C33	C32	120.1(3)
F1	C4	C1	112.1(2)	C33	C34	C35	119.9(3)
F2	C4	F1	107.8(3)	C36	C35	C34	120.1(3)
F2	C4	F3	106.5(3)	C35	C36	C31	120.4(3)
F2	C4	C1	113.0(3)	C38	C37	P	122.7(2)
F3	C4	C1	111.6(2)	C38	C37	C42	119.1(3)
C6	C5	C3	118.0(2)	C42	C37	P	118.2(2)
C6	C5	C10	118.4(2)	C37	C38	C39	120.1(3)
C10	C5	C3	123.5(2)	C40	C39	C38	120.4(3)
C7	C6	C5	120.8(3)	C41	C40	C39	119.7(3)
C8	C7	C6	120.3(3)	C40	C41	C42	120.4(3)
C7	C8	C9	119.6(3)	C41	C42	C37	120.3(3)
C8	C9	C10	120.3(3)	C44	C43	P	118.7(2)
C9	C10	C5	120.6(2)	C44	C43	C48	118.6(3)
N4	C11	C12	112.1(2)	C48	C43	P	122.7(2)
N4	C11	C14	119.3(2)	C43	C44	C45	120.6(3)
C12	C11	C14	128.5(2)	C46	C45	C44	120.0(3)
C13	C12	C11	104.5(2)	C47	C46	C45	119.8(3)
N3	C13	C12	107.8(2)	C46	C47	C48	120.1(3)
N3	C13	C15	124.2(2)	C47	C48	C43	120.9(3)
C12	C13	C15	128.0(2)	N1	B	N3	110.5(2)
F4	C14	F5	106.0(2)	N1	B	N5	110.48(19)
F4	C14	F6	107.7(2)	N5	B	N3	110.3(2)

References

1. Thompson, J. S.; Harlow, R. L.; Whitney, J. F., *J. Am. Chem. Soc.* **1983,** *105* (11), 3522-7, and the references therein.

2. McManus, M. T., *The Plant Hormone Ethylene*. Wiley-Blackwell: 2012; Vol. 44.

3. Saltveit, M. E., *Postharvest Biology and Technology* **1999,** *15* (3), 279-292.

4. Lin, Z.; Zhong, S.; Grierson, D., *Journal of Experimental Botany* **2009,** *60* (12), 3311-3336.

5. Abeles, F. B.; Morgan, P. W.; Saltveit Jr, M. E., CHAPTER 1 - Introduction and Historical Perspectives. In *Ethylene in Plant Biology (Second Edition)*, Academic Press: New York, 1992; pp 1-13.

6. Sisler, E. C.; Grichko, V. P.; Serek, M., Interaction of Ethylene and Other Compounds with the Ethylene Receptor: Agonists and Antagonists. In *Ethylene Action in Plants*, Khan, N. A., Ed. Springer Berlin Heidelberg: Berlin, Heidelberg, 2006; pp 1-34.

7. Sisler, E. C.; Serek, M., *Plant Biology* **2003,** *5* (5), 473-480.

8. Mayerhofer, H.; Panneerselvam, S.; Kaljunen, H.; Tuukkanen, A.; Mertens, H. D. T.; Mueller-Dieckmann, J., *J. Biol. Chem.* **2014**.

9. Burg, S. P.; Burg, E. A., *Plant Physiol.* **1967,** *42* (1), 144-152.

10. Rodriguez, F. I.; Esch, J. J.; Hall, A. E.; Binder, B. M.; Schaller, G. E.; Bleeckert, A. B., *Science* **1999,** *283* (5404), 996-998.

11. Binder, B. M.; Rodriguez, F. I.; Bleecker, A. B.; Patterson, S. E., *FEBS Letters* **2007,** *581* (26), 5105-5109.

12. Lacey, R. F.; Binder, B. M., *J. Inorg. Biochem.* **2014,** *133*, 58-62.

13. Evans, D. E.; Bengochea, T.; Cairns, A. J.; Dodds, J. H.; Hall, M. A., *Plant Cell Environ.* **1982,** *5* (1), 101-107.

14. Gamble, R. L.; Coonfield, M. L.; Schaller, G. E., *Proceedings of the National Academy of Sciences* **1998,** *95* (13), 7825-7829.

15. Sisler, E. C.; Serek, M., *Physiologia Plantarum* **1997,** *100* (3), 577-582.

16. Sisler, E. C.; Serek, M.; Dupille, E.; Goren, R., *Plant Growth Regul.* **1999,** *27* (2), 105-111.

17. Pirrung, M. C.; Bleecker, A. B.; Inoue, Y.; Rodríguez, F. I.; Sugawara, N.; Wada, T.; Zou, Y.; Binder, B. M., *Chem. Biol.* **2008,** *15* (4), 313-321.

18. Serek, M.; Woltering, E. J.; Sisler, E. C.; Frello, S.; Sriskandarajah, S., *Biotechnol. Adv.* **2006,** *24* (4), 368-381.

19. Kofranek, A. M.; Paul, J. L. In *THE VALUE OF IMPREGNATING CUT STEMS WITH HIGH CONCENTRATIONS OF SILVER NITRATE*, International Society for Horticultural Science (ISHS), Leuven, Belgium: 1975; pp 199-206.

20. Veen, H.; van de Geijn, S. C., *Planta* **1978,** *140* (1), 93-96.

21. van Doom, W. G.; Woltering, E. J. In *Developments in the Use of Growth Regulators for the Maintance of Post-Harvest Quality in Cut Flowers and Potted*

Plants, International Society for Horticultural Science (ISHS), Leuven, Belgium: 1991; pp 195-210.

22. Knee, M., *Postharvest Biology and Technology* **1995,** *6* (1), 121-128.

23. Arora, A.; Padua, G. W., *Journal of Food Science* **2010,** *75* (1), R43-R49.

24. Ahmad, N.; Bhatnagar, S.; Dubey, S. D.; Saxena, R.; Sharma, S.; Dutta, R., Nanopackaging in Food and Electronics. In *Nanoscience in Food and Agriculture 4*, Ranjan, S.; Dasgupta, N.; Lichtfouse, E., Eds. Springer International Publishing: Cham, 2017; pp 45-97.

25. Trofimenko, S., *J. Am. Chem. Soc.* **1967,** *89* (24), 6288-6294.

26. Kulkarni, N. V.; Dash, C.; Jayaratna, N. B.; Ridlen, S. G.; Karbalaei Khani, S.; Das, A.; Kou, X.; Yousufuddin, M.; Cundari, T. R.; Dias, H. V. R., *Inorg. Chem.* **2015,** *54* (23), 11043-11045.

27. Kulkarni, N. V.; Das, A.; Jayaratna, N. B.; Yousufuddin, M.; Dias, H. V. R., *Inorg. Chem.* **2015,** *54* (11), 5151-5153.

28. Jayaratna, N. B.; Pardue, D. B.; Ray, S.; Yousufuddin, M.; Thakur, K. G.; Cundari, T. R.; Dias, H. V. R., *Dalton Trans.* **2013,** *42* (43), 15399-15410.

29. Hirsch, J.; George, S. D.; Solomon, E. I.; Hedman, B.; Hodgson, K. O.; Burstyn, J. N., *Inorg. Chem.* **2001,** *40* (10), 2439-2441.

30. Porchia, M.; Dolmella, A.; Gandin, V.; Marzano, C.; Pellei, M.; Peruzzo, V.; Refosco, F.; Santini, C.; Tisato, F., *Eur. J. Med. Chem.* **2013,** *59*, 218-226.

31. Dias, H. V. R.; Gorden, J. D., *Inorg. Chem.* **1996,** *35* (2), 318-24.

32. Dias, H. V. R.; Richey, S. A.; Diyabalanage, H. V. K.; Thankamani, J., *J. Organometallic Chem.* **2005,** *690* (8), 1913-1922.

33. Dias, H. V. R.; Lovely, C. J., *Chem. Rev.* **2008,** *108* (8), 3223-38.

34. Ridlen, S. G.; Wu, J.; Kulkarni, N. V.; Dias, H. V. R., *Eur. J. Inorg. Chem.* **2016,** *2016* (15-16), 2573-2580.

35. Trofimenko, S., *Chem. Rev.* **1993,** *93* (3), 943-80.

36. Trofimenko, S., *Scorpionates: The Coordination Chemistry of Polypyrazolylborate Ligands*. Imperial College: London, 1999.

37. Pettinari, C.; Santini, C., *Comp. Coord. Chem. II* **2004,** *1*, 159-210.

38. Santini, C.; Pellei, M.; Lobbia, G. G.; Papini, G., *Mini-Rev. Org. Chem.* **2010,** *7* (2), 84-124.

39. Pettinari, C., *Scorpionates II: Chelating Borate Ligands*. Imperial College Press: London, 2008.

40. Dias, H. V. R.; Lu, H.-L.; Ratcliff, R. E.; Bott, S. G., *Inorg. Chem.* **1995,** *34* (8), 1975-6.

41. Dias, H. V. R.; Jin, W.; Kim, H.-J.; Lu, H.-L., *Inorg. Chem.* **1996,** *35* (8), 2317-28.

42. Dias, H. V. R.; Gioia Lobbia, G.; Papini, G.; Pellei, M.; Santini, C., *Eur. J. Inorg. Chem.* **2009,** (26), 3935-3941.

43. Dias, H. V. R.; Alidori, S.; Lobbia, G. G.; Papini, G.; Pellei, M.; Santini, C., *Inorg. Chem.* **2007,** *46* (23), 9708-9714.

44. Kou, X.; Wu, J.; Cundari, T. R.; Dias, H. V. R., *Dalton Trans.* **2009,** (6), 915-917.

45. Kou, X.; Dias, H. V. R., *Dalton Trans.* **2009,** (36), 7529-7536.

46. Jayaratna, N. B.; Gerus, I. I.; Mironets, R. V.; Mykhailiuk, P. K.; Yousufuddin, M.; Dias, H. V. R., *Inorg. Chem.* **2013,** *52* (4), 1691-1693.

47. Dias, H. V. R.; Wang, X.; Diyabalanage, H. V. K., *Inorg. Chem.* **2005,** *44* (21), 7322-7324.

48. Dias, H. V. R.; Wu, J.; Wang, X.; Rangan, K., *Inorg. Chem.* **2007,** *46* (6), 1960-1962.

49. Dias, H. V. R.; Kim, H.-J., *Organometallics* **1996,** *15* (25), 5374-5379.

50. Dias, H. V. R.; Wang, X., *Dalton Trans.* **2005,** (18), 2985-2987, and the references therein.

51. Dias, H. V. R.; Wu, J., *Organometallics* **2012,** *31* (4), 1511-1517.

52. Dias, H. V. R.; Kim, H.-J.; Lu, H.-L.; Rajeshwar, K.; de Tacconi, N. R.; Derecskei-Kovacs, A.; Marynick, D. S., *Organometallics* **1996,** *15* (13), 2994-3003.

53. Dias, H. V. R.; Browning, R. G.; Richey, S. A.; Lovely, C. J., *Organometallics* **2005,** *24*, 5784.

54. Dias, H. V. R.; Browning, R. G.; Richey, S. A.; Lovely, C. J., *Organometallics* **2004,** *23*, 1200.

55. Dias, H. V. R.; Browning, R. G.; Polach, S. A.; Diyabalanage, H. V. K.; Lovely, C. J., *J. Am. Chem. Soc.* **2003,** *125*, 9270-9271.

56. Rangan, K.; Fianchini, M.; Singh, S.; Dias, H. V. R., *Inorg. Chim. Acta* **2009,** *362* (12), 4347-4352.

57. Diaz-Requejo, M. M.; Perez, P. J., *Chem. Rev.* **2008,** *108* (8), 3379-3394.

58. Lovely, C. J.; Flores, J. A.; Meng, X.; Dias, H. V. R., *Synlett* **2009,** (1), 129-132.

59. Esser, B.; Schnorr, J. M.; Swager, T. M., *Angew. Chem., Int. Ed.* **2012,** *51* (23), 5752-5756.

60. Gorun, S. M.; Hu, Z.; Stibrany, R. T.; Carpenter, G., *Inorg. Chim. Acta* **2000,** *297* (1-2), 383-388.

61. Hu, Z.; Williams, R. D.; Tran, D.; Spiro, T. G.; Gorun, S. M., *J. Am. Chem. Soc.* **2000,** *122* (14), 3556-3557.

62. Diaconu, D.; Hu, Z.; Gorun, S. M., *J. Am. Chem. Soc.* **2002,** *124* (8), 1564-1565.

63. Krishnamoorthy, P.; Browning, R. G.; Singh, S.; Sivappa, R.; Lovely, C. J.; Dias, H. V. R., *Chem. Commun.* **2007**, 731-732.

64. Lovely, C. J.; Browning, R. G.; Badarinarayana, V.; Dias, H. V. R., *Tetrahedron Lett.* **2005,** *46*, 2453.

65. Dias, H. V. R.; Lu, H.-L.; Kim, H.-J.; Polach, S. A.; Goh, T. K. H. H.; Browning, R. G.; Lovely, C. J., *Organometallics* **2002,** *21* (7), 1466-1473, and the references therein.

66. Chisholm, M. H.; Eilerts, N. W.; Huffman, J. C.; Iyer, S. S.; Pacold, M.; Phomphrai, K., *J. Am. Chem. Soc.* **2000,** *122* (48), 11845-11854.

67. Dias, H. V. R.; Jin, W., *Inorg. Chem.* **2003,** *42* (17), 5034-5036.

68. Schneider, J. L.; Carrier, S. M.; Ruggiero, C. E.; Young, V. G., Jr.; Tolman, W. B., *J. Am. Chem. Soc.* **1998,** *120* (44), 11408-11418.

69. Dias, H. V. R.; Jin, W., *J. Am. Chem. Soc.* **1995,** *117* (45), 11381-2.

70. Dias, H. V. R.; Lu, H.-L., *Inorg. Chem.* **1995,** *34* (21), 5380-2.

71. Dias, H. V. R.; Jin, W., *Inorg. Chem.* **1996,** *35* (12), 3687-3694.

72. Dias, H. V. R.; Polach, S. A.; Goh, S.-K.; Archibong, E. F.; Marynick, D. S., *Inorg. Chem.* **2000,** *39* (17), 3894-3901.

73. Dias, H. V. R.; Wang, Z., *Inorg. Chem.* **2000,** *39* (16), 3724-3727.

74. Dias, H. V. R.; Polach, S. A., *Inorg. Chem.* **2000,** *39* (21), 4676-4677.

75. Ayers, A. E.; Dias, H. V. R., *Inorg. Chem.* **2002,** *41* (12), 3259-3268.

76. Dias, H. V. R.; Ayers, A. E., *Polyhedron* **2002,** *21* (5-6), 611-618.

77. van Waasbergen, L. G.; Fajdetic, I.; Fianchini, M.; Dias, H. V. R., *J. Inorg. Biochem.* **2007,** *101* (8), 1180-1183.

78. Dias, H. V. R.; Batdorf, K. H.; Fianchini, M.; Diyabalanage, H. V. K.; Carnahan, S.; Mulcahy, R.; Rabiee, A.; Nelson, K.; van Waasbergen, L. G., *J. Inorg. Biochem.* **2006,** *100* (1), 158-160.

79. Dias, H. V. R.; Goh, T. K. H. H., *Polyhedron* **2004,** *23* (2-3), 273-282.

80. Dias, H. V. R.; Wang, Z.; Jin, W., *Inorg. Chem.* **1997,** *36* (27), 6205-6215.

81. Dias, H. V. R.; Wu, J., *Angew. Chem., Int. Ed.* **2007,** *46*, 7814 - 7816.

82. Dias, H. V. R.; Wu, J., *Euro. J. Inorg. Chem.* **2008**, 509-522, and **2008**, 2113.

83. Dias, H. V. R., *Pure Appl. Chem.* **2010,** *82* (3), 649-656.

84. Dias, H. V. R.; Fianchini, M., *Comments Inorg. Chem.* **2007,** *28* (1-2), 73-92.

85. Dash, C.; Rasika Dias, H. V., Synthesis and Reactivity of Gold–Olefin Complexes. In *PATAI'S Chemistry of Functional Groups*, John Wiley & Sons, Ltd: 2009.

86. Beyer, E. M., Jr., *Plant Physiol.* **1979,** *63* (1), 169-73.

87. Davies, K. M.; Hobson, G. E.; Grierson, D., *J. Plant Physiology* **1990,** *135* (6), 708-13.

88. Ecker, J. R., *Science* **1995,** *268* (5211), 667-75.

89. Halevy, A. H., *Acta Horticulturae* **1995,** *394* (Plant Bioregulators in Horticulture--1994), 37-43, and the references therein.

90. Reid, M. S.; Evans, R. Y.; Dodge, L. L.; Mor, Y., *J. Am. Soc. for Horticultural Science* **1989,** *114* (3), 436-40.

91. Schaller, G. E.; Bleecker, A. B., *Science* **1995,** *270* (5243), 1809-11.

92. Williams, C. M.; Mander, L. N., *Tetrahedron* **2001,** *57* (3), 425-447.

93. van Beek, T. a.; Subrtova, D., *Phytochemical Analysis* **1995,** *6* (1), 1-19.

94. Safarik, D. J.; Eldridge, R. B., *Ind. Eng. Chem. Res.* **1998,** *37* (7), 2571-2581.

95. Eldrige, R. B., *Ind. Eng. Chem. Res.* **1993,** *32* (10), 2208-12.

96. Lee, H.; Kim, D. B.; Kim, S.-H.; Kim, H. S.; Kim, S. J.; Choi, D. K.; Kang, Y. S.; Won, J., *Angew. Chem. Int. Ed.* **2004,** *43* (23), 3053-3056.

97. Jose, B.; Ryu, J. H.; Lee, B. G.; Lee, H.; Kang, Y. S.; Kim, H. S., *Chem. Commun.* **2001,** (20), 2046-2047.

98. Kim, H. S.; Bae, J. Y.; Park, S. J.; Lee, H.; Bae, H. W.; Kang, S. O.; Lee, S. D.; Choi, D. K., *Chem. Eur. J.* **2007,** *13* (9), 2655-2660.

99. Nymeijer, K.; Visser, T.; Brilman, W.; Wessling, M., *Ind. Eng. Chem. Res.* **2004,** *43* (11), 2627-2635, and the references therein.

100. Nymeijer, D. C.; Visser, T.; Assen, R.; Wessling, M., *Separ. Purific. Tech.* **2004,** *37* (3), 209-220.

101. Linic, S.; Piao, H.; Adib, K.; Barteau, M. A., *Angew. Chem., Int. Ed.* **2004,** *43* (22), 2918-2921.

102. Serafin, J. G.; Liu, A. C.; Seyedmonir, S. R., *J. Mol. Catal. (A)* **1998,** *131* (1-3), 157-168.

103. Van Santen, R. A.; Kuipers, H. P. C. E., *Adv. Catal.* **1987,** *35*, 265-321.

104. Weissermel, K.; Arpe, H.-J., *Industrial Organic Chemistry*. 3rd ed.; VCH: Weinheim, 1997; p 144.

105. Min, B. K.; Friend, C. M., *Chem. Rev.* **2007,** *107* (6), 2709-2724.

106. Schmidbaur, H.; Schier, A., *Gold Organometallics, in Comprehensive Organometallic Chemistry III*. Elsevier: Amsterdam, 2007; Vol. 2, p 251-307.

107. Hashmi, A. S. K., *Chem. Rev.* **2007,** *107* (7), 3180-3211.

108. Del Ministro, E.; Renn, O.; Rueegger, H.; Venanzi, L. M.; Burckhardt, U.; Gramlich, V., *Inorg. Chim. Acta* **1995,** *240* (1-2), 631-9.

109. Kazi, A. B.; Dias, H. V. R.; Tekarli, S. M.; Morello, G. R.; Cundari, T. R., *Organometallics* **2009,** *28* (6), 1826-1831.

110. Dias, H. V. R.; Fianchini, M.; Cundari, T. R.; Campana, C. F., *Angew. Chem. Int. Ed.* **2008,** *47* (3), 556-559.

111. Nechaev, M. S.; Rayon, V. M.; Frenking, G., *J. Phys. Chem. A* **2004,** *108* (15), 3134-3142.

112. Frenking, G.; Froehlich, N., *Chem. Rev.* **2000,** *100* (2), 717-774.

113. Reisinger, A.; Trapp, N.; Knapp, C.; Himmel, D.; Breher, F.; Ruegger, H.; Krossing, I., *Chem. Eur. J.* **2009,** *15* (37), 9505-9520.

114. Pyykkö, P., *Chem. Rev.* **2012,** *112* (1), 371-384.

115. Bayler, A.; Schier, A.; Bowmaker, G. A.; Schmidbaur, H., *J. Am. Chem. Soc.* **1996,** *118* (29), 7006-7007.

116. Omary, M. A.; Rawashdeh-Omary, M. A.; Gonser, M. W. A.; Elbjeirami, O.; Grimes, T.; Cundari, T. R.; Diyabalanage, H. V. K.; Gamage, C. S. P.; Dias, H. V. R., *Inorg. Chem.* **2005,** *44* (23), 8200-8210.

117. Fujisawa, K.; Imai, S.; Moro-oka, Y., *Chem. Lett.* **1998,** (2), 167-168.

118. Flores, J. A.; Dias, H. V. R., *Inorg. Chem.* **2008,** *47* (11), 4448-4450.

119. Cinellu, M. A.; Minghetti, G.; Cocco, F.; Stoccoro, S.; Zucca, A.; Manassero, M.; Arca, M., *Dalton Trans.* **2006,** (48), 5703-5716, and the references therein.

120. Munakata, M.; Kitagawa, S.; Kosome, S.; Asahara, A., *Inorg. Chem.* **1986,** *25* (15), 2622-7.

121. Sheldrick George, M., *Acta Cryst. A* **2008,** *64* (Pt 1), 112-22.

122. Dolomanov, O. V.; Bourhis, L. J.; Gildea, R. J.; Howard, J. A. K.; Puschmann, H., *J. Appl. Crystallogr.* **2009,** *42* (2), 339-341.

123. Fulmer, G. R.; Miller, A. J. M.; Sherden, N. H.; Gottlieb, H. E.; Nudelman, A.; Stoltz, B. M.; Bercaw, J. E.; Goldberg, K. I., *Organometallics* **2010,** *29* (9), 2176-2179.

124. Hu, Z.; George, G. N.; Gorun, S. M., *Inorg. Chem.* **2001,** *40* (19), 4812-4813.

125. Nakazawa, J.; Terada, S.; Yamada, M.; Hikichi, S., *J. Am. Chem. Soc.* **2013,** *135* (16), 6010-6013.

126. Pellei, M.; Papini, G.; Lobbia, G. G.; Ricci, S.; Yousufuddin, M.; Dias, H. V. R.; Santini, C., *Dalton Trans.* **2010,** *39* (38), 8937-8944.

127. van Dijkman, T. F.; Siegler, M. A.; Bouwman, E., *Dalton Trans.* **2015,** *44* (48), 21109-21123.

128. Zhao, N.; Bullinger, J. C.; Van Stipdonk, M. J.; Stern, C. L.; Eichhorn, D. M., *Inorg. Chem.* **2008,** *47* (13), 5945-5950.

129. Urbano, J.; Belderrain, T. R.; Nicasio, M. C.; Trofimenko, S.; Diaz-Requejo, M. M.; Perez, P. J., *Organometallics* **2005,** *24* (7), 1528-1532.

130. Bucher, U. E.; Currao, A.; Nesper, R.; Rueegger, H.; Venanzi, L. M.; Younger, E., *Inorg. Chem.* **1995,** *34* (1), 66-74.

131. Fekl, U.; van Eldik, R.; Lovell, S.; Goldberg, K. I., *Organometallics* **2000,** *19* (18), 3535-3542.

132. Fuentes, M. A.; Olmos, A.; Munoz, B. K.; Jacob, K.; Gonzalez-Nunez, M. E.; Mello, R.; Asensio, G.; Caballero, A.; Etienne, M.; Perez, P. J., *Chem. Eur. J.* **2014,** *20* (35), 11013-11018.

133. Fujisawa, K.; Yoshida, M.; Miyashita, Y.; Okamoto, K.-i., *Polyhedron* **2009,** *28* (8), 1447-1454.

134. Ghosh, C. K.; Hoyano, J. K.; Krentz, R.; Graham, W. A. G., *J. Am. Chem. Soc.* **1989,** *111* (14), 5480-1.

135. Han, R.; Ghosh, P.; Desrosiers, P. J.; Trofimenko, S.; Parkin, G., *J. Chem. Soc., Dalton Trans.* **1997,** (20), 3713-3717.

136. Joshi, H. K.; Arvin, M. E.; Durivage, J. C.; Gruhn, N. E.; Carducci, M. D.; Westcott, B. L.; Lichtenberger, D. L.; Enemark, J. H., *Polyhedron* **2004,** *23* (2-3), 429-438.

137. Renn, O.; Vananzi, L. M.; Marteletti, A.; Gramlich, V., *Helv. Chim. Acta* **1995,** *78* (4), 993-1000.

138. Romero, N.; Vendier, L.; Dinoi, C.; Etienne, M., *Dalton Trans.* **2014,** *43* (26), 10114-10119.

139. Sirianni, E. R.; Yap, G. P. A.; Theopold, K. H., *Inorg. Chem.* **2014,** *53* (17), 9424-9430.

140. van Dijkman, T. F.; Siegler, M. A.; Bouwman, E., *Eur. J. Inorg. Chem.* **2016,** (15-16), 2586-2594.

141. Elliott, E. L.; Hernandez, G. A.; Linden, A.; Siegel, J. S., *Org. Biomol. Chem.* **2005,** *3* (3), 407-413.

142. Loas, A.; Gorun, S. M., *Eur. J. Inorg. Chem.* **2016,** (15-16), 2648-2657.

143. Lupinetti, A. J.; Strauss, S. H.; Frenking, G., *Progress Inorg. Chem.* **2001,** *49*, 1-112.

144. Shufler, S. L.; Sternberg, H. W.; Friedel, R. A., *J. Am. Chem. Soc.* **1956,** *78* (12), 2687-2688.

145. Souma, Y.; Iyoda, J.; Sano, H., *Inorg. Chem.* **1976,** *15* (4), 968-970.

146. Gava, R.; Olmos, A.; Noverges, B.; Varea, T.; Álvarez, E.; Belderrain, T. R.; Caballero, A.; Asensio, G.; Pérez, P. J., *ACS Catal.* **2015,** *5* (6), 3726-3730.

147. Dias, H. V. R.; Fianchini, M., *Angew. Chem., Int. Ed.* **2007,** *46* (13), 2188-2191.

148. Santini, C.; Gioia Lobbia, G.; Pettinari, C.; Pellei, M.; Valle, G.; Calogero, S., *Inorg. Chem.* **1998,** *37* (5), 890-900.

149. Miller, G. R.; Yankowsky, A. W.; Grim, S. O., *J. Chem. Phys.* **1969,** *51* (8), 3185-3190.

150. Kruck, M.; Munoz, M. P.; Bishop, H. L.; Frost, C. G.; Chapman, C. J.; Kociok-Köhn, G.; Butts, C. P.; Lloyd-Jones, G. C., *Chem. Eur. J.* **2008,** *14* (26), 7808-7812.

151. Hierso, J.-C., *Chem. Rev.* **2014,** *114* (9), 4838-4867.

152. Alvarez, S., *Dalton Trans.* **2013,** *42* (24), 8617-8636.

153. Gioia Lobbia, G.; Hanna, J. V.; Pellei, M.; Pettinari, C.; Santini, C.; Skelton, B. W.; White, A. H., *Dalton Trans.* **2004,** (6), 951-958.

154. Santini, C.; Gioia Lobbia, G.; Pellei, M.; Pettinari, C.; Valle, G.; Calogero, S., *Inorg. Chim. Acta* **1998,** *282* (1), 1-9.

155. Youm, K.-T.; Huh, S.; Park, Y. J.; Park, S.; Choi, M.-G.; Jun, M.-J., *Chem. Commun.* **2004,** (21), 2384-2385.

156. Kühl, O., *Phosphorus-31 NMR Spectroscopy*. 2008; p XIV, 132.

157. Trofimenko, S., *J. Am. Chem. Soc.* **1966,** *88* (8), 1842-1844.

158. Effendy; Lobbia, G. G.; Pettinari, C.; Santini, C.; Skelton, B. W.; White, A. H., *Inorg. Chim. Acta* **2000,** *308* (1-2), 65-72.

159. Finar, I. L.; Lord, G. H., *J. Chem. Soc.* **1959,** (0), 1819-1823.

160. Trofimenko, S., *J. Am. Chem. Soc.* **1970,** *92* (17), 5118-5126.

161. Harris, R. K.; Howes, B. R., *Journal of Molecular Spectroscopy* **1968,** *28* (2), 191-203.

162. Krieck, S.; Koch, A.; Hinze, K.; Müller, C.; Lange, J.; Görls, H.; Westerhausen, M., *Eur. J. Inorg. Chem.* **2016,** *2016* (15-16), 2332-2348.

163. Reger, D. L., *Comments Inorg. Chem.* **1999,** *21* (1-3), 1-28.

164. Cavallo, L.; Cucciolito, M. E.; De Martino, A.; Giordano, F.; Orabona, I.; Vitagliano, A., *Chem. Eur. J.* **2000,** *6* (7), 1127-1139.

165. Pettinari, C.; Santini, C., 1.10 - Polypyrazolylborate and Scorpionate Ligands A2 - McCleverty, Jon A. In *Comprehensive Coordination Chemistry II*, Meyer, T. J., Ed. Pergamon: Oxford, 2003; pp 159-210.

166. Byers, P. K.; Stone, F. G. A., *J. Chem. Soc. Dalton Trans.* **1991,** (1), 93-9.

167. Perez, P. J.; Diaz-Requejo, M. M., *Copper Organometallics, in Comprehensive Organometallic Chemistry III*. Elsevier: Amsterdam, 2007; Vol. 2, p 153-195.

168. Pike, R. D., *Organometallics* **2012,** *31* (22), 7647-7660.

169. Xu, Q., *Coord. Chem. Rev.* **2002,** *231* (1-2), 83-108.

170. Reger, D. L.; Grattan, T. C.; Brown, K. J.; Little, C. A.; Lamba, J. J. S.; Rheingold, A. L.; Sommer, R. D., *J. Organomet. Chem.* **2000,** *607* (1–2), 120-128.

171. Bigmore, H. R.; Lawrence, S. C.; Mountford, P.; Tredget, C. S., *Dalton Trans.* **2005,** (4), 635-651.

172. Neurock, M.; Zhang, X.; Olken, M.; Jones, M.; Hickman, D.; Calverley, T.; Gulotty, R., *J. Phys. Chem. B* **2001,** *105* (8), 1562-1572.

173. Lee, S., *Methanol Synthesis Technology*. CRC Press: Boca Raton, FL., 1990; p 1-22.

174. Capracotta, M. D.; Sullivan, R. M.; Martin, J. D., *J. Am. Chem. Soc.* **2006,** *128* (41), 13463-13473, and the references therein.

175. Reger, D. L.; Collins, J. E.; Rheingold, A. L.; Liable-Sands, L. M., *Organometallics* **1996,** *15* (8), 2029-32.

176. Klaui, W.; Berghahn, M.; Frank, W.; Reiss, G. J.; Schonherr, T.; Rheinwald, G.; Lang, H., *Eur. J. Inorg. Chem.* **2003,** (11), 2059-2070.

177. Fujisawa, K.; Ono, T.; Ishikawa, Y.; Amir, N.; Miyashita, Y.; Okamoto, K.-I.; Lehnert, N., *Inorg. Chem.* **2006,** *45* (4), 1698-1713.

178. Kujime, M.; Kurahashi, T.; Tomura, M.; Fujii, H., *Inorg. Chem.* **2007,** *46* (2), 541-551.

179. Hsu, S. C. N.; Chen, H. H. Z.; Lin, I. J.; Liu, J.-J.; Chen, P.-Y., *J. Organomet. Chem.* **2007,** *692* (17), 3676-3684.

180. Miller, K. E.; Schopp, L. M.; Nesseth, K. N.; Moore, C.; Rheingold, A. L.; Daley, C. J. A., *Acta Crystallographica Section E* **2009,** *65* (11), m1354-m1355.

181. Rocha, B. G. M.; Wanke, R.; Guedes da Silva, M. F. C.; Luzyanin, K. V.; Martins, L. M. D. R. S.; Smolénski, P.; Pombeiro, A. J. L., *J. Organomet. Chem.* **2012,** *714*, 47-52.

182. Pampaloni, G.; Peloso, R.; Belletti, D.; Graiff, C.; Tiripicchio, A., *Organometallics* **2007,** *26* (17), 4278-4286.

183. Pampaloni, G.; Peloso, R.; Graiff, C.; Tiripicchio, A., *Dalton Trans.* **2006,** (29), 3576-3583.

184. Chou, C.-C.; Su, C.-C.; Yeh, A., *Inorg. Chem.* **2005,** *44* (17), 6122-6128.

185. Good, C. D.; Ritter, D. M., *J. Am. Chem. Soc.* **1962,** *84* (7), 1162-1166.

186. Otero, A.; Fernández-Baeza, J.; Antiñolo, A.; Tejeda, J.; Lara-Sánchez, A.; Sánchez-Barba, L.; Rodríguez, A. M.; Maestro, M. A., *J. Am. Chem. Soc.* **2004,** *126* (5), 1330-1331.

187. Otero, A.; Fernández-Baeza, J.; Antiñolo, A.; Tejeda, J.; Lara-Sánchez, A.; Sánchez-Barba, L. F.; Sánchez-Molina, M.; Rodríguez, A. M.; Bo, C.; Urbano-Cuadrado, M., *Organometallics* **2007,** *26* (17), 4310-4320.

188. Cavallo, L.; Macchioni, A.; Zuccaccia, C.; Zuccaccia, D.; Orabona, I.; Ruffo, F., *Organometallics* **2004,** *23* (9), 2137-2145, and the references therein.

189. Hahn, C., *Chem. Eur. J.* **2004,** *10* (23), 5888-5899.

190. Dai, X.; Warren, T. H., *Chem. Commun.* **2001,** (19), 1998-1999.

191. Dias, H. V. R.; Singh, S.; Flores, J. A., *Inorg. Chem.* **2006,** *45* (22), 8859-8861.

192. Bartell, L. S.; Roth, E. A.; Hollowell, C. D.; Kuchitsu, K.; Young, J. E., Jr., *J. Chem. Phys.* **1965,** *42* (8), 2683-6.

193. Groom, C. R.; Bruno, I. J.; Lightfoot, M. P.; Ward, S. C., *Acta Crystallographica Section B* **2016,** *72* (2), 171-179.

194. Steinborn, D.; Potechin, V. V.; Gerisch, M.; Bruhn, C.; Schmidt, H., *Transition Metal Chemistry* **1999,** *24* (1), 67-70.

195. Powell, D. B.; Scott, J. G. V.; Sheppard, N., *Spectrochim. Acta, Part A* **1972,** *28* (2), 327-35.

196. Maekawa, M.; Tominaga, T.; Okubo, T.; Kuroda-Sowa, T.; Munakata, M., *Eur. J. Inorg. Chem.* **2009,** *2009* (28), 4225-4231.

197. Hebben, N.; Himmel, H.-J.; Eickerling, G.; Herrmann, C.; Reiher, M.; Herz, V.; Presnitz, M.; Scherer, W., *Chem. Eur. J.* **2007**, in press; and the references therein.

198. Manceron, L.; Andrews, L., *J. Phys. Chem.* **1986,** *90* (19), 4514-28.

199. Straub, B. F.; Eisentrager, F.; Hofmann, P., *Chem. Commun.* **1999,** (24), 2507-2508.

200. Flores, J. A.; Badarinarayana, V.; Singh, S.; Lovely, C. J.; Dias, H. V. R., *Dalton Trans.* **2009,** (37), 7648-7652.

201. Adiraju, V. A. K.; Flores, J. A.; Yousufuddin, M.; Dias, H. V. R., *Organometallics* **2012,** *31* (22), 7926-7932.

202. Van Nes, G. J. H.; Vos, A., *Acta Cryst. (B)* **1979,** *35* (11), 2593-601.

203. Boni, A.; Pampaloni, G.; Peloso, R.; Belletti, D.; Graiff, C.; Tiripicchio, A., *J. Organomet. Chem.* **2006,** *691* (26), 5602-5609.

204. Zhang, Z.; Cui, D.; Trifonov, A. A., *Eur. J. Inorg. Chem.* **2010,** *2010* (18), 2861-2866.

205. Bellott, B. J.; Girolami, G. S., *Organometallics* **2009,** *28* (7), 2046-2052.

206. Salomon, R. G.; Kochi, J. K., *J. Am. Chem. Soc.* **1973,** *95* (10), 3300-3310.

207. Beyer, E. M., *Plant Physiol.* **1976,** *58* (3), 268-271.

Biographical Information

Shawn G. Ridlen earned a Bachelor of Science in Chemistry from the University of West Georgia (UWG), located in Carrollton, GA, in 2010. During his last year at UWG, he conducted inorganic synthesis research under the supervision of Dr. Megumi Fujita. Shawn earned a Master of Science in Chemistry from the University of North Carolina at Charlotte (UNCC), located in Charlotte, NC, in 2012. Here he joined the lab of Dr. Jordan Poler and conducted research in inorganic synthesis with a focus on enantiopure ruthenium complexes, electronic characterization, and photophysical characterization with applications in the self-assembly of nanomaterials. In 2012, Shawn began his doctoral studies under the guidance of Dr. Rasika Dias at the University of Texas at Arlington (UTA), located in Arlington, TX. Shawn has worked on numerous projects, but his research mainly focused on the isolation of rare coinage metal adducts of poly(pyrazolyl)borates. After receiving his degree from UTA, Shawn plans to begin a career in industry.